The Role of Epigenetics and Type 2 Epithelial-Mesenchymal Transitions in Trachoma

Tamsyn Ruth Derrick

Thesis submitted in accordance with the requirements for the degree of

Doctor of Philosophy

University of London
September 2015

Department of Clinical Research

Faculty of Infectious and Tropical Diseases

LONDON SCHOOL OF HYGIENE & TROPICAL MEDICINE

Declaration

I declare that the work presented in this thesis is my own. Where information has been derived from other sources, I confirm that this has been indicated within the thesis.

Signature   Date: 26th September 2015

Tamsyn Derrick

Abstract

Trachoma is the leading infectious cause of blindness worldwide and is initiated by repeated infection of the conjunctiva with *Chlamydia trachomatis* (Ct). In some individuals this causes chronic inflammation and fibrosis that progresses in the absence of Ct. The work presented in this thesis sought to determine the role and contribution of miRNA and epithelial-mesenchymal transition (EMT) in various stages of trachomatous disease. Epithelial cells did not differentially express miRNA at 48 hours post infection with virulent plasmid-competent and avirulent plasmid-free ocular strains of Ct. Expression of inflammatory cytokines and growth factors were increased in response to virulent Ct infection but the induction of EMT was not detected in response to either strain. In a set of 161 samples from children living in a trachoma hyper-endemic region in Guinea-Bissau, miR-155 was upregulated in children with active trachoma and current Ct infection and miR-184 was downregulated in children with active trachoma with and without Ct infection. In a set of 194 samples from adults in The Gambia, miR-1285 and miR-147b were upregulated in inflammatory trachomatous scarring. Differential expression of these miR indicates the regulation of inflammation, wound healing and cell proliferation pathways. Immunohistochemistry was used to study conjunctival biopsies from Tanzanian adults with trachomatous trichiasis and found increased epithelial expression of the pro-inflammatory mediator and antimicrobial peptide S100A7 and connective tissue growth factor. Pro-inflammatory cytokine IL-1β expression was increased in the subepithelium relative to controls. Trichiasis cases had increased disruption of collagen deposition patterns and increased sub-clinical inflammatory cell infiltrates, but no differences in epithelial atrophy and myofibroblasts were detected relative to controls. There was no evidence for the occurrence of EMT in biopsy tissue from trachomatous trichiasis cases. These data suggest that EMT does not have a major role in conjunctival fibrosis and highlight the importance of inflammation in trachomatous pathology.

Preface

This thesis is presented as a 'Research Paper Style Thesis' in accordance with submission guidelines provided by the London School of Hygiene and Tropical Medicine. Chapters indicated in bold italics in the Table of Contents are either published articles, papers that have been submitted or papers that have been formatted for submission in peer-reviewed journals. Details of publication/submission are included in a cover sheet preceding each of these chapters. Author contributions are detailed on page 6 of this thesis. Other chapters include supporting information and data that were not written up for publication, all of which were written by Tamsyn Derrick.

Acknowledgements

List of contributors to the work presented in this thesis

Name	Position	Contribution
Martin Holland	Reader, LSHTM	PhD supervisor
Matthew Burton	Senior Research Fellow, LSHTM	PhD co-supervisor
Chrissy h. Roberts	Lecturer, LSHTM	Laboratory and data analysis advice, review contributor (Chapter 2; "Host genetic association studies and Trachoma")
Anna Last	Clinical lecturer, LSHTM	Clinical grader and sample collector, review contributor (Chapter 2; "Chlamydial Genomics and Pathogenesis")
Sarah Burr	Lecturer, LSHTM	Logistical field support from MRC The Gambia unit, review contributor (Chapter 2; "Bacterial Ecology of the Conjunctiva and Trachoma")
Eunice Cassama	Ophthalmic nurse, Ministerio de Saude Publica, Guinea Bissau	Fieldwork: finding participants and collecting informed consent
Megha Rajasekhar	MRC The Gambia Unit	miRNA extraction
Hassan Joof & Pateh Makalo	MRC The Gambia Unit	Sample collection and fieldwork in The Gambia
Omar Camara	MRC The Gambia Unit	Driver
Robin Bailey	Professor, LSHTM	Statistical support
David Mabey	Professor, LSHTM	PhD project support
Meno Nabicassa	Ministerio de Saude Publica, Guinea Bissau	Fieldwork project support
Hodan Jama	Biomedical scientist, Institute of Ophthalmology	IHC laboratory advice and support
Phil Luthert	Professor, Institute of Ophthalmology	IHC grading
David Essex	Laboratory manager, Institute of Ophthalmology	IHC project support
Patrick Massae	Researcher, Kilimanjaro Christian Medical Centre	IHC biopsy sample preparation
Victor Hu	Honorary lecturer, LSHTM	IHC data interpretation advice
Lesley Cutcliffe	Molecular microbiology group, University of Southampton	Training in chlamydial culture
Rod Markham-David	NA	Fieldwork: Clinical photography

LSHTM: London School of Hygiene and Tropical Medicine
MRC: Medical Research Council
IHC: immunohistochemistry

Table of Contents

List of abbreviations

Ct: *Chlamydia trachomatis*

Cm: *Chlamydia muridarum*

N: Healthy control (no clinical evidence of trachoma)

TF: *Trachomatous inflammation – follicular*

TI: *Trachomatous inflammation – intense*

Active trachoma: TF and/or TI

TS: Trachomatous scarring

TSI: Trachomatous scarring with clinically significant inflammation

TT: Trachomatous trichiasis

SAFE: Surgery, Antibiotics, Facial cleanliness and Environmental improvements

MDA: Mass drug administration

EMT: Epithelial-mesenchymal transition

miR: MicroRNA (miRNA)

PRR: Pattern recognition receptor

TLR: Toll-like Receptor

IFU: Infection forming units

MOI: Multiplicity of infection

PBS: Phosphate buffered saline

RIN: RNA integrity number

MEM: Minimum essential medium

DMEM: Dulbecco's modified eagle medium

HEp-2 cells: Human epithelial type 2 cells

HCjE cells: Human conjunctival epithelial cells

ddPCR: Droplet-digital polymerase chain reaction

RPP30: *Homo sapiens* RNase P/MRP 30-kDa subunit gene (DNA endogenous control)

omcB: *Chlamydia trachomatis* outer membrane gene (encoded on Ct chromosome)

qPCR: Quantitative polymerase chain reaction

RPLP0: *Homo sapiens* Ribosomal Protein Large P0 gene (mRNA endogenous control)

U6: Small nuclear RNA (miRNA endogenous control)

dCT: Delta cycle threshold value

hpi: Hours post infection

FC: Fold change

AUC: Area Under the Curve

IHC: Immunohistochemistry

GM-CSF: Granulocyte-macrophage colony-stimulating factor (CSF2)

CTGF: Connective tissue growth factor

PDGF: Platelet-derived growth factor

TGFβ: Transforming growth factor beta

EGF: Epidermal growth factor

CC1: Cleaved caspase 1

MMP: Matrix metalloproteinase

List of Figures

AF: Additional file

S: Supplementary file

List of Tables

AF: Additional file
S: Supplementary file

Chapter 1: Introduction

1.1 Introduction to trachoma

Trachoma is initiated by infection of the tarsal conjunctiva with the intracellular bacterium *Chlamydia trachomatis* (Ct). Sightsavers International estimates that every 15 minutes a person looses sight as a result of trachoma [1]. As such, trachoma remains the world's leading infectious cause of blindness despite significant efforts to control and eliminate the disease [2]. Trachoma is currently considered endemic in 51 countries worldwide and only seven formerly endemic countries have reached target elimination thresholds [2]. Forty million people are currently estimated to have active trachoma and eight million people suffer with un-operated trichiasis [3]. The Alliance for Global Elimination of Blinding Trachoma has set the goal of 2020 for the elimination of trachoma. The aim is to control trachoma through the implementation of **S**urgery for trichiasis, **A**ntibiotics to treat infection, **F**acial cleanliness and **E**nvironmental improvements to reduce transmission (SAFE). Currently 31 trachoma-endemic countries implement SAFE, which is effective in controlling trachoma if well conducted. Azithromycin is the antibiotic of choice used in mass drug administration (MDA) programmes for trachoma control. There are additional beneficial effects of azithromycin MDA, including reduced all-cause mortality [4] and potential to reduce clinical disease through its anti-inflammatory properties [5]. There remains a need to pursue vaccine development however as there are circumstances when SAFE is poorly effective and there is uncertainty about its universal application. The lack of randomized controlled trials examining the effectiveness of the F and E components for the interruption of transmission, alongside the historical lack of molecular laboratory tools able to identify transmission events raises questions on the basic understanding of their effectiveness. Additional concerns with the A component include the long-term use of antibiotics in populations where MDA has failed to control disease [6] and introduction of resistance in other bacterial species [7]. It is also not currently understood whether effective mass treatment leads to arrested immunity and it is unclear what impact the elimination of ocular chlamydial exposure in childhood might exert later in adolescent and adult urogenital disease. *Chlamydiae* can reside in the gastrointestinal tract in the absence of clinical disease and this has led to the suggestion that azithromycin treatment failures (at least in urogenital disease) may be because gastrointestinal *Chlamydiae* are refractory to azithromycin treatment and can act as a source for auto-inoculation [8,9]. Although implementation of MDA is effective in reducing the prevalence of Ct infection [10], re-infection is common and may be re-introduced by migrants [11]. Furthermore there is evidence that scarring trachoma progresses in the absence of Ct infection [12], therefore it is likely that a large number

of individuals will continue to progress towards trichiasis even once Ct infection is controlled at the population level. Epilation provides a temporary relief from minor trichiasis and surgery to rotate the tarsal conjunctiva is currently the main intervention for major trichiasis, however recurrence rates from trichiasis surgery can reach 60% by 3 years [13]. In order to prevent the progressive fibrosis leading to trichiasis, a better understanding of the causative mechanism is required. A vaccine offering effective long-term protection against disease in both ocular and urogenital chlamydial disease remains desirable.

There are a number of classification systems for the clinical signs of trachoma. Under the WHO simplified grading system, the presence of five or more follicles on the conjunctival surface is classified as trachomatous inflammation follicular (TF). Ct infection is independently associated with TF (OR=11.2 (95% CI 6.9–18.1) [14]), although this value varies between populations depending on disease sign prevalence and becomes disassociated from TF once prevalence is low. Repeated Ct infection in endemic communities can trigger chronic conjunctival inflammation (trachomatous inflammation intense, TI) in some individuals, causing conjunctival fibrosis (trachomatous scarring, TS). Ct infection is rarely found in adults with scarring [12], suggesting that early life Ct infection is an important priming event that may establish a stable pro-fibrotic environment. Progressive fibrosis may lead to entropion, inward turning or mis-directed lashes (trachomatous trichiasis, TT) all of which abrade the corneal surface. This abrasive damage may lead to corneal opacity (CO) and blindness. Figure 1.1 shows reflective *in vivo* confocal microscopy scans, histology sections and photographs of the tarsal conjunctiva that illustrate the changes in tissue architecture that occur in the different stages of trachomatous disease.
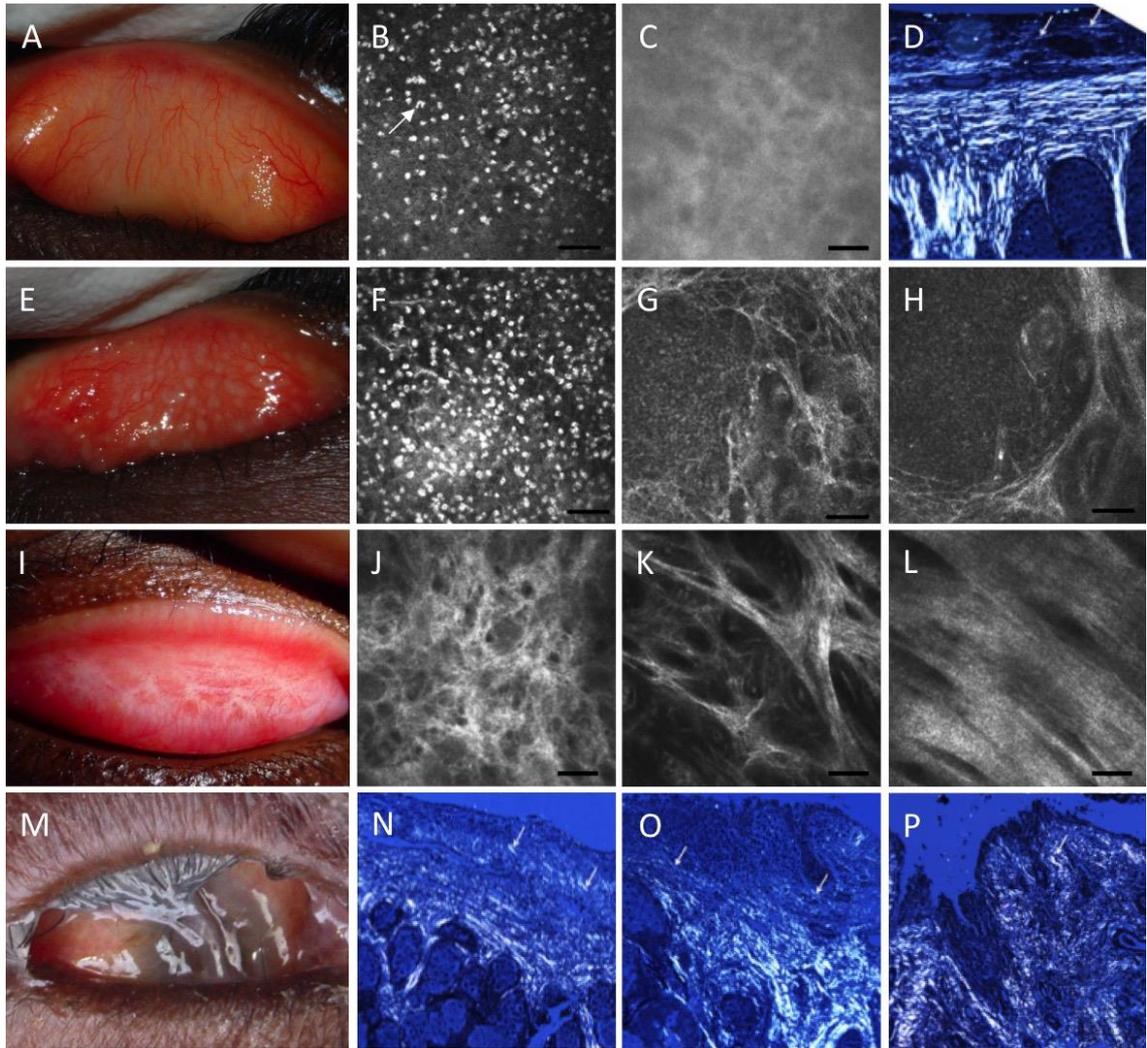
Figure 1.1. Images from a normal healthy eye (A-D) and from individuals with follicular trachoma (E-H), trachomatous scarring (I-L), trichiasis and progressive scarring (M-P). *A, E, I and M are photographs of the tarsal conjunctiva showing normal appearance (A), papillary inflammation and follicles (E), bands of trachomatous scarring (I) and extreme trichiasis and corneal opacity (M). B, C, F, G, H, J, K and L are in vivo confocal microscopy images of the tarsal conjunctiva at various depths (the bar represents 50μm). A moderate number of inflammatory nuclei are present in the sub-epithelium of a healthy eye (B), whereas a higher number are present in trachomatous inflammation (F). Follicles can be seen in (G) and (H). The connective tissue of the healthy conjunctiva is amorphous (C), whereas successive grades of trachomatous scarring are seen as a heterogeneous clumpy appearance (J), defined tissue bands that make up <50% of the scan area (K) and defined bands that make up >50% of the scan area (L). D and N-P are histological images of tissue scarring using polarized light (original magnification x100). In the healthy conjunctiva, collagen fibers are parallel (arrows) with the surface epithelium (D), whereas progressive disorganization of this appearance is observed in scarring (N-P). Images are kindly provided with permission*

from Matthew Burton and Victor Hu and are adapted from Hu et al., 2011 [15] *and Hu et al., 2013* [16]*.*

The human trachoma vaccine trials that took place in the 1960s concluded that some short-term strain-specific protection from infection was induced, amidst concerns that pathology was exacerbated in some cases, supported by data from monkey models [17]. The data from these large placebo-controlled trials has been recently reinterpreted in the context of current grading systems and our current knowledge of disease pathogenesis. Only trial III in The Gambia recorded evidence of conjunctival scarring. Two doses of prophylactic vaccination made from two live strains in mineral oil were given three weeks apart to children aged 0-4 years old. There was no protection from active trachoma, however the vaccinated group had a reduced prevalence of scarring disease two years later [18]. When all three Gambian trials are reviewed in the context of what is now known about disease pathogenesis, vaccine-induced exacerbation of disease may not be a significant concern, raising hopes that current vaccine formulations may be successful [17,19]. Understanding the immunology and pathology of trachomatous disease is therefore essential for the development of a vaccine that invokes a protective, and not a pathogenic, host response.

1.2 Anatomy of the tarsal conjunctiva in trachoma

The conjunctiva is a mucous membrane that lines the insides of the eyelids and the white of the eyeball (the sclera). The palpebral (tarsal) conjunctiva lines the inner eyelid, the bulbar conjunctiva covers the sclera and the fornix conjunctiva forms a junction between the tarsal and bulbar sections. The conjunctival epithelium is formed of a non-keratinized layer of columnar and squamous stratified epithelial cells 2-5 cells thick, which is interspersed with goblet cells [20]. Goblet cells are highly differentiated epithelial cells and their primary role is to produce mucins, which, in addition to the membrane-associated mucins produced by apical epithelial cells, prevent desiccation of the ocular surface and trap commensal and pathogenic bacteria [21]. Other innate immune functions of the conjunctival epithelium include tight junctions between cells that prevent pathogen entry, release of antimicrobial peptides and expression of pattern recognition receptors (PRRs). PRRs are found on the cell membrane or in the cytosol and can respond to pathogen associated molecular patterns (PAMPs) or damage associated molecular patterns (DAMPs). PRRs include Toll-like Receptors

(TLRs), NOD-like receptors (NLRs), C-type Lectin receptors (CLRs) and RIG-I-like receptors (RLRs).

Beneath the epithelium lies the stroma, or connective tissue, which is separated from the epithelium by the basement membrane. The stroma is made up of fibroblasts and contains blood vessels, nerves and sebaceous glands (glands which secrete sebum to lubricate the skin). The superficial stroma contains lymphoid tissue, which is not present in children <3 months of age [22]. As a result, neonates cannot make conjunctival follicles and instead respond with papillary inflammation [23]. Beneath the stroma lies the tarsal plate, which is made up of dense connective tissue (mainly collagen type I) and gives the eyelid its structure.

Upon recognition of a pathogen via a PRR, epithelial cells secrete cytokines and chemokines that recruit and activate innate immune cells, which subsequently activates the adaptive immune system. Follicles are generated in the subepithelial tissue, consisting of germinal centers (immature proliferating lymphocytes) surrounded by mature lymphocytes and plasma cells. Follicles can be seen by eye as small white dots. Papillary inflammation is the formation of numerous tiny projections of tissue around central vascular cores. When papillary inflammation is severe the conjunctiva appears swollen, red and deep vessels are obscured [24]. Repeated rounds of inflammation in trachoma are thought to drive scarring in the tarsal plate, though the mechanism is unknown (discussed further below) Accumulation of scarring in the tarsal plate causes it to contract, causing entropion (infolding of the eyelid) and trichiasis (ingrowth of the eyelashes).

1.3 Wound healing

Infection and inflammation can cause tissue damage. The body responds to tissue damage through the process of wound healing, which has four distinct phases. These are hemostasis (clot formation), inflammation, proliferation and remodeling. In the inflammatory phase, immune cells including recruited macrophages and resident fibroblasts release pro-inflammatory cytokines, growth factors and matrix metalloproteinases (MMPs). As well as countering infection, these factors stimulate keratinocyte and fibroblast proliferation and extracellular-matrix (ECM) deposition. Activated fibroblasts known as myofibroblasts migrate into the wound space, deposit ECM and contract the wound to form a scar. These myofibroblasts originate both from local activated fibroblasts and from bone marrow-derived fibroblast-like cells that are

recruited to the wound. It is also thought that some myofibroblasts originate from local epithelial cells via epithelial-mesenchymal transition [25]. The wound is re-epithelialized and finally remodeled, whereby collagen type III (deposited during the proliferation phase) is replaced and realigned with collagen type I and unwanted cells are removed by apoptosis.

Aberrant inflammation can greatly affect the normal course of wound healing. Embryos heal wounds without scar formation before the third trimester and the wound is associated with a lower level of inflammation [26]. Likewise adult oral wounds have a lower inflammatory component and scarring is less severe [27]. In an environment of chronic inflammation an aberrant wound healing response is triggered, leading to progressive fibrosis and organ damage. In the conjunctiva, chronic inflammation associated with trachoma and other diseases such as Stephen-Johnson syndrome, linear Immunoglobulin A disease (LAD), ocular cicatricial pemphigoid (OCP) or chronic atopic keratoconjunctivitis can lead to progressive scarring and eventually loss of organ function [12,28–30].

1.4 Chlamydia trachomatis

Ct is a gram-negative-like intracellular bacterium with a biphasic developmental cycle that infects host epithelial cells (Figure 1.2). Chlamydial strains are separated into three biovars that preferentially (though not exclusively) infect distinct sites in the human body: trachoma, urogenital and LGV (lymphogranuloma venereum). Serovars A-C infect the conjunctival epithelium, causing trachoma. Serovars D-K infect the epithelial lining of the genital tract and cause urethritis. Serovars L1-3 can also infect the genital tract and rectum but are more invasive, surviving in macrophages and spreading to local lymph nodes, causing a disease known as LGV and proctitis in men who have sex with men. Although serovars A-C and D-K are thought not to disseminate and to remain in the epithelium, there is growing evidence that the gastrointestinal tract could be a reservoir of urogenital Ct infection and could result in autoinoculation [8,31]. Ct has also been detected in the joints, blood and other tissues of humans [32–34].
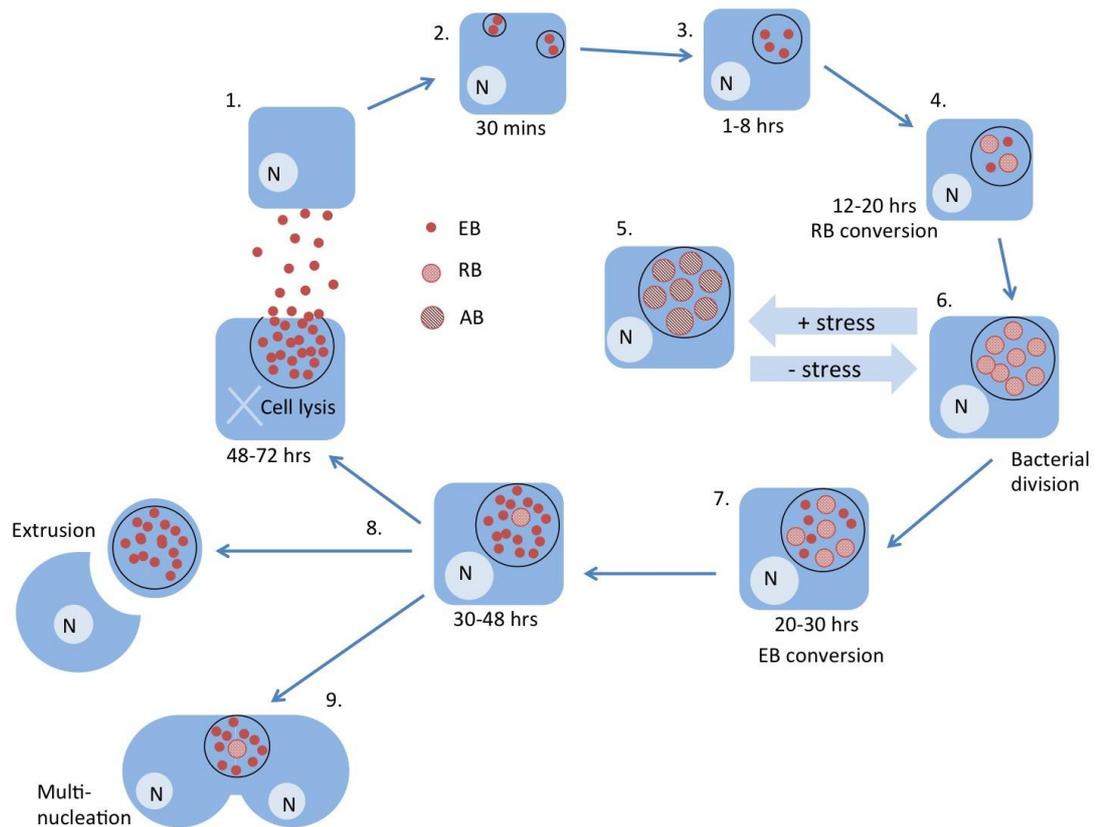
Figure 1.2. Ct developmental cycle. EB: elementary body, RB: reticulate body, AB: aberrant body, N: nucleus. Elementary bodies (EBs) are the smaller, infectious form. EBs attach to the host cell membrane and are endocytosed (1), forming an intracellular vacuole known as an inclusion body (2). Multiple inclusion bodies in a cell fuse into one (3). Phago-lysosomal fusion is blocked, providing an intracellular niche for the bacteria [35]. *EBs undergo differentiation into larger reticulate bodies (RBs) (4). Stress, such as penicillin or interferon gamma (IFNγ), can induce RBs to enter a reversible state of persistence (ABs) (5). RBs multiply by binary fission inside the inclusion (6), then differentiate back into EBs (7), whereupon they are released by cell lysis or extrusion to continue the infection cycle* [36] *(8). Ct can also prevent host cell cytokinesis, leading to the formation of multinucleated cells* [37–39] *(9). The timepoint (in hours) at which each stage of the developmental cycle occurs after initial EB attachment and entry is shown.*

The host cell receptors involved in Ct attachment and entry have not been fully defined. The epidermal growth factor receptor (EGFR), fibroblast growth factor receptor (FGFR) and platelet-derived growth factor receptor-β (PDGFRβ) are thought to be involved in chlamydial attachment [40–43] and activation of EGFR was required for Ct

development [43]. Tyrosine phosphorylated proteins accumulate at the entry site [44,45] and actin polymerization forms a scaffold around the nascent inclusion [46]. Ct possesses a number of virulence factors that enable it to form a protective intracellular niche in which to complete the developmental cycle and to avoid the host immune response, discussed further in the following section (section 1.5). RBs divide by binary fission inside the inclusion, doubling their numbers every 2-3 hours. They are thought to go through 6-10 rounds of replication before differentiating back into EBs, yielding 64-1024 EBs from a single infecting EB [47–49]. The Ct inclusion is then thought to be released by extrusion or lysis of the host cell [36] (Figure 1). These two processes were found to occur at near equivalent frequencies [36]. There is evidence to suggest that cells can repair their membrane following release of Ct, remaining viable and a suitable host in which residual EBs can complete another developmental cycle [50]. Location of the Ct inclusion on the cells equator can block cytokinesis, leading to formation of multinucleated cells, which is thought to confer a growth advantage to Ct via an increase in golgi content (an important source of lipids for Ct) [37–39]. If the host cell divides successfully however it is thought that only one daughter cell inherits the inclusion. If there are two inclusions in the dividing cell, both daughters may inherit one each or one daughter may inherit both [39].

Stressors such as IFNγ, penicillin and nutrient starvation can induce a state of persistence in chlamydial development *in vitro*. Upon induction of persistence, RBs transition into aberrant forms (ABs; Figure 1) which are usually larger and do not divide. ABs are non-cultivable and have altered metabolism, antigen, transcriptional and non-coding RNA profiles [51–54], however they remain viable. Genome replication continues but cytokinesis of the AB does not occur. Upon removal of the stress stimuli, RBs are thought to bud off the AB and continue the normal developmental cycle [55]. Chlamydial persistence is well described *in vitro* (reviewed in [56]), however until recently [57] there has been little evidence to suggest that persistence occurs in humans *in vivo* at urogenital or ocular anatomical sites.

The developmental cycle of Ct takes longer in ocular serovars in comparison to urogenital serovars (D-K and L2) [58]. Urogenital serovars converted from RBs back to EBs within 20-24 hours and completed the developmental cycle by 30-48 hours post infection of cell lines *in vitro*. In ocular serovars EB conversion began around 30-36 hours and the developmental cycle completed by 48-68 hours post infection [58]. Genomic replication was also slower in serovar A (A/HAR-13) compared to D (D/UW-3/Cx) and L2 (L2/434/Bu). Considerable variation occurs within serovars between

strains however; serovar A strain A2497 has been reported to grow faster than L2/434/Bu (Richard Haywood; personal communications).

1.5 *Chlamydia trachomatis* virulence factors

Defining the identity and function of chlamydial virulence factors has previously been restricted due to the obligate intracellular growth requirement of the pathogen. However, significant advances have been made in recent years and our understanding of chlamydial virulence mechanisms has grown rapidly [59–64]. Virulence factors identified through whole genome sequencing analysis and *in vitro* and animal studies include the polymorphic outer membrane protein family (Pmp's) [65–68], the type three secretion system (T3SS) and effectors [69–71], genes involved in tryptophan [72–74] and glycogen [59,75] biosynthesis, members of the *incA* [76,77] and phospholipase D [78,79] families, genes from the heat shock protein family [80,81], the chlamydial cytotoxin [82] and plasmid-encoded genes implicated in the regulation of chromosomal virulence factors [83–85]. These virulence factors are described in detail elsewhere [86], however the chlamydial cytotoxin and the plasmid are discussed further below.

The chlamydial cytotoxin is located in the plasticity zone (PZ), a site of extensive genomic variation between the chlamydial serovars [87,88]. The function of the toxin is thought to involve GTPase inactivation and guanylate binding protein neutralization resulting in IFNγ resistance [82,89,90]. IFNγ stimulation of cells *in vitro* and *in vivo* induces transcription of genes that co-operate to eliminate intracellular bacteria, suggesting that inhibition of this mechanism may contribute to the pathogenesis of chlamydial disease [90]. The genomic organisation of the cytotoxin varies such that oculogenital strains have a single gene with a large deletion, lymphogranuloma venereum (LGV) strains lack the gene entirely, whilst the closely related *C. muridarum* (Cm) has three intact copies [91,92]. This most likely reflects the IFNγ evasion mechanism employed by Cm in the mouse compared with that employed by urogenital strains in humans [125, 112]. Since ocular strains lack a functional *trp* operon, required for synthesis of the essential amino acid tryptophan, and only have a partial toxin, how they evade IFNγ is not fully understood. Ocular chlamydial infection of mice does not reproduce the clinical features of disease seen in humans, whereas ocular chlamydial infection of Guinea-Pigs and non-human primates (NHPs) more closely models active trachoma in humans [93,94]. The differences between model species and chlamydial strains regarding chlamydial virulence [91,92], infection course [95,96] and immune

response [97] highlight the importance of using appropriate model experimental systems.

The chlamydial plasmid has been shown to function as a virulence factor in urogenital murine and ocular NHP models [85,93]. Phenotypic differences vary between plasmid-cured and wild-type strains with respect to infectivity, glycogen accumulation, induction of inflammation and activation of toll-like receptor pathways [75,98]. Plasmid deletion mutagenesis studies showed that deletion of the plasmid-encoded *pgp4* gene results in an *in vitro* phenotype identical to that of a plasmid-free strain [83]. Bacterial transcriptome analysis found a decrease in transcript levels of a subset of chromosomal genes in a naturally occurring plasmid-free strain of *Ct*, demonstrating that the plasmid is a transcriptional regulator of virulence-associated genes [84]. The failure of plasmid-free Ct to produce and store glycogen might confer a survival disadvantage in nutrient limited settings, such as at mucosal surfaces [84]. Maintenance of the plasmid at the relatively low copy number of 5-6 plasmids per genome [99] carries inherent risk of plasmid-loss during cell partition [100], but naturally occurring plasmid-free strains are rare [101–103]. This suggests that 5-6 plasmid copies may maximize infectivity or intracellular survival whilst provoking minimal host immune response. Recent host transcriptome studies suggest that the plasmid may stimulate host cell expression of PD-L1, which induces programmed cell death in immune effector cells, suggesting a possible mechanism for plasmid virulence [104,105]. The plasmid is clearly strongly selected for during successful infection or transmission [98] and studies have shown that a plasmid-cured *Ct* strain is less virulent in ocular infection of macaques, does not cause pathology and can function as a live attenuated vaccine [139]. The absence of pathology in animal models infected with plasmid-free Ct suggests that parallel study of the host response to plasmid-competent and plasmid-free Ct will bring us closer to understanding the immunopathology of trachoma.

1.6 Immunopathology of trachoma

Despite extensive research, the mechanistic link between chronic inflammation and progressive scarring remains elusive [12]. The scarring observed in both trachoma and urogenital disease is thought to be a result of the host response to infection rather than a direct effect of the bacteria. Defining the features of protective versus pathogenic immunological responses in chlamydial disease (reviewed in [106]) is crucial to understanding disease and for efficacious vaccine design.

Currently, two models have been put forward to explain the immunopathogenesis of chlamydial disease: the immunological and cellular paradigms. The traditional immunological paradigm implicates the adaptive immune system. Initial studies on chlamydial infection found that repeated infection exacerbated inflammation and that inflammatory pathology continued in the absence of Ct. At first, a delayed type hypersensitivity (DTH) reaction triggered by a chlamydial antigen was hypothesized. The chlamydial heat shock protein 60 (HSP60) was considered a candidate antigen to trigger DTH, but was not found to exacerbate pathology when tested in a guinea-pig model [107]. Antibodies to HSP60 predicted a 2-3 fold higher risk of Ct pelvic inflammatory disease (PID) in humans and higher levels of antibodies specific to HSP60 were found in women with the most severe forms of urogenital disease [108]. Likewise antibodies to HSP60 were associated with tubal factor infertility (TFI) and inflammatory trachoma [109,110], however it remains unclear whether these antibodies cause pathology or are a result of a greater number or more severe episodes of infection. More recent screening of sera from trichiasis patients and controls detected differential patterns of antibody recognition for a number of Ct antigens, however HSP60 responses were not significantly different [111].

Previous research demonstrated that individuals with scarring trachoma had Th2 patterns of cytokine expression [112], whereas those with strong Th1 responses efficiently cleared infection [113]. This opposed the DTH theory and suggested that a Th2 response was either ineffectual at clearing infection or led to enhanced pathology and that CD4+ Th1 IFNγ responses were a key element of protective immunity in trachoma. Both CD8+ and CD4+ T cell infiltrates are associated with the conjunctival follicles that are characteristic of TF however CD4+ T cells are thought to outnumber CD8+ [114]. NK cells have more recently been identified as a major early source of IFNγ in response to Ct [115]. Despite the primary function of CD8+ T cells in defense against intracellular pathogens, data from murine models previously found a limited role for CD8+ T cells in anti-Ct immunity [116]. Recent evidence in the macaque model of trachoma challenges this theory and suggests that depletion of CD8+ T cells can abrogate protective immunity [117]. Characterization of the roles of each of these cell types in chronic scarring trachoma has proved difficult to address however, largely due to the long-term natural history of scarring disease.

Stephens suggested an alternative model of disease [118] in which epithelial cells at the infection site play a central role as mediators of the innate immune response.

Epithelial cells infected with Ct secrete a number of proinflammatory cytokines and growth factors, such as IL-8, GROα, IL-1α, IL-6 and granulocyte-macrophage colony-stimulating factor (GM-CSF). The secretion of these cytokines is delayed compared to the kinetics of secretion upon infection with other invasive bacteria and persists throughout the 2-4 day developmental cycle of Ct. The secretion of IL-1α by infected cells was shown to up-regulate pro-inflammatory cytokine production by neighboring uninfected cells, promoting a strong inflammatory response [119]. Lymphocytes of the adaptive immune system are attracted to the infection site by the chemotactic gradient and subsequent infections include memory populations that amplify the response. Ct infected cells also secreted the pro-fibrotic cytokine IL-11, a member of the IL-6 family [120,121]. Recent evidence from a primary-like polarized epithelial cell model showed that IL-11 was secreted preferentially from the basolateral membrane and IL1ra from the apical membrane in Ct-infected cells [122]. The T cell chemokines RANTES and IP10 were also down-regulated in productively Ct-infected cells, suggesting that Ct attempts to avoid stimulation of the immune response in order to maintain its intracellular niche, potentially leading to longer infections and chronic pathology [122]. Recent genome-wide scale array studies from clinical samples support Stephens' hypothesis. Expression profiling of children in The Gambia with active trachoma versus healthy controls revealed a strong up-regulation of the innate immune response [123]. Along with the expected infiltration of neutrophils, lymphocytes and the inflammatory cytokine pathways consistent with histopathology [124], the natural killer (NK) cell response was also enhanced. A transcriptome study conducted in Ethiopian adults with either trachomatous trichiasis (TT) or TT with inflammation (TTI) versus healthy controls found that despite less than 1% Ct infection prevalence, markers of ongoing sub-clinical inflammation and tissue remodeling were evident in the TT group and were more pronounced in the TTI group [125]. These markers were consistent with an activated and pro-inflammatory epithelium. There was a lack of evidence for a pro-fibrotic Th2 response and a very limited Th1 response. Subsequent targeted quantitative-PCR studies have re-emphasized the role of the innate immune response in trachoma in both children and adults [126,127]. These studies found antimicrobial peptides psoriasin (*S100A7*), *DEFb4A* and *SAA1*, inflammatory cytokines *IL-17, IL-1β* and *TNF*, inflammatory chemokines (*CCL18* and *CXCL5*), *MMPs* and *CTGF* were up-regulated in trachomatous disease. Increased *IL-17* expression was highlighted as characteristic of active trachoma and is thought to coordinate the pro-inflammatory response [126].

Overall these studies suggest that clearance of Ct infection requires an appropriate acute Th1 response with IFNγ and CD8+ T cells. They also support the case for the central role of epithelial cells in ongoing trachomatous inflammation and pathogenesis that leads to TT. This would imply that neither the cellular nor the immunological paradigm can fully explain disease, but that active cross talk between cellular (innate epithelial cell responses) and immunological (adaptive immunity) systems is required. A failure to generate an effective Th1 response to clear Ct infection (leading to chronic infection and inflammation), combined with an overactive innate epithelial inflammatory response throughout an individuals life might be risk factors for scarring progression.

1.7 Small RNAs and chlamydial disease

One possible explanation for the chronic inflammation and continued presence of active disease signs in populations once ocular Ct infection has been controlled is epigenetic change of the host cell state. "Epigenetics" describes changes in gene expression that are heritable through cell division, without alteration to the DNA sequence itself. These changes can be applied directly to DNA (CpG methylation), the proteins DNA is packaged around (chromatin modifications such as histone methylation or acetylation) and to the transcribed message (micro RNA mediated silencing).

Only 20% of transcription across the human genome is associated with protein-coding genes [128] and it has become clear that many of the non protein-coding RNA species that are transcribed have important regulatory roles. These non-coding RNA species include micro RNA (miRNA), short interfering RNA (siRNA), piwi-interacting RNA (piRNA), small nucleolar RNAs (snoRNA), other small RNA and long non-coding RNA (lncRNA (>200 nucleotides)).

MiRNA (miR) are short (18-22 nucleotide) single stranded sequences of RNA that post-transcriptionally regulate gene expression. MiRNA encoding sequences make up only around 2% of the human genome, but are estimated to regulate >60% of protein-coding genes [129]. Single or small numbers of miR can be master regulators of entire biological pathways and thus their abnormal expression can lead to disease. MiR regulate gene expression through binding to complementary messenger RNA (mRNA) sequences in the cytosol in association with Argonaute proteins, forming a RNA-induced silencing complex (RISC), leading to inhibition or degradation of the target mRNA [130]. The "seed sequence" of the miR, nucelotides 2-7 from the five prime end,

guides target selection [131]. Half of known miR are found in polycistronic units and are expressed in parallel, often sharing structure and function [132,133]. Due to flexibility in binding complementarity an individual miR can target hundreds of different genes, and a gene might be targeted by many different miR [133], forming a complex network of regulation. Abnormal expression of miR may occur by the same factors regulating expression of any gene, including epigenetic control of pre-miR transcription or SNP's in the miR coding sequence. MiR expression can also be regulated at the post-transcriptional level (as pre-miR or mature miR), by RNA-binding proteins or by circular RNAs that can act as 'sponges' [134–137]. Due to the far-reaching and complex roles of miR, a small change in expression can have a profound effect on tissue homeostasis.

MiR are an important part of the host response to bacteria, both pathogenic and commensal. Inflammation must be tightly regulated; excess can lead to organ damage whereas insufficient inflammation may facilitate the dissemination of infection. Several miR are well characterized as having important roles in the immune response against bacteria (reviewed in [138–140]). MiR-146 and miR-155 are up-regulated in immune cells following infection with a range of bacteria, including *Helicobacter pylori*, *Salmonella enterica*, *Listeria monocytogenes*, *Francisella tularensis* and *Mycobacterium* species. Both miR-155 and miR-146 function in negative feedback loops to prevent excessive inflammation by silencing targets in the TLR4 signalling pathway. MiR-155 also maintains TNF expression and is essential for an appropriate adaptive immune response. The miR response to Ct infection in humans has not previously been investigated, however, others have examined the expression of miR during urogenital infection of mice with Ct or Cm. Distinct patterns of miR expression were elicited by two strains of Cm that varied in virulence in the murine genital tract [141]. MiR-223-3p and miR-18a-5p were induced in mice by both strains at 24 hours post-infection. Interestingly, miR-155 expression was increased in response to avirulent Cm, but not in response to the virulent strain of Cm. The failure to up-regulate miR-155 in the virulent infection model could indicate an absence of the negative feedback loop that is required to prevent excessive inflammation, leading to the increased pathology that was observed. Gupta and colleagues investigated miR expression following Cm infection in the murine genital model at a later time point. At 6 days post bacterial challenge, miR-125b-5p, -135a, -16, -214, -30c, 30-e, -182, 183 and -23b were down-regulated in the lower genital tract and miR-146 and -451 were up-regulated [142]. These changes were not maintained at 12 days post infection. Knockdown of -125b-5p, -30c and -182 led to a failure to control Cm infection and in

CD4-/- mice, levels of miR-125b-5p, -182, -183 and -135 were up-regulated relative to wild type infected mice. MiR-125b maintains the naivety of T cells and is down-regulated upon their differentiation and maturation [143]. MiR-125b also targets TNF and is thought to maintain the inactivity of macrophages in the absence of bacterial TLR stimulation [138]. MiR-125b down-regulation may therefore be required for an appropriate immune response. Igietseme and colleagues have shown that upon urogenital infection of mice with a virulent LGV Ct strain (L2), murine miR-21, -103, -107, let-7i and -92b were down-regulated in the oviducts, though the time-point at which these changes in expression are observed is unclear [144].

Overexpression of miR-146a in psoriatic skin lesions has been linked to a SNP in the miR-146 gene in a large cohort of Chinese patients [145]. Wang and colleagues looked at the association of polymorphisms in miR-146a and the NRLP3 inflammasome in association with susceptibility and severity of urogenital Ct infection in two cohorts of Dutch and Finnish women [146]. A SNP in NLRP3 was found to associate with lower abdominal pain in Ct positive women, however, no link with miR-146a was found.

Transcriptome arrays comparing gene expression at various stages of trachomatous disease have found many thousands of genes are differentially regulated [123,125]. Given that single or small numbers of miR can regulate entire biological pathways, the study of miR in trachoma offers a chance to reduce some of this complexity to identify the key pathways that are dysregulated. As a preliminary step, a data mining approach (MSigDB) was used to identify miR that were enriched for predicted targets within lists of differentially regulated genes from four trachoma transcriptomes. The results are shown in Table 1.1. Of interest are the miR with known roles in the regulation of EMT, which is discussed further below. A number of miR that have been identified as differentially expressed in Ct and Cm infection are enriched for targets in these datasets, particularly in the comparison of active disease with Ct infection against controls, which is closest biologically to these murine models. Many of the miR were predicted to have roles regulating cell proliferation and apoptosis. This could be reflective of *Ct* preventing host cell apoptosis to maintain the intracellular niche or T cell and fibroblast proliferation contributing to inflammation and fibrosis, however, a drawback of using data mining techniques is the relative abundance of cancer-related miR associations and pathways that dominate the literature.

Table 1.1. MiR predicted to regulate differentially expressed transcripts from four array datasets.

miR Functional categories	MsigDb predicted miR based on differentially regulated mRNA transcripts (FC>1.5 Adj.P<0.01) from 4 trachoma transcriptomes			
	Active disease with Ct infection (GSE20436)	Active disease (GSE20430)	Trachomatous Scarring disease with inflammation (GSE24383)	Trachomatous trichiasis with inflammation (GSE23705)
Inflammation / Infection	LET-7 family [144] MIR-125A/B [142] MIR-19A/B		MIR-511	LET-7 family [144] MIR-19A/B MIR-224 MIR-29A/B/C
EMT/fibrosis	MIR-200B/C, MIR-429 MIR-506			MIR-200B/C, MIR-429 MIR-29A/B/C MIR-506 MIR-520D
Cell cycle/ Cancer	LET-7 family [144] MIR-124A MIR-125A/B [142] MIR-15 family MIR-17-5P, MIR-20A/B, MIR-106A/B, MIR-519D MIR-19A/B MIR-218 MIR-23A/B [142] MIR-30A/B/C/D/E-5P [142] MIR-519A/B/C MIR-524 MIR-9	MIR-518A-2 MIR-186 MIR-130A/B, MIR-301	MIR-128A/B MIR-21 [141,144] MIR-26A/B MIR-519A/B/C	LET-7 family [144] MIR-19A/B MIR-22 MIR-224 MIR-25, MIR-32, MIR-92, MIR-363, MIR-367 [144] MIR-516-3P MIR-519A/B/C MIR-520D
Other	MIR-130A/B, MIR-301		MIR-153	MIR-27A/B MIR-516-5P

Phenotype comparisons are as follows: Normal healthy (N) children age 1-9 versus those with active trachoma (TF) and Ct infection (GSE20436); children age 1-9 with TF (with or without Ct infection) versus N (GSE20430); N adults versus adults with trachomatous scarring and clinical inflammation (TSI) (GSE24383); and N adults versus adults with trichiasis and clinical inflammation (TTI) (GSE23705). Enriched miR are grouped into functional categories based well characterized roles in the literature. References show published studies that identify miR in bold as differentially expressed in chlamydial infection.

The study of miR can thus advance our understanding of the key biological pathways involved in health and disease processes and how they are controlled. In addition, due to their relatively small numbers and profound effects, miR can also be used as diagnostic tools, biomarkers and therapeutic targets. Expression levels of just a few

miR in tissue, blood or plasma have been suggested as biomarkers for early larynx carcinoma [147], breast cancer [148], drug-resistant epilepsy [149] and Alzheimer's disease [150]. Furthermore miRNA levels can be manipulated *in vivo* for therapeutic purposes [151]. Silencing of miR-155 in mice, which is upregulated upon LPS stimulation, by systemic administration of an anti-miR (a complementary sequence to bind and inhibit miR-155) led to a downregulation of granulocyte colony stimulating factor in murine splenocyte cells, thus conferring targeted silencing of miR-155 with the potential to reduce acute or chronic inflammatory disease [152]. A systemic anti-miR-122 drug was safe and effective following Phase 2a human clinical trials for the treatment of Hepatitis C virus, due to the requirement of human miR-122 for viral replication [153]. The study of miR expression in human chlamydial disease, which has not yet been reported, will advance our understanding of the key biological pathways under control in various stages of the disease process. It might also enable us to find a small number of miR that could identify individuals at increased risk of future scarring sequelae, and could enable the development of therapeutic interventions in these individuals. Alternatively, an early miRNA correlate of protection from scarring sequelae could be used to assess vaccine efficacy.

1.8 Epithelial-mesenchymal transition and chlamydial disease

EMT is a reversible process by which epithelial cells differentiate into mesenchymal cells. Currently 3 types of EMT are recognised. In type-I EMT, epithelial cells differentiate into mesenchymal cells to migrate around the growing embryo during fetal development. These mesenchymal cells can then transform back into epithelia through the reverse process of mesenchymal-epithelial transition (MET) to establish new distant sites of epithelial tissue. Type-II EMT is associated with inflammation-induced tissue fibrosis and type-III EMT occurs in cancer when epithelial tumors metastasize. It is thought that the 3 types of EMT have similar stimuli, signaling cascades and regulation [154,155]. Endothelial cells also differentiate into mesenchymal cells when subjected to the same stimuli (EndMT) and can contribute to cardiac fibrosis [156].

Type-II EMT (EMT-2) occurs in response to inflammation and can lead to loss of organ function through pathological fibrosis. Inflammatory cytokines, growth factors and MMPs activate a chain of transcription factors that cause a down-regulation of epithelial characteristics in cells and gain of mesenchymal properties. The basement membrane is degraded by MMPs, allowing differentiating cells to migrate into the interstitial tissue [157]. New mesenchymal cells can then acquire a myofibroblast

phenotype [158], secreting collagen 1 and expressing α-smooth muscle actin and therefore contributing to extracellular matrix deposition and 'wound' contraction. EMT-2 is known to contribute to the pathology of many fibrotic diseases, including kidney fibrosis [158], idiopathic pulmonary fibrosis [159], cardiac and liver fibrosis [156,160]. In a murine model of liver fibrosis up to 45% of fibroblasts were found to have originated from hepatocytes [156,160]. Evidence of EMT has been shown in both acute wound healing and in chronic fibrotic (hypertrophic) scars where there is also evidence of unresolved inflammation [161]. EMT-2 ceases when inflammatory stimuli stop; therefore it appears that EMT-2 only becomes pathological in an environment of chronic inflammation. Having said that, EMT cells can be resistant to apoptosis (reviewed in [162]), possibly arising from the need for resilient cells to seed new sites of epithelial tissue in embryonic development. In addition to resisting apoptosis, EMT cells can acquire stem-cell-like properties allowing self-renewal [163–165], a property which is known to play a role in various cancers and which could contribute to the chronic fibrosis that is observed in trachoma. EMT-activating transcription factor ZEB1 represses expression of the stemness-inhibiting miR-200 family, therefore releasing expression of stem cell factors and leading to EMT and self-renewal. The *in silico* analysis presented in Table 1 suggests that the miR-200 family may be associated with trachoma.

Primary hepatocytes infected with Hepatitis C virus *in vitro* have been shown to up-regulate biomarkers of EMT [166]. LPS-treated intrahepatic biliary epithelial cells up-regulate TGFβ1 *in vitro* and stimulate EMT through the TGFβ1/SMAD2/3 pathway [167]. EMT-2 has also been observed during Herpes virus infection *in vitro* and *in vivo* and following *E. coli* infection *in vitro* [168,169]. *Helicobacter pylori* virulence factors VacA and CagA disrupt epithelial cell tight junctions and polarity [170–172] and up-regulation of EMT transcription factors and biomarkers in gastric cell lines requires both the *cag* pathogenicity island and NFkB activation [173,174]. EMT can thus be stimulated indirectly through inflammatory signals or directly by pathogens. Ct infected epithelial cells in *ex vivo* fallopian tube tissue show phenotypic changes characteristic of EMT, such as decreased polarity and cell adhesion [175]. The WNT pathway was up-regulated and β-catenin was recruited to the chlamydial inclusion. Loss of epithelial cell-cell adhesion, N-cadherin/β-catenin complex formation and recruitment of β-catenin to the chlamydial inclusion has also been observed *in vitro* [176]. Nectin-1, an integral molecule of epithelial cell tight junctions and adherens junctions was down-regulated at the post-transcriptional level by 85% in Ct infected HeLa cells, which was

dependent on live infection [177]. Disruptions to key components of the WNT and Notch signaling pathways, inter-cellular junctions and adhesion and cytoskeletal remodeling have been identified by RNA-sequencing as early as one hour post-infection of HeLa cells with serovar E Ct [178]. Transcriptomic profiling of TT and subsequent gene-set enrichment analysis has also shown significant enrichment in members of the WNT pathway [125,179]. These data therefore support a role for WNT signaling in both active infection and later stages of chlamydial disease. Given that WNT signaling stimulates EMT *in vitro* [180] and the Akt/β-catenin pathway mediates EMT activation following HCV and *H. pylori* infection [166,172], it is tempting to speculate that Ct induces EMT-2 in the conjunctival epithelium, either directly or via Ct-induced inflammation.

EMT-2 (hereafter referred to as EMT) might therefore present a mechanism by which trachomatous inflammation leads to fibrosis in the tarsal plate. Knowledge of this mechanism might enable targeted interventions or rational vaccine design.

1.9 Overall summary

A large number of individuals remain at risk of progressing to scarring trachoma and trichiasis. There is therefore a need to understand the immunopathogenesis of the disease in order to develop therapeutic treatments to halt scarring progression or to develop a protective vaccine. It is also hoped that research on the immunopathogenesis of trachoma might be transferable to urogenital chlamydial disease, for which is it more difficult to obtain clear clinical phenotypes to correlate with laboratory findings. Preliminary evidence suggests that EMT might have a role in the inflammation-induced fibrosis of chlamydial disease, and miR could be master regulators of the inflammatory and fibrotic pathways that lead to progressive trachomatous scarring. The chlamydial plasmid has a role in pathogen virulence and the resulting host immunopathology, and as such might effect EMT induction or miR regulation. The Ct plasmid is therefore a tool with which to investigate the role of these factors in chlamydial disease.

1.10 References

1. Sightsavers (2012) Sightsavers Annual Review: 24. doi:MISC12.

2. Alliance WHO, Elimination G, Trachoma B, Oms A (2014) Weekly epidemiological record Relevé épidémiologique hebdomadaire. 96: 421–428.

3. Mariotti SP, Pascolini D, Rose-Nussbaumer J (2009) Trachoma: global magnitude of a preventable cause of blindness. Br J Ophthalmol 93: 563–568. doi:10.1136/bjo.2008.148494.

4. Keenan JD, Ayele B, Gebre T, Zerihun M, Zhou Z, et al. (2011) Childhood mortality in a cohort treated with mass azithromycin for trachoma. Clin Infect Dis 52: 883–888. doi:10.1093/cid/cir069.

5. Giamarellos-Bourboulis EJ (2008) Macrolides beyond the conventional antimicrobials: a class of potent immunomodulators. Int J Antimicrob Agents 31: 12–20. doi:10.1016/j.ijantimicag.2007.08.001.

6. Jimenez V, Gelderblom HC, Mann Flueckiger R, Emerson PM, Haddad D (2015) Mass Drug Administration for Trachoma: How Long Is Not Long Enough? PLoS Negl Trop Dis 9: e0003610. doi:10.1371/journal.pntd.0003610.

7. Coles CL, Mabula K, Seidman JC, Levens J, Mkocha H, et al. (2013) Mass distribution of azithromycin for trachoma control is associated with increased risk of azithromycin-resistant Streptococcus pneumoniae carriage in young children 6 months after treatment. Clin Infect Dis 56: 1519–1526. doi:10.1093/cid/cit137.

8. Rank RG, Yeruva L (2014) Hidden in plain sight: chlamydial gastrointestinal infection and its relevance to persistence in human genital infection. Infect Immun 82: 1362–1371. doi:10.1128/IAI.01244-13.

9. Craig AP, Kong FYS, Yeruva L, Hocking JS, Rank RG, et al. (2015) Is it time to switch to doxycycline from azithromycin for treating genital chlamydial infections in women? Modelling the impact of autoinoculation from the gastrointestinal tract to the genital tract. BMC Infect Dis 15: 200. doi:10.1186/s12879-015-0939-3.

10. Cumberland P, Edwards T, Hailu G, Harding-Esch E, Andreasen A, et al. (2008) The impact of community level treatment and preventative interventions on trachoma prevalence in rural Ethiopia. Int J Epidemiol 37: 549–558. doi:10.1093/ije/dyn045.

11. West SK, Munoz BE, Mkocha H, Gaydos C, Quinn T (2015) Risk of Infection with Chlamydia trachomatis from Migrants to Communities Undergoing Mass Drug Administration for Trachoma Control. Ophthalmic Epidemiol 22: 170–175. doi:10.3109/09286586.2015.1010687.

12. Burton MJ, Rajak SN, Hu VH, Ramadhani A, Habtamu E, et al. (2015)

Pathogenesis of progressive scarring trachoma in Ethiopia and Tanzania and its implications for disease control: two cohort studies. PLoS Negl Trop Dis 9: e0003763. doi:10.1371/journal.pntd.0003763.

13. Hu VH, Harding-Esch EM, Burton MJ, Bailey RL, Kadimpeul J, et al. (2010) Epidemiology and control of trachoma: systematic review. Trop Med Int Health 15: 673–691. doi:10.1111/j.1365-3156.2010.02521.x.

14. Last AR, Burr SE, Weiss HA, Harding-Esch EM, Cassama E, et al. (2014) Risk Factors for Active Trachoma and Ocular Chlamydia trachomatis Infection in Treatment-Naïve Trachoma-Hyperendemic Communities of the Bijagós Archipelago, Guinea Bissau. PLoS Negl Trop Dis 8: e2900. doi:10.1371/journal.pntd.0002900.

15. Hu VH, Massae P, Weiss HA, Cree IA, Courtright P, et al. (2011) In vivo confocal microscopy of trachoma in relation to normal tarsal conjunctiva. Ophthalmology 118: 747–754. doi:10.1016/j.ophtha.2010.08.029.

16. Hu VH, Holland MJ, Cree I a, Pullin J, Weiss H a, et al. (2013) In vivo confocal microscopy and histopathology of the conjunctiva in trachomatous scarring and normal tissue: a systematic comparison. Br J Ophthalmol 97: 1333–1337. doi:10.1136/bjophthalmol-2013-303126.

17. Mabey DCW, Hu VH, Bailey RL, Burton MJ, Holland MJ, et al. (2014) TOWARDS A SAFE AND EFFECTIVE CHLAMYDIAL VACCINE: LESSONS FROM THE EYE. In: Schachter J, Byrne G, Chernesky MA, Clarke IN, Darville T, et al., editors. Chlamydial Infections. Proceedings of the Thirteenth International Symposium on Human Chlamydial Infections. Asilomar Conference Grounds, California. Vol. 32. pp. 489–492. doi:10.1016/j.vaccine.2013.10.016.

18. Sowa S, Sowa J, Collier LH, Blyth WA (1969) Trachoma vaccine field trials in The Gambia. J Hyg (Lond) 67: 699–717.

19. Bailey RL, Burton MJ, Mabey DCW (2014) TRACHOMA VACCINE TRIALS IN THE GAMBIA. In: Schachter J, Byrne G, Chernesky MA, Clarke IN, Darville T, et al., editors. Chlamydial Infections. Proceedings of the Thirteenth International Symposium on Human Chlamydial Infections. Asilomar Conference Grounds, California. pp. 485–488.

20. Goldman L (n.d.) Goldman's Cecil Medicine. 24th ed. Philadelphia: Elsevier Saunders. 2426 p.

21. Argüeso P, Gipson IK (2001) Epithelial mucins of the ocular surface: structure, biosynthesis and function. Exp Eye Res 73: 281–289. doi:10.1006/exer.2001.1045.

22. Kanski JJ (1999) Clinical ophthalmology: a systematic approach. 4th ed. Oxford:

Butterworth-Heinemann.

23. THYGESON P (1957) Etiology and differential diagnosis of non-trachomatous follicular conjunctivitis. Bull World Health Organ 16: 995–1011.

24. Solomon AW, Peeling RW, Foster A, Mabey DCW (2004) Diagnosis and assessment of trachoma. Clin Microbiol Rev 17: 982–1011, table of contents. doi:10.1128/CMR.17.4.982-1011.2004.

25. Lee K, Nelson CM (2012) New insights into the regulation of epithelial-mesenchymal transition and tissue fibrosis. Elsevier Inc. 171-221 p. doi:10.1016/B978-0-12-394305-7.00004-5.

26. Martin P, Parkhurst SM (2004) Parallels between tissue repair and embryo morphogenesis. Development 131: 3021–3034. doi:10.1242/dev.01253.

27. Szpaderska AM, Zuckerman JD, DiPietro LA (2003) Differential injury responses in oral mucosal and cutaneous wounds. J Dent Res 82: 621–626.

28. Ahmed M, Zein G, Khawaja F, Foster CS (2004) Ocular cicatricial pemphigoid: pathogenesis, diagnosis and treatment. Prog Retin Eye Res 23: 579–592. doi:10.1016/j.preteyeres.2004.05.005.

29. Chiou AG-Y, Florakis GJ, Kazim M (1998) Management of Conjunctival Cicatrizing Diseases and Severe Ocular Surface Dysfunction. Surv Ophthalmol 43: 19–46. doi:10.1016/S0039-6257(98)00005-8.

30. Tuft SJ, Kemeny DM, Dart JKG, Buckley RJ (1991) Clinical Features of Atopic Keratoconjunctivitis. Ophthalmology 98: 150–158. doi:10.1016/S0161-6420(91)32322-4.

31. Yeruva L, Spencer N, Bowlin AK, Wang Y, Rank RG (2013) Chlamydial infection of the gastrointestinal tract: a reservoir for persistent infection. Pathog Dis 68: 88–95. doi:10.1111/2049-632X.12052.

32. Gerard HC, Stanich JA, Whittum-Hudson JA, Schumacher HR, Carter JD, et al. (2010) Patients with Chlamydia-associated arthritis have ocular (trachoma), not genital, serovars of C. trachomatis in synovial tissue. Microb Pathog 48: 62–68. doi:10.1016/j.micpath.2009.11.004.

33. Hernandez-Trejo M, Herrera-Gonzalez NE, Escobedo-Guerra MR, Haro-Cruz M de J de, Moreno-Verduzco ER, et al. (2014) Reporting detection of Chlamydia trachomatis DNA in tissues of neonatal death cases. J Pediatr (Rio J) 90: 182–189. doi:10.1016/j.jped.2013.09.002.

34. Zigangirova N a., Rumyantseva YP, Morgunova EY, Kapotina LN, Didenko L V., et al. (2013) Detection of C. trachomatis in the serum of the patients with urogenital chlamydiosis. Biomed Res Int 2013. doi:10.1155/2013/489489.

35. Heinzen R, Scidmore M, Rockey D, Hackstadt T (1996) Differential interaction

with endocytic and exocytic pathways distinguish parasitophorous vacuoles of Coxiella burnetii and Chlamydia trachomatis. Infect Immun 64: 796–809.

36. Hybiske K, Stephens RS (2007) Mechanisms of host cell exit by the intracellular bacterium Chlamydia. Proc Natl Acad Sci U S A 104: 11430–11435. doi:10.1073/pnas.0703218104.

37. Sun HS, Wilde A, Harrison RE (2011) Chlamydia trachomatis Inclusions Induce Asymmetric Cleavage Furrow Formation and Ingression Failure in Host Cells. Mol Cell Biol 31: 5011–5022. doi:10.1128/MCB.05734-11.

38. Sun HS, Sin AT-W, Poirier M, Harrison RE (2015) Chlamydia Trachomatis Inclusion Disrupts Host Cell Cytokinesis to Enhance Its Growth in Multinuclear Cells. J Cell Biochem. doi:10.1002/jcb.25258.

39. Campbell S, Richmond SJ, Yates P (1989) The Development of Chlamydia trachomatis Inclusions within the Host Eukaryotic Cell during Interphase and Mitosis. J Gen Microbiol: 1153–1165.

40. Mölleken K, Becker E, Hegemann JH (2013) The Chlamydia pneumoniae invasin protein Pmp21 recruits the EGF receptor for host cell entry. PLoS Pathog 9: e1003325. doi:10.1371/journal.ppat.1003325.

41. Elwell CA, Ceesay A, Kim JH, Kalman D, Engel JN (2008) RNA interference screen identifies Abl kinase and PDGFR signaling in Chlamydia trachomatis entry. PLoS Pathog 4: e1000021. doi:10.1371/journal.ppat.1000021.

42. Kim JH, Jiang S, Elwell CA, Engel JN (2011) Chlamydia trachomatis Co-opts the FGF2 Signaling Pathway to Enhance Infection. PLoS Pathog 7: e1002285. doi:10.1371/journal.ppat.1002285.

43. Patel AL, Chen X, Wood ST, Stuart ES, Arcaro KF, et al. (2014) Activation of epidermal growth factor receptor is required for Chlamydia trachomatis development. BMC Microbiol 14: 277. doi:10.1186/s12866-014-0277-4.

44. Fawaz FS, van Ooij C, Homola E, Mutka SC, Engel JN (1997) Infection with Chlamydia trachomatis alters the tyrosine phosphorylation and/or localization of several host cell proteins including cortactin. Infect Immun 65: 5301–5308.

45. Birkelund S, Johnsen H, Christiansen G (1994) Chlamydia trachomatis serovar L2 induces protein tyrosine phosphorylation during uptake by HeLa cells. Infect Immun 62: 4900–4908.

46. Kumar Y, Valdivia RH (2008) Actin and intermediate filaments stabilize the Chlamydia trachomatis vacuole by forming dynamic structural scaffolds. Cell Host Microbe 4: 159–169. doi:10.1016/j.chom.2008.05.018.

47. Mathews SA, Volp KM, Timms P (1999) Development of a quantitative gene expression assay for Chlamydia trachomatis identified temporal expression of

sigma factors. FEBS Lett 458: 354–358.

48. Shaw EI, Dooley CA, Fischer ER, Scidmore MA, Fields KA, et al. (2000) Three temporal classes of gene expression during the Chlamydia trachomatis developmental cycle. Mol Microbiol 37: 913–925.

49. Wilson DP, Mathews S, Wan C, Pettitt AN, McElwain DLS (2004) Use of a quantitative gene expression assay based on micro-array techniques and a mathematical model for the investigation of chlamydial generation time. Bull Math Biol 66: 523–537. doi:10.1016/j.bulm.2003.09.001.

50. Beatty WL (2007) Lysosome repair enables host cell survival and bacterial persistence following Chlamydia trachomatis infection. 9: 2141–2152. doi:10.1111/j.1462-5822.2007.00945.x.

51. Carrasco JA, Tan C, Rank RG, Hsia R, Bavoil PM (2011) Altered developmental expression of polymorphic membrane proteins in penicillin-stressed Chlamydia trachomatis. Cell Microbiol 13: 1014–1025. doi:10.1111/j.1462-5822.2011.01598.x.

52. Gérard HC, Krauße-Opatz B, Wang Z, Rudy D, Rao JP, et al. (2001) Expression of Chlamydia trachomatis genes encoding products required for DNA synthesis and cell division during active versus persistent infection. Mol Microbiol 41: 731–741. doi:10.1046/j.1365-2958.2001.02550.x.

53. Abdelrahman YM, Rose L a., Belland RJ (2011) Developmental expression of non-coding RNAs in Chlamydia trachomatis during normal and persistent growth. Nucleic Acids Res 39: 1843–1854. doi:10.1093/nar/gkq1065.

54. Belland RJ, Nelson DE, Virok D, Crane DD, Hogan D, et al. (2003) Transcriptome analysis of chlamydial growth during IFN-gamma-mediated persistence and reactivation. Proc Natl Acad Sci U S A 100: 15971–15976. doi:10.1073/pnas.2535394100.

55. Skilton RJ, Cutcliffen LT, Barlow D, Wang Y, Salim O, et al. (2009) Penicillin induced persistence in Chlamydia trachomatis: high quality time lapse video analysis of the developmental cycle. PLoS One 4: e7723. doi:10.1371/journal.pone.0007723.

56. Wyrick PB (2010) Chlamydia trachomatis persistence in vitro: an overview. J Infect Dis 201 Suppl : S88–S95. doi:10.1086/652394.

57. Lewis ME, Belland RJ, AbdelRahman YM, Beatty WL, Aiyar AA, et al. (2014) Morphologic and molecular evaluation of Chlamydia trachomatis growth in human endocervix reveals distinct growth patterns. Front Cell Infect Microbiol 4: 71. doi:10.3389/fcimb.2014.00071.

58. Miyairi I, Mahdi OS, Ouellette SP, Belland RJ, Byrne GI (2006) Different growth

rates of Chlamydia trachomatis biovars reflect pathotype. J Infect Dis 194: 350–357. doi:10.1086/505432.

59. Wang Y, Kahane S, Cutcliffe LT, Skilton RJ, Lambden PR, et al. (2011) Development of a Transformation System for Chlamydia trachomatis: Restoration of Glycogen Biosynthesis by Acquisition of a Plasmid Shuttle Vector. PLoS Pathog 7: e1002258. doi:10.1371/journal.ppat.1002258.

60. Kari L, Goheen MM, Randall LB, Taylor LD, Carlson JH, et al. (2011) Generation of targeted Chlamydia trachomatis null mutants. Proc Natl Acad Sci 108: 7189–7193. doi:10.1073/pnas.1102229108.

61. Johnson CM, Fisher DJ (2013) Site-specific, insertional inactivation of incA in Chlamydia trachomatis using a group II intron. PLoS One 8: e83989. doi:10.1371/journal.pone.0083989.

62. Nguyen B, Valdivia R (2014) A chemical mutagenesis approach to identify virulence determinants in the obligate intracellular pathogen Chlamydia trachomatis. Methods Mol Biol 1197: 347–358. doi:10.1007/978-1-4939-1261-2_20.

63. Kokes M, Dunn JD, Granek JA, Nguyen BD, Barker JR, et al. (2015) Integrating chemical mutagenesis and whole-genome sequencing as a platform for forward and reverse genetic analysis of Chlamydia. Cell Host Microbe 17: 716–725. doi:10.1016/j.chom.2015.03.014.

64. Mueller KE, Wolf K, Fields KA (2016) Gene Deletion by Fluorescence-Reported Allelic Exchange Mutagenesis in Chlamydia trachomatis. MBio 7. doi:10.1128/mBio.01817-15.

65. Stephens RS, Kalman S, Lammel C, Fan J, Marathe R, et al. (1998) Genome sequence of an obligate intracellular pathogen of humans: Chlamydia trachomatis. Science 282: 754–759.

66. Longbottom D, Russell M, Dunbar SM, Jones GE, Herring AJ (1998) Molecular cloning and characterization of the genes coding for the highly immunogenic cluster of 90-kilodalton envelope proteins from the Chlamydia psittaci subtype that causes abortion in sheep. Infect Immun 66: 1317–1324.

67. Stothard DR, Toth GA, Batteiger BE (2003) Polymorphic membrane protein H has evolved in parallel with the three disease-causing groups of Chlamydia trachomatis. Infect Immun 71: 1200–1208.

68. Gomes JP, Nunes A, Bruno WJ, Borrego MJ, Florindo C, et al. (2006) Polymorphisms in the nine polymorphic membrane proteins of Chlamydia trachomatis across all serovars: evidence for serovar Da recombination and correlation with tissue tropism. J Bacteriol 188: 275–286.

doi:10.1128/JB.188.1.275-286.2006.

69. Rockey DD, Heinzen RA, Hackstadt T (1995) Cloning and characterization of a Chlamydia psittaci gene coding for a protein localized in the inclusion membrane of infected cells. Mol Microbiol 15: 617–626.

70. Hsia RC, Pannekoek Y, Ingerowski E, Bavoil PM (1997) Type III secretion genes identify a putative virulence locus of Chlamydia. Mol Microbiol 25: 351–359.

71. Hefty PS, Stephens RS (2006) Chlamydial Type III Secretion System Is Encoded on Ten Operons Preceded by Sigma 70-Like Promoter Elements. J Bacteriol 189: 198–206. doi:10.1128/JB.01034-06.

72. Caldwell HD, Wood H, Crane D, Bailey R, Jones RB, et al. (2003) Polymorphisms in Chlamydia trachomatis tryptophan synthase genes differentiate between genital and ocular isolates. J Clin Invest 111: 1757–1769. doi:10.1172/JCI17993.

73. Wood H, Fehlner-Gardner C, Berry J, Fischer E, Graham B, et al. (2003) Regulation of tryptophan synthase gene expression in Chlamydia trachomatis. Mol Microbiol 49: 1347–1359.

74. Carlson JH, Wood H, Roshick C, Caldwell HD, McClarty G (2006) In vivo and in vitro studies of Chlamydia trachomatis TrpR:DNA interactions. Mol Microbiol 59: 1678–1691. doi:10.1111/j.1365-2958.2006.05045.x.

75. O'Connell CM, AbdelRahman YM, Green E, Darville HK, Saira K, et al. (2011) Toll-like receptor 2 activation by Chlamydia trachomatis is plasmid dependent, and plasmid-responsive chromosomal loci are coordinately regulated in response to glucose limitation by C. trachomatis but not by C. muridarum. Infect Immun 79: 1044–1056. doi:10.1128/IAI.01118-10.

76. Hackstadt T, Scidmore-Carlson MA, Shaw EI, Fischer ER (1999) The Chlamydia trachomatis IncA protein is required for homotypic vesicle fusion. Cell Microbiol 1: 119–130.

77. Suchland RJ, Rockey DD, Bannantine JP, Stamm WE (2000) Isolates of Chlamydia trachomatis that occupy nonfusogenic inclusions lack IncA, a protein localized to the inclusion membrane. Infect Immun 68: 360–367.

78. Nelson DE, Crane DD, Taylor LD, Dorward DW, Goheen MM, et al. (2005) Inhibition of Chlamydiae by Primary Alcohols Correlates with the Strain-Specific Complement of Plasticity Zone Phospholipase D Genes. Infect Immun 74: 73–80. doi:10.1128/IAI.74.1.73-80.2006.

79. Taylor LD, Nelson DE, Dorward DW, Whitmire WM, Caldwell HD (2010) Biological characterization of Chlamydia trachomatis plasticity zone MACPF domain family protein CT153. Infect Immun 78: 2691–2699.

doi:10.1128/IAI.01455-09.

80. LaVerda D, Albanese LN, Ruther PE, Morrison SG, Morrison RP, et al. (2000) Seroreactivity to Chlamydia trachomatis Hsp10 correlates with severity of human genital tract disease. Infect Immun 68: 303–309.

81. Kol A, Lichtman AH, Finberg RW, Libby P, Kurt-Jones EA (2000) Cutting edge: heat shock protein (HSP) 60 activates the innate immune response: CD14 is an essential receptor for HSP60 activation of mononuclear cells. J Immunol 164: 13–17.

82. Carlson JH, Hughes S, Hogan D, Cieplak G, Sturdevant DE, et al. (2004) Polymorphisms in the Chlamydia trachomatis cytotoxin locus associated with ocular and genital isolates. Infect Immun 72: 7063–7072. doi:10.1128/IAI.72.12.7063-7072.2004.

83. Song L, Carlson JH, Whitmire WM, Kari L, Virtaneva K, et al. (2013) Chlamydia trachomatis Plasmid-Encoded Pgp4 Is a Transcriptional Regulator of Virulence-Associated Genes. Infect Immun 81: 636–644. doi:10.1128/IAI.01305-12.

84. Carlson JH, Whitmire WM, Crane DD, Wicke L, Virtaneva K, et al. (2008) The Chlamydia trachomatis plasmid is a transcriptional regulator of chromosomal genes and a virulence factor. Infect Immun 76: 2273–2283. doi:10.1128/IAI.00102-08.

85. Frazer LC, Darville T, Chandra-Kuntal K, Andrews CW, Zurenski M, et al. (2012) Plasmid-cured Chlamydia caviae activates TLR2-dependent signaling and retains virulence in the guinea pig model of genital tract infection. PLoS One 7: e30747. doi:10.1371/journal.pone.0030747.

86. Derrick T, Roberts C, Last AR, Burr SE, Holland MJ (2015) Trachoma and Ocular Chlamydial Infection in the Era of Genomics. Mediators Inflamm.

87. Read TD, Brunham RC, Shen C, Gill SR, Heidelberg JF, et al. (2000) Genome sequences of Chlamydia trachomatis MoPn and Chlamydia pneumoniae AR39. Nucleic Acids Res 28: 1397–1406.

88. Read TD, Myers GSA, Brunham RC, Nelson WC, Paulsen IT, et al. (2003) Genome sequence of Chlamydophila caviae (Chlamydia psittaci GPIC): examining the role of niche-specific genes in the evolution of the Chlamydiaceae. Nucleic Acids Res 31: 2134–2147.

89. Belland RJ, Scidmore MA, Crane DD, Hogan DM, Whitmire W, et al. (2001) Chlamydia trachomatis cytotoxicity associated with complete and partial cytotoxin genes. Proc Natl Acad Sci U S A 98: 13984–13989. doi:10.1073/pnas.241377698.

90. Tietzel I, El-Haibi C, Carabeo RA (2009) Human guanylate binding proteins

potentiate the anti-chlamydia effects of interferon-gamma. PLoS One 4: e6499. doi:10.1371/journal.pone.0006499.

91. Thomson NR, Holden MTG, Carder C, Lennard N, Lockey SJ, et al. (2008) Chlamydia trachomatis: genome sequence analysis of lymphogranuloma venereum isolates. Genome Res 18: 161–171. doi:10.1101/gr.7020108.

92. Fan B, Van Der Pol B, Nelson D (2008) Do chlamydial cytotoxins mediate IFN-g immune evasion. Proceedings of the European Society for Chlamydia Research 6. pp. 165–171.

93. Kari L, Whitmire WM, Olivares-Zavaleta N, Goheen MM, Taylor LD, et al. (2011) A live-attenuated chlamydial vaccine protects against trachoma in nonhuman primates. J Exp Med 208: 2217–2223. doi:10.1084/jem.20111266.

94. Monnickendam MA, Darougar S, Treharne JD, Tilbury AM (1980) Development of chronic conjunctivitis with scarring and pannus, resembling trachoma, in guinea-pigs. Br J Ophthalmol 64: 284–290.

95. Lyons JM, Ito JI, Peña AS, Morré SA (2005) Differences in growth characteristics and elementary body associated cytotoxicity between Chlamydia trachomatis oculogenital serovars D and H and Chlamydia muridarum. J Clin Pathol 58: 397–401. doi:10.1136/jcp.2004.021543.

96. Ito JIJ, Lyons JM, Airo-Brown LP (1990) Variation in virulence among oculogenital serovars of Chlamydia trachomatis in experimental genital tract infection. Infect Immun 58: 2021–2023.

97. Zschaler J, Schlorke D, Arnhold J (2014) Differences in innate immune response between man and mouse. Crit Rev Immunol 34: 433–454.

98. Russell M, Darville T, Chandra-Kuntal K, Smith B, Andrews CW, et al. (2011) Infectivity acts as in vivo selection for maintenance of the chlamydial cryptic plasmid. Infect Immun 79: 98–107. doi:10.1128/IAI.01105-10.

99. Last AR, Roberts C h, Cassama E, Nabicassa M, Molina-Gonzalez S, et al. (2014) Plasmid copy number and disease severity in naturally occurring ocular Chlamydia trachomatis infection. J Clin Microbiol 52: 324–327. doi:10.1128/JCM.02618-13.

100. Twigg AJ, Sherratt D (1980) Trans-complementable copy-number mutants of plasmid ColE1. Nature 283: 216–218.

101. Thomas NS, Lusher M, Storey CC, Clarke IN (1997) Plasmid diversity in Chlamydia. Microbiology 143 (Pt 6: 1847–1854.

102. An Q, Radcliffe G, Vassallo R, Buxton D, O'Brien WJ, et al. (1992) Infection with a plasmid-free variant Chlamydia related to Chlamydia trachomatis identified by using multiple assays for nucleic acid detection. J Clin Microbiol 30: 2814–2821.

103. Peterson EM, Markoff BA, Schachter J, de la Maza LM (1990) The 7.5-kb plasmid present in Chlamydia trachomatis is not essential for the growth of this microorganism. Plasmid 23: 144–148.

104. Porcella SF, Carlson JH, Sturdevant DE, Sturdevant GL, Kanakabandi K, et al. (2015) Transcriptional Profiling of Human Epithelial Cells Infected with Plasmid-Bearing and Plasmid-Deficient Chlamydia trachomatis. Infect Immun 83: 534–543. doi:10.1128/IAI.02764-14.

105. Fankhauser SC, Starnbach MN (2014) PD-L1 limits the mucosal CD8+ T cell response to Chlamydia trachomatis. J Immunol 192: 1079–1090. doi:10.4049/jimmunol.1301657.

106. Hu VH, Holland MJ, Burton MJ (2013) Trachoma: Protective and Pathogenic Ocular Immune Responses to Chlamydia trachomatis. PLoS Negl Trop Dis 7: e2020. doi:10.1371/journal.pntd.0002020.

107. Rank RG, Dascher C, Bowlin AK, Bavoil PM (1995) Systemic immunization with Hsp60 alters the development of chlamydial ocular disease. Invest Ophthalmol Vis Sci 36: 1344–1351.

108. Wagar EA, Schachter J, Bavoil P, Stephens RS (1990) Differential human serologic response to two 60,000 molecular weight Chlamydia trachomatis antigens. J Infect Dis 162: 922–927.

109. Skwor T, Kandel RP, Basravi S, Khan A, Sharma B, et al. (2010) Characterization of humoral immune responses to chlamydial HSP60, CPAF, and CT795 in inflammatory and severe trachoma. Invest Ophthalmol Vis Sci 51: 5128–5136. doi:10.1167/iovs.09-5113.

110. Budrys NM, Gong S, Rodgers AK, Wang J, Louden C, et al. (2012) Chlamydia trachomatis antigens recognized in women with tubal factor infertility, normal fertility, and acute infection. Obstet Gynecol 119: 1009–1016. doi:10.1097/AOG.0b013e3182519326.

111. Lu C, Holland MJ, Gong S, Peng B, Bailey RL, et al. (2012) Genome-wide identification of Chlamydia trachomatis antigens associated with trachomatous trichiasis. Invest Ophthalmol Vis Sci 53: 2551–2559. doi:10.1167/iovs.11-9212.

112. Holland MJ, Bailey RL, Hayes LJ, Whittle HC, Mabey DC (1993) Conjunctival scarring in trachoma is associated with depressed cell-mediated immune responses to chlamydial antigens. J Infect Dis 168: 1528–1531.

113. Holland MJ, Bailey RL, Conway DJ, Culley F, Miranpuri G, et al. (1996) T helper type-1 (Th1)/Th2 profiles of peripheral blood mononuclear cells (PBMC); responses to antigens of Chlamydia trachomatis in subjects with severe trachomatous scarring. Clin Exp Immunol 105: 429–435.

114. Abu el-Asrar a M, Geboes K, Tabbara KF, al-Kharashi S a, Missotten L, et al. (1998) Immunopathogenesis of conjunctival scarring in trachoma. Eye (Lond) 12 (Pt 3a: 453–460. doi:10.1038/eye.1998.104.

115. Gall A, Horowitz A, Joof H, Natividad A, Tetteh K, et al. (2011) Systemic effector and regulatory immune responses to chlamydial antigens in trachomatous trichiasis. Front Microbiol 2: 10. doi:10.3389/fmicb.2011.00010.

116. Brunham RC, Rey-Ladino J (2005) Immunology of Chlamydia infection: implications for a Chlamydia trachomatis vaccine. Nat Rev Immunol 5: 149–161. doi:10.1038/nri1551.

117. Olivares-Zavaleta N, Whitmire WM, Kari L, Sturdevant GL, Caldwell HD (2014) CD8+ T cells define an unexpected role in live-attenuated vaccine protective immunity against Chlamydia trachomatis infection in macaques. J Immunol 192: 4648–4654. doi:10.4049/jimmunol.1400120.

118. Stephens RS (2003) The cellular paradigm of chlamydial pathogenesis. Trends Microbiol 11: 44–51.

119. Rasmussen SJ, Eckmann L, Quayle AJ, Shen L, Zhang YX, et al. (1997) Secretion of proinflammatory cytokines by epithelial cells in response to Chlamydia infection suggests a central role for epithelial cells in chlamydial pathogenesis. J Clin Invest 99: 77–87. doi:10.1172/JCI119136.

120. Dessus-Babus S, Darville TL, Cuozzo FP, Ferguson K, Wyrick PB (2002) Differences in innate immune responses (in vitro) to HeLa cells infected with nondisseminating serovar E and disseminating serovar L2 of Chlamydia trachomatis. Infect Immun 70: 3234–3248.

121. Zhu Z, Lee CG, Zheng T, Chupp G, Wang J, et al. (2001) Airway inflammation and remodeling in asthma. Lessons from interleukin 11 and interleukin 13 transgenic mice. Am J Respir Crit Care Med 164: S67–S70.

122. Buckner LR, Lewis ME, Greene SJ, Foster TP, Quayle AJ (2013) Chlamydia trachomatis infection results in a modest pro-inflammatory cytokine response and a decrease in T cell chemokine secretion in human polarized endocervical epithelial cells. Cytokine 63: 151–165. doi:10.1016/j.cyto.2013.04.022.

123. Natividad A, Freeman TC, Jeffries D, Burton MJ, Mabey DCW, et al. (2010) Human conjunctival transcriptome analysis reveals the prominence of innate defense in Chlamydia trachomatis infection. Infect Immun 78: 4895–4911. doi:10.1128/IAI.00844-10.

124. Barron AL (1988) Microbiology of Chlamydia . Barron AL, editor CRC Press. pp. 193–208 p.

125. Burton MJ, Rajak SN, Bauer J, Weiss H a, Tolbert SB, et al. (2011) Conjunctival

transcriptome in scarring trachoma. Infect Immun 79: 499–511. doi:10.1128/IAI.00888-10.

126. Burton MJ, Ramadhani A, Weiss HA, Hu V, Massae P, et al. (2011) Active trachoma is associated with increased conjunctival expression of IL17A and profibrotic cytokines. Infect Immun 79: 4977–4983. doi:10.1128/IAI.05718-11.

127. Hu VH, Weiss HA, Ramadhani AM, Tolbert SB, Massae P, et al. (2012) Innate immune responses and modified extracellular matrix regulation characterize bacterial infection and cellular/connective tissue changes in scarring trachoma. Infect Immun 80: 121–130. doi:10.1128/IAI.05965-11.

128. Kapranov P, Cheng J, Dike S, Nix DA, Duttagupta R, et al. (2007) RNA maps reveal new RNA classes and a possible function for pervasive transcription. Science 316: 1484–1488. doi:10.1126/science.1138341.

129. Friedman RC, Farh KK-H, Burge CB, Bartel DP (2009) Most mammalian mRNAs are conserved targets of microRNAs. Genome Res 19: 92–105. doi:10.1101/gr.082701.108.

130. Martinez J, Patkaniowska A, Urlaub H, Lührmann R, Tuschl T (2002) Single-Stranded Antisense siRNAs Guide Target RNA Cleavage in RNAi. Cell 110: 563–574. doi:10.1016/S0092-8674(02)00908-X.

131. Vejnar CE, Zdobnov EM (2012) miRmap: Comprehensive prediction of microRNA target repression strength. Nucleic Acids Res. doi:10.1093/nar/gks901.

132. Bartel DP (2004) MicroRNAs: genomics, biogenesis, mechanism, and function. Cell 116: 281–297.

133. Ambros V (2004) The functions of animal microRNAs. Nature 431: 350–355. doi:10.1038/nature02871.

134. Memczak S, Jens M, Elefsinioti A, Torti F, Krueger J, et al. (2013) Circular RNAs are a large class of animal RNAs with regulatory potency. Nature 495: 333–338. doi:10.1038/nature11928.

135. Hansen TB, Jensen TI, Clausen BH, Bramsen JB, Finsen B, et al. (2013) Natural RNA circles function as efficient microRNA sponges. Nature 495: 384–388. doi:10.1038/nature11993.

136. van Kouwenhove M, Kedde M, Agami R (2011) MicroRNA regulation by RNA-binding proteins and its implications for cancer. Nat Rev Cancer 11: 644–656. doi:10.1038/nrc3107.

137. Viswanathan SR, Daley GQ, Gregory RI (2008) Selective blockade of microRNA processing by Lin28. Science 320: 97–100. doi:10.1126/science.1154040.

138. Staedel C, Darfeuille F (2013) MicroRNAs and bacterial infection. Cell Microbiol

15: 1496–1507. doi:10.1111/cmi.12159.

139. Eulalio A, Schulte L, Vogel J (2012) The mammalian microRNA response to bacterial infections. RNA Biol 9: 742–750. doi:10.4161/rna.20018.

140. Maudet C, Mano M, Eulalio A (2014) MicroRNAs in the interaction between host and bacterial pathogens. FEBS Lett 588: 4140–4147. doi:10.1016/j.febslet.2014.08.002.

141. Yeruva L, Myers GSA, Spencer N, Creasy HH, Adams NE, et al. (2014) Early microRNA expression profile as a prognostic biomarker for the development of pelvic inflammatory disease in a mouse model of chlamydial genital infection. MBio 5: e01241–14. doi:10.1128/mBio.01241-14.

142. Gupta R, Arkatkar T, Yu J-J, Wali S, Haskins WE, et al. (2015) Chlamydia muridarum Infection Associated Host MicroRNAs in the Murine Genital Tract and Contribution to Generation of Host Immune Response. Am J Reprod Immunol 73: 126–140. doi:10.1111/aji.12281.

143. Rossi RL, Rossetti G, Wenandy L, Curti S, Ripamonti A, et al. (2011) Distinct microRNA signatures in human lymphocyte subsets and enforcement of the naive state in CD4+ T cells by the microRNA miR-125b. Nat Immunol 12: 796–803. doi:10.1038/ni.2057.

144. Igietseme JU, Omosun Y, Partin J, Goldstein J, He Q, et al. (2013) Prevention of chlamydia-induced infertility by inhibition of local caspase activity. J Infect Dis 207: 1095–1104. doi:10.1093/infdis/jit009.

145. Zhang W, Yi X, Guo S, Shi Q, Wei C, et al. (2014) A single-nucleotide polymorphism of miR-146a and psoriasis: an association and functional study. J Cell Mol Med 18: 2225–2234. doi:10.1111/jcmm.12359.

146. Wang W, Stassen FR, Surcel H-M, Ohman H, Tiitinen a, et al. (2009) Analyses of polymorphisms in the inflammasome-associated NLRP3 and miRNA-146A genes in the susceptibility to and tubal pathology of Chlamydia trachomatis infection. Drugs Today (Barc) 45 Suppl B: 95–103.

147. Wang Y, Chen M, Tao Z, Hua Q, Chen S, et al. (2013) Identification of predictive biomarkers for early diagnosis of larynx carcinoma based on microRNA expression data. Cancer Genet 206: 340–346. doi:10.1016/j.cancergen.2013.09.005.

148. Mar-Aguilar F, Mendoza-Ramírez JA, Malagón-Santiago I, Espino-Silva PK, Santuario-Facio SK, et al. (2013) Serum circulating microRNA profiling for identification of potential breast cancer biomarkers. Dis Markers 34: 163–169. doi:10.3233/DMA-120957.

149. Wang J, Tan LL, Tan LL, Tian Y, Ma J, et al. (2015) Circulating microRNAs are

promising novel biomarkers for drug-resistant epilepsy. Sci Rep 5: 10201. doi:10.1038/srep10201.

150. Dong H, Li J, Huang L, Chen X, Li D, et al. (2015) Serum MicroRNA Profiles Serve as Novel Biomarkers for the Diagnosis of Alzheimer ' s Disease. Dis Markers 2015.

151. van Rooij E, Purcell AL, Levin AA (2012) Developing microRNA therapeutics. Circ Res 110: 496–507. doi:10.1161/CIRCRESAHA.111.247916.

152. Worm J, Stenvang J, Petri A, Frederiksen KS, Obad S, et al. (2009) Silencing of microRNA-155 in mice during acute inflammatory response leads to derepression of c/ebp Beta and down-regulation of G-CSF. Nucleic Acids Res 37: 5784–5792. doi:10.1093/nar/gkp577.

153. Janssen HL, Reesink HW, Lawitz EJ, Zeuzem S, Rodriguez-Torres M, et al. (2013) Treatment of HCV infection by targeting microRNA. N Engl J Med 368: 1685–1694. doi:10.1056/NEJMoa1209026.

154. Kalluri R, Weinberg RA (2009) Review series The basics of epithelial-mesenchymal transition. 119. doi:10.1172/JCI39104.1420.

155. Zeisberg M, Neilson EG (2009) Biomarkers for epithelial-mesenchymal transitions. J Clin Invest 119: 1429–1437. doi:10.1172/JCI36183.

156. Zeisberg EM, Tarnavski O, Zeisberg M, Dorfman AL, McMullen JR, et al. (2007) Endothelial-to-mesenchymal transition contributes to cardiac fibrosis. Nat Med 13: 952–961. doi:10.1038/nm1613.

157. Okada H, Strutz F, Danoff TM, Kalluri R, Neilson EG (1996) Possible mechanisms of renal fibrosis. Contrib Nephrol 118: 147–154.

158. Iwano M, Plieth D, Danoff TM, Xue C, Okada H, et al. (2002) Evidence that fibroblasts derive from epithelium during tissue fibrosis. J Clin Invest 110: 341–350. doi:10.1172/JCI15518.

159. Chilosi M, Poletti V, Zamò A, Lestani M, Montagna L, et al. (2003) Aberrant Wnt/beta-catenin pathway activation in idiopathic pulmonary fibrosis. Am J Pathol 162: 1495–1502.

160. Zeisberg M, Yang C, Martino M, Duncan MB, Rieder F, et al. (2007) Fibroblasts derive from hepatocytes in liver fibrosis via epithelial to mesenchymal transition. J Biol Chem 282: 23337–23347. doi:10.1074/jbc.M700194200.

161. Yan C, Grimm WA, Garner WL, Qin L, Travis T, et al. (2010) Epithelial to mesenchymal transition in human skin wound healing is induced by tumor necrosis factor-alpha through bone morphogenic protein-2. Am J Pathol 176: 2247–2258. doi:10.2353/ajpath.2010.090048.

162. Thiery JP, Acloque H, Huang RYJ, Nieto MA (2009) Epithelial-mesenchymal

transitions in development and disease. Cell 139: 871–890. doi:10.1016/j.cell.2009.11.007.

163. Morel A-P, Lièvre M, Thomas C, Hinkal G, Ansieau S, et al. (2008) Generation of breast cancer stem cells through epithelial-mesenchymal transition. PLoS One 3: e2888. doi:10.1371/journal.pone.0002888.

164. Wellner U, Schubert J, Burk UC, Schmalhofer O, Zhu F, et al. (2009) The EMT-activator ZEB1 promotes tumorigenicity by repressing stemness-inhibiting microRNAs. Nat Cell Biol 11: 1487–1495. doi:10.1038/ncb1998.

165. Mani SA, Guo W, Liao M-J, Eaton EN, Ayyanan A, et al. (2008) The epithelial-mesenchymal transition generates cells with properties of stem cells. Cell 133: 704–715. doi:10.1016/j.cell.2008.03.027.

166. Bose SK, Meyer K, Di Bisceglie AM, Ray RB, Ray R (2012) Hepatitis C virus induces epithelial-mesenchymal transition in primary human hepatocytes. J Virol 86: 13621–13628. doi:10.1128/JVI.02016-12.

167. Zhao L, Yang R, Cheng L, Wang M, Jiang Y, et al. (2011) LPS-induced epithelial-mesenchymal transition of intrahepatic biliary epithelial cells. J Surg Res 171: 819–825. doi:10.1016/j.jss.2010.04.059.

168. Pozharskaya V, Torres-González E, Rojas M, Gal A, Amin M, et al. (2009) Twist: a regulator of epithelial-mesenchymal transition in lung fibrosis. PLoS One 4: e7559. doi:10.1371/journal.pone.0007559.

169. Cane G, Ginouvès A, Marchetti S, Buscà R, Pouysségur J, et al. (2010) HIF-1alpha mediates the induction of IL-8 and VEGF expression on infection with Afa/Dr diffusely adhering E. coli and promotes EMT-like behaviour. Cell Microbiol 12: 640–653. doi:10.1111/j.1462-5822.2009.01422.x.

170. Papini E, Satin B, Norais N, de Bernard M, Telford JL, et al. (1998) Selective increase of the permeability of polarized epithelial cell monolayers by Helicobacter pylori vacuolating toxin. J Clin Invest 102: 813–820. doi:10.1172/JCI2764.

171. Amieva MR, Vogelmann R, Covacci A, Tompkins LS, Nelson WJ, et al. (2003) Disruption of the epithelial apical-junctional complex by Helicobacter pylori CagA. Science 300: 1430–1434. doi:10.1126/science.1081919.

172. Murata-Kamiya N, Kurashima Y, Teishikata Y, Yamahashi Y, Saito Y, et al. (2007) Helicobacter pylori CagA interacts with E-cadherin and deregulates the beta-catenin signal that promotes intestinal transdifferentiation in gastric epithelial cells. Oncogene 26: 4617–4626. doi:10.1038/sj.onc.1210251.

173. Yin Y, Grabowska AM, Clarke PA, Whelband E, Robinson K, et al. (2010) Helicobacter pylori potentiates epithelial:mesenchymal transition in gastric

cancer: links to soluble HB-EGF, gastrin and matrix metalloproteinase-7. Gut 59: 1037–1045. doi:10.1136/gut.2009.199794.

174. Baud J, Varon C, Chabas S, Chambonnier L, Darfeuille F, et al. (2013) Helicobacter pylori initiates a mesenchymal transition through ZEB1 in gastric epithelial cells. PLoS One 8: e60315. doi:10.1371/journal.pone.0060315.

175. Kessler M, Zielecki J, Thieck O, Mollenkopf H-J, Fotopoulou C, et al. (2011) Chlamydia Trachomatis Disturbs Epithelial Tissue Homeostasis in Fallopian Tubes via Paracrine Wnt Signaling. Am J Pathol 180: 198–186. doi:10.1016/j.ajpath.2011.09.015.

176. Prozialeck WC, Fay MJ, Lamar PC, Pearson CA, Sigar I, et al. (2002) Chlamydia trachomatis disrupts N-cadherin-dependent cell-cell junctions and sequesters beta-catenin in human cervical epithelial cells. Infect Immun 70: 2605–2613.

177. Sun J, Kintner J, Schoborg R V (2008) The host adherens junction molecule nectin-1 is downregulated in Chlamydia trachomatis-infected genital epithelial cells. Microbiology 154: 1290–1299. doi:10.1099/mic.0.2007/015164-0.

178. Humphrys MS, Creasy T, Sun Y, Shetty AC, Chibucos MC, et al. (2013) Simultaneous transcriptional profiling of bacteria and their host cells. PLoS One 8: e80597. doi:10.1371/journal.pone.0080597.

179. Holland MJ, Jeffries D, Pattison M, Korr G, Gall A, et al. (2010) Pathway-focused arrays reveal increased matrix metalloproteinase-7 (matrilysin) transcription in trachomatous trichiasis. Invest Ophthalmol Vis Sci 51: 3893–3902. doi:10.1167/iovs.09-5054.

180. Chen H-C, Zhu Y-T, Chen S-Y, Tseng SCG (2012) Wnt signaling induces epithelial-mesenchymal transition with proliferation in ARPE-19 cells upon loss of contact inhibition. Lab Invest 92: 676–687. doi:10.1038/labinvest.2011.201.

Chapter 2: Aims and hypotheses

2.1 Purpose

Repeated chlamydial infection of the conjunctiva throughout childhood appears to prime or imprint the conjunctiva, causing some individuals in endemic communities to become chronically inflamed and develop fibrosis that persists throughout their lives, even in the absence of detectable Ct infection. This fibrosis leads to trichiasis, pain and blindness. The mechanisms that drive chronic immunopathology and the reasons why only a proportion of Ct-exposed individuals go on to develop scarring trachoma are not currently understood.

Inflammatory episodes are a major risk factor for scarring progression. Inflammation can induce EMT, whereby epithelial cells differentiate into pro-fibrotic mesenchymal cells and contribute to tissue fibrosis in the underlying stroma. MiR are small single-stranded RNA species that regulate gene expression post-transcriptionally and single or small numbers of miR can hold tight control over inflammatory and pro-fibrotic pathways. Ocular infections with plasmid-free Ct strains result in reduced inflammatory pathology in animal models and thus might lead to attenuated EMT induction and differential miR responses. The roles of EMT and miR in human ocular chlamydial disease, their contribution to trachomatous scarring and the effect of the Ct plasmid on EMT and miR responses have not yet been investigated.

The purpose of this thesis was to investigate a) whether differential expression of miR is associated with the pathological changes in the conjunctiva that occur in response to and continue in the absence of Ct, b) whether EMT occurs in response to inflammation in the conjunctiva and contributes to the fibrotic pathology of trachoma and c) what effect the presence of the Ct plasmid has on EMT induction and miR expression.

2.2 Hypotheses

1. Single or small numbers of miR that control inflammatory and fibrotic pathways are differentially expressed in the conjunctiva during active and scarring trachoma.
2. Infection of epithelial cell lines with plasmid-free and plasmid-competent Ct strains induces differential expression of miR.
3. Ct infection and inflammation induce EMT in conjunctival epithelial cells and this process contributes to trachomatous scarring *in vivo*.
4. A plasmid-free ocular strain of Ct is attenuated in the induction of pathological miR, inflammation and EMT responses.

2.3 Aims

1. To examine the expression of miR in the conjunctiva of individuals with scarring trachoma in the presence of clinical inflammation and from individuals with active trachoma (trachomatous inflammation – follicular and/or trachomatous inflammation – intense) in the presence of Ct infection relative to normal healthy controls.
2. To examine the expression of miR in plasmid-free and plasmid-competent Ct infected relative to uninfected epithelial cell lines.
3. To examine the induction of inflammation and EMT in epithelial cells *in vitro* in response to infection with plasmid-free and plasmid-competent Ct strains.
4. To investigate the presence and localisation of pro-inflammatory mediators, growth factors and EMT biomarkers in tissue from individuals with trichiasis at the protein level.

2.4 Specific Objectives

1. To identify miR associated with scarring trachoma in the presence and absence of clinically significant inflammation using qPCR.
2. To establish infection models in clinically relevant epithelial cell lines *in vitro* with ocular plasmid-free and plasmid-competent Ct strains.
3. To examine miR expression in epithelial cells in response to plasmid-free and plasmid-competent Ct strains using small RNA sequencing by synthesis (SBS) technology and quantitative real-time PCR (qPCR).
4. To identify miRNA associated with active trachoma in the presence and absence of current Ct infection using SBS and qPCR.
5. To determine whether miRNA can be used as classifiers of disease in active and scarring trachoma.
6. To examine induction of inflammation and EMT in epithelial cells in response to plasmid-free and plasmid-competent Ct strains using qPCR, microscopy and a scratch wound model.
7. To investigate the expression of pro-inflammatory mediators, growth factors and biomarkers of EMT in tissue from individuals with trichiasis using immunohistochemistry (IHC).

Chapter 3: Research article:

Conjunctival MicroRNA Expression in Inflammatory Trachomatous Scarring

RESEARCH PAPER COVER SHEET

PLEASE NOTE THAT A COVER SHEET MUST BE COMPLETED FOR EACH RESEARCH PAPER INCLUDED IN A THESIS.

SECTION A – Student Details

Student	Tamsyn Derrick
Principle Supervisor	Martin Holland
Thesis Title	The Role of Epigenetics and Type 2 Epithelial-Mesenchymal Transitions in Trachoma

If the Research Paper has previously been published please complete Section B, if not please move to Section C

SECTION B – Paper already published

Where was the work published?	PLoS Neglected Tropical Diseases		
When was the work published?	14.03.2013		
If the work was published prior to registration for your research degree, give a brief rationale for its inclusion	NA		
Have you retained the copyright for the work?*	Article is open access under a Creative Commons Attribution 4.0 International liicense	Was the work subject to academic peer review?	Yes

*If yes, please attach evidence of retention. If no, or if the work is being included in its published format, please attach evidence of permission from the copyright holder (publisher or other author) to include this work.

SECTION C – Prepared for publication, but not yet published

Where is the work intended to be published?	
Please list the paper's authors in the intended authorship order:	
Stage of publication	

SECTION D – Multi-authored work

For multi-authored work, give full details of your role in the research included in the paper and in the preparation of the paper. (Attach a further sheet if necessary)	I performed the majority of the laboratory work (all except miRNA extraction from 63 samples), I analysed the data, interpreted the findings and wrote the manuscript.

Student signature: _Tamsyn Derrick_   **Date:** 26.9.2015
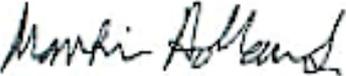
Supervisor signature: _Martin Holland_   **Date:** 28.9.2015

Conjunctival MicroRNA Expression in Inflammatory Trachomatous Scarring

Tamsyn Derrick[1]*, **Chrissy h. Roberts**[1], **Megha Rajasekhar**[1], **Sarah E. Burr**[1,2], **Hassan Joof**[2], **Pateh Makalo**[2], **Robin L. Bailey**[1], **David C. W. Mabey**[1], **Matthew J. Burton**[3], **Martin J. Holland**[1]

1 Department of Clinical Research, Faculty of Infectious Tropical Diseases, London School of Hygiene and Tropical Medicine, London, United Kingdom, 2 Medical Research Council Unit, The Gambia, Fajara, Banjul, The Gambia, West Africa, 3 International Centre for Eye Health, Department of Clinical Research, Faculty of Infectious Tropical Diseases, London School of Hygiene and Tropical Medicine, London, United Kingdom

Abstract

Purpose: Trachoma is a fibrotic disease of the conjunctiva initiated by *Chlamydia trachomatis* infection. This blinding disease affects over 40 million people worldwide yet the mechanisms underlying its pathogenesis remain poorly understood. We have investigated host microRNA (miR) expression in health (N) and disease (conjunctival scarring with (TSI) and without (TS) inflammation) to determine if these epigenetic differences are associated with pathology.

Methods: We collected two independent samples of human conjunctival swab specimens from individuals living in The Gambia (n = 63 & 194). miR was extracted, and we investigated the expression of 754 miR in the first sample of 63 specimens (23 N, 17 TS, 23 TSI) using Taqman qPCR array human miRNA genecards. Network and pathway analysis was performed on this dataset. Seven miR that were significantly differentially expressed between different phenotypic groups were then selected for validation by qPCR in the second sample of 194 specimens (93 N, 74 TS, 22 TSI).

Results: Array screening revealed differential expression of 82 miR between N, TS and TSI phenotypes (fold change >3, p<0.05). Predicted mRNA targets of these miR were enriched in pathways involved in fibrosis and epithelial cell differentiation. Two miR were confirmed as being differentially expressed upon validation by qPCR. miR-147b is significantly up-regulated in TSI versus N (fold change = 2.3, p = 0.03) and miR-1285 is up-regulated in TSI versus TS (fold change = 4.6, p = 0.005), which was consistent with the results of the qPCR array.

Conclusions: miR-147b and miR-1285 are up-regulated in inflammatory trachomatous scarring. Further investigation of the function of these miR will aid our understanding of the pathogenesis of trachoma.

Introduction

Chlamydia trachomatis (*Ct*) is the causative agent of trachoma, the leading cause of blindness that results from infection. Forty million people have active trachoma and eight million people suffer with unoperated trichiasis [1]. Repeated infection of the conjunctiva by this intracellular bacterium during childhood causes a chronic inflammatory response, leading to progressive fibrosis and scarring in adult life. Scarring distorts the conjunctiva and the eyelashes are pulled inward to the extent that they scratch the cornea (trichiasis), causing pain and eventually blindness.

Chronic trachomatous inflammation is known to continue in the absence of current *Ct* infection and is believed to drive the continued scarring process, however the mechanisms by which this occurs are not completely understood [2]. Messenger RNA (mRNA) expression profiling of each clinical stage of trachoma has revealed many thousands of mRNAs that are differentially expressed [2,3]. Key pathways that are differentially regulated in

the conjunctiva are innate inflammatory pathways and extracellular matrix modifiers. MicroRNAs (miR) are known to have significant roles in the regulation of inflammation, fibrosis and cell differentiation [4–7] and can be dysregulated upon bacterial infection [8,9].

miR are post-transcriptional regulators of gene expression. They are single-stranded RNA molecules typically 18–22 nucleotides in length. miR bind to complementary mRNA sequences in association with the RNA-induced silencing complex (RISC), causing transcriptional degradation of the transcript or repression of its translation [10]. The seed sequence (5′ nucleotides 2–7) of the miR guides target selection [11]. Complementary target sequence sites are usually, though not exclusively, found in the 3′ untranslated region (UTR) of mRNA transcripts. For a given miR complementary sequence sites may be present on a few or several hundred different mRNA targets, indicating the potential for a few miRs to regulate complete biological processes. Indeed, a relatively small total number of miR are thought to regulate over a third of

58

Author Summary

Trachoma is a debilitating disease that affects 40 million people worldwide. It can cause progressive fibrosis of the upper eyelid and blindness, yet the mechanism is poorly understood. We have investigated the expression of short sequences of genetic material (microRNA) that regulate gene expression. We screened for the expression of 754 microRNA sequences (miR) in genetic material isolated from conjunctival swab samples from individuals in trachoma-endemic communities in The Gambia. This sample included healthy controls, individuals with trachomatous scarring and individuals with trachomatous scarring in the presence of clinically significant inflammation. We found 82 miR that were differentially expressed. Computer simulations predict that these miR regulate genes in epithelial cell differentiation, inflammation and fibrosis pathways, all of which are involved in the scarring process. We then validated the expression of seven of these differentially expressed miR in a second larger biological sample set from The Gambia. We confirmed that miR-147b and miR-1285 have increased expression in individuals with trachomatous scarring in the presence of clinically significant inflammation. Further investigation into the functions of these miR will aid our understanding of this disease and present opportunities to develop treatments for ocular fibrotic diseases.

all protein-coding genes [12]. miR have profound roles in the regulation of many biological processes and interest in their various functions in health and disease is growing. The number of known mature miR (http://www.mirbase.org/) is increasing rapidly as research in this area quickly unravels miR biology.

The ability of miR to regulate entire pathways offers investigators an opportunity to reduce the complexity of the trachoma transcriptome [2]. We suggest that the differential regulation of just a few miR in trachomatous disease may underlie the substantial differences in mRNA expression that characterize each phenotypic trachoma group. This reduction in complexity will enable more targeted research into the mechanisms of disease and may identify new potential therapeutic approaches.

Methods

Ethical permission, study participants and clinical assessment

The study was conducted in accordance with the tenets of the Declaration of Helsinki. The Ethics Committee of the Gambian Government/Medical Research Council Unit, and the ethics committee of the London School of Hygiene and Tropical Medicine approved the study. Samples were drawn from an archive built up under the MRC study numbers SCC729, SCC1177 and SCC1274 with specific approval for miR gene expression studies under SCC L2011.03. The samples described in this paper were collected from individuals recruited in trachoma-endemic communities across the whole geographic range of The Gambia, West Africa. Written informed consent was taken from individuals at the time of sample collection. For those participants aged <16 years that wished to take part in the study consent was obtained from a parent/guardian. All samples were anonymized. Cases of trachomatous scarring (TS) were identified from screening records, community ophthalmic nurse referral and opportunistic rapid screening. Control individuals with normal conjunctivae were selected by matching for age, sex, ethnicity and location. Clinical phenotypes were assessed in the field by experienced field supervisors trained and regularly assessed in trachoma grading. FPC scores [13] were assigned and grades were agreed by two experienced trachoma physicians using high-resolution photographic records taken in the field using a Nikon D3000 SLR camera with a VR AF-S micro Nikkor 105 mm 1:2.8G ED lens. Photographs were taken at the time of sample collection. Individuals were grouped into the following clinical phenotypes for analysis: individuals with trachomatous scarring (TS) had a C score between 1–3 (mild to severe scarring) and a P score of 0 or 1 (none or mild inflammation), individuals with trachomatous scarring in the presence of clinically significant inflammation (TSI) had a C score of 1–3 and a P score of 2 or 3 (moderate to severe inflammation), and control samples from individuals with normal healthy conjunctivae (N) had no conjunctival scarring (C0), papillary inflammation (P0) or follicles (F0).

Sample collection and processing

Swabs were taken from the upper tarsal conjunctiva using Dacron polyester-tipped swabs (Hardwood Products Company) and stored in 250 µl RNA*later* (Ambion, Life Technologies) on ice blocks in the field and then archived at −20°C until processed.

Taqman microfluidic array miR genecards

A total of 63 specimens from the archive were selected for miR expression array profiling. Specimens were selected as representative examples of each phenotype group using the FPC scores. As control samples for these experiments, individuals with normal conjunctivae matched on age, sex, ethnicity and location were selected. MiR was extracted from swabs using the Qiagen Allprep DNA/RNA/protein kits with a modification to collect small non-coding RNAs. DNase1 digestion (Qiagen) was included. Total RNA purity was assessed by spectrophotometry using a nanodrop ND-1000 (Thermo Fisher Scientific). Reverse transcription and pre-amplification were performed using Megaplex human primer pools Av2.1 and Bv3.0 following the manufacturer's instructions (Taqman, Life Technologies). Quantitative PCR was performed using 72 µl of pre-amplified cDNA as template in the PCR master mix for the TaqMan Array Human MicroRNA genecards (Av2.0 and Bv3.0). Thermal cycling was performed on a 7900HT thermal cycler (Life Technologies). Plates were held at 50°C for 2 minutes, 94.5°C for 10 minutes, then underwent 40 cycles of 97°C for 30 seconds and one minute at 59.7°C. A total of 754 of the most well characterised unique human miR from Sanger miRBase V.14 (www.**mirbase**.org/) were screened. Sanger miRBase V.14 was the latest version of the miR database at the time of screening.

Array analysis

qPCR cycle threshold (C_T) values were processed in SDS RQ manager (Life technologies); the threshold was set to 0.05 and baselines were detected automatically. Data from each array were uploaded and analysed using the High Throughput qPCR Package (HTqPCR) in Bioconductor R (www.bioconductor.org, www.r-project.org) [14]. Sample profiles were excluded from the analysis when the median C_T value for the array was 40 since the majority of the C_T values were either close to threshold or undetermined. Individual miR were retained in the analysis only when expressed (C_T value<40) by at least five specimens. A and B genecard data were analysed separately due to differences in specimen performance on each card. Data were normalized to reduce technical bias in the analysis by a number of different standard methods (supplementary figure S1A & B). The coefficient of variation, standard deviation and correlation of raw against normalized data were used to evaluate the suitability of each

method of normalisation, as described in Deo *et al.* (2011) [15]. The 'Norm rank invariant' method was chosen as the most effective normalisation strategy for both A and B cards (supplementary figure S1A & B). The distribution of the raw and Norm rank invariant normalized C_T values are shown in supplementary figure S2 A–D. Differential expression was then assessed by empirical Bayes/moderated t-tests using HTqPCR in Bioconductor R. These data are deposited within the NCBI GEO public database (GSE37717) and, in line with MIQE guidelines [16], details are included as supplementary table S1.

MiR abundance

Relative abundance of miR in the conjunctiva was calculated from array C_T data. An average was taken of the normalized C_T values for all specimens (including all phenotypes) for each miR on A and B cards. The general equation for estimating relative differences in PCR was then applied to these values: $2^{-(CT\_target - CT\_calibrator)}$ where the calibrator was the most abundant miR (miR-1274B). For each miR this value was then divided by the sum of all these values to create a relative abundance.

Network analysis

A network graph based on the specimen-to-specimen Pearson correlation was generated Biolayout express 3D v2.2 (www.biolayout.org/) [17]. The overall miR expression correlation matrix and graph were constructed from the rank invariant normalized raw C_T data. The graph was arranged according to patient clinical classification (N, TS, TSI). Pearson correlation coefficients (r)>0.7 were retained and used as cut-offs in network construction. Nodes in the graph are individual miR linked by an edge if r>0.7. The graph was then clustered using a Markov Clustering algorithm using default inflation values. The partitioned clusters of expression contain sets of miR that exhibit a very strong degree of co-expression across the sample. Cluster content is independent of differential expression level. The co-expression clusters were then investigated *in silico* at the individual and pathway levels.

Pathway analysis

miR that were differentially expressed in the arrays at a significance level of p<0.05 and with a fold change (FC) over three (up or down-regulated) were entered into pathway analysis.

Table 1. Sample demographic details before and after quality control exclusion for full array analysis.

All samples before filtering	N (n=23)	TS (n=17)	TSI (n=23)
Male [Female]	7 [16]	4 [13]	7 [16]
Mean age (min-max)	44.58 (3–78)	42.59 (8–75)	50.31 (3–85)
Samples included following A genecard quality control exclusion	n=16	n=15	n=9
Male [Female]	5 [11]	4 [11]	2 [7]
Mean age (min-max)	48 (8–78)	43.8 (8–75)	44.9 (4–80)
Papillary hypertrophy			
0	16	14	0
1	0	1	0
2	0	0	3
3	0	0	6
Conjunctival scarring			
0	16	0	0
1	0	0	0
2	0	13	9
3	0	2	0
Samples included following B genecard quality control exclusion	n=10	n=12	n=7
Male [Female]	3 [7]	4 [8]	1 [6]
Mean age (min-max)	43 (8–70)	44.5 (8–75)	41.9 (4–80)
Papillary hypertrophy			
0	10	11	0
1	0	1	0
2	0	0	2
3	0	0	5
Conjunctival scarring			
0	10	0	0
1	0	0	0
2	0	11	7
3	0	1	0

FPC grading scores (0–3) are shown for each phenotypic group.
Footnote: Age ranges between phenotypic groups are not significantly different within and between A and B genecard groups (Wilcoxon test p>0.05). Fewer B genecards were passed filtering as these cards were designed to cover less abundant miR.
doi:10.1371/journal.pntd.0002117.t001

60
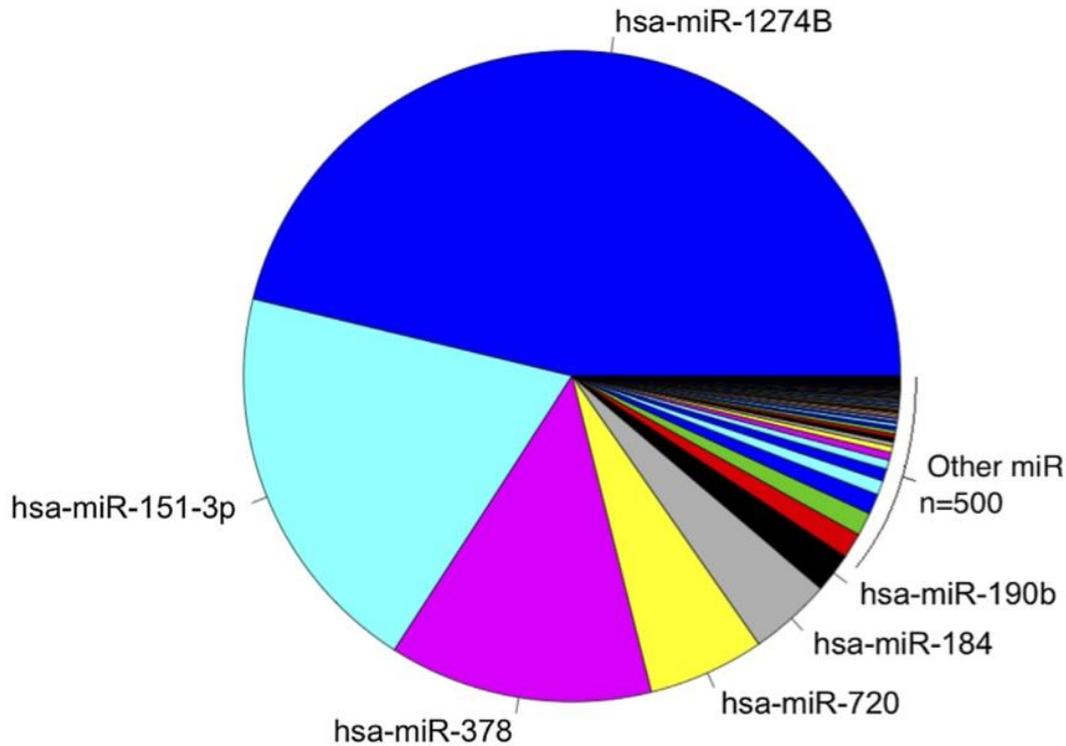
Figure 1. Relative abundance of miR in the conjunctiva. Abundance of all miR tested expressed relative to miR-1274B. Abundance was calculated from cycle threshold values irrespective of sample phenotype.
doi:10.1371/journal.pntd.0002117.g001

DIANA-microT v4.0 (Beta version) target prediction was used in the DIANA mirPath software [18]. Multiple miRNA analysis was used for the significant miR within each comparison group.

Extraction of miR for quantitative real-time PCR

Total RNA including miR was extracted from swabs using a Qiagen miRNeasy kit, incorporating a DNase1 digestion step.

Total RNA purity was assessed by spectrophotometry using a nanodrop ND-1000 (Thermo Fisher Scientific). miR was reverse transcribed using miScript II RT kit with the hiFlex buffer as per the manufacturer's instructions (Qiagen). qPCR was carried out using miScript Primer Assays and the miScript SYBR Green PCR kit (Qiagen) on a 7900HT thermal cycler (Life Technologies). Ten microlitres of RT product was diluted in 100 μl H$_2$0 and 0.5 μl

Figure 2. Network co-expression analysis. Clusters of co-expressed miR are shown, calculated from normalized array data irrespective of phenotype. Clusters are highlighted according to the pathway most enriched upon pathway analysis of miR in each cluster.
doi:10.1371/journal.pntd.0002117.g002

61

Table 2. Number of differentially expressed miR in array results.

	N v TS	N v TSI	TS v TSI	Total
FC>3 p<0.05*	7	35	40	82
Up	3	22	21	46
Down	4	13	19	36
FC>3 p<0.01*	5	12	19	36
Up	2	10	13	25
Down	3	2	6	11

*p-values were not adjusted or controlled by false discovery rate. We calculated 1518 independent tests of significance on the entire array data set and estimate that this would result in a false positivity rate of 50% when accepting unadjusted p>0.05.

doi:10.1371/journal.pntd.0002117.t002

was used as template in each qPCR assay, with 0.5 µl specific miR forward primer assay, 1 µl water, 0.5 µl universal reverse primer and 2.5 µl SYBR green master mix, in a total reaction volume of 5 µl. Each assay was performed in quadruplicate, including no template controls for each miR and for each specimen. Cycling conditions were as follows: 15 minutes at 95°C, followed by 70 cycles of 15 seconds at 94°C, 30 seconds at 55°C, and 30 seconds at 70°C. Data were collected at 94°C and 70°C. qPCR was run for 70 cycles to minimize the number of undetermined values. Fifteen percent of all miR assays had a C_T value over 40.

qPCR analysis

C_T values were derived in SDS RQ manager (ABI, Life technologies), with a threshold of 0.05 and an automatic baseline.

Four replicate tests were used to calculate the geometric mean after outliers were removed. Analysis was done in R. Specimens were removed from the analysis if the endogenous control snoU6 (U6) C_T values were $\geq 2\times$ the standard deviation (s.d.) of the mean of all U6 C_Ts in the sample. For analysis purposes, any assay that did not amplify by 70 cycles was assigned a C_T value of 80 (19 assays out of a total 1552). Target C_T values for each specimen were normalized to U6 using $\Delta C_T = C_{T\ target} - C_{T\ U6}$. For each miR within each phenotype group, the Shapiro-Wilk method was used to test for normality of distribution in the raw-data. For each comparison (N v TS, N v TSI, TS v TSI) we calculated the fold change in miR expression between the phenotypic groups, using $2^{-\Delta CT(median\ phenotype\ 1)} - \Delta CT(median\ phenotype\ 2)$. We used the Wilcoxon rank sum test (with continuity correction) to test for differences in the expression of each miR between phenotypic groups as the majority of the data were not normally distributed. Details of the qPCR and analysis in line with MIQE are included in supplementary table S1.

Results

Array samples

Sixty-three specimens were tested by miRNA array cards. Twenty-three specimens were excluded from A genecard profiles and 34 specimens from B genecard profiles. Basic demographic and clinical phenotype data are shown in table 1 both before and after filtering and these show that there was no systematic loss of any specific sample type based on clinical phenotype, age or sex as a result of the filtering process.

Basic characteristics of miR expression in the conjunctiva: Abundance and co-expression analysis

Following the filtering procedures described, 506/754 miRs were included in the final analysis. Relative abundance of all of
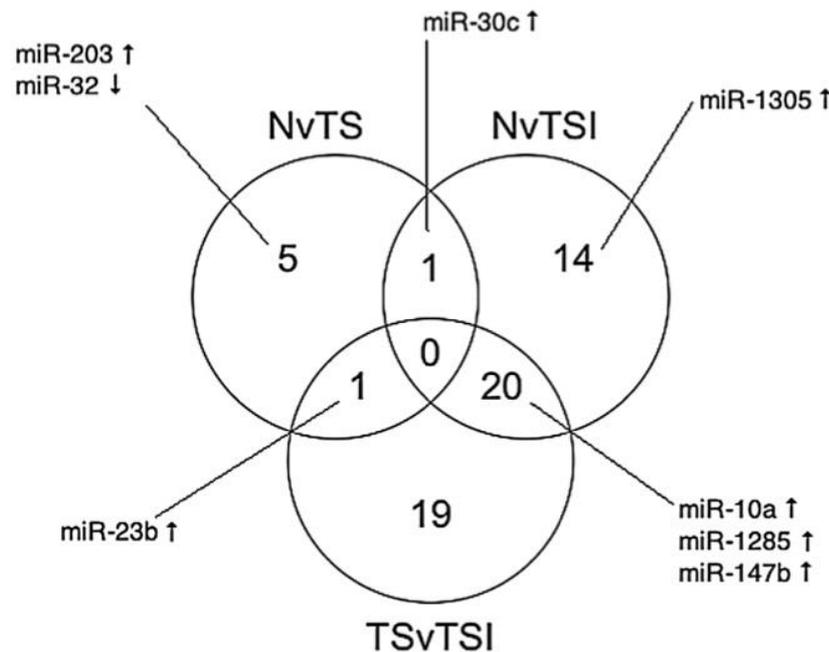
Figure 3. Venn diagram of differentially expressed miR. Venn diagram showing the number of differentially expressed (FC>3, p<0.05) miR that are unique or that overlap between the different clinical phenotypes. Selected miR of interest are shown with arrows illustrating whether they are up- or down-regulated in the indicated comparison group. An upward facing arrow indicates up-regulation and a downward facing arrow indicates down-regulation. * miR-23b is up-regulated in N v TS but down-regulated in the TS v TSI comparison group.
doi:10.1371/journal.pntd.0002117.g003

62
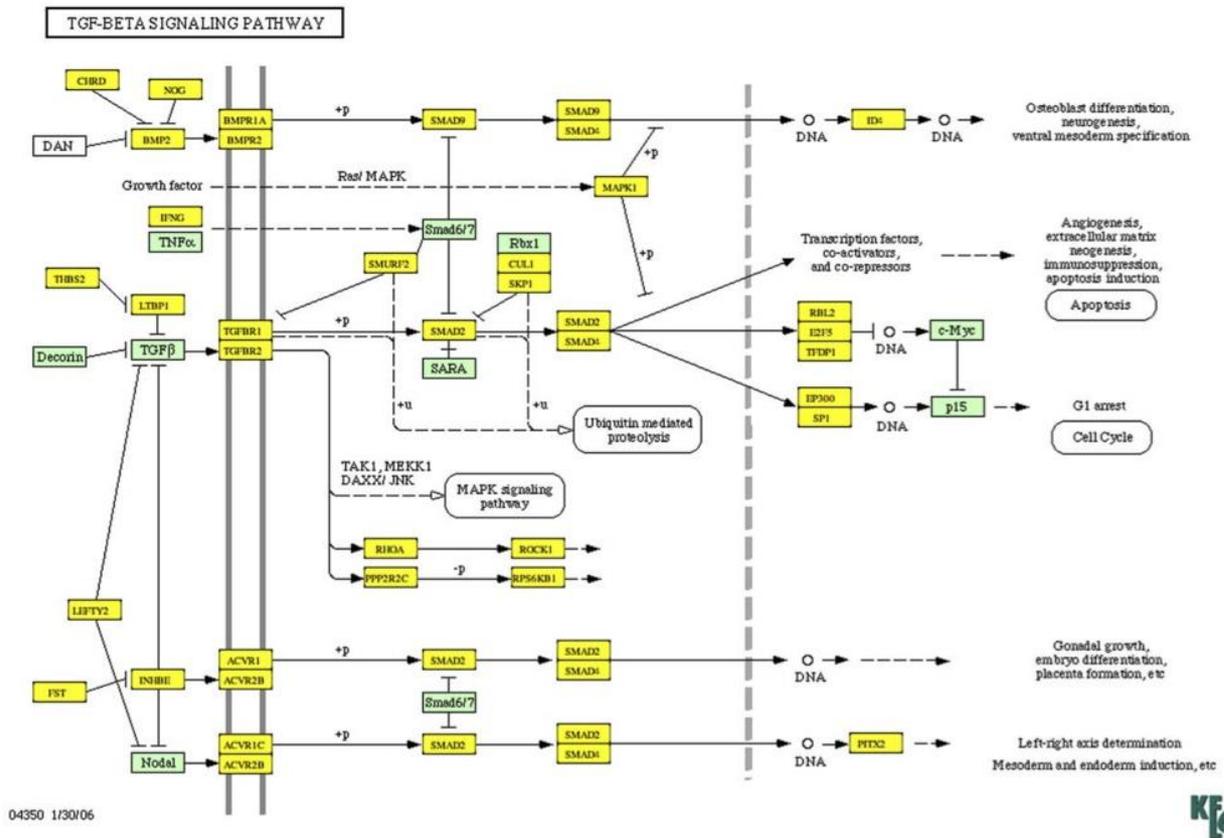
Figure 4. TGF-β signaling pathway. Genes highlighted in yellow are predicted targets of miR differentially regulated in N v TSI (35 miR) (FC>3 p<0.05). Genes highlighted in green are not predicted targets.
doi:10.1371/journal.pntd.0002117.g004

506 expressed miR in the conjunctiva was calculated from the C_T data. Of the miR that were tested, just six constitute 90% of total miR present in the conjunctival samples (figure 1). miR-1274B has the highest overall expression and miR-623 the lowest. Networks of co-expression, independent of differential expression, based on rank invariant C_T values were explored in the entire data set of 506 miR using Biolayout express 3D. The undirected graph contained 126 miR connected by 215 edges. Markov clustering partitioned the network into 11 clusters of co-expressed miR. These clusters ranged in size from 23 to 4 co-expressed miR and accounted for 80 miR in the original network. Each of the 11 clusters is laid out in figure 2 and the specific miR content of each cluster is available in supplementary table S2. The major biology revealed by these co-expression clusters indicates that these miR target mRNA in four major pathways. These are repeatedly identified and are shown in figure 2. The MAPK signaling pathway and focal adhesion pathway contain the largest number of miR target genes and have the highest levels of enrichment (over-representation).

Differential expression analysis

A total of 82 miR are differentially expressed across the comparison groups (FC>3, p<0.05) (supplementary table S3). The number of up- and down-regulated miR in each comparison is shown in table 2. A miR that is up-regulated in the N v TS comparison has a lower C_T value in TS relative to N. The same applies to N v TSI and TS v TSI, where the latter is up- or down-regulated relative to the former in each comparison. A larger number of miR are differentially expressed in comparisons with the TSI phenotype. Fewer miR are down-regulated than up-regulated, particularly in the N v TSI group.

Twenty miR are differentially expressed in both N v TSI and TS v TSI comparisons (figure 3) indicating they might be features of inflammation. In contrast, very few miR are shared with the N v TS miR gene set and there are none that overlap between all three groups. This indicates that TSI and TS phenotypes are distinct and have characteristic miR signatures.

Of the 103 miR found in the networks by Markov clustering, 15 had some evidence of differential regulation based on p-value alone. miR-492 and miR-548d were both up-regulated (4.9 and 3.2 times respectively) in TSI individuals compared to controls whilst 3 miR (miR-508, miR-509 and miR-664) were >3 fold down-regulated. The miR precursor let-7b showed modest evidence of differential up-regulation in TS individuals versus normal controls (p = 0.037).

Pathway analysis

Differentially expressed miR in each comparison group (FC>3 p<0.05) were entered into DIANA mirPath pathway analysis. The top ten most enriched pathways for each comparison are listed in table 3, where a greater −ln(p-value) reflects increasing enrichment of miR targets within a pathway. Many of the same pathways are enriched in each comparison group, despite little overlap in miR between the N v TS, N v TSI and TS v TSI groups (figure 3). Axon guidance, focal adhesion, and the TGF-β signaling pathway are all present in all three

63

Table 3. DIANA mirPath pathway analysis on differentially expressed miR in each comparison group (p<0.05 and FC>3).

Pathway	# Target genes in pathway	−ln(p-value)
N v TS (n = 7)		
Axon guidance	52	25.39
Focal adhesion	70	24.14
Epidermal growth factor receptor (ErbB) signaling pathway	40	23.02
Renal cell carcinoma	31	17.13
Glioma	29	16.39
Tight junction	48	15.51
Non-small cell lung carcinoma	25	14.35
Regulation of actin cytoskeleton	65	14.3
Small cell lung cancer	34	14.15
TGF-β signaling pathway	35	13.93
N v TSI (n = 35)		
Focal adhesion	94	19.86
Axon guidance	66	18.49
Regulation of actin cytoskeleton	97	17.43
MAPK signaling pathway	113	17.23
TGF-β signaling pathway	51	16.93
ErbB signaling pathway	50	16.77
Ribosome	2	16.58
Ubiquitin mediated proteolysis	66	15.68
Wnt signaling pathway	71	14.58
Oxidative phosphorylation	11	13.61
TS v TSI (n = 40)		
Axon guidance	77	24.39
Adherens junctions	52	24.34
MAPK signaling pathway	127	18.99
Ribosome	3	18.95
Wnt signaling pathway	82	18.49
TGF-β signaling pathway	56	17.39
Focal adhesion	100	16.77
Oxidative phosphorylation	13	15.88
Ubiquitin mediated proteolysis	72	15.25
Renal cell carcinoma	43	13.2

doi:10.1371/journal.pntd.0002117.t003

groups. A large number of genes in the TGF-β pathway are predicted targets of differentially expressed miR in the N v TSI comparison (figure 4). Within the TGF-β pathway, 53% of transcripts are differentially regulated based on differences found in a mRNA transcriptome array using Ethiopian conjunctival samples (GSE23705) from similar phenotypic groups [2]. Analysis was also carried out on each phenotypic comparison group split into up- and down-regulated gene sets (supplementary table S5). Interestingly, TGF-β is enriched in the down-regulated gene set for each comparison group. Given that this pathway is enriched for miR targets that would be silenced and these miR are down-regulated, this would suggest an up-regulation or release of the TGF-β signaling pathway. Analysis was also performed on the 20 miR differentially expressed in both N v TSI and TS v TSI comparisons, with enrichment again in MAPK, TGF-β and *Wnt* pathways (supplementary table S6), supporting the hypothesis that these miR are characteristic of the

major pathways under miR control in the conjunctiva and are perturbed by inflammation.

Validation of differential expression of selected miR using an alternative RT-qPCR system

In the validation set it was not feasible to assay the expression of all the potentially differentially expressed miR and we selected for follow-up a small number of miR that exhibited a high FC, low p-value and homogeneity in the raw data. Seven miR were selected for follow-up (supplementary table S7) including three miR that were differentially regulated in the N v TS comparison (miR-30c, miR-32, miR-203) and four from the N v TSI comparison (miR-10a, miR-147b, miR-1285, miR-1305). Each candidate miR was tested for differential expression in a second sample of 194 independent archival Gambian clinical specimens, selected as representative examples of each phenotype group. In these experiments, small nucleolar (sno) U6 RNA was used as the

64

Table 4. qPCR sample demographic summary including FPC grading scores (0–3) for each phenotypic group.

Specimen number in each group	C (n = 93)	TS (n = 74)	TSI (n = 22)
Male [Female]	23 [70]	19 [55]	8 [14]
Mean age (min-max)	51.4 (16–87)	51.7 (16–80)	47.7 (2–80)
Papillary hypertrophy score	Number of samples		
0	91	36	0
1	2	38	0
2	0	0	19
3	0	0	3
Conjunctival scarring score	Number of samples		
0	93	0	0
1	0	9	1
2	0	61	15
3	0	4	6

Footnote: Age ranges between phenotypic groups were not significantly different (Wilcoxon test p>0.05). One individual in the TS group also had a follicular grade (F) of 1, and three individuals in TSI had F3.
doi:10.1371/journal.pntd.0002117.t004

Discussion

Array analysis revealed that a large number of miR are potentially differentially regulated between different disease states and healthy controls. Trachomatous scarring with inflammation (TSI) has a distinct miR signature compared to scarring trachoma (TS). TS may be a less active disease process than TSI as fewer miR were differentially regulated. On validation, two miR remained significantly differentially regulated. MiR-147b was up-regulated in individuals with TSI compared to N and miR-1285 was up-regulated in people with TSI compared to those with TS alone. In a transcriptome analysis of similar phenotypic comparison groups in Ethiopians with scarring trachoma [2], 25% of predicted targets of miR-1285 and 52% of predicted targets of miR-147b predicted targets (TargetScan v6.2) were differentially regulated (adjusted p<0.05).

MiR-1285 directly targets the 3′UTR of p53 mRNA in HEK 293T cells [19]. The loss of p53 is associated with many cancers via disruption of the normal function of p53 in the initiation of apoptosis and growth arrest. In contrast, Hidaka and colleagues [20] find miR-1285 to be a tumor suppressor. Expression levels of miR-1285 were reduced in clinical samples of renal cell carcinoma (RCC) compared to healthy mucosa and miR-1285 transfection in RCC cell lines *in vitro* led to inhibition of cell proliferation, migration and invasion [20]. The authors verified transglutaminase 2 (TGM2) as a target of miR-1285. Interestingly, TGM2 is linked to several cancers and the process of epithelial-mesenchymal transition (EMT) [21]. EMT can be initiated by chronic inflammation [22] and is implicated in the pathology of many fibrotic diseases [23], so could have a role in trachomatous disease. The conflicting conclusions of these studies are likely due to the different cell types used. *In vitro* studies in primary conjunctival epithelia will be required to understand the function of miR-1285 in chlamydial infection and trachoma.

There is limited literature on the clinical significance of changes in miR-147b expression, but it is known to be down-regulated in rectal cancer [24]. This is consistent with the ability of miR-147b to induce apoptosis four days post-transfection in A549 cells [25]. *Mmu*-miR-147, a functional homologue of human miR-147b, is induced by multiple toll-like-receptor (TLR) signals and negatively regulates inflammation in murine macrophages [26]. It acts in a negative feedback loop to prevent excessive inflammation. Bertero and colleagues [25] showed that LPS (bacterial lipopolysaccharide) and TNFα strongly induced hsa-miR-147b expression in A549 cells *in vitro*; supporting the hypothesis that miR-147b has a

calibrator snoU6 C_T values were not different between the phenotypic groups, which implied that it was a stably expressed reference gene (supplementary information figure S3). Five specimens were excluded because they had outlying snoU6 values (average C_T>2 s.d. of the sample mean), leaving a total of 189 specimens to be tested for statistical differences in expression levels. Summary statistics for these 189 specimens are shown in table 4.

Data were tested for differential expression between the three phenotypic groups as is presented for the analysis of the array data (N, TS and TSI). Only miR-1285 and miR-147b showed a significant difference between the different phenotypic groups in this validation set (table 5). MiR-147b was up-regulated 2.3 fold in individuals with TSI relative to N (p = 0.0332). This is consistent with the array results in which miR-147b was up-regulated 9.6 fold in individuals with TSI versus N. MiR-1285 was up-regulated 4.6 fold in TSI relative to TS (p = 0.005). This is also consistent with the array results in which miR-1285 was up-regulated 16 fold in TSI versus TS.

Table 5. Results of qPCR differential expression analysis.

miR	Median deltaCT (IQR)			N v TS		N v TSI		TS v TSI	
	N	TS	TSI	Fold difference	p-value*	Fold difference	p-value*	Fold difference	p-value*
miR-10a	16.3 (14.7–18.9)	16.1 (13.7–20.4)	17.4 (14.5–20)	1.149	0.554	0.467	0.353	0.406	0.248
miR-30c	5.3 (3.5–6.7)	5 (2.8–7.2)	5.9 (3.8–7.6)	1.231	0.813	0.660	0.761	0.537	0.362
miR-32	14 (11–18.1)	14.6 (11.9–18)	15.2 (13.3–17.1)	0.660	0.403	0.435	0.332	0.660	0.845
miR-147b	6.4 (5–9.6)	6.8 (4.8–10.7)	5.2 (3.1–7.8)	0.758	0.783	2.297	0.033	3.031	0.078
miR-203	4.6 (2.2–5.1)	3.7 (1.9–5.8)	3.8 (1.2–6.3)	1.866	0.097	1.741	0.234	0.933	0.706
miR-1285	7 (5.1–8.7)	8 (5.4–9.7)	5.8 (3.8–8)	0.5	0.214	2.297	0.059	4.595	0.006
miR-1305	12.7 (11–14)	12.6 (9.3–14.6)	12.5 (10.6–13.7)	1.072	0.535	1.149	0.562	1.072	0.709

*Unadjusted p-values are presented. With no inflation of p-values the chance of finding one or more significant differences in 21 tests = 65.9%. Bonferroni's adjustment indicates critical p-value = 0.002 and assuming outcomes are moderately correlated (r = 0.5) then a critical p-value = 0.01 would be required.
doi:10.1371/journal.pntd.0002117.t005

65

homologous role in the regulation of inflammation in humans. The up-regulation of miR-147b seen in the TSI phenotypic group may reflect ongoing and uncontrolled inflammation. Understanding the role of miR-147b in TSI should also be aided by further *in vitro* functional studies.

MiR-23b-5p is up-regulated in TS relative to both N (FC = 3.6 p = 0.026) and TSI (FC = 5.8 p = 0.008) (figure 3), indicating that it might be a feature of scarring in the absence of inflammation. MiR-23b is a member of the miR-23b cluster, which includes miR-27b and miR-24-1. This cluster is known to target members of the TGF-β signaling pathway [27]. An up-regulation of miR-23b, as is seen in scarred individuals, would lead to a decrease in TGF-β signaling. Although this may seem counterintuitive, any dysregulation of the TGF-β signaling pathway could lead to aberrant wound healing [28]. MiR-23b is also anti-inflammatory through inhibition of NFkB activation [29], preventing up-regulation of inflammatory cytokines such as IL-17. In turn, IL-17 inhibits miR-23b, leading to inflammation. An up-regulation of IL-17A is associated with active trachomatous disease [30]. The relative down-regulation of miR-23b in TSI compared to TS and N conjunctival samples could reflect a down-regulation of this miR's expression by IL-17 in individuals with TSI.

MiR-30c was up-regulated 15 fold in N v TS (p = 0.01) and 11 fold in N v TSI (p = 0.04) in the microarray experiments. This miR is thought to regulate fibrinolysis and collagen production through targeting serine protease inhibitor SERPINE1 and connective tissue growth factor (CTGF) respectively [31]. Over expression of this miR is known to inhibit the proliferative and migratory properties of endometrial cancer cells [32], however qPCR validation found no association of this miR with disease.

Pathway analysis revealed that many of the same pathways are enriched amongst predicted targets of differentially expressed miR in each comparison group. This is surprising due to the minimal overlap of differentially expressed miR in N v TS compared with the other groups. Many of these pathways are characteristic of epithelial cell and fibroblast communication, differentiation and fibrosis. In particular, the *Wnt* pathway has been implicated in the disruption of epithelial cell homeostasis and the pathology of *C. trachomatis* infection [33]. Importantly, epithelial cell differentiation, development and cytoskeleton remodeling pathways (including TGF-β and *Wnt*) are enriched in gene sets from a differential expression analysis of transcriptome data of similar phenotypic groups in Ethiopians [2]. Of all the members of the KEGG defined TGF-β pathway, 53% are differentially regulated in this Ethiopian transcriptome [2]. We theorise that the miR that are differentially expressed in this study are at least partly responsible for the observed changes in the normal function of the *Wnt* and TGF-β pathways in trachoma patients.

Investigation of miR abundance in the conjunctiva shows that most miR have very low levels of expression, with just a few making up the vast majority of the population. MiR-1274B is the most highly abundant miR in the conjunctiva, but the nature of this miR has been called in to question. A previous study [34] found evidence that miR-1274B may not be a canonical miR, rather that it is a tRNA-derived small RNA (tsRNA). tsRNAs are thought to be abundant in the genome [26] and may have a role similar to miR in regulating gene functions [35]. It may be the case that the high abundance of miR-1274B can be explained simply by its origin in tRNA and the generally high abundance of tRNA in cells. Regardless of this uncertainty over its designation as either a miR or a tsRNA, a role for miR-1274B in the regulation of gene expression cannot be excluded at this time.

The discrepancy between the array results and qPCR validation could be due to a high number of false positives accepted in the initial analysis or as a result of a number of technical differences leading to differential miR isolation, extraction, amplification bias and normalisation [36]. Different methods of miRNA isolation and qPCR were employed in this study in the screening and validation stages which could introduce technical variation [37]. In addition, a non-proscriptive filtering process was used in the identification of potentially differentially expressed miR. Acceptance of a high number of potential false positive associations at this initial filtering stage was considered acceptable based on the arguments presented by Rothman [38] on principles of p-value adjustment and enabled us to explore the wider biology of miR conjunctival expression (supplementary table S4). As a result, many of the miR chosen for follow up in the validation clinical samples appear not to be differentially regulated. This highlights the need to verify array-profiling results even when the method of choice is the apparently robust gold standard technique to examine differential expression [39–41]. Furthermore the design of the B genecards, which cover less abundant miR, adds difficulty to analysis pipeline. Even with pre-amplification the amount of genetic material that can be obtained from a conjunctival swab is very small. Specimens were judged to perform less well on B genecards leading to the exclusion of a larger number of specimens, resulting in a reduction of the number of biological replicates in each phenotypic group and therefore some loss of statistical power. The raw and analysed data is publicly available in the NCBI GEO.

This is the first description and initial identification of specific miR expression in an ocular fibrotic disease of humans. It is possible that these miR play a role in other ocular surface inflammatory diseases. We highlight the major pathways under the control of miR that are expressed in the conjunctival epithelium and suggest that it is plausible that dysregulation of expression in these miR leads to the release of the TGF-β signaling pathway in trachomatous disease. Two miR with significantly increased expression in trachomatous scarring and inflammation were identified (miR-147b and miR-1285). In order to understand the mechanisms by which these miR may contribute to health and disease of the conjunctiva the associations of miR-147b and miR-1285 with trachomatous disease now requires further study. A combination of *in vitro* experimentation in model systems and *in vivo* application in animal models will also facilitate our understanding of this association and whether these miR are reflective or causative effectors of disease. Research in this area of RNA biology is a rapidly evolving field that is only now beginning to realize its potential. We hope that its application to trachomatous disease may lead to the development of therapeutics or biomarkers for the diagnosis and treatment of trachoma and other fibrotic ocular pathologies.

Supporting Information

Figure S1 Supplementary figure S1A & B. Coefficient of variation (CV) for uncorrected and normalized array data for A and B card genesets. Various methods of normalization were tested (Left to right: uncorrected data, geometric mean, quantile, delta-C_T using RQ manager, delta-C_T using geNorm, norm rank invariance, scale rank invariance).
(TIFF)

Figure S2 Supplementary figure S2A–D. Boxplots of C_T distribution for each sample in A and B geneset groups after quality control filtering before normalization (A, B), and after normalization (C, D).
(TIFF)

Figure S3 Boxplots of endogenous control snoRNA U6 raw C_T distribution in each phenotype group. These distributions are not significantly different (Kruskal-Wallis p = 0.5469).
(TIFF)

Table S1 MIQE guidelines for array and qPCR processing.
(XLS)

Table S2 MiR in the 11 clusters derived from Markov chain clustering algorithm of array data. Footnote: The most enriched pathway among predicted targets of miR in each cluster is shown with values and FC for each miR from the array analysis.
(XLSX)

Table S3 Differentially regulated miR (FC>3 p<0.05) in each phenotypic comparison group in the array analysis.
(XLSX)

Table S4 Number and percentage of false positives in trachoma miR array study. Footnote: With no inflation of p-values the chance of finding one or more significant differences in 1518 tests = 100%. Bonferroni's adjustment indicates critical p-value = 3.38×10^{-5} and assuming outcomes are moderately correlated (r = 0.5) then a critical p-value = 0.001 would be required.
(XLSX)

Table S5 Pathway analysis of up- and down-regulated miR in the array analysis (FC>3 p<0.05).
(XLSX)

Table S6 Pathway analysis on 20 miR differentially expressed (FC>3 p<0.05) in both N v TSI and TS v TSI comparisons.
(XLSX)

Table S7 MiScript primer assays used in qPCR validation: accession number and mature miR sequence.
(XLSX)

Acknowledgments

Author Contributions

Obtained funding: DCWM RLB MJH MJB. Conceived and designed the experiments: MJH DCWM. Performed the experiments: TD MJH MR ChR. Analyzed the data: TD ChR MJH RLB MJB. Contributed reagents/materials/analysis tools: SEB PM HJ TD MJH. Wrote the paper: TD MJH.

References

1. Mariotti SP, Pascolini D, Rose-Nussbaumer J (2009) Trachoma: global magnitude of a preventable cause of blindness. Br J Ophthalmol 93: 563–568. doi:10.1136/bjo.2008.148494.

2. Burton MJ, Rajak SN, Bauer J, Weiss HA, Tolbert SB, et al. (2011) Conjunctival transcriptome in scarring trachoma. Infect Immun 79: 499–511. doi:10.1128/IAI.00888-10.

3. Natividad A, Freeman TC, Jeffries D, Burton MJ, Mabey DCW, et al. (2010) Human conjunctival transcriptome analysis reveals the prominence of innate defense in Chlamydia trachomatis infection. Infect Immun 78: 4895–4911. doi:10.1128/IAI.00844-10.

4. Oertli M, Engler DB, Kohler E, Koch M, Meyer TF, et al. (2011) MicroRNA-155 Is Essential for the T Cell-Mediated Control of Helicobacter pylori Infection and for the Induction of Chronic Gastritis and Colitis. J Immunol 187: 3578–3586. doi:10.4049/jimmunol.1101772.

5. Gregory PA, Bert AG, Paterson EL, Barry SC, Tsykin A, et al. (2008) The miR-200 family and miR-205 regulate epithelial to mesenchymal transition by targeting ZEB1 and SIP1. Nat Cell Biol 10: 593–601. doi:10.1038/ncb1722.

6. Cushing L, Kuang PP, Qian J, Shao F, Wu J, et al. (2011) miR-29 is a major regulator of genes associated with pulmonary fibrosis. Am J Respir Cell Mol Biol 45: 287–294. doi:10.1165/rcmb.2010-0323OC.

7. Lu TX, Hartner J, Lim E-J, Fabry V, Mingler MK, et al. (2011) MicroRNA-21 limits in vivo immune response-mediated activation of the IL-12/IFN-gamma pathway, Th1 polarization, and the severity of delayed-type hypersensitivity. J Immunol 187: 3362–3373. doi:10.4049/jimmunol.1101235.

8. Zhu Y, Jiang Q, Lou X, Ji X, Wen Z, et al. (2012) MicroRNAs up-regulated by CagA of Helicobacter pylori induce intestinal metaplasia of gastric epithelial cells. PLoS One 7: e35147. doi:10.1371/journal.pone.0035147.

9. Izar B, Mannala GK, Mraheil MA, Chakraborty T, Hain T (2012) microRNA Response to Listeria monocytogenes Infection in Epithelial Cells. International Journal of Molecular Sciences 13: 1173–1185. doi:10.3390/ijms13011173.

10. Martinez J, Patkaniowska A, Urlaub H, Lührmann R, Tuschl T (2002) Single-Stranded Antisense siRNAs Guide Target RNA Cleavage in RNAi. Cell 110: 563–574. doi:10.1016/S0092-8674(02)00908-X.

11. Vejnar CE, Zdobnov EM (2012) miRmap: Comprehensive prediction of microRNA target repression strength. Nucleic Acids Res 40: 11673–83. doi:10.1093/nar/gks901.

12. Lewis BP, Burge CB, Bartel DP (2005) Conserved seed pairing, often flanked by adenosines, indicates that thousands of human genes are microRNA targets. Cell 120: 15–20. doi:10.1016/j.cell.2004.12.035.

13. Dawson CR, Jones BR TM (1981) Guide to Trachoma Control. Geneva: World Health Organization.

14. Dvinge H, Bertone P (2009) HTqPCR: high-throughput analysis and visualization of quantitative real-time PCR data in R. Bioinformatics 25: 3325–3326. doi:10.1093/bioinformatics/btp578.

15. Deo A, Carlsson J, Lindlöf A (2011) How to choose a normalization strategy for miRNA quantitative real-time (qPCR) arrays. J Bioinform Comput Biol 9: 795–812.

16. Bustin SA, Beaulieu J-F, Huggett J, Jaggi R, Kibenge FSB, et al. (2010) MIQE précis: Practical implementation of minimum standard guidelines for fluorescence-based quantitative real-time PCR experiments. BMC Mol Biol 11: 74. doi:10.1186/1471-2199-11-74.

17. Goldovsky L, Cases I, Enright AJ, Ouzounis CA (2005) BioLayout(Java): versatile network visualisation of structural and functional relationships. Appl Bioinformatics 4: 71–74.

18. Papadopoulos GL, Alexiou P, Maragkakis M, Reczko M Hatzigeorgiou AG (2009) DIANA-mirPath: Integrating human and mouse microRNAs in pathways. Bioinformatics 25 (15): 1991–1993. doi: 10.10.

19. Tian S, Huang S, Wu S, Guo W, Li J, et al. (2010) MicroRNA-1285 inhibits the expression of p53 by directly targeting its 3′ untranslated region. Biochem Biophys Res Commun 396: 435–439. doi:10.1016/j.bbrc.2010.04.112.

20. Hidaka H, Seki N, Yoshino H, Yamasaki T, Yamada Y, et al. (2012) Tumor suppressive microRNA-1285 regulates novel molecular targets: aberrant expression and functional significance in renal cell carcinoma. Oncotarget 3: 44–57.

21. Shao M, Cao L, Shen C, Satpathy M, Chelladurai B, et al. (2009) Epithelial-to-mesenchymal transition and ovarian tumor progression induced by tissue transglutaminase. Cancer Res 69: 9192–9201. doi:10.1158/0008-5472.CAN-09-1257.

22. Kalluri R, Weinberg RA (2009) Review series The basics of epithelial-mesenchymal transition. J Clin Invest. 119 (6): 1420–8. doi:10.1172/JCI39104.1420.

23. Kalluri R, Neilson EG (2003) Epithelial-mesenchymal transition and its implications for fibrosis. J Clin Invest 112: 1776–1784. doi:10.1172/JCI20530.

24. Gaedcke J, Grade M, Camps J, Søkilde R, Kaczkowski B, et al. (2012) The Rectal Cancer microRNAome - microRNA Expression in Rectal Cancer and Matched Normal Mucosa. Clin Cancer Res 18: 4919–4930. doi:10.1158/1078-0432.CCR-12-0016.

25. Bertero T, Grosso S, Robbe-Sermesant K, Lebrigand K, Hénaoui I-S, et al. (2012) "Seed-Milarity" Confers to hsa-miR-210 and hsa-miR-147b Similar Functional Activity. PLoS One 7: e44919. doi:10.1371/journal.pone.0044919.

26. Liu G, Friggeri A, Yang Y, Park Y-J, Tsuruta Y, et al. (2009) miR-147, a microRNA that is induced upon Toll-like receptor stimulation, regulates murine macrophage inflammatory responses. Proc Natl Acad Sci U S A 106: 15819–15824. doi:10.1073/pnas.0901216106.

27. Rogler CE, Levoci L, Ader T, Massimi A, Tchaikovskaya T, et al. (2009) MicroRNA-23b cluster microRNAs regulate transforming growth factor-beta/bone morphogenetic protein signaling and liver stem cell differentiation by targeting Smads. Hepatology 50: 575–584. doi:10.1002/hep.22982.

28. Bavan L, Midwood K, Nanchahal J (2011) A New Avenue for Wound Healing Research. BioDrugs 25: 27–41. doi:10.2165/11585010-000000000-00000.

29. Zhu S, Pan W, Song X, Liu Y, Shao X, et al. (2012) The microRNA miR-23b suppresses IL-17-associated autoimmune inflammation by targeting TAB2, TAB3 and IKK-α. Nat Med 18: 1077–1086. doi:10.1038/nm.2815.

30. Burton MJ, Ramadhani A, Weiss HA, Hu V, Massae P, et al. (2011) Active trachoma is associated with increased conjunctival expression of IL17A and profibrotic cytokines. Infect Immun 79: 4977–4983. doi:10.1128/IAI.05718-11.

31. Duisters RF, Tijsen AJ, Schroen B, Leenders JJ, Lentink V, et al. (2009) miR-133 and miR-30 regulate connective tissue growth factor: implications for a role

10

67

of microRNAs in myocardial matrix remodeling. Circ Res 104: 170–8. doi:10.1161/CIRCRESAHA.108.182535.

32. Zhou H, Xu X, Xun Q, Yu D, Ling J, et al. (2012) microRNA-30c negatively regulates endometrial cancer cells by targeting metastasis-associated gene-1. Oncol Rep 27: 807–812. doi:10.3892/or.2011.1574.

33. Kessler M, Zielecki J, Thieck O, Mollenkopf H-J, Fotopoulou C, et al. (2011) Chlamydia Trachomatis Disturbs Epithelial Tissue Homeostasis in Fallopian Tubes via Paracrine Wnt Signaling. Am J Pathol 180: 198–186. doi:10.1016/j.ajpath.2011.09.015.

34. Schopman NCT, Heynen S, Haasnoot J, Berkhout B (2010) A miRNA-tRNA mix-up: tRNA origin of proposed miRNA. RNA Biol 7: 573–576. doi:10.4161/rna.7.4.13141.

35. Cole C, Sobala A, Lu C, Thatcher SR, Bowman A, et al. (2009) Filtering of deep sequencing data reveals the existence of abundant Dicer-dependent small RNAs derived from tRNAs. RNA 15: 2147–2160. doi:10.1261/rna.1738409.

36. Thomas ME, Bueno M, Wirapati P, Lefort K, Dotto GP, et al. (2009) Impact of normalization on miRNA microarray expression profiling. RNA 15 (3): 493–501. doi:10.1261/rna.1295509.contrast.

37. Ach RA, Wang H, Curry B (2008) Measuring microRNAs: comparisons of microarray and quantitative PCR measurements, and of different total RNA prep methods. BMC Biotechnol 8: 69. doi:10.1186/1472-6750-8-69.

38. Rothman KJ (1986) Modern epidemiology. 2nd edition. Little Brown & Co.

39. Canales RD, Luo Y, Willey JC, Austermiller B, Barbacioru CC, et al. (2006) Evaluation of DNA microarray results with quantitative gene expression platforms. Nat Biotechnol 24: 1115–1122. doi:10.1038/nbt1236.

40. Git A, Dvinge H, Osborne M, Kutter C, Hadfield J, et al. (2010) Systematic comparison of microarray profiling , real-time PCR, and next-generation sequencing technologies for measuring differential microRNA expression: 991–1006. doi:10.1261/rna.1947110.one.

41. VanGuilder HD, Vrana KE, Freeman WM (2008) Twenty-five years of quantitative PCR for gene expression analysis. Biotechniques 44: 619–626. doi:10.2144/000112776.

68

Chapter 4: Establishing *Chlamydia trachomatis* infection in HCjE and HEp-2 epithelial cell lines

4.1 Use of HCjE cells and HEp-2 cells for modelling the epithelial response to Ct infection

HEp-2 and HeLa cells are human epithelial cell lines that are commonly used for Ct infection models. HEp-2 cells were originally derived from an epidermoid carcinoma of the larynx, however due to the presence of HeLa cell chromosome markers they are suspected to be contaminated by HeLa cells. The HEp-2 cells used in this study were a kind gift from collaborators at the University of Southampton and the original source is unknown. The American Tissue Type Collection (ATCC) HEp-2 cell line CCL-23 is positive for keratin by immunoperoxidase staining and contains human papilloma viral DNA sequences and HeLa marker chromosomes. HeLa cells were derived from a glandular adenocarcinoma of the cervix [1].

Although used widely in studies, there are data to suggest that HeLa cells (and therefore HEp-2 cells) may not be an appropriate cell line in which to study the host response to Ct infection. RNA and DNA sequencing of a HeLa Kyoto cell line discovered evidence of a chromosomal rearrangement event (chromothripsis) and alarming levels of aneuploidy and differential gene expression in cell cycle and DNA repair pathways [2]. Ct modulates the host cell cycle in order to optimize bacterial replication and survival [3,4], which could be affected by the abnormal expression of cell cycle genes with unknown consequences. What is more, there are mixed reports concerning the expression of TLRs and downstream members of TLR signalling pathways in HeLa cells, which are crucial in pathogen recognition. Wyllie *et al.,* found that ATCC HeLa cells (exact strain not reported) did not express TLR1, TLR2 or MD-2 (a cofactor required for TLR4 function) mRNA [5]. Kurt-Jones *et al.,* also examined gene expression in ATCC HeLa cells (exact strain not reported) and found that TLR2 and TLR8 were not expressed and that HeLa were unresponsive to TLR2 stimuli, although cytokines were secreted in response to TNFα [6]. In contrast, another study reported that all 10 TLRs were expressed in HeLa cells, also using gene expression analysis (ATCC#: CCL-2) [7]. Plasmid-free strains of Ct fail to activate TLR2 and as a result do not induce pathology in the murine genital tract [8]. A lack of specific TLR machinery in HeLa cells would lead to an aberrant innate cellular response to infection, with the potential to mislead researchers.

Studies using more physiologically appropriate cell lines and polarized epithelial cell models have shown that Ct entry, productivity, response to antimicrobial drugs and host responses differ in comparison to Ct infection of non-polarized epithelial cell

monolayers [9–12]. Infectivity of a serovar E strain of Ct was higher in endometrial HEC-1B cells relative to HeLa and McCoy cells when cells were grown in monolayer (flask) cultures [9]. When cells were cultured three-dimensionally on collagen-coated microcarrier beads the Ct developmental cycle completed faster in all three cell lines relative to monolayer cultures, however in HEC-1B cells Ct entry was faster, genome replication was greater and progeny from were slightly more infectious relative to HeLa and McCoy cells [9]. In contrast, the more virulent strain L2 that disseminates *in vivo* and causes LGV showed equal attachment, entry and growth productivity in polarized HeLa and HEC-1B and non-polarized HeLa cells [13]. This perhaps reflects the virulence of L2 and might suggest that growth of less virulent ocular (serovars A-C) and urogenital (serovars D-K) strains of Ct is more susceptible to changes in the local environment. A recent study using a primary-like immortalized endocervical epithelial cell model found that polarized cells localized expression of certain inflammatory mediators to the apical or basal surface in response to infection with a serovar D strain of Ct [12]. These data indicate that growth of ocular Ct strains may be more successful and the host response more complex when using cellular models that better mimic the *in vivo* environment.

For investigation of the ocular response to Ct infection it was therefore desirable to use an epithelial cell line of conjunctival origin. Three conjunctival epithelial cell lines have been reported in the literature: HCjE, IOBA-NHC [14] and Wong-Kilbourne derivative of Chang conjunctiva (ChWK), however ChWK cells are suspected to be contaminated by HeLa cells [15,16]. Primary cells were not used in this PhD project due to the reported difficulty in obtaining and growing pure primary epithelial cells from conjunctival tissue.

The HCjE cell line was established by James G. Rheinwald and colleagues in 2002 [17]. Primary conjunctival keratinocytes from an 82-year-old clinically normal man were grown from explanted or minced tissue. These cells were determined to be genetically normal and were co-cultivated through 1-4 serial passages with feeder cells (mitomycin-treated Swiss 3T3J2 cells). Following this they were cultured in keratinocyte serum-free medium supplemented with bovine pituitary extract, epidermal growth factor (EGF) and calcium chloride [17]. HCjE cells were engineered to express hTERT (to prevent telomere shortening), a p-16 insensitive mutant of cdk4 (to abolish p-16 control) and a dominant negative mutant of p53 (to abolish p53 function). All three of these mutations were necessary to achieve immortality of this cell line. The differentiation characteristics of this cell line were subsequently investigated by Gipson and colleagues in 2003 [18]. The keratin and mucin expression repertoire of HCjE cells

was shown to be similar to that of native epithelial cells and cells stratified when grown on plastic, type I collagen and when implanted into severe combined immunodeficient (SCID) mice [18]. Stratified apical cells flattened and produced membrane-associated mucins, however basal cell polarity was not detected and HCjE cells failed to fully differentiate into polarized epithelium. Despite a subpopulation of HCjE cells expressing small amounts of the goblet-cell specific mucin, MUC5AC, goblet cells that had differentiated from HCjE cells could not be detected [18].

One study has compared the growth of an ocular serovar A strain of Ct, A/HAR-13, in HeLa and HCjE cells [19]. Cells were grown on cell culture plastic (24 well plates), were not polarized or stratified and were infected with Ct inoculum in sucrose phosphate glutamate and were rocked at 37°C for 2 hours to facilitate infection. A/HAR-13 grew faster in HCjE cells than in HeLa cells, whereas urogenital Ct serovars grew faster in HeLa cells. The authors concluded that this reflected the tissue tropism of Ct serovars.

This project sought to use the HCjE cell line to investigate the conjunctival epithelial cell response to Ct infection. The HCjE cells used were a kind gift from the laboratory of Professor Ilene Gipson (Harvard University). The specific objectives were to establish Ct infection models in HEp-2 cells and to perform experiments in the more physiologically appropriate HCjE cell line. This chapter reports the growth kinetics of Ct in these two cell lines and the methods used to investigate Ct infectivity in HCjE cells.

4.2. Methods

In vitro culture and Ct infection of human epithelial cell lines

Human epithelial type 2 (HEp-2) cells were cultured in MEM (Gibco, Life Technologies) supplemented with 1% gentamicin (Gibco), 10% FBS (Gibco), and 1% L-glutamine (Gibco). For *in vitro* experiments, cells were seeded in 12 well plates at $3x10^5$ cells per well in MEM. An immortalized human conjunctival epithelial cell line (HCjE) was cultured in Keratinocyte serum-free medium (K-sfm) with L-Glutamine (Gibco) supplemented with $25\mu g/ml$ bovine pituitary extract (Gibco), 0.2ng/ml epidermal growth factor (Gibco), $0.4mM$ $CaCl_2$ (Sigma) and 5% gentamicin and incubated at 37°C with 5% atmospheric CO_2. For experiments, HCjE cells were seeded in 12 well plates at $3x10^5$ cells per well. Initial infection experiments cultured HCjE cells in K-sfm throughout. For later HCjE cell infection experiments, cells were seeded in 1:1 K-sfm [with supplements]: Dulbecco's Modified Eagle Medium: Nutrient Mixture F12 (DMEM/F12) [with 10% FBS, 1% gentamicin and 1% L-glutamine] (Gibco) and were switched to DMEM/F12 [with supplements] upon infection 24 hours later. Cell lines were tested for Mycoplasma contamination upon receipt and regularly thereafter using the LookOut® Mycoplasma PCR Detection kit (Sigma-Aldrich) following the manufacturers instructions. Methods to test cell line identity such as human lymphocyte antigen (HLA) testing, karyotyping, isoenzyme or short tandem repeat (STR) analyses were not performed.

HEp-2 and HCjE cells were infected with serovar A Ct strains: A2497 (described in [20]), its plasmid cured counterpart (A2497P-) [21] and A/HAR-13 [20] and LGV strain L2/434/Bu [22]. Cells were infected 24 hours after seeding at a multiplicity of infection (MOI) of 0.5 or 1 and with or without the addition of cycloheximide where described. Cycloheximide (Sigma) was used at a final concentration of $1\mu g/ml$. Ct cultures and mock-infected cells were centrifuged at 1800 r.p.m. for 1 hr to facilitate infection and were incubated at 37°C in 5% CO_2. Cells were not washed after the addition of Ct inoculum or centrifugation. DEAE-Dextran (Sigma) was used instead of centrifugation where described. Twenty-four hours after seeding, media was removed from wells and replaced with Hanks Balanced Salt Solution (HBSS) (Gibco) containing 30mg/L DEAE-Dextran. Wells were left to stand at room temperature for 20 minutes. HBSS and DEAE-Dextran were removed, cells were washed in HBSS and Ct inoculum in media was added. After one hour of incubation at 37°C the inoculum was removed, cells were washed in HBSS and media was added. Two or six replicates were carried out for each

experiment where described. At the indicated timepoints post-infection (hpi), media was removed and cells were washed in 1X PBS (Sigma). Productive infection was measured by ddPCR and through visualization of inclusions using confocal and phase microscopy.

Nucleic acid extraction

Three hundred microliters of lysis buffer (Norgen Biotek) was added to each well and cells were harvested by scraping. Total RNA and DNA were extracted using the Norgen RNA and DNA purification kit according to the manufacturers instructions.

Ct infection load by droplet digital PCR

Droplet-digital PCR was carried out to quantitate Ct infection, as described previously (Chapter 4; [23,24]). An initial assay detecting Ct *omcB* and human *RPP30* endogenous control was carried out on all samples to determine Ct load. Another assay detecting Ct *omcB* and Ct plasmid DNA was performed to check for cross contamination of plasmid competent Ct in plasmid-free Ct cultures. Ct *omcB* and human *RPP30* primer and probe sequences are described elsewhere (Chapter 4). The Ct plasmid primer and probe sequences were forward: 5' CAGCTTGTAGTCCTGCTTGAGAGA 3', reverse: 5' CAAGAGTACATCGGTCAACGAAGA 3', probe: [HEX] CCCCACCATTTTTCCGGAGCGA [BHQ1]. Thermal cycling conditions were as follows: 95°C hold for 10 minutes, followed by 40 cycles of 95°C for 10 seconds and 60°C for 20 seconds with a final hold of 98°C for 12 minutes. ddPCR was performed on a Bio-Rad QX100 Instrument and data were collected using Quantalife software (Bio-Rad). Copy number was calculated in R using previously published scripts [23].

Confocal microscopy

Cell monolayers were seeded on glass coverslips and at 48 hpi media was removed and cells were washed in 1X PBS. Two hundred μl ice cold 100% methanol was added to each well for 10 minutes. Cells were washed in 1X PBS and incubated in 200 μl 1% w/v BSA/PBS for 30 minutes at room temperature to block non-specific fluorescence. Cells were incubated for 30 minutes in the dark with 100 μl of a 1% v/v solution of anti-*Chlamydia trachomatis* MOMP antibody (FITC) (ab30951; Abcam) in 1% w/v

BSA/PBS. Cells were washed 3x in 1X PBS for 5 minutes each wash. DAPI dilactate (1μg/ml (Sigma)) was added for 5 minutes. Cells were washed 3x in 1X PBS. Slides were mounted with coverslips and viewed on a Zeiss LSM510 confocal microscope at 40X magnification. Images were captured using the tile function in Volocity, V5.5.1 (PerkinElmer).

Qiagen RT^2 Profiler antibacterial response PCR arrays

RNA was reverse transcribed using MiScript RTII kits with the HiFlex buffer (Qiagen) to synthesise a cDNA library. Qiagen RT^2 profiler antibacterial response qPCR array cards were carried out using RT^2 SYBR Green ROX qPCR master mix (Qiagen) following the manufacturers instructions. PCR was performed on a 7500HT 96-well Standard block PCR instrument (Applied Biosystems, ThermoFisher Scientific, Life Technologies).

4.3 Ct growth in HEp-2 and HCjE cells

4.3.1 Growth of ocular serovars in HEp-2 cells

HEp-2 cells grew quickly, were small and round and had the pavement-like morphology characteristic of epithelial cells. Inclusions could be seen by phase microscopy between 48-72 hours post infection with Ct. Cells were free of Mycoplasma on all occasions tested.

The Ct chromosomal copy number (*omcB*) of A2497, A2497P- and A/HAR-13 decreased between 0 and 12 hours post infection (hpi) in HEp-2 cells. By 24 hpi, A2497 *OmcB* copies began to increase, whereas A2497P- took slightly longer and an increase was seen at 48 hpi. Levels of A2497 and A2497P- were comparable by 48 hpi. A/HAR-13 growth was not as successful in comparison to A2497 and A2497P-. Although A/HAR-13 copy numbers increased by 48 hpi, the total number of *OmcB* copies was still lower than that of the starting inoculum (Figure 4.1). This difference was clearly evident by microscopy of chlamydial inclusions in HEp-2 cell monolayers (Figure 4.2). A2497 and A2497P- achieved comparable numbers of inclusions, whereas far fewer inclusions could be seen in A/HAR-13 infected cells. A2497P- formed the "bulls-eye" inclusions characteristic of plasmid-free Ct [25–27], with inclusions appearing donut-like and hollow in the middle. These can be seen in more detail in the insert of Figure 4.2B. In contrast A2497 inclusions were solid throughout. A2497 and A2497P- inclusions were angular and enlarged to fill the cell cytoplasm, whereas A/HAR-13 inclusions were small and round. No plasmid DNA was detected in the DNA of A2497P- infected cells (data not shown).
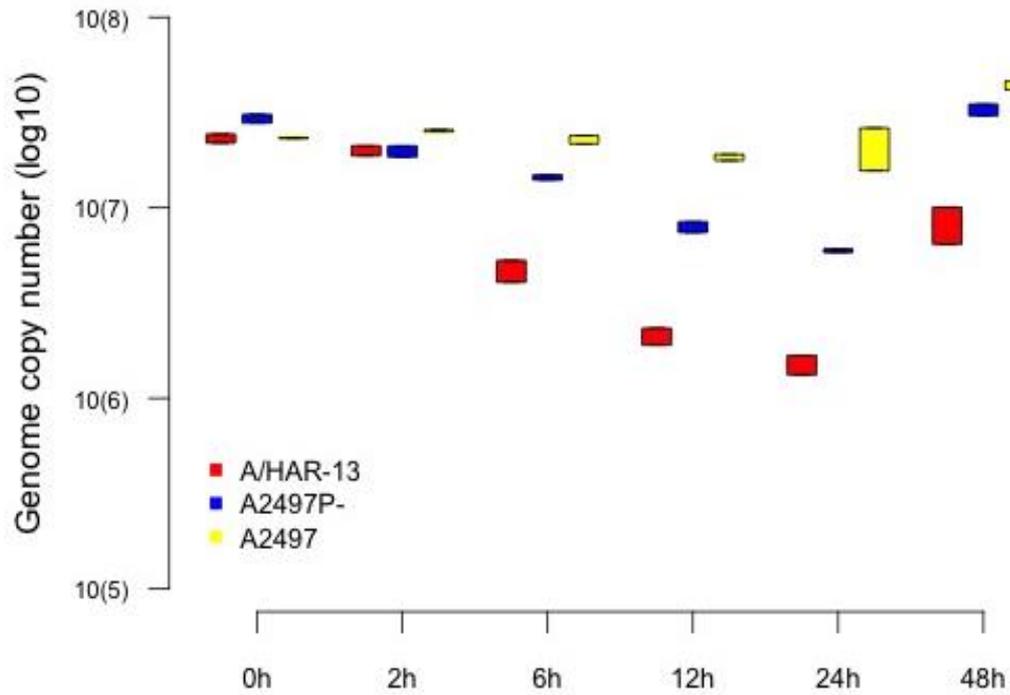
*Figure 4.1. Genome copy number (*omcB*) of A/HAR-13, A2497P- and A2497 strains of Ct in HEp-2 cells at the indicated timepoints post-infection. Cells were infected at an MOI of 1. Genome copy number is shown on a log(10) scale. Timepoints post-infection are shown on a non-linear scale. Two replicates of each timepoint/infection were carried out. Boxes show the range between the two values (one from each replicate). Red: A/HAR-13, Blue: A2497P-, Yellow: A2497.*
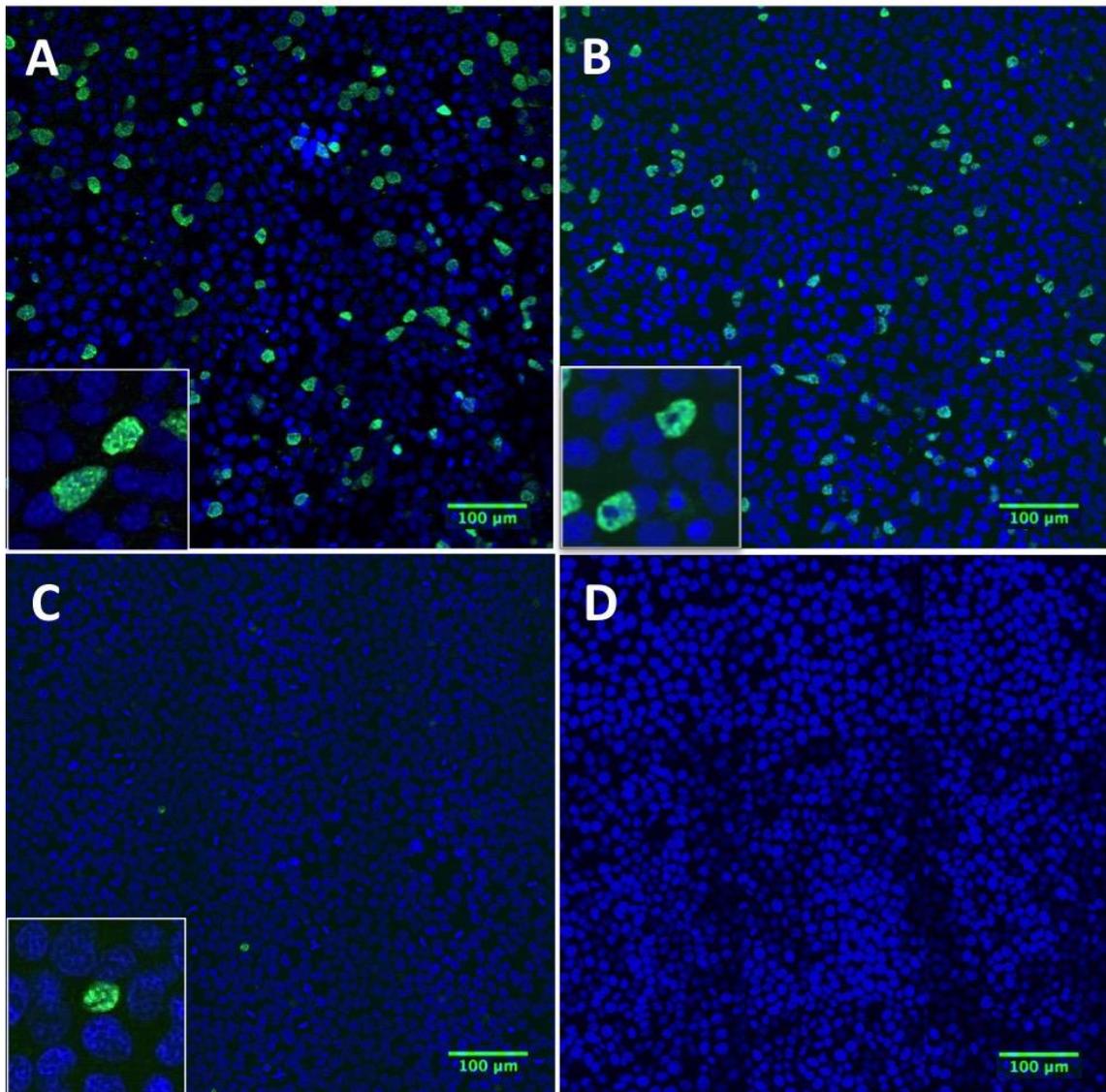
Figure 4.2. HEp-2 cell monolayers infected with Ct strains A2497 (A), A2497P- (B), A/HAR-13 (C) and mock-infected cells (D) at 48 hpi. "Bulls-eye" inclusions can be seen for A2497P- infected cells in the insert of (B). Cell nuclei were stained with DAPI (blue) and Ct inclusions were stained with anti-C. trachomatis MOMP antibody (FITC (green)). Cells were infected at an MOI of 1 and viewed at 40X magnification. Representative photomicrographs were taken from one of two replicates for each condition. Inserts show a section of each field at a greater magnification. Scale bars represent 100µm.

4.3.2 Growth of ocular serovars in HCjE cells

HCjE cells were slow growing and were larger than HEp-2 cells. Cells were flattened and difficult to see clearly using phase microscopy, particularly once confluency was

achieved, however the pavement-like morphology could be seen. Cells were free of Mycoplasma on all occasions tested.

HCjE cells were infected with the same inoculum and volume that was used to infect HEp-2 cells in section 4.3.1. In contrast to HEp-2 cells, all Ct strains failed to grow productively in HCjE cells (Figure 4.3). The genome copy number of A2497 and A2497P- decreased consistently over time, even up to 144 hpi. A/HAR-13 genome copy number decreased at a faster rate than A2497 and A2497P- (similar to HEp-2 cells), however it increased slightly between 72 and 144 hpi. The lack of productive infection was evident through microscopy; very few inclusions could be identified and they were small and round, similar to A/HAR-13 growth in HEp-2 cells (Figure 4.4). No plasmid DNA was detected in A2497P- infected cell DNA (data not shown).
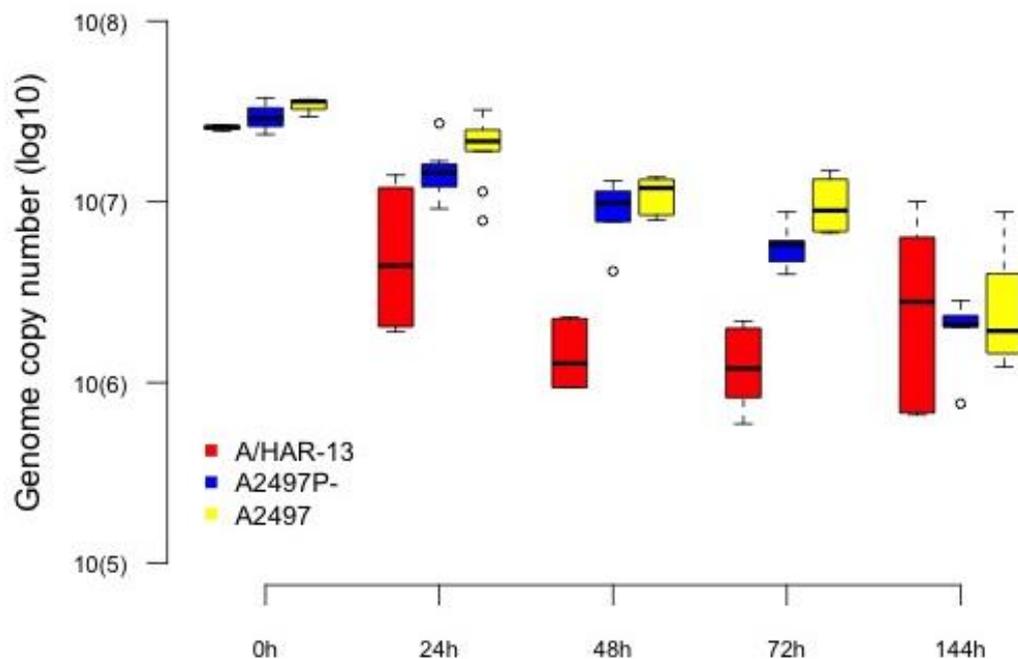
Figure 4.3. Genome copy number (omcB) of A/HAR-13, A2497P- and A2497 strains of Ct in HCjE cells at the indicated timepoints post-infection. Genome copy number is shown on a log(10) scale. Timepoints post-infection are shown on a non-linear scale. Cells were infected at an MOI of 1. Boxplots show the median (thick black horizontal line), the interquartile range (solid coloured box) and the minimum and maximum values (dotted line or empty circles) of the six replicates for each timepoint/infection. Red: A/HAR-13, Blue: A2497P-, Yellow: A2497.
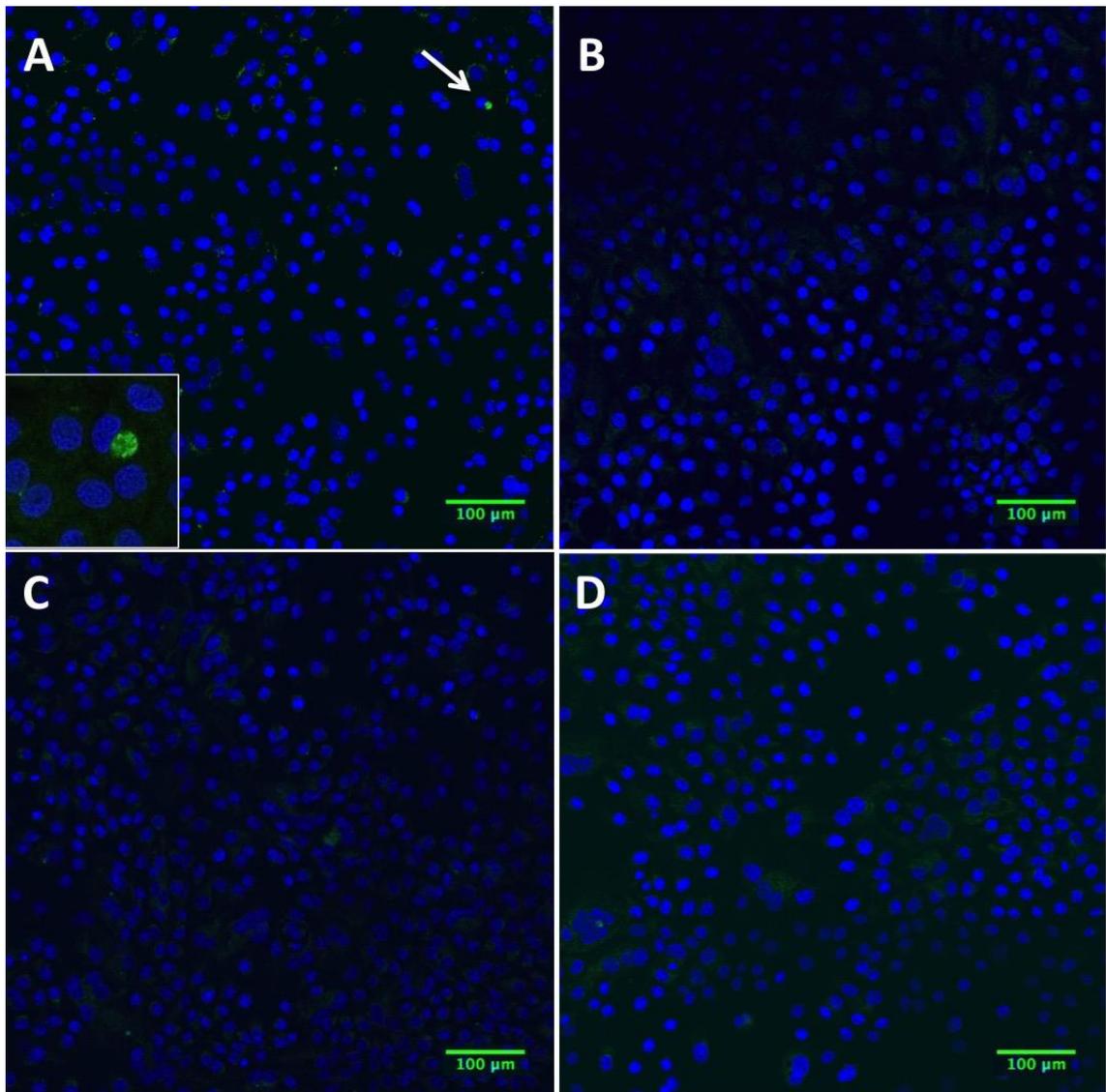
Figure 4.4. HCjE cell monolayers infected with Ct strains A2497 (A), A2497P- (B), A/HAR-13 (C) and mock-infected cells (D) at 48 hpi. Cell nuclei were stained with DAPI (blue) and Ct inclusions were stained with anti-C. trachomatis MOMP antibody (FITC (green)). Cells were infected with an MOI of 1 and viewed at 40X magnification. Representative photomicrographs were taken from one of two replicates for each condition. The arrow indicates a Ct inclusion, shown at greater magnification in the insert. Scale bars represent 100μm.

4.4 Optimization of Ct growth in HCjE cells

4.4.1 Infection medium and facilitation

The addition of serum to HCjE cells is thought to slow cell replication and promote differentiation. HCjE cells can be switched to DMEM/F12 media containing FCS in order to promote differentiation and stratification [18]. The calcium and tryptophan levels in the media of K-sfm (in which HCjE cells were grown and infected in section *4*.3.2), MEM (in which HEp-2 cells were grown) and DMEM/F12 were compared (Table 4.1). The calcium concentration of K-sfm was lower than that of MEM and DMEM/F12, whereas tryptophan levels were comparable. In case of low calcium or the differentiation state of HCjE cells hindering chlamydial growth, the infectivity of Ct in HCjE cells grown in DMEM/F12 was investigated.

Table 4.1. Nutrient levels in media used for HEp-2 and HCjE cells

	Calcium (mg/L)	Tryptophan (mg/L)
K-sfm	80	8.98
MEM	200	10
DMEM/F12	116.6	9.02

Footnote: total nutrient levels are shown after addition of supplements.

Centrifugation was used to facilitate chlamydial infection in the experiments described above. DEAE-Dextran is an alternative method that polarizes cell membranes and is thought to facilitate uptake of EBs by cells. HCjE (seeded and infected in K-sfm) and HEp-2 cells were infected with A2497, A2497P- and A/HAR-13 (three wells of each condition) and were centrifuged for one hour at 1800 rpm, as was used in all previous infections (Section 4.3). Another three wells of each Ct strain in each cell line were treated with DEAE-Dextran prior to infection. HCjE cells were seeded in 1:1 K-sfm:DMEM/F12 and switched to DMEM/F12 upon infection 24 hours later. Cells were stained at 48 hpi and inclusions were viewed using confocal microscopy. Images were taken using the tile function, recording 9 images of adjacent fields that were then stitched together. One such tiled image was taken per well so that three images were taken per cell line/infection. The number of cells and the number of inclusions in each image were counted using ImageJ. Infectivity was calculated [(number of infected cells/total number of cells)*100) for each of the three images and the average is shown in Table 4.2.

Table 4.2. Average infectivity achieved by ocular Ct strains at 48 hpi in HEp-2 and HCjE cells.

Ct strain	HEp-2 cells		HCjE cells	
	Centrifuge	Dextran	Centrifuge (K-sfm)	Dextran (DMEM/F12)
A2497p+	22.40%	22.20%	6%	4.30%
A2497p-	1.30%	1.90%	0.80%	0.60%
A/HAR-13	0.20%	0.20%	0.40%	0.50%

The infectivity of Ct in HCjE cells grown in DMEM/F12 and infected using DEAE-Dextran was no different to the infectivity achieved using centrifugation and K-sfm media. There was also no difference in infectivity achieved by DEAE-Dextran versus centrifugation in HEp-2 cells. The inocula used in this experiment were derived from different Ct harvests to the experiments described above and the differences in infectivity between A2497 and A2497P- are likely due to inaccurate quantification of inclusion forming units (IFU) in the inoculum, rather than differential infectivity. Identical volumes of inoculum for each Ct strain were added to each cell line. The power to detect differences in infection success in HCjE cells was limited by calculating infectivity as very few inclusions could be identified using centrifugation or DEAE-Dextran. Quantifying genome copy number by ddPCR at various timepoints post infection might have revealed more subtle differences owing to different media and infection facilitators. Another limitation of this experiment was that the effects of DMEM/F12 and DEAE-Dextran cannot be differentiated and they may have cancelled each other out. They would have best been performed as independent conditions, with the addition of centrifugation and DEAE-Dextran (combined).

4.4.2 Growth of an LGV strain of Ct in HCjE and HEp-2 cells

Virulent LGV strain L2 was grown in HEp-2 and HCjE cells in order to compare growth kinetics and infectivity to that of ocular strains. L2 does not require infection facilitation due to its virulence. HCjE cells were seeded in 1:1 K-sfm:DMEM/F12 and infected in DMEM/F12. Genome copy number of L2 dropped between 0 and 24 hpi, however it increased again by 48 hpi and steadily increased over time in both cell lines (Figure 4.5). Genome copy number decreased to much lower levels in HCjE cells compared to HEp-2 cells. Despite amplification of L2 genome copy number in HCjE cells, the load at 72 and 144 hpi remained lower than that of the starting inoculum. Large inclusions of L2 were clearly seen through phase microscopy of HCjE cells, however there were far

fewer than in HEp-2 cells (Figure 4.6). Inclusion morphology was equivalent in both cell lines.
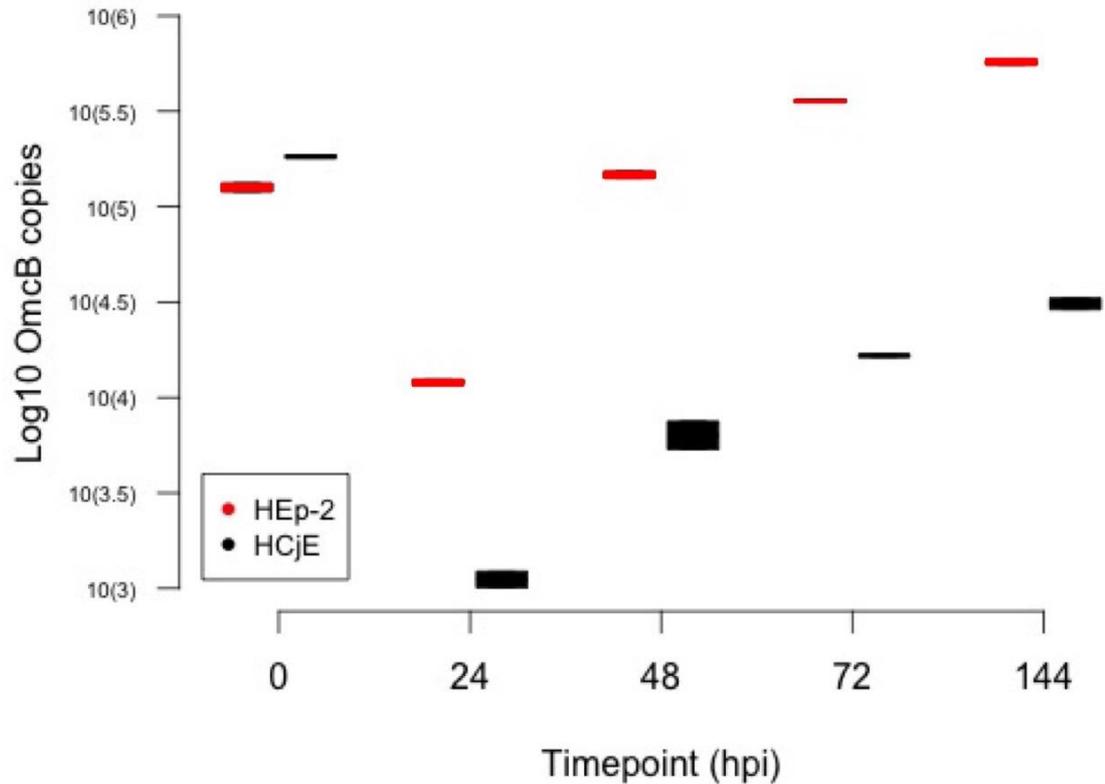
*Figure 4.5. Genome copy number (*omcB*) of Ct strain L2 in HCjE and HEp-2 cells at the indicated timepoints post-infection. Genome copy number is shown on a log(10) scale. Timepoints (hours post-infection (hpi)) are shown on a non-linear scale. Cells were infected at an MOI of 0.5. Two replicates of each timepoint/infection were performed. Boxes show the range between the two values (one from each replicate). Red: HEp-2 cells, Black: HCjE cells.*
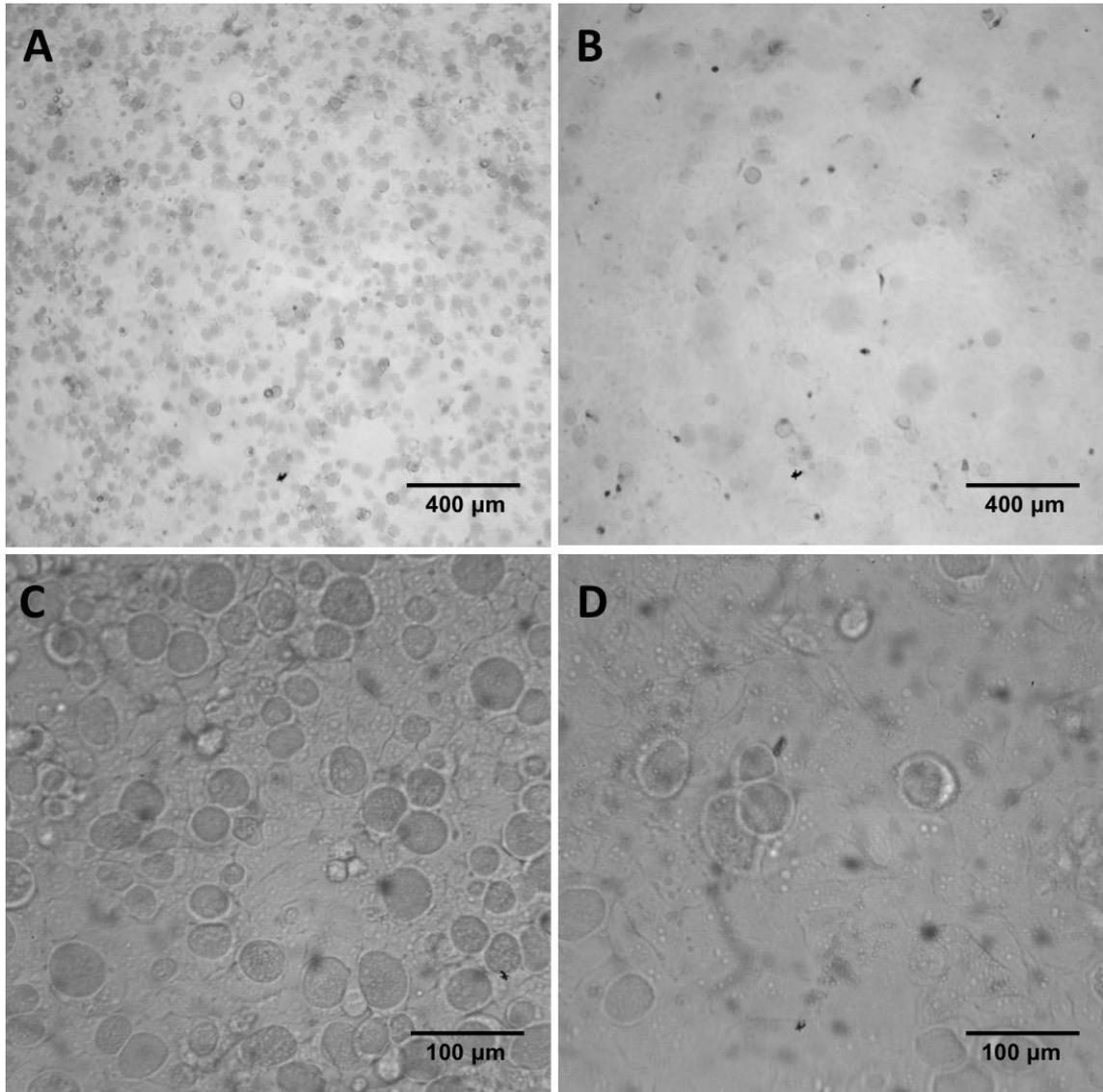
Figure 4.6. HCjE and HEp-2 cell monolayers infected with Ct strain L2 at 48 hpi. (A) and (C) are L2 infected HEp-2 cells, (B) and (D) are L2 infected HCjE cells. (A) and (B) were taken at 5X magnification, (C) and (D) were taken at 20X magnification. Cells were infected at an MOI of 0.5. Representative photomicrographs were taken from one of three replicates for each cell line.

4.4.3 Ct growth in the presence of cycloheximide

In order to address whether the production of innate antimicrobial mediators by HCjE cells inhibited Ct growth, HEp-2 and HCjE cells were infected with A2497, A2497P- and A/HAR-13 in the presence and absence of cycloheximide and the genome copy number was quantified at 48 hpi. The mean *OmcB* load of A2497P- and A2497 in HEp-2 cells increased in the presence of cycloheximide (Figure 4.7), however the genome copy number of A/HAR-13 did not. The high variation in genome copy number of Ct

infected cycloheximide-treated HEp-2 cells was partly due to an abnormal amount of cell death in 2/6 biological replicates, for reasons unknown, therefore the overall yield was lower. Ct growth in HCjE cells was not improved in the presence of cycloheximide; in fact it was reduced (Figure 4.7). Unfortunately genome copy number was not measured over time; therefore it was not clear whether there was any growth of Ct in HCjE cells or whether it steadily declined over time as in section 4.3.2.
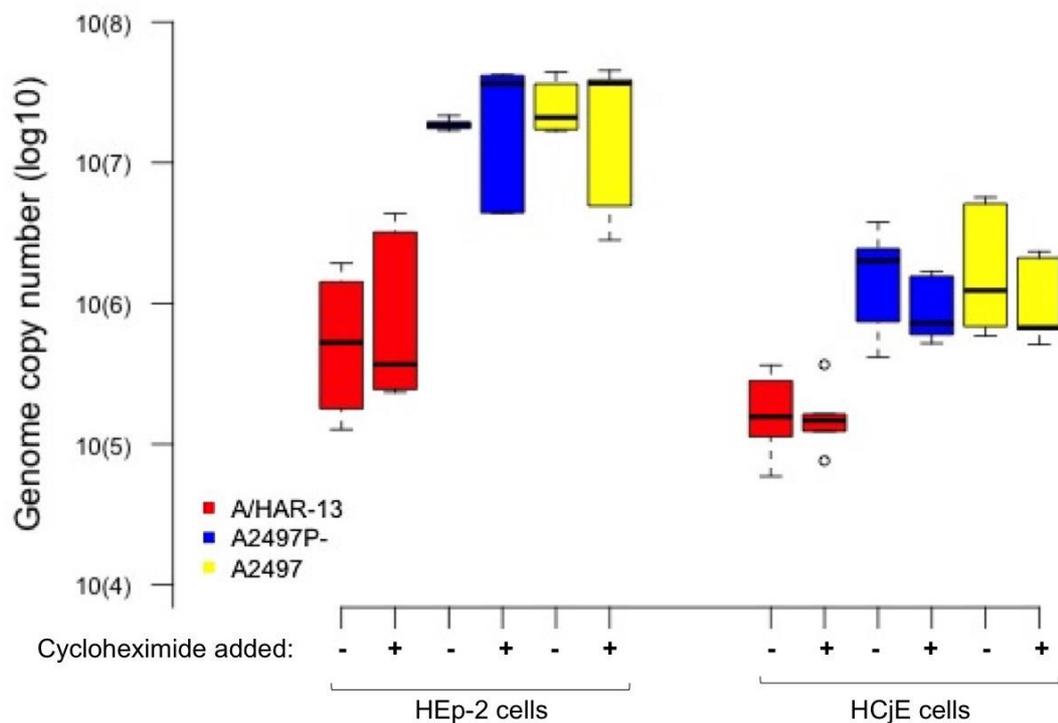
Figure 4.7. Genome copy number (omcB) of ocular Ct strains in HEp-2 and HCjE cells at 48 hpi in the presence (C+) and absence (C-) of cycloheximide. Genome copy number is shown on a log(10) scale. Cells were infected at an MOI of 1. Six replicates of each timepoint/infection were performed. Red: A/HAR-13, Blue: A2497P-, Yellow: A2497.

4.5 Profiling the PRR and associated signaling pathways repertoire in HEp-2 cells.

Although HCjE cells were a preferable choice of cell line for conducting *in vitro* investigations of the host epithelial response to ocular Ct infection, productive infection of Ct in HCjE cells was not achieved. Their slow growth was also a limiting factor in the number of optimization experiments that could be performed given the number of experimental repeats, conditions and timepoints required. Many researchers use HEp-2 and HeLa cells to study the host response to both urogenital and ocular Ct infection [26,28–30]. This is likely due to the ease and speed of growing these cells in large numbers and the productive infection of Ct that can be achieved. This also perhaps reflects the relative difficulty in establishing Ct infection in other cell lines. Limited resources were available for further optimization of Ct growth in HCjE cells or to source another conjunctival cell line/primary cells; therefore in order to complete aims 2 and 3 (Chapter 2) of this PhD project, the suitability of the HEp-2 cell line for *in vitro* experiments was evaluated.

Due to controversy in the literature, the PRR profile of HEp-2 cells was investigated in order ensure they could respond appropriately to Ct infection. As a proof of principle, two Qiagen RT^2 antibacterial response qPCR arrays were performed using cDNA from uninfected HEp-2 cells (at 0h) and HEp-2 cells 6 hours post infection with A2497. Each qPCR card contains 5 housekeeping genes and 84 genes that are involved in the antibacterial response. The geometric mean of the 5 housekeeping genes was taken and subtracted from each target separately for each card to give a delta cycle threshold value (dCT). The fold change of gene expression in A2497 infected HEp-2 cells was compared to gene expression in uninfected cells using the delta delta Ct method [31]. All 84 antibacterial response genes had cycle thresholds ≤35 in uninfected HEp-2 cells, except NLRP3, which had a cycle threshold value of 36.7. Thirty-seven genes were downregulated in A2497 infected cells (6 hpi) and 18 genes were upregulated (FC ≥1.5) (Table 4.3). TLRs 1, 2, 4, 5, 6, 9 and co-factors LY96 (MD-2) and CD14 were expressed by HEp-2 cells (TLR1, 4, 5, 6 and CD14 had a FC <1.5 and are not shown in Table 4.3). Among the most upregulated genes were C reactive protein (CRP), NOD-like receptor proteins 1 and 3 (NLRP1/3), TLR2, inflammatory cytokines TNF and IL8 and CARD9 (a regulator of NOD signaling and cell apoptosis). Among the most downregulated genes were the antimicrobial peptide PRTN3, MD-2 (TLR4 cofactor), MEFV (pyrin; regulates inflammation), CARD6 (apoptosis related) and IFNB1 (antiviral and pro-inflammatory). Several genes in the NOD-like receptor, TLR

signaling, inflammatory response and antimicrobial pathways were downregulated. Statistical testing was not performed as only one card (one repeat) was performed for uninfected HEp-2 cells (-VE 0h) and A2497 infected HEp-2 cells (A2497 6h).

Table 4.3. Expression of antibacterial response genes with ≥1.5 fold change in A2497 infected HEp-2 cells at 6 hpi (A2497 6 h) relative to uninfected HEp-2 cells (-VE 0h).

Gene Symbol	dCT* -VE 0h	dCT* A2497 6h	Fold Change
NOD-Like receptor signalling			
MEFV	12.378	14.98	0.16
SUGT1	0.658	2.41	0.30
HSP90AA1	-1.882	-0.37	0.35
PSTPIP1	13.448	14.84	0.38
NLRC4	7.168	8.31	0.45
NOD2	12.388	13.42	0.49
XIAP	6.798	6.01	1.73
BIRC3	5.748	4.92	1.78
NLRP1	16.958	15.27	3.22
NLRP3	18.128	14.51	12.28
Signaling Downstream of Antibacterial Responses			
MAP2K1	5.558	6.54	0.51
CHUK (IKKα)	5.108	5.7	0.66
JUN	10.348	9.69	1.58
RELA	6.298	5.64	1.58
MAPK3	8.398	7.59	1.75
Antimicrobial peptides			
PRTN3	16.178	20.88	0.04
MPO	12.968	14.62	0.32
CTSG	14.038	15.62	0.33
BPI	12.278	13.81	0.35
LTF	12.848	14.3	0.37
LYZ	14.958	16.07	0.46
CAMP	12.238	12.94	0.61
SLPI	6.278	5.61	1.59
Apoptosis			
CARD6	7.858	10.02	0.22
RIPK2	4.138	5.49	0.39
MAPK8 (JNK1)	5.348	6.25	0.54
PYCARD	11.878	12.56	0.62
AKT1	7.428	6.8	1.55
CASP1	12.618	11.75	1.83

CARD9	15.648	13.25	5.27
Inflammatory response			
IFNB1	13.428	15.77	0.20
CCL5	6.388	8.37	0.25
IL12B	11.898	13.71	0.28
APCS	11.648	13.37	0.30
IL12A	7.368	8.95	0.33
SLC11A1	9.748	10.96	0.43
LBP	11.768	12.85	0.47
RAC1	0.808	1.69	0.54
CCL3	13.908	14.56	0.64
IL8	9.668	8.25	2.67
TNF	15.208	12.61	6.05
CRP	16.728	12.74	15.87
TLR signalling			
LY96 (MD-2)	12.998	15.48	0.18
TLR9	15.198	16.63	0.37
PIK3CA	4.158	5.58	0.37
MAP3K7	3.138	4.33	0.44
IRAK3	9.898	10.93	0.49
IRF5	10.728	11.61	0.54
TRAF6	5.878	6.5	0.65
MYD88	6.178	6.8	0.65
TIRAP	11.688	11.01	1.60
TOLLIP	10.118	9.32	1.74
IRAK1	7.978	6.92	2.08
TLR2	15.368	14.24	2.19
Other bacterial PRRs			
DMBT1	13.118	13.97	0.55

*dCT = delta cycle threshold value, normalized to the mean of 5 housekeeping genes
(ACTB, B2M, GAPDH, HPRT1, RPLP0)

4.6 Discussion

Productive growth was achieved of A2497, A2497P- and L2 Ct strains in HEp-2 cells. A/HAR-13 growth in HEp-2 cells was less successful and by 48 hpi the genome copy number was still slightly lower than that of the starting inoculum. Unfortunately genome copy number in HEp-2 cells was not measured beyond 48 hpi however it might be expected to increase further. Genome copy number decreased at early timepoints post infection and increased between 24 and 48 hpi. The HEp-2 cells used in these experiments possessed the normal repertoire of PRRs and responded to Ct infection by upregulating inflammatory (IL-8, TNF, CRP) and pathogen-response genes (NLRP1/3, CARD9, TLR2). More genes were downregulated than upregulated in A2497 infected cells at 6 hpi. This might reflect interference by Ct with host response pathways or negative feedback by the host cell to prevent excessive stimulation and inflammation. No significant differences in gene expression were detected until 24 hpi in A2497 infected HeLa cells using a transriptome microarray however [26], suggesting that with more biological repeats and statistical testing these differences may not be significant. These data suggest that HEp-2 cells can initiate a normal and appropriate innate immune response to Ct infection.

Productive growth of Ct was not achieved in HCjE cells and this was a limitation to this project. The genome copy number of ocular strains decreased steadily over time. A/HAR-13 genome copy numbers decreased lower than A2497 and A2497P-, however in contrast to A2497 and A2497P- there was a slight increase between 72 and 144 hpi. The virulent Ct strain L2 proliferated in both cell lines from 24 hpi, however the initial fall in genome copy number was much larger in HCjE cells and did not recover enough to match the genome copy number in the starting inoculum, even at 144 hpi. Nutrient-rich HCjE differentiation medium, DEAE-Dextran and cycloheximide did not improve Ct growth in HCjE cells.

Cycloheximide inhibits protein synthesis in eukaryotic organisms. Addition of cycloheximide to Ct cultures at a concentration that suppresses, but does not completely inhibit host protein synthesis, increases chlamydial yield [32,33]. This is thought to allow Ct to harness host machinery and nutrients to enhance its own growth. As expected, addition of cycloheximide increased yield of ocular strains in HEp-2 cells but surprisingly this was not the case in HCjE cells. HEp-2 cells grow quickly and are not inhibited by contact once confluence is achieved, therefore inhibiting growth by adding cycloheximide presumably provides a large pool of nutrients for Ct. In contrast,

HCjE cells grow slowly and are inhibited once confluent. The addition of differentiation medium (DMEM/F12) further inhibits growth and promotes stratification. It is therefore reasonable to speculate that adding cycloheximide to HCjE cells does not significantly increase the pool of nutrients available to Ct, so there is no growth advantage. This has previously been observed for *C. pneumonia* (Cpn) growth in polarized epithelial cell models where cycloheximide had a negligible impact [34].

The production of innate antimicrobial mediators by HCjE cells, such as have been described for other immortalized primary epithelial cell lines [35], might have interfered with chlamydial growth. In this case the addition of cycloheximide might have prevented production of these antimicrobials and permitted Ct growth, but this was not the case. Cycloheximide was added at the point of infection however so constitutively expressed antimicrobials may have been present and sufficient to prevent infection. Cycloheximide could be added prior to the addition of Ct inoculum (over an extended timecourse due to the unknown longevity of potential antimicrobial mediators in culture medium) to investigate this further.

It was previously reported that the ocular Ct strain A/HAR-13 grew faster in HCjE cells than in HeLa cells, owing to ecological niche adaptation, although the IFU achieved at the final timepoint (48hpi) was the same in both cell lines [19]. L2 grew faster in HeLa and achieved higher final IFUs in HeLa compared to HCjE [19]. In my hands, A/HAR-13 grew very poorly in both HCjE and HEp-2 cells and growth was even less successful in HCjE cells. This observation is supported by data from Kari *et al.*, who found that A2497 produced ~10 fold more recoverable IFU than A/HAR-13 when grown in HeLa cells [20]. The Ct strains A2497, A2497P- and A/HAR-13 used in this study were kind gifts from Laszlo Kari (Rocky Mountains Laboratories, NIH, USA). HCjE cells were isolated in 2003, therefore the A/HAR-13/HCjE cell infection experiments published by Miyairi *et al.,* [19] in 2006 were performed soon after establishment of the cell line and the Ct strains were likely from different stocks. It is possible that genetic changes relating to infection susceptibility of HCjE cells and infectivity of A/HAR-13 accumulated through multiple passages in different laboratories over time, which could explain some of the differences in growth and infectivity [36–40]. Unfortunately karyotyping or other tests to ensure the HCjE cell line was correct were not performed, therefore the possibility that the HCjE cells used in these experiments were not genetically normal cannot be ruled out. Human lymphocyte antigen (HLA) testing, karyotyping, isoenzyme, short tandem repeat (STR) analyses or other such methods should be performed before any further work with this cell line takes place.

Interestingly, A/HAR-13 showed a slight increase in genome copy number in HCjE cells between 72 and 144 hpi. This could indicate a more successful method of natural reinfection of host cells following the first infection cycle. Alternatively it could be due to HCjE cells having differentiated into a more infection-susceptible phenotype over time in culture. This observation was strain specific however as it did not occur in A2497 or A2497P- infected HCjE cells.

Genome copy number of ocular strains in HCjE cells declined steadily over time, whereas L2 showed evidence of genome amplification in HCjE cells. L2 had a comparable growth curve in both cell lines, however the initial drop in genome copy number was much steeper in HCjE cells. Given that HCjE cells did not appear to actively inhibit Ct growth, as no improvement was observed upon addition of cycloheximide, this might suggest that the problem lies in entry into the host cell. L2 is more virulent and disseminates to the lymph nodes *in vivo*, whereas ocular strains remain in the conjunctival epithelium. Perhaps the enhanced virulence of L2 allowed more effective entry into host cells and once inside successful growth was achieved. It is possible that a cell surface receptor required for chlamydial attachment and entry was absent from HCjE cells, or that the mucins produced by HCjE cells, particularly on the apical surface [18], were more effective at preventing Ct penetration and attachment. The entry of Ct into host cells could be examined by electron microscopy or cryo-electron tomography as described previously [10,41] in order to investigate this further.

The rocking method of Ct infection facilitation was used by Miyairi *et al.,* to achieve productive infection of A/HAR-13 in HCjE cells [19]. In a polarized immortalized endocervical epithelial cell model, the rocking method of Ct infection facilitation only achieved 25% infection whereas the centrifugation method achieved >95% infection [12]. The production of mucins by polarized immortalized endocervical epithelial cells [35] was thought to explain why the rocking method was less efficient [12]. One might speculate that the same would be true for HCjE cells due to their own mucin expression profile [18], however, given that attachment and entry stages might be limiting factors for Ct infection of HCjE cells, alternative infection methods such as the rocking method and centrifugation and DEAE-Dextran in combination [33] should be investigated. Miyairi *et al.,* also infected HCjE cells 24 hours after seeding [19], however cells could be left to differentiate and stratify in culture for 7-10 days before addition of Ct. HCjE cells could also be blind passaged with a strain such as A2497, with addition of much higher IFUs of Ct, to try and force adaptation to this cell line.

Purposefully forcing selection in this way however could negate the objective of obtaining physiological and clinically relevant data from an *in vitro* model. Alternatively, another conjunctival cell line could be used. ChWK cells are thought to be contaminated by HeLa cells and were transcriptionally more dissimilar to conjunctival epithelium and primary conjunctival epithelial cells than IOBA-NHC cells [15,16]. IOBA-NHC cells or primary conjunctival epithelial cells could be investigated as an alternative to HCjE cells.

The HEp-2 cells described herein had a complete PRR expression profile and upregulated appropriate innate immune response genes following Ct infection. These data contrast some of the reported literature about the limitations of this cell line, suggesting that they are an acceptable (although not ideal) cell line in which to perform investigations of the host response to Ct infection. Unfortunately it was not possible to achieve productive Ct infection in HCjE cells. In order to investigate miRNA expression and EMT induction *in vitro* in response to Ct infection, HEp-2 cells were used for subsequent experiments. Whilst HEp-2 cells were able to respond appropriately by the parameters tested, the results of these *in vitro* experiments should be interpreted with an understanding of their limitations.

4.7 References

1. Jones HW, McKusick VA, Harper PS, Wuu KD (1971) George Otto Gey. (1899-1970). The HeLa cell and a reappraisal of its origin. Obstet Gynecol 38: 945–949.
2. Landry JJM, Pyl PT, Rausch T, Zichner T, Tekkedil MM, et al. (2013) The Genomic and Transcriptomic Landscape of a HeLa Cell Line. G3 (Bethesda). doi:10.1534/g3.113.005777.
3. Greene W, Zhong G (2003) Inhibition of host cell cytokinesis by Chlamydia trachomatis infection. J Infect 47: 45–51.
4. Balsara ZR, Misaghi S, Lafave JN, Starnbach MN (2006) Chlamydia trachomatis infection induces cleavage of the mitotic cyclin B1. Infect Immun 74: 5602–5608. doi:10.1128/IAI.00266-06.
5. Wyllie DH, Kiss-Toth E, Visintin A, Smith SC, Boussouf S, et al. (2000) Evidence for an Accessory Protein Function for Toll-Like Receptor 1 in Anti-Bacterial Responses. J Immunol 165: 7125–7132. doi:10.4049/jimmunol.165.12.7125.
6. Kurt-Jones EA, Sandor F, Ortiz Y, Bowen GN, Counter SL, et al. (2004) Use of murine embryonic fibroblasts to define Toll-like receptor activation and specificity. J Endotoxin Res 10: 419–424. doi:10.1179/096805104225006516.
7. Nishimura M, Naito S (2005) Tissue-specific mRNA expression profiles of human toll-like receptors and related genes. Biol Pharm Bull 28: 886–892.
8. O'Connell CM, AbdelRahman YM, Green E, Darville HK, Saira K, et al. (2011) Toll-like receptor 2 activation by Chlamydia trachomatis is plasmid dependent, and plasmid-responsive chromosomal loci are coordinately regulated in response to glucose limitation by C. trachomatis but not by C. muridarum. Infect Immun 79: 1044–1056. doi:10.1128/IAI.01118-10.
9. Guseva N V, Dessus-Babus S, Moore CG, Whittimore JD, Wyrick PB (2007) Differences in Chlamydia trachomatis serovar E growth rate in polarized endometrial and endocervical epithelial cells grown in three-dimensional culture. Infect Immun 75: 553–564. doi:10.1128/IAI.01517-06.
10. Wyrick PB, Choong J, Davis CH, Knight ST, Royal MO, et al. (1989) Entry of genital Chlamydia trachomatis into polarized human epithelial cells. Infect Immun 57: 2378–2389.
11. Wyrick PB, Davis CH, Knight ST, Choong J (1993) In-vitro activity of azithromycin on Chlamydia trachomatis infected, polarized human endometrial epithelial cells. J Antimicrob Chemother 31: 139–150.
12. Buckner LR, Lewis ME, Greene SJ, Foster TP, Quayle AJ (2013) Chlamydia trachomatis infection results in a modest pro-inflammatory cytokine response and a decrease in T cell chemokine secretion in human polarized endocervical epithelial cells. Cytokine 63: 151–165. doi:10.1016/j.cyto.2013.04.022.
13. Dessus-Babus S, Moore CG, Whittimore JD, Wyrick PB (2008) Comparison of Chlamydia trachomatis serovar L2 growth in polarized genital epithelial cells grown in three-dimensional culture with non-polarized cells. Microbes Infect 10: 563–570. doi:10.1016/j.micinf.2008.02.002.
14. Diebold Y (2003) Characterization of a Spontaneously Immortalized Cell Line (IOBA-NHC) from Normal Human Conjunctiva. Invest Ophthalmol Vis Sci 44: 4263–4274. doi:10.1167/iovs.03-0560.
15. Lavappa KS (1978) Survey of ATCC stocks of human cell lines for HeLa

contamination. In Vitro 14: 469–475.

16. Tong L, Diebold Y, Calonge M, Gao J, Stern ME, et al. (2009) Comparison of gene expression profiles of conjunctival cell lines with primary cultured conjunctival epithelial cells and human conjunctival tissue. Gene Expr 14: 265–278. doi:10.3727/105221609788681231.

17. Rheinwald JG, Hahn WC, Ramsey MR, Wu JY, Guo Z, et al. (2002) A two-stage, p16(INK4A)- and p53-dependent keratinocyte senescence mechanism that limits replicative potential independent of telomere status. Mol Cell Biol 22: 5157–5172.

18. Gipson IK (2003) Mucin Gene Expression in Immortalized Human Corneal-Limbal and Conjunctival Epithelial Cell Lines. Invest Ophthalmol Vis Sci 44: 2496–2506. doi:10.1167/iovs.02-0851.

19. Miyairi I, Mahdi OS, Ouellette SP, Belland RJ, Byrne GI (2006) Different growth rates of Chlamydia trachomatis biovars reflect pathotype. J Infect Dis 194: 350–357. doi:10.1086/505432.

20. Kari L, Whitmire WM, Carlson JH, Crane DD, Reveneau N, et al. (2008) Pathogenic diversity among Chlamydia trachomatis ocular strains in nonhuman primates is affected by subtle genomic variations. J Infect Dis 197: 449–456. doi:10.1086/525285.

21. Kari L, Whitmire WM, Olivares-Zavaleta N, Goheen MM, Taylor LD, et al. (2011) A live-attenuated chlamydial vaccine protects against trachoma in nonhuman primates. J Exp Med 208: 2217–2223. doi:10.1084/jem.20111266.

22. Caldwell HD, Kuo CC, Kenny GE (1975) Antigenic analysis of Chlamydiae by two-dimensional immunoelectrophoresis. II. A trachoma-LGV-specific antigen. J Immunol 115: 969–975.

23. Roberts CH, Last A, Molina-Gonzalez S, Cassama E, Butcher R, et al. (2013) Development and evaluation of a next-generation digital PCR diagnostic assay for ocular Chlamydia trachomatis infections. J Clin Microbiol 51: 2195–2203. doi:10.1128/JCM.00622-13.

24. Last AR, Roberts C h, Cassama E, Nabicassa M, Molina-Gonzalez S, et al. (2014) Plasmid copy number and disease severity in naturally occurring ocular Chlamydia trachomatis infection. J Clin Microbiol 52: 324–327. doi:10.1128/JCM.02618-13.

25. Song L, Carlson JH, Whitmire WM, Kari L, Virtaneva K, et al. (2013) Chlamydia trachomatis Plasmid-Encoded Pgp4 Is a Transcriptional Regulator of Virulence-Associated Genes. Infect Immun 81: 636–644. doi:10.1128/IAI.01305-12.

26. Porcella SF, Carlson JH, Sturdevant DE, Sturdevant GL, Kanakabandi K, et al. (2015) Transcriptional Profiling of Human Epithelial Cells Infected with Plasmid-Bearing and Plasmid-Deficient Chlamydia trachomatis. Infect Immun 83: 534–543. doi:10.1128/IAI.02764-14.

27. Wang Y, Kahane S, Cutcliffe LT, Skilton RJ, Lambden PR, et al. (2013) Genetic Transformation of a Clinical (Genital Tract), Plasmid-Free Isolate of Chlamydia trachomatis: Engineering the Plasmid as a Cloning Vector. PLoS One 8: e59195. doi:10.1371/journal.pone.0059195.

28. Prozialeck WC, Fay MJ, Lamar PC, Pearson CA, Sigar I, et al. (2002) Chlamydia trachomatis disrupts N-cadherin-dependent cell-cell junctions and sequesters beta-catenin in human cervical epithelial cells. Infect Immun 70: 2605–2613.

29. Sun J, Kintner J, Schoborg R V (2008) The host adherens junction molecule nectin-1 is downregulated in Chlamydia trachomatis-infected genital epithelial cells. Microbiology 154: 1290–1299. doi:10.1099/mic.0.2007/015164-0.

30. Humphrys MS, Creasy T, Sun Y, Shetty AC, Chibucos MC, et al. (2013) Simultaneous transcriptional profiling of bacteria and their host cells. PLoS One 8: e80597. doi:10.1371/journal.pone.0080597.

31. Livak KJ, Schmittgen TD (2001) Analysis of relative gene expression data using real-time quantitative PCR and the 2(-Delta Delta C(T)) Method. Methods 25: 402–408. doi:10.1006/meth.2001.1262.

32. Ripa KT, Mårdh PA (1977) Cultivation of Chlamydia trachomatis in cycloheximide-treated mccoy cells. J Clin Microbiol 6: 328–331.

33. Sabet SF, Simmons J, Caldwell HD (1984) Enhancement of Chlamydia trachomatis infectious progeny by cultivation of HeLa 229 cells treated with DEAE-dextran and cycloheximide. J Clin Microbiol 20: 217–222.

34. Törmäkangas L, Markkula E, Lounatmaa K, Puolakkainen M (2010) Chlamydia pneumoniae infection in polarized epithelial cell lines. Infect Immun 78: 2714–2722. doi:10.1128/IAI.01456-09.

35. Buckner LR, Schust DJ, Ding J, Nagamatsu T, Beatty W, et al. (2011) Innate immune mediator profiles and their regulation in a novel polarized immortalized epithelial cell model derived from human endocervix. J Reprod Immunol 92: 8–20. doi:10.1016/j.jri.2011.08.002.

36. Sambuy Y, De Angelis I, Ranaldi G, Scarino ML, Stammati A, et al. (2005) The Caco-2 cell line as a model of the intestinal barrier: influence of cell and culture-related factors on Caco-2 cell functional characteristics. Cell Biol Toxicol 21: 1–26. doi:10.1007/s10565-005-0085-6.

37. Yu H, Cook TJ, Sinko PJ (1997) Evidence for diminished functional expression of intestinal transporters in Caco-2 cell monolayers at high passages. Pharm Res 14: 757–762.

38. Briske-Anderson MJ, Finley JW, Newman SM (1997) The influence of culture time and passage number on the morphological and physiological development of Caco-2 cells. Proc Soc Exp Biol Med 214: 248–257.

39. Wenger SL, Senft JR, Sargent LM, Bamezai R, Bairwa N, et al. (2004) Comparison of established cell lines at different passages by karyotype and comparative genomic hybridization. Biosci Rep 24: 631–639. doi:10.1007/s10540-005-2797-5.

40. Miyairi I, Laxton JD, Wang X, Obert CA, Arva Tatireddigari VRR, et al. (2011) Chlamydia psittaci Genetic Variants Differ in Virulence by Modulation of Host Immunity. J Infect Dis 204: 654–663. doi:10.1093/infdis/jir333.

41. Nans A, Saibil HR, Hayward RD (2014) Pathogen-host reorganization during Chlamydia invasion revealed by cryo-electron tomography. Cell Microbiol 16: 1457–1472. doi:10.1111/cmi.12310.

Chapter 5: Collection and processing of samples from individuals with active trachoma and controls for miRNA expression analysis

5.1 Study site

The Bijagós Archipelago of Guinea-Bissau is a group of ~88 islands found approximately 60km from the coast of Guinea-Bissau, West Africa (Figure 5.1). Guinea-Bissau has a human development index (HDI) of 0.396 and is ranked 177/196 in the world based on 2014 estimates [1]. The gross domestic product (GDP) estimate for 2014 was $598 per capita [2]. Infrastructure links and healthcare access in the Bijagós are poor and generally worse than on the mainland due to difficulties in accessibility; travel from Bissau to Bubaque, the capital of the Bijagós, can take ~10 hours by local dugout boat. Bad weather, strong tides and a lack of navigational aids or phone signal can make the journey dangerous. The inhabitants of the Bijagós are largely subsistence farmers and fishermen. The climate of the Bijagós Archipelago is humid and warm with an average daytime temperature of 27.3^{0}C and a rainy season between June and October. An initial population-based trachoma survey carried out on four islands in 2012 found that the overall prevalence of active trachoma was 11% and Ct infection was 18% [3]. In 1 to 9 year olds the prevalence of active trachoma was 22% and the prevalence of Ct infection in was 25% [3]. These rates are extremely high, particularly for an area that has adequate water access; trachoma is thought to be more prevalent in hot arid environments [4]. This prevalence of TF qualified the Bijagós for mass drug administration (MDA) with Azithromycin. The current World Health Organization (WHO) recommendations are to treat with three annual rounds of MDA all members of a district where the prevalence of active trachoma in 1-9 year olds (TF_{1-9}) is between 10-29%, alongside implementation of other components of the SAFE strategy [5]. Following three years of MDA TF_{1-9} should be reassessed with an impact survey, after which a decision is made whether to continue MDA (if TF_{1-9} remains >10%) or stop (if TF_{1-9} <5%). If a district has TF_{1-9} between 5-10%, within-district communities should be assessed and treated separately by the same principles and promotion of facial cleanliness and environmental improvements should continue. This fieldwork was planned so that samples could be collected from individuals on Islands that were treatment naïve i.e. before the initiation of MDA, which took place as scheduled immediately after collection of these samples (April 2014).

Figure 5.1. Map of Guinea-Bissau, West Africa. Source: [6]*.*

5.2 Study design

The aim of this study was to investigate miRNA expression in the conjunctiva of individuals with TF and concurrent Ct infection (TF Ct+) and in healthy controls with no clinical evidence of trachoma (N). Based on our knowledge of TF and Ct prevalence in this population before MDA treatment [3], we aimed to collect matched case-control samples from 200 children aged between 1 and 9. By collecting 100 samples from children with TF, we expected ~50 TF Ct+ and ~50 TF cases without current Ct infection (TF Ct-). Control samples were collected from children matched by age, gender and village. There were no prior data on miRNA expression in active trachoma upon which to base power calculations. We therefore used data from our previous study on miRNA expression in adults with scarring and inflammatory trachoma to calculate the sample size required (Chapter 6 [7]). Using these data we calculated that a sample size of 49 cases and 49 controls would give 81% power to detect a 2.3 fold change in miR expression in 1-9 year olds with 99% confidence (alpha = 0.0025). This alpha level would allow for adjustment for multiple comparisons of 20 miRNA and would still maintain power and confidence to detect the effect size.

Informed consent forms, spare data collection forms and certificates of ethical approval from both the LSHTM ethics committee and the Comitê Nacional de Ética e Saúde of Guinea-Bissau are attached in the appendix.

5.3 Logistics of sample collection

5.3.1 Field team, travel and equipment

The field base was on the largest island in the Bijagós Archipelago, Bubaque. The field team and fieldwork infrastructure were established previously by Dr Anna Last and included a boat and local skipper for travel to and from study islands. The field study was coordinated through The Gambia MRC Unit. Travel from The Gambia MRC Unit to Bissau, the capital of Guinea-Bissau, by road took ~7 hours, travelling through Senegal and then into Guinea-Bissau. Travel from Bissau to Bubaque by speedboat then took ~2 hours. A liquid nitrogen dry shipper was brought from The Gambia MRC Unit for sample storage in Bubaque. Due to the need to maintain a cold-chain, the field team returned to Bubaque at the end of each day of fieldwork to transfer samples into the dry shipper.

Travel to and from the islands each day by boat often took several hours. Many of the islands in the Bijagós Archipelago are surrounded by mangroves (Figure 5.2) and the skipper identified suitable landing sites where the field team could walk to the nearest village. This often involved walking through deep mud and forests. Tides had to be kept in mind to ensure access to the boat upon returning from the village; therefore the time available to collect samples on each island was often very limited. There was minimal or no mobile phone reception.

The field team consisted of a trained examiner that performed clinical grading and took swab samples (Dr. Anna Last), a nurse who collected informed consent and recorded initial screening data (Eunice Cassama or Eduardo Muscate), a clinical photographer who took conjunctival photographs (Rod Markham-David) and a data collector (Tamsyn Derrick). Data was collected using Eyescores ([8]; attached in appendix) an electronic system that was modified for the particular requirements of this field study. Equipment brought to each study site included: a laptop for running Eyescores, back-up data collection paper forms, consent forms, boxes containing tubes for swabs (pre-filled with RNA*later®* and with unique ID labels attached), a cool-box, envelopes for buccal swabs with unique ID labels, buccal brushes and ocular swabs, examination gloves, ethanol spray, a wipe-clean tablecloth, a 2.5X binocular magnifying loupe for

clinical examination, a camera for clinical photography (including spare batteries) and waste disposal bags (which were brought back to the field base for appropriate disposal).

Figure 5.2. Fieldwork in the Bijagós Archipelago. Clockwise from top left: walking to the boat through the mangroves; collecting samples from children in a village; searching for the boat; walking to a village on the island of Orangozinho.

5.3.2. Participant enrolment

The most time and cost-efficient way to collect samples from 1-9 year olds was to visit schools, however individual households were visited if this was not possible. On arrival at a school or household permission was requested from the headmaster or parent to screen children for trachoma. Headmasters are the children's guardians whilst they are at school and ethically, headmasters have the authority to give consent to take samples. Children were invited to have their eyes screened for evidence of active

trachoma using the WHO simplified grading system [9]. Cases were defined as individuals with *trachomatous inflammation – follicular* (TF) in both eyes. Controls were defined as individuals with no clinical evidence of follicles, papillary inflammation or cicatricial scarring. Upon identification of a case, informed consent was requested from the parent or headmaster. If consent was given the individual was graded for trachoma using the more detailed FPC grading system [10] and two swabs and a photograph were taken from their left tarsal conjunctiva. A buccal brush sample was taken for DNA analysis. Upon enrollment of a case, a control individual of the same age and gender (identified through screening) was invited to participate. If an exact age and sex match could not be found or did not wish to participate, a sample from the closest match was obtained. The examiner changed gloves between examination of each participant.

5.3.3 Sample collection and maintenance of the cold chain

Two swab samples were taken from the inverted left tarsal conjunctiva of each study participant using standard methodology [3,11]. Swabs were horizontally passed across the tarsal conjunctiva three times, rotating the swab by 1/3rd with each pass. Swabs were immediately and individually placed into sterile tubes filled with 250μl RNA*later®* (Ambion) and were stored in a cool-box filled with ice packs. Control swabs were pre-marked and selected at random (1 per 50 samples) and were passed three times 10cm in front of the eye, ensuring no contact was made. Control swabs were processed identically to sample swabs. Samples were transferred to a liquid nitrogen dry shipper within 8 hours. Every week the liquid nitrogen dry shipper containing samples was transported to Bissau on the mainland by speedboat or plane. To coincide with this trip a colleague from The Gambia MRC Unit drove to Bissau and brought a new empty liquid nitrogen dry shipper. Dry shippers were exchanged and samples were taken back to The Gambia MRC Unit for storage at -80^0C. Buccal brush samples were stored in envelopes (unsealed to allow them to dry) and were stored and transported at room temperature. Samples were subsequently shipped at -80^0C from The Gambia MRC Unit to LSHTM.

5.3.4 Summary

Sample collection took three weeks in total. One hundred and sixty three samples (81 cases, 82 controls) were collected from children living on 7 islands, 6 islands of which were treatment-naïve at the time of sample collection.

5.4 Optimization of total RNA and DNA extraction from clinical swabs

5.4.1. Methods

Cell culture

Human epithelial type 2 (HEp-2) cells were cultured in Minimum Essential Medium (MEM) (Gibco, ThermoFisher Scientific) supplemented with 1% gentamicin (Gibco), 10% fetal bovine serum (FBS) (Gibco), and 1% L-glutamine (Gibco) and were incubated at 37°C in 5% atmospheric CO_2. HEp-2 cells were infected with 0.5 MOI of Ct strain L2/434/Bu [12]. Cells were scraped into RNA*later*® (Ambion, ThermoFisher Scientific) 48 hours post infection and homogenate was stored at -80^0C. Where indicated in the text, ocular swab samples were taken from the conjunctivae of healthy volunteers at LSHTM using standard methodology (described above) and were stored at -80^0C in 250µl RNAlater® until use.

Nucleic acid purification

Extraction of nucleic material was performed using the Qiagen AllPrep RNA/DNA/miRNA Universal kit (Qiagen), Norgen total RNA/DNA purification kit (Norgen Biotek), Zymo Quick-RNA™ MiniPrep kit (Zymo Research) and the Zymo Direct-zol RNA MiniPrep kit (Zymo Research) where described and following the manufacturers instructions. β-mercaptoethanol was added to lysis buffers to inhibit RNAses where it was recommended by the kit manufacturer. RNA was quantified using Qubit® fluorometric quantitation (ThermoFisher Scientific) and NanoDrop spectrophotometry (ThermoFisher Scientific) and quality was assessed using an Agilent RNA 6000 nano kit on a 2100 Bioanalyzer instrument (Agilent technologies). Bead beating was performed using MP Bio lysing matrices and an MP Bio FastPrep-24 bead beater (MP Biomedicals).

Droplet-digital PCR assay for DNA quantitation

Droplet-digital PCR (ddPCR) was carried out to quantitate the Ct chromosomal gene omcB and *Homo sapiens* RNase P/MRP 30-kDa subunit gene (*RPP30*), as described previously [13,14]. Human *RPP30* primer and probe sequences were forward: 5' AGATTTGGACCTGCGAGCG 3', reverse: 5' GAGCGGCTGTCTCCACAAGT 3', probe: 5' [HEX] TTCTGACCTGAAGGCTCTGCGCG [BHQ1] 3'. Ct *omcB* primer and probe

sequences were forward: 5' GACACCAAAGCGAAAGACAACAC 3', reverse: 5'
ACTCATGAACCGGAGCAACCT 3', probe: 5' [FAM]
CCACAGCAAAGAGACTCCCGTAGACCG [BHQ1] 3'. ddPCR mix had a final volume
of 20µl and contained final concentrations of 1X ddPCR supermix (Bio-Rad), 0.3µM of
primer and probes and 4.95µl sample DNA. Droplet generation and droplet reading
was carried out according to the manufacturers instructions. Thermal cycling conditions
were as follows: 95°C hold for 10 minutes, followed by 40 cycles of 95°C for 10
seconds and 60°C for 20 seconds with a final hold of 98°C for 12 minutes. ddPCR was
performed on a Bio-Rad QX100 Instrument and data were collected using Quantalife
software (Bio-Rad). DNA copy number was calculated in R (https://www.r-project.org)
using a previously published script [13].

Quantitative polymerase chain reaction (qPCR) for RNA quantitation

Total RNA was reverse transcribed using miScript RTII kits with the HiFlex buffer
(Qiagen) to synthesize a cDNA library containing miRNA and mRNA. Six µl RNA was
added to the reverse transcription reaction, which had a final volume of 20µl. Reverse
transcription was performed following the manufacturers instructions. Ten µl cDNA was
diluted in 100µl dH$_2$O for use in qPCR in order to dilute out components of the reverse
transcription reaction. Upon initial optimization of qPCR, optimal exponential curves
were achieved by diluting the cDNA 1:10.

qPCR for mRNA was performed with Power SYBR Green PCR master mix
(ThermoFisher Scientific) according to the manufacturers instructions, using mRNA
specific primers for *Homo sapiens* Ribosomal Protein Large P0 gene (RPLP0). Primers
were designed using using NCBI gene data (http://www.ncbi.nlm.nih.gov/gene/),
Primer3 (http://primer3.wi.mit.edu) and SIM4 (http://pbil.univ-
lyon1.fr/members/duret/cours/inserm210604/exercise4/sim4.html) software. *RPLP0*
primer sequences were forward: 5' ATCTGCTTGGAGCCCACAT 3' and reverse: 5'
GCGACCTGGAAGTCCAACTA 3'. mRNA qPCR mix had a final volume of 5µl and
contained final concentrations of 1X Power SYBR green master mix, 0.25µM of forward
and reverse primers and 0.5µl sample cDNA. Cycling conditions were 10 minutes at
95°C followed by 40 cycles of 15 seconds at 95°C and 1 minute at 60°C.

qPCR for miRNA was performed using the miScript SYBR Green PCR kit with a
miScript Primer Assay for the endogeneous control small nucleolar RNA U6 (Qiagen),
as described previously (Chapter 6; [7]). miRNA qPCR mix had a final volume of 5µl

and contained 2.5µl miScript SYBR green PCR master mix, 0.5µl of specific miR forward primer assay, 0.5µl universal reverse primer assay, 0.5µl sample cDNA and 1µl dH$_2$0.

All qPCR was performed on a 7900HT thermal cycler (Applied Biosystems, ThermoFisher Scientific) and 4 technical repeats were performed for each sample/assay. Raw cycle thresholds were analyzed in R.

5.4.2. Purpose of optimization

The purpose of this fieldwork was to obtain clinical samples for small RNA analysis by Illumina TruSeq small RNA sequencing and qPCR. For Illumina TruSeq small RNA sequencing a total RNA starting input of 1µg in 5µl and an RNA Integrity Number (RIN) ≥8 was required. DNA was also required from these samples for the diagnosis of Ct infection and for possible future DNA methylation studies or Ct genome sequencing. For methylation studies buccal brush samples were collected to provide a DNA background sample for each individual and these buccal samples were processed separately. In our previous study on miRNA expression using genetic material from clinical swab samples, 23/63 (35.6%) samples tested on low density Taqman qPCR arrays were discarded from the analysis due to a low concentration of genetic material (Chapter 3 [7]). The isolation of total RNA and DNA of a high quality and quantity from ocular swabs was therefore imperative.

Two swab samples were taken from the left conjunctiva of each individual in order to maximize the quantity of genetic material that could be isolated. The two swabs could be pooled together for extraction of total RNA and DNA (most cost efficient), or they could be processed separately, in which case RNA could be isolated from one swab and DNA from the other, or RNA and DNA could be isolated from both. A variety of commercial kits are available for genetic material extraction. It is thought that a lower yield is achieved when isolating multiple fractions from one sample, particularly for miRNA, which is already at low concentration. This is likely due to the increased number of washes the sample undergoes. The risk of sample loss, especially when using filter columns, is also higher when samples are of a lower concentration. In this case a higher yield and quality might be obtained by extracting total RNA only from one swab (and DNA from the other). It is unclear however what variation exists in the cellular fractions collected by the first and second swab and what impact this might have when diagnosing and quantifying Ct from one swab and relating it to

transcriptional data from the other. Summaries of the extraction kits compared during optimization are given in Table 5.1.

Table 5.1. Summary of the commercially available extraction kits tested.

Kit	Fractions obtained	Format	Lysis method
Qiagen AllPrep RNA/DNA/miRNA Universal kit	RNA, DNA, miRNA	Spin-column	Guanidinium thiocyanate
Norgen total RNA/DNA purification kit	Total RNA, DNA	Spin-column	Guanidinium thiocyanate
Zymo Quick-RNA™ MiniPrep kit	Total RNA	Spin-column	Guanidinium thiocyanate
Zymo Direct-zol RNA MiniPrep kit	Total RNA	Spin-column	Trizol (Guanidinium thiocyanate-phenol-chloroform)

Should sufficient DNA remain after the primary objectives these samples could also be of use for future analysis of the ocular microbiome. Bead beating aids the lysis of some bacterial cell walls during the lysis stage of DNA purification. Small beads were added to the sample tube with lysis buffer and the tube was vortexed in a specialized tissue homogeniser (MP Bio FastPrep-24 bead beater (MP Biomedicals)) at high intensity. Bead beating is thought to be an essential step for obtaining high yields of DNA (particularly from gram-positive bacteria) and for obtaining an accurate representation of bacterial species present in clinical samples [15]. Bead beating was tested in this optimization process in order to permit future microbiome analysis in these samples.

The material used for optimization was derived from cultured cells or from ocular swabs taken from colleagues at the LSHTM. DNA carriers can enhance sample recovery of low concentration samples during the extraction process, however they were not used in case of interference with downstream applications and to enable quantitation of true sample concentration.

5.4.3 Qiagen and Norgen extraction kits with MP Bio Lysing matrix beads

Qiagen and Norgen kits that purify multiple fractions were tested with inclusion of a bead beating step in the initial lysis stage. A variety of different bead matrices are commercially available, optimized for various extraction goals. Upon consultation with MP Biomedicals, lysing matrices A and E were recommended for this application of miRNA, RNA and DNA extraction from ocular swab samples. Lysing matrix E (LE) contains 1.4 mm ceramic spheres, 0.1 mm silica spheres, and one 4 mm glass bead. Lysing matrix A (LA) contains garnet matrix and one 1/4 inch ceramic sphere. Ct (L2) infected HEp-2 cells were scraped into RNA*later®* and stored in aliquots at -80^{0}C. One hundred microliters of this human cell/Ct homogenate was pipetted onto Dacron swabs and swabs were placed in a 2ml tube containing 250µl RNA*later®*, using the exact procedure and reagents used in the field.

Four swabs were extracted using the Norgen total RNA/DNA purification kit, two of which were lysed with LE and two with LA. Another four swabs were extracted using the Qiagen Universal RNA/DNA/miRNA kit, two of which were lysed with LE and two with LA. Swabs were removed from RNA*later®* and were added to 2ml tubes containing lysing matrices. Six hundred microliters of Qiagen or Norgen lysis buffer was added to ensure the swab was completely submerged. All 8 swabs were bead beaten for 2 1-minute pulses at 6.0m/s. This was advised to be long enough to pulverize the swab without causing damage to the genetic material. Two 1-minute pulses were performed with a 5 minute interval in-between to prevent over-heating (sample temperature is thought to increase by 10^{0}C for every minute of bead beating). Tubes were centrifuged at 4°C for 10 minutes to pellet debris. The lysate was collected and added to the filter column of the relevant purification kit. Genetic material was extracted following the manufacturers instructions. ddPCR was performed to quantify human and chlamydial DNA. Total RNA (Norgen kit) and miRNA (Qiagen kit) fractions were reverse transcribed and qPCR was performed for the endogenous control small nucleolar RNA U6 and miR-146a to determine miRNA concentration. NanoDrop was performed on RNA and DNA (data not shown). Results are shown in Table 5.2.

Table 5.2. Yield and quality of miRNA and DNA obtained using two bead beating methods with Qiagen and Norgen extraction kits.

Lysis and extraction method	ddPCR DNA[a]		qPCR miRNA[b]	
	Ct omcB	Human RPP30	U6	miR-146a
1 LE Qiagen	0.00	0.00	30.49	≥ 40
2 LE Qiagen	0.00	0.76	≥ 40	≥ 40
1 LA Qiagen	18.62	0.72	≥ 40	≥ 40
2 LA Qiagen	61.77	1.29	33.32	≥ 40
1 LE Norgen*	1275.43	45.77	22.70	32.24
2 LE Norgen	172.87	6.22	24.05	32.60
1 LA Norgen	31.55	2.08	24.64	32.49
2 LA Norgen	38.17	1.67	24.15	33.39

Swabs used in this experiment were spiked with cultured cells.

[a] DNA concentration in copies/µl of extracted DNA is shown

[b] Mean cycle threshold is shown of four technical repeats

LE: Lysing matrix E, LA: Lysing matrix A.

1 and 2 = first and second repeat of each condition.

* Sample was processed with amendments to the protocol

RNA and DNA yields were poor from the four extraction variations. Despite adding 600µl lysis buffer, very little lysate was recovered from the bead beaten tubes even after centrifugation. Beads and swab debris took up most of the space in the 2ml tube, particularly the large glass and ceramic beads. One Norgen LE sample was accidentally lost during the extraction process. It was repeated with amendments: the large ceramic bead was removed from the tube, 800µl lysis buffer was added and it was pulsed for 40 seconds at 6.0m/s rather than 2 minutes (sample indicated with a *). Much more lysate was recovered from this swab and DNA and miRNA concentrations were ~10 fold higher.

NanoDrop data (not shown) was highly variable and did not correlate with ddPCR and qPCR values. NanoDrop is inaccurate at low concentrations as values are highly affected by the presence of contaminants. Three Qiagen RNA samples had very good concentrations by NanoDrop, however the absorbance was high and peaks were apparent at 230nm for these three samples. Guanidine isothiocyanate absorbs at 230nm therefore this peak was likely due to buffer carryover. Guanidine isothiocyanate is a chaotropic agent and a protein denaturant, therefore its presence in the RNA sample could have inhibited the enzymes used in reverse transcription and qPCR, which might explain why miRNA was barely detected in these samples by qPCR.

Guanidine isothiocyanate is also present in the Norgen lysis buffer however no carry-over was detected.

5.4.4 Norgen extraction kit with and without bead beating

In order to validate these results the effect of bead beating was investigated further using the Norgen purification kit. Eight ocular swabs (two from each volunteer) were taken from colleagues by a clinician (Dr Anna Last) using the same method and reagents used in the field. Four swabs (one from each volunteer) were removed from RNA*later®* and placed into LE tubes containing 600µl Norgen lysis buffer. These were bead beaten for 40 seconds at 6.0m/s and centrifuged at 4°C for 30 seconds at full speed. Roughly 500µl lysate was recovered from these swabs. The other four swabs were placed into a 2ml tube containing 600µl Norgen lysis buffer and were vortexed for 1 minute without beads. Roughly 600µl lysate was recovered from these swabs. Total RNA and DNA was extracted from all 8 swabs following the manufacturers instructions and DNA concentration was quantified by ddPCR (Table 5.3).

Table 5.3. DNA yield obtained using the Norgen kit with and without bead beating.

Lysis method	Human RPP30[a]
LE 1	80.44
LE 2	27.69
LE 3	10.58
LE 4	23.42
Vortex 1	419.07
Vortex 2	604.38
Vortex 3	428.85
Vortex 4	755.48

[a] DNA concentration in copies/µl of extracted DNA is shown
LE: Lysing matrix E, Vortex: Vortex only
1-4: Volunteer ID

Around 10 fold less DNA was obtained by bead beating relative to vortexing alone. This loss could be due to the high temperature and additional processing to which samples were exposed, the lower volume of lysis buffer recovered or to shearing and damage of nucleic acids by the mechanical force and abrasion of beat beating (aimed at lysing tough bacterial or fungal cell walls). Beat beating is advantageous for investigation of the microbiome or for lysis of tough sample material. As this was not

necessary and was not a primary research objective for these samples, bead beating was excluded from further use.

5.4.5 Comparison of extraction kits with one or two swabs per tube during lysis

The next step was to determine whether the two swabs from each individual should be lysed and extracted together or separately. Lysing swabs separately before pooling might increase the risk of cross-contamination however it might increase yield. Material from HEp-2 cells scraped into RNA*later®* and stored at -80^{0}C was used. One hundred microliters of this material was pipetted onto each swab and swabs were added to tubes containing 250µl RNA*later®*. Tubes were stored at -80^{0}C until extraction. All swabs were extracted within one day.

Norgen total RNA/DNA purification, Qiagen Universal RNA/DNA/miRNA and Zymo Quick-RNA™ MiniPrep kits were compared. Three repeats were performed of two variations: a) one swab was placed into a tube containing 600µl lysis buffer and b) two swabs were placed into one tube containing 600µl lysis buffer and were extracted as one. The Qiagen kit was included for the one swab condition only in order to validate previous results (Table 5.2). Swabs in lysis buffer were vortexed for 1 minute then centrifuged at 4°C for 1 minute. Extraction was performed following the manufacturers instructions. Roughly the same quantity of lysate was recovered from tubes containing one and two swabs.

The concentration and quality of RNA was assessed using NanoDrop (data not shown), Qubit and Agilent bioanalyser. DNA was quantified by ddPCR and mRNA and miRNA concentration were measured by qPCR for the endogenous controls RPLP0 and U6. Results are shown in Table 5.4. The highest yield and quality of miRNA, RNA and DNA were obtained by vortexing one swab individually and extracting material using the Norgen total RNA/DNA purification kit, despite there being double the input material in the two-swab condition. The Qiagen kit performed well for DNA but very poorly for RNA (no additional RNA wash steps were included). Zymo Quick-RNA™ MiniPrep kit performed worse than the Norgen kit and purified RNA only.

Table 5.4. Comparison of three extraction kits with one or two swabs per tube during lysis

Lysis and extraction method	DNA RPP30[a]	mRNA RPLP0[b]	miRNA U6[b]	Agilent RIN	Agilent RNA pg/ul	Qubit RNA ng/ml
Norgen:						
1 swab	114.21	22.66	18.93	9.4	4722.9	246
1 swab	67.99	23.65	20.7	9.3	6285	108
1 swab	108.43	22.14	19.66			199
2 swabs	51.55	26.15	21.33	NA	30	97
2 swabs	44.00	33.15	25.44	8.9	878	<20
2 swabs	38.80	≥ 40	≥ 40			<20
Zymo Quick-Prep:						
1 swab	-	30.86	≥ 40	9.1	51	30
1 swab	-	24.33	30.6	NA	2.3	<20
1 swab	-	36.81	≥ 40			<20
2 swabs	-	29.1	26.06	7.2	211	46.6
2 swabs	-	35.02	29.55	NA	9	21
2 swabs	-	≥ 40	≥ 40			<20
Qiagen:						
1 swab	103.55	≥ 40	≥ 40	NA	3.2	28.4
1 swab	28.31	≥ 40	≥ 40	NA	5.7	<20
1 swab	401.74	≥ 40	≥ 40			<20

Swabs used in this experiment were spiked with cultured cells.

[a] *DNA concentration in copies/µl of extracted DNA is shown*

[b] *Mean cycle threshold is shown of four technical repeats*

5.4.6. Comparison of Norgen and Zymo Direct-zol extraction kits and lysis methods

The Norgen kit was compared to the Zymo Direct-zol total RNA extraction kit, which differs to the others in that it uses Trizol. Conditions were: a) One swab vortexed and processed individually in 600µl lysis buffer and b) two swabs vortexed in separate tubes in 400µl lysis buffer and the 800µl combined lysate was pooled for extraction on one column. Two swabs were vortexed and processed as one in 600µl lysis buffer again using the Norgen kit, which confirmed the poor results using this method (Table 5.5). Surprisingly no RNA was detected using the Zymo Direct-zol kit. Lysing two swabs in individual tubes and combining the lysate for extraction on one column provided the highest quality and quantity of miRNA, RNA and DNA. RNA extracted using the Norgen kit had RIN values ≥8, sufficient for small RNA sequencing.

Table 5.5. Comparison of lysis methods using Norgen and Zymo Direct-Zol kits

Lysis and extraction method	DNA RPP30[a]	mRNA RPLP0[b]	miRNA U6[b]	Agilent RIN	Agilent RNA pg/ul	Qubit RNA ng/ml
Norgen:						
1 swab 600µl LB	377.74	22.59	19.34	8.4	24160	411
1 swab 600µl LB	247.53	23.52	25.78	8.2	9716	306
(1 swab 400µl LB)*2	559.94	22.19	18.55	8	11433	477
(1 swab 400µl LB)*2	343.08	21.5	17.36	8	18515	620
2 swabs 600µl LB	213.31	22.92	18.65	8.2	11179	470
2 swabs 600µl LB	217.31	25.28	20.1	3.5	880	177
Zymo Direct-zol:						
1 swab 600µl LB		≥ 40	≥ 40	NA	11	<20
1 swab 600µl LB		≥ 40	≥ 40	NA	21	<20
(1 swab 400µl LB)*2		≥ 40	≥ 40	NA	5.4	<20
(1 swab 400µl LB)*2		≥ 40	≥ 40	NA	9	<20

Swabs used in this experiment were spiked with cultured cells.

[a] DNA concentration in copies/µl of extracted DNA is shown

[b] Mean cycle threshold is shown of four technical repeats

LB: Lysis buffer

Zymo Direct-zol RNA samples had a small peak at 270nm on the absorbance spectrum by NanoDrop (data not shown) characteristic of phenol contamination. Contamination with Trizol or chaotropic agents could inhibit the PCR, however the RNA concentration was also very low using fluorometric (Qubit) and spectrophotometric (NanoDrop) methods. Despite swabs being removed from RNA*later®* before addition to the Tri-reagent, it is possible that excess RNA*later®* carryover interfered with the extraction chemistry such that the RNA did not enter the aqueous phase. This was not investigated further as adequate results for total RNA and DNA were obtained using the Norgen kit and the Zymo Direct-zol kit isolates RNA only.

5.4.7. Optimization summary

For the samples tested in this study, vortexing swabs individually, pooling the lysate and extracting total RNA and DNA using the Norgen purification kit was the most cost-efficient method and yielded high quality and quantity nucleic acids. Bead beating was detrimental to yield and quality of nucleic acids and would perhaps only be worthwhile

for these samples if isolating DNA from bacteria for microbiome analysis. A previous microbiome study using material from ocular swabs used Mo Bio extraction and bead beating kits and did not isolate more fragile RNA species from the same samples [16]. The study achieved an average read depth of 7684 per sample using Roche-454 deep sequencing and retained 84% (220/260) samples after quality control. It is possible there is a trade-off of a loss of overall (or host) DNA in order to obtain DNA from a representative sample of the bacterial species present, however this finding may be limited to the reagents tested in this study, which was not fully optimized for bead beating. The Qiagen kit yielded a good quantity of DNA but guanidine isothiocyanate carryover was detected in the RNA, which likely inhibited downstream reactions. The Zymo Quick-prep mini kit yielded RNA of a lower concentration and quality to Norgen and the Zymo Direct-zol kit did not work at all in these experiments. This is unlikely to be an accurate reflection of the kit, as Trizol is thought to extract RNA of the highest quality and yield. Further optimization of this kit could reveal it's true potential, however this was not undertaken in the current study due to the disadvantage of the kit only isolating RNA.

5.5 Summary

All clinical samples were subsequently processed by lysing two swabs from each individual separately and pooling the lysate for extraction with the Norgen kit. Gloves and workspace were cleaned between processing of each sample to minimize cross-contamination. Of the 163 clinical samples extracted, 51 had a total RNA RIN value ≥ 8. None of the 163 samples had a total RNA concentration sufficient to meet the Illumina input requirements of 1µg in 5µl total RNA. The highest sample concentration was 74.6ng/µl (373ng in 5µl). Ten case-control samples were chosen of the highest RNA concentration and quality and were normalized to the concentration of the lowest sample (120ng in 5µl) for entry into the sequencing pipeline. The sample selection process is described in Figure 5.3. Illumina TruSeq small RNA sequencing was performed successfully and results are described in Chapter 5.
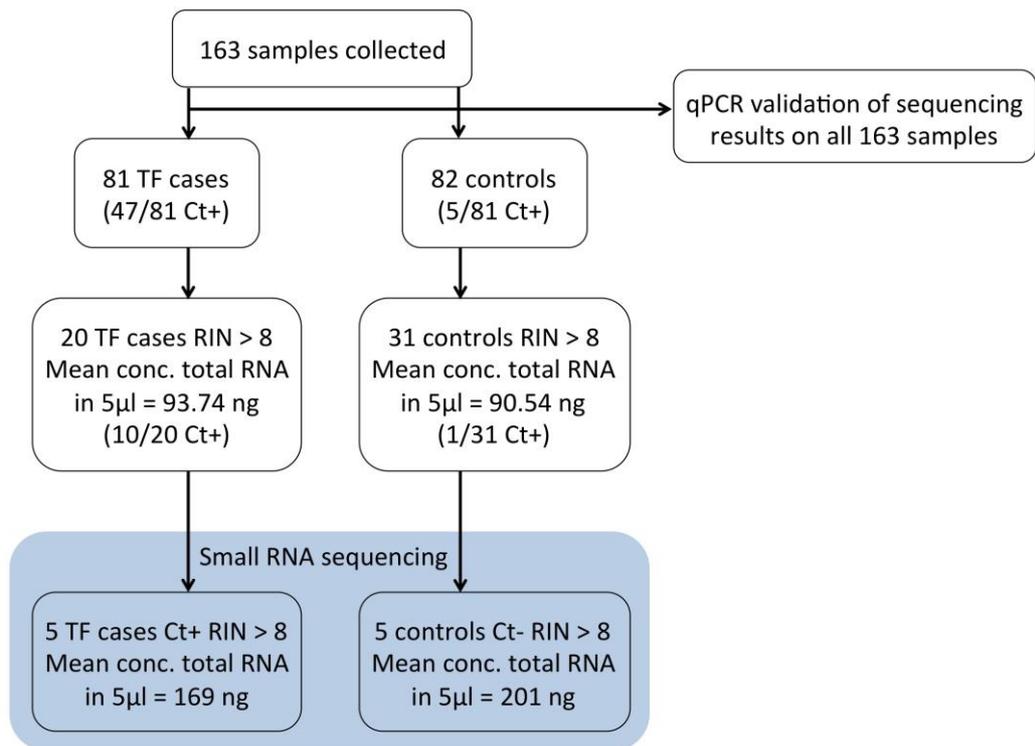
Figure 5.3. Sample selection process for small RNA sequencing. Ct+ = Ct positive, Ct- = Ct negative.

5.6 References

1. Programme UND (n.d.) 2014 Human Development Report Summary: 2014.
2. 'Guinea-Bissau'. International Monetary Fund (n.d.). Available: http://www.imf.org/external/pubs/ft/weo/2014/02/weodata/weorept.aspx?sy=201 3&ey=2019&scsm=1&ssd=1&sort=country&ds=.&br=1&c=654&s=NGDPD%2C NGDPDPC%2CPPPGDP%2CPPPPC%2CLP&grp=0&a=&pr.x=36&pr.y=17. Accessed 4 September 2015.
3. Last AR, Burr SE, Weiss HA, Harding-Esch EM, Cassama E, et al. (2014) Risk Factors for Active Trachoma and Ocular Chlamydia trachomatis Infection in Treatment-Naïve Trachoma-Hyperendemic Communities of the Bijagós Archipelago, Guinea Bissau. PLoS Negl Trop Dis 8: e2900. doi:10.1371/journal.pntd.0002900.
4. Ramesh A, Kovats S, Haslam D, Schmidt E, Gilbert CE (2013) The impact of climatic risk factors on the prevalence, distribution, and severity of acute and chronic trachoma. PLoS Negl Trop Dis 7: e2513. doi:10.1371/journal.pntd.0002513.
5. World Health Organisation (2010) WHO Report on the 3rd Global Scientific Meeting on Trachoma.
6. Infoplease. Guinea-Bissau (n.d.).
7. Derrick T, Roberts C h., Rajasekhar M, Burr SE, Joof H, et al. (2013) Conjunctival MicroRNA Expression in Inflammatory Trachomatous Scarring. PLoS Negl Trop Dis 7: e2117. doi:10.1371/journal.pntd.0002117.
8. Roberts CH, Mtuy T, Derrick T, Burton MJ, Holland MJ (2013) Eyescores: an open platform for secure electronic data and photographic evidence collection in ophthalmological field studies. Br J Ophthalmol: bjophthalmol – 2012–302653 – . doi:10.1136/bjophthalmol-2012-302653.
9. WHO simplified trachoma grading system. (2004). Community Eye Health 17: 68.
10. Dawson CR, Jones BR TM, Dawson CR, Jones BR, Tarizzo ML, World Health Organization (1981) Guide to trachoma control in programmes for the prevention of blindness. 56 p.
11. Keenan JD, Lakew T, Alemayehu W, Melese M, Porco TC, et al. (2010) Clinical activity and polymerase chain reaction evidence of chlamydial infection after repeated mass antibiotic treatments for trachoma. Am J Trop Med Hyg 82: 482–487. doi:10.4269/ajtmh.2010.09-0315.
12. Caldwell HD, Kuo CC, Kenny GE (1975) Antigenic analysis of Chlamydiae by two-dimensional immunoelectrophoresis. II. A trachoma-LGV-specific antigen. J Immunol 115: 969–975.
13. Roberts CH, Last A, Molina-Gonzalez S, Cassama E, Butcher R, et al. (2013) Development and evaluation of a next-generation digital PCR diagnostic assay for ocular Chlamydia trachomatis infections. J Clin Microbiol 51: 2195–2203. doi:10.1128/JCM.00622-13.
14. Last AR, Roberts C h, Cassama E, Nabicassa M, Molina-Gonzalez S, et al. (2014) Plasmid copy number and disease severity in naturally occurring ocular Chlamydia trachomatis infection. J Clin Microbiol 52: 324–327. doi:10.1128/JCM.02618-13.
15. Guo F, Zhang T (2012) Biases during DNA extraction of activated sludge

samples revealed by high throughput sequencing. Appl Microbiol Biotechnol 97: 4607–4616. doi:10.1007/s00253-012-4244-4.

16. Zhou Y, Holland MJ, Makalo P, Joof H, Roberts C h, et al. (2014) The conjunctival microbiome in health and trachomatous disease: a case control study. Genome Med 6: 99. doi:10.1186/s13073-014-0099-x.

Chapter 6: Research article: Inverse relationship between microRNA-155 and -184 expression with increasing conjunctival inflammation during ocular *Chlamydia trachomatis* infection

RESEARCH PAPER COVER SHEET

PLEASE NOTE THAT A COVER SHEET MUST BE COMPLETED FOR EACH RESEARCH PAPER INCLUDED IN A THESIS.

SECTION A – Student Details

Student	Tamsyn Derrick
Principle Supervisor	Martin Holland
Thesis Title	The Role of Epigenetics and Type 2 Epithelial-Mesenchymal Transitions in Trachoma

If the Research Paper has previously been published please complete Section B, if not please move to Section C

SECTION B – Paper already published

Where was the work published?	BMC Infectious Diseases		
When was the work published?	3.2.2016		
If the work was published prior to registration for your research degree, give a brief rationale for its inclusion	NA		
Have you retained the copyright for the work?*	Article is open access under a Creative Commons Attribution 4.0 International liicense	Was the work subject to academic peer review?	Yes

*If yes, please attach evidence of retention. If no, or if the work is being included in its published format, please attach evidence of permission from the copyright holder (publisher or other author) to include this work.

SECTION C – Prepared for publication, but not yet published

Where is the work intended to be published?	
Please list the paper's authors in the intended authorship order:	
Stage of publication	

SECTION D – Multi-authored work

For multi-authored work, give full details of your role in the research included in the paper and in the preparation of the paper. (Attach a further sheet if necessary)	I designed the study, conducted the fieldwork, performed all laboratory work, analysed the data, interpreted the findings and wrote the manuscript.

Student signature: **Date:** 26.9.15
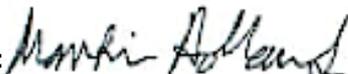
Supervisor signature: **Date:** 28.9.15

Inverse relationship between microRNA-155 and -184 expression with increasing conjunctival inflammation during ocular *Chlamydia trachomatis* infection

Tamsyn Derrick[1], Anna R. Last[1], Sarah E. Burr[1,2], Chrissy H Roberts[1], Meno Nabicassa[3], Eunice Cassama[3], Robin L. Bailey[1], David C. W. Mabey[1], Matthew J. Burton[1], Martin J. Holland[1]

[1]Faculty of Infectious and Tropical Diseases, London School of Hygiene and Tropical Medicine, London, United Kingdom

[2]Disease Control and Elimination Theme, Medical Research Council Unit, The Gambia

[3]Programa Nacional de Saude de Visao, Ministerio de Saude Publica, Bissau, Guinea Bissau

Corresponding Author: Tamsyn Derrick (tamsyn.derrick@lshtm.ac.uk)

Anna.Last@lshtm.ac.uk, Sarah.Burr@lshtm.ac.uk, Chrissy.Roberts@lshtm.ac.uk, eunicassama27@gmail.com, pnlcegueira@yahoo.com.br, Robin.Bailey@lshtm.ac.uk, David.Mabey@lshtm.ac.uk, Matthew.Burton@lshtm.ac.uk, Martin.holland@lshtm.ac.uk

Abstract

Background: Trachoma, a preventable blinding eye disease, is initiated by ocular infection with *Chlamydia trachomatis* (Ct). We previously showed that microRNAs (miR) -147b and miR-1285 were up-regulated in inflammatory trachomatous scarring. During the initial stage of disease, follicular trachoma with current Ct infection, the differential expression of miR has not yet been investigated.

Methods: Conjunctival samples were collected from 163 children aged 1-9 years old living in a trachoma-endemic region of Guinea Bissau, West Africa. Small RNA sequencing (RNAseq) was carried out on samples from five children with follicular trachoma and current Ct infection and five children with healthy conjunctivae and no Ct infection. Small RNAseq was also carried out on human epithelial cell lines infected with ocular Ct strains A2497 and isogenic plasmid-free A2497 *in vitro.* Results were validated by quantitative PCR (qPCR) in 163 clinical samples.

Results: Differential expression of RNAseq data identified 12 miR with changes in relative expression during follicular trachoma, of which 9 were confirmed as differentially expressed by qPCR (miR-155, miR-150, miR-142, miR-181b, miR-181a, miR-342, miR-132, miR-4728 and miR-184). MiR-155 and miR-184 expression had a direct relationship with the degree of clinical inflammation. MiR-155 was up-regulated (OR=2.533 ((95% CI = 1.291 – 4.971); P=0.0069) and miR-184 was down-regulated (OR=0.416 ((95% CI = 0.300 – 0.578); P= $1.61*10^{-7}$) as the severity of clinical inflammation increased. Differential miR expression was not detected in HEp-2 or HCjE epithelial cells 48 hours post infection with Ct *in vitro*. HCjE cells, a conjunctival epithelial cell line, had a markedly different miR background expression compared to HEp-2 cells.

Conclusions: In follicular trachoma, expression of miR-155 and miR-184 is correlated with the severity of inflammation. This likely reflects host regulation of the immune response and a prolonged period of wound healing following the clearance of Ct. Prolonged healing may be associated with subsequent development of scarring trachoma.

Keywords: Chlamydia trachomatis; trachoma; miRNA; Inflammation; RNAseq; miR-155; miR-184; follicular trachoma.

Background

Trachoma is the leading infectious cause of blindness worldwide and is initiated by infection of the conjunctival epithelium with the obligate intracellular bacterium *Chlamydia trachomatis* (Ct). In trachoma-endemic areas children suffer repeated episodes of infection and the effects of the associated immune response, which is characterized by a follicular conjunctivitis. In some individuals this triggers a chronic inflammatory response, causing scarring of the eyelid over the course of the lifetime of the individual, often in the absence of detectable Ct infection [1]. Conjunctival fibrosis causes entropion (in-turning of the lid margin) and subsequent trichiasis, the inward turning of eyelashes, which scratch the cornea causing mechanical damage leading to blinding corneal opacification in a proportion of cases. The mechanisms of fibrotic progression in the absence of Ct infection and the reason why only some individuals in trachoma-endemic communities develop scarring despite similar exposure to infection are unknown.

Trachoma is endemic in 51 countries and is associated with visual impairment in 2.2 million people worldwide (of whom 1.2 million are irreversibly blind) [2]. The World Health Organization (WHO) strategy for the elimination of trachoma ("SAFE") consists of mass distribution of antibiotics (MDA) to communities to treat infection, surgery for trichiasis, promotion of facial hygiene and environmental and sanitation improvements such as provision of latrines to reduce transmission [3].

Whilst MDA is generally effective, there are concerns regarding its efficacy in hyper-endemic settings such as Ethiopia, where trachoma prevalence remains high despite >5 years of biannual MDA in some districts [4]. High recurrence rates of trichiasis following lid margin rotation surgery [5] and the presence of follicular trachoma and incident scarring in populations where Ct infection prevalence has been controlled [1, 6] are also of concern. In order to develop an anti-Ct vaccine that invokes a protective immune response and to design therapeutic treatments to halt progressive scarring, a better understanding of the immunopathology of chlamydial disease is required.

Experimental conjunctival Ct infection of human volunteers found the incubation period to be between 2 and 19 days post inoculation [7, 8], whilst mathematical models based on data from disease and infection studies in trachoma-endemic communities estimated this period as around 17 days [9]. Although some infected individuals remain

asymptomatic, many will develop clinical signs of follicular trachoma, such as lymphoid follicles and papillary inflammation. The median duration of follicular trachoma has been observed to decrease with age; from 13.2 weeks in 0-4 year olds to 1.7 weeks in individuals of 15 years or more [10]. The cumulative incidence rate of follicular trachoma is also reduced threefold with age, implying that some degree of protective immunity is acquired [10]. There is a lag time between the clearance of infection and the disappearance of clinical signs of follicular trachoma on both an individual (median time of five weeks [9]) and population level [11, 12].

MicroRNA (miR) are small single-stranded RNA species that regulate gene expression post-transcriptionally. MiR can have profound effects on health and disease and there are many examples in which abnormal expression of a single [13] or small number [14] of miR are associated with disease. We have previously found that miR-147b and miR-1285 are up-regulated in adult cases of scarring and inflammatory trachoma [15]. Others have investigated the miR response to Ct and *C. muridarum* (Cm) in the murine genital tract [16–18], but the miR response to Ct in human disease has not yet been reported. In this study we examine the miR response in clinical cases of follicular trachoma with Ct infection and during Ct infection of cultured human epithelial cells.

Methods

Ethics, consent and permissions

The study was conducted in accordance with the declaration of Helsinki and was approved by the Ethics committee of the London School of Hygiene and Tropical Medicine (reference: 6433) and the Comité Nacional de Ética em Saúde of Guinea Bissau (reference: 012/CNES/INASA/2013). Written informed consent was obtained from a parent or guardian before participants were enrolled in the study.

Clinical sample collection

Prospective samples were collected from children aged from 1 to 9 years residing on seven islands of the Bijagos Archipelago, Guinea Bissau, 6 islands of which were trachoma treatment naïve at the time of sample collection. Children were screened for clinical signs of trachoma by a trained clinician using the WHO 1981 FPC scoring system [19]. Individuals presenting with follicular trachoma scores of "F2" or "F3" were roughly equivalent to "Trachomatous Inflammation − Follicular (TF)" in the WHO simplified trachoma grading system [20] and are hereafter referred to as TF cases. Individuals with pronounced papillary hypertrophy and diffuse infiltration (score "P3") were equivalent to "Trachomatous Inflammation − Intense (TI)" in the WHO simplified grading system. Individuals with no clinical signs of follicles (F0), papillary hypertrophy (P0) or conjunctival scarring (C0) were classed as normal healthy controls (N). A case was defined as a child with TF in both eyes irrespective of P score. A healthy control was enrolled for each TF case where a case was defined as an individual with an F-score ≥F2. Cases and controls were matched by age, gender and village.

Two conjunctival samples were taken from the left upper tarsal conjunctiva of each participant with Dacron swabs (Puritan, Guilford, ME, USA) using standard methodology [21, 22]. Swabs were stored in RNAlater (Ambion, Life technologies, Carlsbad CA, USA) and kept in a cold chain in the field before subsequent storage at -80°C. The two swabs from each individual were pooled for RNA and DNA extraction.

In vitro culture and Ct infection of human epithelial cell lines

Human epithelial type 2 (HEp-2) cells were cultured in Minimum Essential Medium

(MEM) (Gibco, Life Technologies) supplemented with 1% gentamicin (Gibco), 10% fetal bovine serum (FBS) (Gibco), and 1% L-glutamine (Gibco). For the *in vitro* experiments, cells were seeded in 12 well plates at $3x10^5$ cells per well in MEM. An immortalized human conjunctival epithelial cell line (HCjE) was cultured in Keratinocyte serum free medium (K-sfm) (Gibco) supplemented with 25μg/ml bovine pituitary extract (Gibco), 0.2ng/ml epidermal growth factor (Gibco), 0.4mM $CaCl_2$ (Sigma, St. Louis, MO, USA) and 5% gentamicin and incubated at 37°C with 5% atmospheric CO_2. For experiments, HCjE cells were seeded in 12 well plates at $3x10^5$ cells per well in 1:1 K-sfm [with supplements]: Dulbecco's Modified Eagle Medium: Nutrient Mixture F12 (DMEM/F12) [with 10% FBS, 1% gentamicin and 1% L-glutamine] (Gibco) and were switched to DMEM/F12 [with supplements] upon infection 24 hours later.

HEp-2 and HCjE cells were infected with 3 different ocular-derived serovar A Ct strains: A2497 (described in [23]), its plasmid cured counterpart (A2497P-) [24] and A/HAR-13 [23]. Cells were infected 24 hours after seeding at a multiplicity of infection (MOI) of 1 and without the addition of cycloheximide. Ct cultures and mock-infected cells were centrifuged at 1800 r.p.m. for 1 hr to facilitate infection and were then incubated at 37°C in 5% CO_2. Six replicates were carried out for each biological condition. At 48 hours post-infection (hpi), media was removed and cells were washed in 1X phosphate-buffered saline (PBS) (Sigma). Productive infection was measured by digital PCR, as detailed below, and through visualization of inclusions using confocal microscopy.

Microscopy

Cell monolayers were seeded on glass coverslips and at 48 hpi media was removed and cells were washed in 1X PBS. 200 μl ice cold 100% methanol was added to each well for 10 minutes. In order to block the cells, they were washed in 1X PBS and incubated in 200 μl 1% w/v bovine serum albumin (BSA)/PBS for 30 minutes at room temperature. Cells were then incubated for 30 minutes in the dark with 100 μl of a 1% v/v solution of anti-Chlamydia trachomatis MOMP antibody (FITC) (ab30951, Abcam, Cambridge, UK) in 1% w/v BSA/PBS. Cells were washed 3x in 1X PBS for 5 minutes each wash. DAPI dilactate (1μg/ml (Sigma)) was added for 5 minutes. Cells were washed 3x in 1X PBS. Slides were mounted with coverslips and viewed on a Zeiss LSM510 confocal microscope at 40X magnification. Images were captured using the tile function in Volocity, V5.5.1 (PerkinElmer, Waltham, MA, USA).

Nucleic acid extraction

For *in vitro* cultures 300µl lysis buffer (Norgen Biotek, Thorold, ON, Canada) was added to each well and cells were harvested by scraping. Ocular swabs were thawed and added to a 1.5 ml microcentrifuge tube containing 300 µl lysis buffer (Norgen Biotek) and were vortexed for one minute. Total RNA and DNA were extracted from both sample types using the Norgen RNA and DNA purification kit according to the manufacturers instructions. Total RNA was quantified using Qubit® fluorometric quantitation (Life Technologies) and quality was assessed using an Agilent RNA 6000 pico kit on a 2100 Bioanalyzer instrument (Agilent technologies, Santa Clara, CA, USA).

Ct infection load by droplet digital PCR

A droplet-digital PCR assay was carried out to diagnose Ct infection, as described previously [25, 26] with the following modifications. Forward and reverse primers were used at 0.9µM and probes were used 0.2µM. Eight microlitres of sample DNA was added to each reaction. For clinical samples, an initial diagnostic assay detecting Ct plasmid and human RPP30 endogenous control was carried out on all samples. Ct *omcB* and plasmid DNA was then quantified in positive samples to determine Ct load. This assay was also performed on *in vitro* samples to quantitate Ct *omcB* load and to check that there was no cross contamination of plasmid competent Ct in plasmid-free Ct cultures. Primer and probe sequences are described elsewhere [26]. Thermal cycling conditions were as follows: 95°C hold for 10 minutes, followed by 40 cycles of 95°C for 10 seconds and 60°C for 20 seconds with a final hold of 98°C for 12 minutes. ddPCR was performed on a Bio-Rad QX100 Instrument and data were collected using Quantalife software (Bio-Rad, Hercules, CA, USA). Copy number was calculated in R using previously published scripts [25].

Small RNA Sequencing

Small RNA libraries were prepared using TruSeq® Small RNA sample preparation kit (Illumina, San Diego, CA, USA), carried out following the manufacturer's instructions. *In vitro*-derived samples chosen for sequencing had an RNA Integrity number (RIN; where 0 = fully degraded RNA and 10 = best possible quality) > 8 and a concentration

of at least 0.2 µg/µl total RNA. Sample concentrations were normalized prior to small RNA library preparation. Clinical samples chosen for sequencing had an RIN > 8 and were normalized to the sample with the lowest concentration (24 ng/µl). Libraries were sequenced on a MiSeq desktop sequencer (Illumina). Sequencing reads were analyzed as described previously [27] with an amendment such that only reads with a Phred33 score of 30 or more were retained. Differential analysis was performed on read count data using two analysis packages in R, DESeq (which is believed to be conservative) and EdgeR [28–30]. In both methods miR with an average read count across all samples of less than five were excluded from each analysis. P values were adjusted for false discovery rate (FDR) using the Benjamini-Hochberg procedure [31]. Raw and processed sequencing data along with processing workflows are deposited in the NCBI GEO public database (GSE69837).

MiR qPCR and statistical analysis

Total RNA was reverse transcribed and expression levels were quantified by quantitative PCR (qPCR) using the MiScript system (Qiagen, Venlo, Limburg, Netherlands) as described previously [15]. Thermal cycling conditions were 95°C for 15 minutes followed by 40 cycles of 94°C for 15 seconds, 55°C 30 seconds, and 70°C 30 seconds. Data was collected at 70°C. Cycle thresholds were calculated using an automatic baseline and a threshold of 0.1 for all clinical and *in vitro* samples. Differential expression analysis of cycle threshold values was carried out as described previously [15]. FDR adjusted P values were calculated using the Benjamini-Hochberg procedure.

The relationship between conjunctival papillary inflammation (P) score and the expression of miR that were significantly differentially expressed in TF versus N by qPCR was examined using ordinal logistic regression models in R (MASS package [32]). Clinical scores P2 and P3 were combined due to the low number of P3 scores (n=6) and individuals were classified as P0 (n=84), P1 (n=53) and P2/P3 (n=29) as an ordinal response variable. Age, gender and the natural logarithm of Ct *omcB* load were included in the model and miR expression levels (40-delta cycle threshold (ΔCT) value) were included as independent variables. This value (40-ΔCT) was used so that an odds ratio (OR) >1 would reflect an up-regulation of miR expression and vice versa. Univariable ordinal regression was performed for each miR and miR with a P value < 0.05 were included in the final multivariate model. F and P scores were tested for collinearity: A high kappa score and a covariance matrix value near zero indicates

collinearity (0= perfect colinearity, 1= no colinearity). Post-hoc analyses were carried out on miR with a P value <0.05 in the multivariate model. Kruskal-Wallis and post-hoc Kruskal Nemenyi tests (Tukey method) were carried out in R using the PMCMR package [33] to detect pairwise differences between miR expression and collapsed papillary inflammation score. Kruskal Nemenyi test P values were adjusted using the Benjamini-Hochberg procedure.

Results

In vitro infections

HEp-2 and HCjE epithelial cell lines were infected *in vitro* with 3 different serovar A ocular strains of Ct; A/HAR-13, A2497 and plasmid-cured A2497. In HEp-2 cells, virulent A2497 plasmid-competent Ct had the highest mean genome copy number at 48 hpi, which was slightly higher than that of isogenic plasmid-free A2497 (A2497P-) (Figure 1). A/HAR-13 growth was considerably less efficient in these experiments. All 3 strains were substantially less productive in HCjE cells compared to HEp-2 cells, as measured by *omcB* load and microscopy of inclusions (Figure 6.1 and Additional file 6.1). Due to the low productivity of A/HAR-13 infection in HEp-2 and HCjE cells, these samples were not carried forward for small RNA sequencing. A2497 and A2497P- infected HCjE cells were sequenced despite the poor infection productivity in order to contrast small RNA expression between infected HEp-2 and HCjE cells. Small RNA sequencing was performed on mock-infected, A2497 and A2497P- infected HEp-2 and HCjE cells.
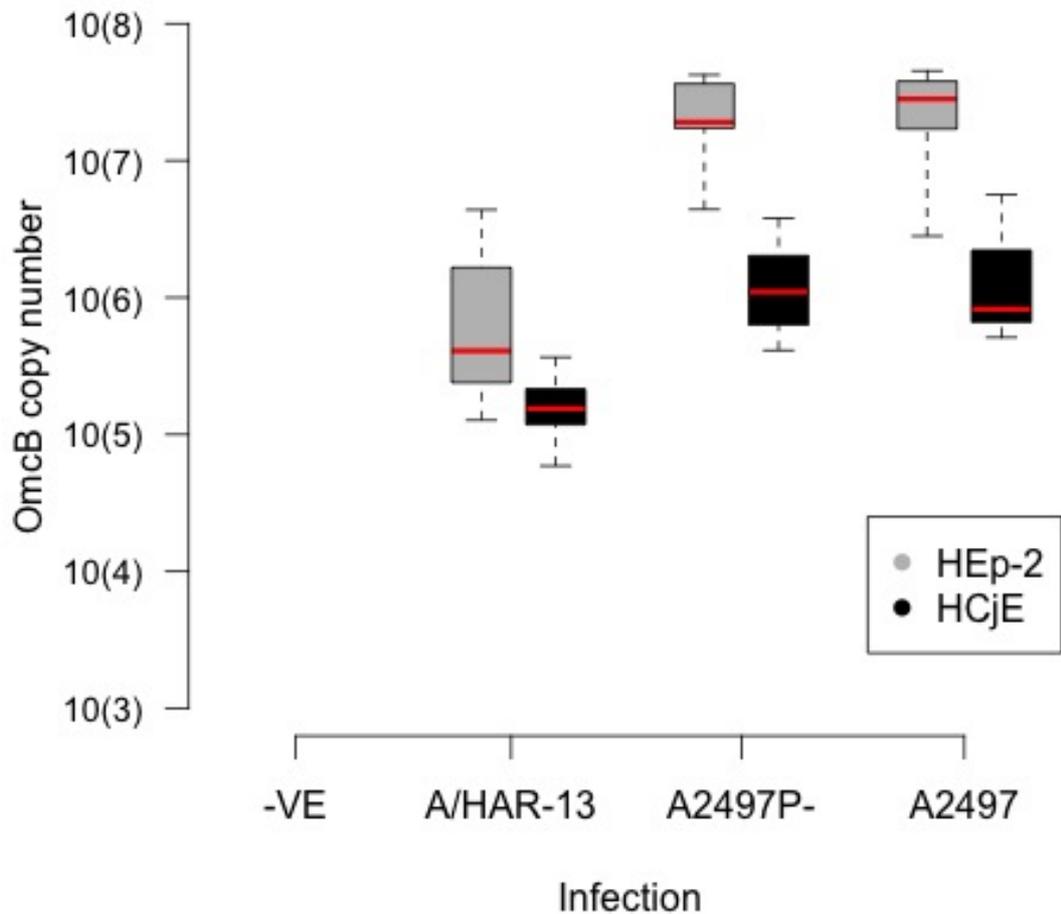
Figure 6.1. Yield of three ocular Ct strains in two epithelial cell lines. *Chlamydial genome copy number of three ocular Ct strains (A2497, A2497p- and A/HAR-13) in HEp-2 and HCjE cells at 48 hpi. Cells were infected at an MOI of 1. Mock-infected cells (-VE) were treated identically except for the addition of Ct inoculum. The mean of the total OmcB genome copy number per well of 6 biological replicates is shown. OmcB copy number is shown on a log(10) scale. Boxplots show the median (horizontal red line), interquartile range (grey or black solid-filled box) and the maximum and minimum values (dotted lines). Grey: HEp-2 cells, Black: HCjE cells.*

In HEp-2 cells, 885 miR were detected in mock-infected cells, 894 miR were detected in A2497 infected cells and 856 miR were detected in A2497P- infected cells. Differential expression of read count data (miR with an average read count <5 excluded) was carried out using EdgeR and DEseq to account for variance in the normalization method. No miR were differentially expressed ($P_{adj} < 0.01$) using either method between mock-infected and A2497 infected (377 miR tested) or between mock-infected and A2497P- infected (378 miR tested) HEp-2 cells (Additional file 6.2).

In HCjE cells, 853 miR were detected in mock-infected cells, 840 miR were detected in A2497 infected cells and 872 miR were detected in A2497P- infected cells. No miR were differentially expressed using EdgeR or DESeq (P_{adj} <0.01) between mock-infected and A2497 infected (357 miR tested) or between mock-infected and A2497P-infected (372 miR tested) HCjE cells (Additional file 6.3).

The miR profile of mock-infected HEp-2 and HCjE cells was analyzed in order to investigate differences between these two cell lines. Four hundred and seven miR had an average read count > 5 in mock-infected HEp-2 and HCjE cells. Strikingly, DESeq identified 136 out of the 407 miR tested with an adjusted P value (P_{adj}) < 0.01 and EdgeR identified 217 miR with P_{adj} < 0.01 (Additional file 6.4). The top 3 most differentially expressed miR were members of the miR-200 family: miR-200b-3p (P_{adj}=2.11 x 10^{-51}, log_2FC=12.3), miR-141-5p (P_{adj}=1.1 x 10^{-32}, log_2FC=9.2), and miR-429 (P_{adj}=1.1 x 10^{-32}, log_2FC= ∞), which were all highly expressed in HCjE cells relative to HEp-2 cells. MiR-429 was detected at an average read count of 379 in mock-infected HCjE cells, whereas it was not detected at all in HEp-2 cells at the sequencing depth achieved.

Clinical sample details

Conjunctival swab samples were collected from 81 cases of TF and 82 clinically normal healthy controls. A summary of sample phenotypes is shown in Table 6.1. Five out of 82 controls and 47/81 cases were positive for Ct DNA (Chi^2 = 55.93, P = 0.0005). The proportion of Ct infected individuals in each clinical category increases with the severity of trachomatous inflammation, both follicular and papillary. Two clinical cases had evidence of conjunctival scarring; one sample was F2, P1, C1 (Ct positive) and the other was F3, P2, C2 (Ct negative). The median Ct plasmid copy number was 1.5 (range 0.4-14.6).

Table 6.1. Trachoma grade and Ct infection load of clinical samples

FPC score	Total (% Male)	Ct positive	Ct *omcB* median[a] copies/swab (IQR)[b]	Human RPP30 median copies/swab (IQR)[b]
Controls (N)				
F0P0C0	82 (41%)	5/82 (6%)	345 (42-1078)	19290 (13310-25810)
TF cases: Breakdown by follicular score				
F2	46 (48%)	20/46 (43.5%)	703 (370-25870)	23900 (15670-39440)
F3	35 (31%)	27/35 (77%)	6050 (1451-15350)	35250 (19120-43250)
TF cases: Breakdown by papillary hypertrophy score				
P1	53 (38%)	22/53 (71%)	656 (433-5238)	23280 (15380-34500)
P2	22 (55%)	19/22 (86%)	12950 (3638-42880)	37750 (21560-48560)
P3	6 (17%)	6/6 (100%	11480 (4169-15720)	43620 (37750-53440)

[a]*Ct omcB median calculated from Ct positive individuals only*
[b]*IQR= inter-quartile range.*

Fifty-one of the 163 clinical samples from which total RNA was extracted had an RIN > 8. Five of the 51 RIN > 8 samples with the highest RNA concentration that had TF with current Ct infection were chosen for sequencing. Five control samples (F0,P0,C0) with the highest RNA concentration and the closest age and sex match to the 5 TF samples were also sequenced. Total RNA concentration of all 10 samples was normalized to the sample with the lowest concentration (24 ng/µl) prior to library preparation. The mean age of the 5 controls was 6.4 years old and the group consisted of 2 males and 3 females. The mean age of the TF group was 6.2 years old and the group consisted of 3 males and 2 females. In the TF group, the sample phenotypes were F2,P1,C0 (n=2), F2,P2,C0 (n=1), F3,P1,C0 (n=1) and F3,P2,C0 (n=1).

MiR expression in clinical samples by RNAseq

Deep sequencing of conjunctival small RNA from 10 clinical samples identified 860 miR. MiR-21-5p was the most highly expressed miR in the conjunctiva of both N and TF cases (Additional file 6.5). MiR with an average read count < 5 in all ten samples were removed. EdgeR revealed 43 miR (P_{adj} < 0.01, FC > 1.5) and DEseq identified 12 miR (P_{adj} < 0.01 FC > 1.5 (Additional file 6.6)) that were differentially expressed between TF cases and controls. All of the significant miR identified by DEseq were also significant using EdgeR.

The differential expression of the 12 miR that were significant in both DESeq and EdgeR analyses was investigated in 163 clinical samples using qPCR. Two miR that were previously found to be up-regulated in inflammatory trachomatous scarring (miR-147b and miR-1285) [15] were also tested by qPCR in these samples. Results were analyzed using the ΔΔCt method [34]. Differential expression was tested in 3 independent clinical phenotype comparisons: TF (n=81) against normal healthy controls (N, n=82), TF with detectable Ct infection (TF Ct+ n=47) against normal healthy controls without detectable Ct infection (N Ct-, n=77), and TF with detectable Ct infection (TF Ct+, n=47) against TF cases without detectable Ct infection (TF Ct-, n=34). Results are shown in Table 6.2. MiR-155, miR-150, miR-142, miR-181b, miR-181a and miR-342 were up-regulated in all 3 comparisons (Figure 6.2). MiR-155, miR-150, miR-142, miR-181b, miR-181a, miR-342 and miR-132 were differentially expressed during current Ct infection. MiR-184 and miR-4728 were down-regulated in TF independently of Ct infection. MiR-184 was the only miR that was significantly differentially expressed between uninfected normal healthy controls (n=77) and Ct negative TF cases (TF Ct- (n=34), P_{adj} = 0.00165, FC = 0.315, data not shown). These results are consistent with the small RNA sequencing results (Additional file 6.6). MiR-147b and miR-1285, which were up-regulated in inflammatory trachomatous scarring [15], were not differentially expressed between TF/TI and N.

Table 6.2. Differential expression analysis of miR by qPCR in 163 clinical samples, in three independent phenotype comparisons.

	TF (n=81) v N (n=82)			TF Ct+ (n=47) V TF Ct- (n=34)			TF Ct+ (n=47) V N Ct- (n=77)		
	P value	Adj P^a	FC^b	P value	Adj P^a	FC^b	P value	Adj P^a	FC^b
miR-184	$5.69*10^{-8}$	$7.96*10^{-7}$	0.30	0.7571	0.7571	0.88	$3.06*10^{-7}$	$1.07*10^{-6}$	0.28
miR-142-5p	$6.46*10^{-7}$	$4.52*10^{-6}$	1.82	$1.63*10^{-5}$	$7.58*10^{-5}$	2.53	$2.3*10^{-12}$	$3.22*10^{-11}$	2.83
miR-155-5p	$1.56*10^{-5}$	$7.29*10^{-5}$	1.73	$9.45*10^{-6}$	$6.62*10^{-5}$	2.50	$1.18*10^{-9}$	$5.51*10^{-9}$	2.58
miR-150-5p	0.0003	0.0011	1.56	$1.41*10^{-6}$	$1.98*10^{-5}$	3.24	$8.56*10^{-10}$	$5.51*10^{-9}$	2.71
miR-181b-5p	0.0010	0.0028	1.33	0.0018	0.005	1.74	$1.58*10^{-6}$	$4.44*10^{-6}$	1.70
miR-342-3p	0.0041	0.0096	1.12	0.0076	0.0178	1.50	0.0001	0.0002	1.34
miR-4728-3p	0.0103	0.0207	0.75	0.0353	0.0617	0.72	0.0005	0.0008	0.65
miR-181a-5p	0.0120	0.0211	1.30	0.0151	0.0301	1.40	0.0003	0.0006	1.54
miR-375	0.0871	0.1355	0.80	0.3054	0.3887	0.81	0.0615	0.0862	0.75
miR-132-3p	0.1628	0.2279	1.09	0.0009	0.0031	1.45	0.0023	0.0035	1.27
miR-10a-5p	0.2654	0.3378	1.16	0.6729	0.7247	0.92	0.3454	0.4030	1.15
miR-146b-3p	0.5491	0.6406	0.95	0.3666	0.4277	1.15	0.9425	0.9425	1.02
miR-147b	0.6203	0.6680	1.07	0.1073	0.1669	1.44	0.2394	0.3047	1.21
miR-1285	0.8683	0.8683	0.98	0.2095	0.2933	0.83	0.4434	0.4775	0.91

Tests for difference were conducted with a T test or Wilcoxon signed rank test if data were not normally distributed. N= Normal, TF= follicular trachoma, Ct+ = Ct infected, Ct- = no Ct infection detected.

^{a}P adj= Adjusted P value, ^{b}FC= Fold chang
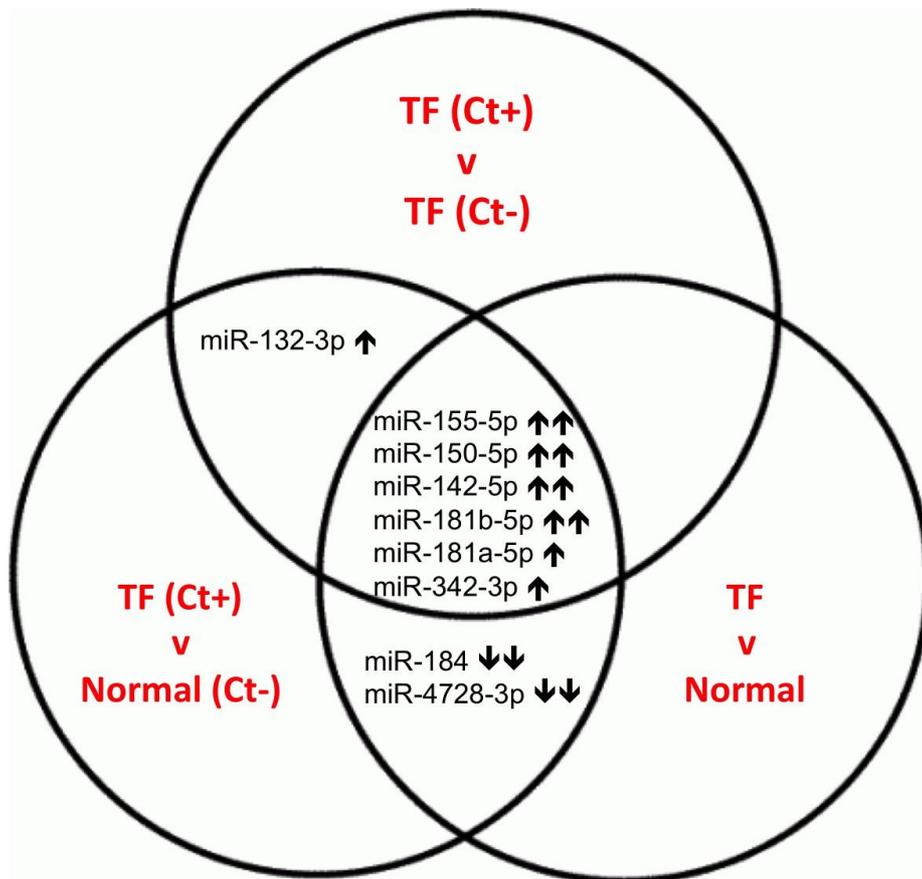
Figure 6.2. Patterns of differential miR expression according to clinical phenotype. MiR expression was measured using qPCR in 163 clinical samples. MiR that were significantly up (upward arrow) or down (downward arrow) regulated inhabit the circles of the phenotype comparisons in which they were differentially regulated. MiR labeled with double arrows had significant differences between groups ($P_{adj} < 0.05$, FC>1.5). MiR with single arrows had significantly different expression ($P_{adj} < 0.05$) but had a FC <1.5 in 2 or 3 of the comparisons shown.

Relationship between clinical papillary inflammation and miR expression

We investigated the relationship between clinical papillary inflammation and miR expression using an ordinal logistic regression model, which allowed us to adjust for confounding variables and estimate the contribution of miR expression to inflammation. Ct load was adjusted for in order to detect miR associated with papillary inflammation independently of Ct infection. Follicular trachoma and papillary hypertrophy were highly collinear (Kappa score = $5.8*10^{15}$, determinant of covariance matrix = $1.92*10^{-21}$)

therefore F score was not included as an independent variable in this analysis as the purpose of this model was to investigate papillary inflammation. MiR-150, -142, -4728, -181A and -181B were up-regulated in follicular trachoma in response to current Ct infection (Figure 2) and were associated with papillary inflammation in univariate regression analyses, but they had no association with papillary inflammation after adjustment for Ct infection load (Additional file 6.7). MiR-155 (OR = 2.533 (95% CI= 1.291 – 4.971), P = 0.007) and miR-184 (OR= 0.416 (95% CI=0.300 – 0.578), P = $1.61*10^{-7}$) were significantly associated with papillary inflammation (Additional file 6.7). MiR-155 expression increases with papillary inflammation score (Figure 6.3). Significant differences in miR-155 expression were found between P0 and P1 (P_{adj} = 0.03), P1 and P2/3 (P_{adj} = 0.019) and P0 and P2/3 (P_{adj} = $3.6*10^{-6}$). MiR-184 expression decreased with papillary inflammation score (Figure 3). Significant differences in miR-184 expression level were found between P0 and P1 (P_{adj} = $5.5*10^{-5}$) and between P0 and P2/3 (P_{adj} = $4.2*10^{-5}$). In separate univariate multinomial logistic regression analyses, no associations were found between miR expression and plasmid copy number in Ct positive individuals (data not shown). Exclusion of the two samples with evidence of trachomatous scarring did not change the outcomes of the differential expression or regression analyses (data not shown).
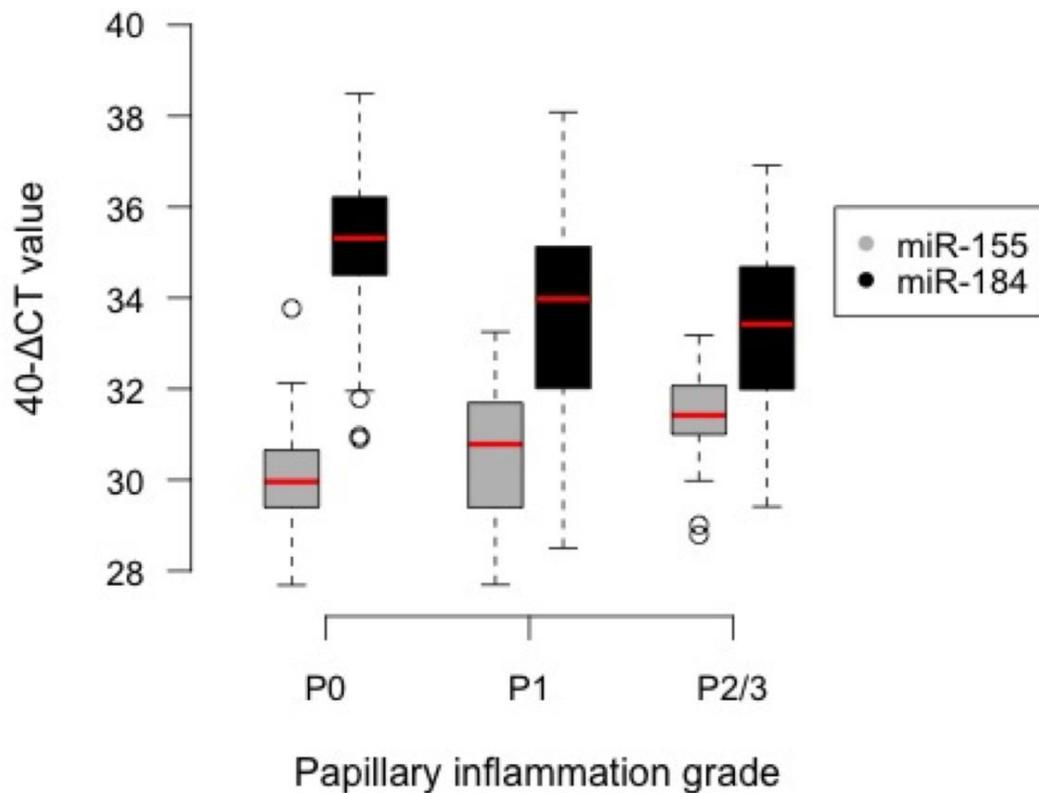
Figure 6.3. MiR expression correlates with clinical inflammation score. *Expression of miR-155 and miR-184 for 163 clinical samples plotted against clinical trachoma papillary hypertrophy score. P2 and P3 categories were combined due to the low number of P3 cases. ΔCT values were calculated by subtracting the endogenous control (snoRNA U6) cycle threshold (CT) value from the CT value of each miR for each individual sample. ΔCT values were inverted (40-ΔCT) in order to show the direction of miR expression. Boxplots show the median (horizontal red line), interquartile range (grey or black solid-filled box) and the maximum and minimum (dotted lines or empty circles) 40-ΔCT values for all samples in each clinical inflammation score group. Grey: miR-155, Black: miR-184.*

Discussion

During Ct infection of the conjunctiva *in vivo* 7 miR were up-regulated. Two miR were down-regulated during follicular trachoma in the absence of Ct. After adjusting for the relationship between miR and Ct infectious load, we found that miR-155 and miR-184 were independently associated with inflammation. We also found that isolated epithelial cells in culture did not differentially regulate miR expression in response to Ct infection.

The Ct plasmid is a known virulence factor [35, 36]. In a non-human primate model of trachoma A2497P- infection is attenuated relative to A2497 and does not lead to ocular pathology [24]. Attempts to elucidate the mechanism of this attenuation are ongoing [37, 38]. In order to understand the contribution of the epithelium, Porcella *et al.* (2015) recently characterized the *in vitro* transcriptome response of HeLa cells infected with A2497 and A2497P- (at an MOI of 1) [39]. Similar transcriptional profiles were induced by A2497 and A2497P- and only modest increases in cytokine and chemokine levels were detected in response to virulent A2497. The authors suggested that their data supports the hypothesis that Ct is a stealth pathogen [40], due to the limited innate pro-inflammatory response induced. We did not detect differential regulation of miR by deep sequencing in HEp-2 or HCjE epithelial cells at 48 hpi with A2497 and A2497P- (also at an MOI of 1). This result is not surprising in HCjE cells due to the lack of productive infection achieved, however more differences might have been expected upon productive infection of HEp-2 cells, particularly as Porcella *et al.,* found the largest transcriptional changes occurred in response to A2497 and A2497P- at 48hpi [39]. Our data could also be interpreted as evidence in support of the stealth pathogen hypothesis and suggests that Ct avoids stimulation of a miR response in epithelial cells. Infection of HeLa cells with *Salmonella typhimurium* revealed the largest changes in miR expression at 4hpi, with minimal changes detected at 24hpi despite infecting with an MOI of 10 [41]. Therefore, it is also possible that changes in epithelial cell miR expression in response to Ct are limited to early time points post infection. Limitations of this experiment were that despite infecting with an MOI of 1 we achieved <50% infectivity (Additional file 6.1) and we sequenced three biological repeats per condition. The expression changes in infected cells were therefore likely diluted by the lack of expression change in neighboring uninfected cells and it is possible that we did not have the statistical power to detect small expression differences.

HEp-2 cells originated from a human laryngeal carcinoma but it is known that many laboratory stocks of HEp-2 cells are contaminated with HeLa cells, which are derived

from a glandular adenocarcinoma of the cervix [42]. HCjE cells are an immortalized cell line generated from a primary conjunctival epithelial culture [43] and may represent an *in vitro* model that better mimics conjunctival epithelial cells *in vivo*. A previous study infected HCjE and HeLa cells with A/HAR-13 at an MOI of 0.3 and reported that A/HAR-13 achieved higher infectious load in HCjE cells compared to HeLa cells [44]. In contrast we were unable to maintain productive infections of 3 ocular strains in HCjE cells, whereas productive infection of HEp-2 cells with A2497 and A2497P- was achieved. These differences could reflect culture adaptation of HCjE cells [45–48] or Ct strains [49] over time or a natural resistance of the HCjE line to infection, perhaps due to expression of mucins or innate antimicrobial effectors [50]. Comparison of mock-infected HEp-2 and HCjE cell lines revealed significant differences in miR profile. Amongst the miR that were most significantly up-regulated in HCjE cells relative to HEp-2 cells were several members of the miR-200 family (Additional file 6.4), which are known to be highly enriched in epithelial tissues [51]. This would suggest that HEp-2 cells present an environment to Ct that is different to conjunctival epithelial cells and might indicate that caution should be used when interpreting data generated from these cultures in comparison to the *in vivo* response.

In vivo, we found that miR-21-5p was the most abundant miR in the conjunctiva of both follicular trachoma cases and healthy control individuals (Additional file 6.5). MiR-21 is transactivated by NFκB [52] and is thought to act in a positive feedback loop in epithelial cells by increasing NFκB activity [53]. The high expression of miR-21 at this mucosal site may reflect NFκB stimulation in an environment of frequent microbial exposure. We previously found that miR-21 was abundant (Ranked 19/503) in the conjunctiva of Gambian adults with and without scarring trachoma [15]. This slight reduction in the relative abundance of miR-21 in adults may reflect the fact that the conjunctival microbiome of adults in The Gambia has reduced richness and diversity of species compared to Gambian children [54] and thus a lower level of microbial stimulation. The reduction in abundance could also be due to differences in microbial exposure between The Gambia and Guinea Bissau, or the different technical approaches used in the two studies such as small RNA purification and quantitation.

In follicular trachoma, the miR expression signature reflects the presence of the immune response. MiR-155, miR-150 and miR-142 are thought to be specific for hematopoietic cells [55] (although miR-155 expression has been reported in epithelial cell lines [56, 57]) and miR-155, miR-150, miR-181a, miR-146 and miR-10a have roles in hematopoiesis (reviewed in [58]). MiR-155 in particular has wide-ranging and

profound effects on the development and function of immune cells (reviewed in [59]). MiR-181b, miR-132, miR-10a and miR-146b negatively regulate inflammation following TLR or NFκB stimulation in order to prevent excessive inflammation and pathology. A brief summary of roles that have been described for these differentially regulated miR relating to inflammation or fibrosis is presented in Additional file 6.8. The expression of these miR following stimulation of innate pathogen recognition pathways explains their up-regulation in response to Ct in this study. We found that expression of miR-150, -181a, -181b, -142 and -4728 were each independently associated with increasing inflammatory score, however, these associations were no longer significant after adjustment for Ct load and miR-co-expression. MiR-155 and miR-184 alone had a strong and direct association with papillary inflammatory score after adjustment for these factors. Pathway analysis was not carried out due to the relatively small and manageable number of differentially expressed miR and the inherent bias of current miR-based pathway analysis software [60].

A number of the miR that were differentially regulated in Ct positive follicular trachoma cases have previously been linked to chlamydial disease. MiR-155-5p, miR-142-5p, miR-142-3p, miR-132-3p and miR-147-3p amongst others were up-regulated during Cm infection of the murine cervix in response to an attenuated strain of Cm, relative to a virulent strain of Cm [16]. The roles attributed to these miR in dampening inflammation possibly explain the reduced pathology observed upon avirulent infection. Another study found that miR-146a was up-regulated in the murine genital tract 6 days post infection with Cm [17]. We did not find miR-147b or miR-1285 to be differentially expressed in Ct positive or Ct negative follicular trachoma cases. This could reflect differences in the inflammatory phenotype between adults with trachomatous scarring and inflammation (TI) that continues in the absence of Ct, compared to younger individuals with chlamydial-induced inflammation (TF and TI). MiR-147b is also hypothesized to dampen inflammation upon LPS and TNFα stimulation [61, 62], therefore regulation of inflammation is a key theme in both stages of trachomatous disease. No differentially regulated miR were detected in healthy control adults versus individuals with scarring trachoma in our previous study; differences were only detected in comparisons against trachomatous scarring with inflammation [15]. These data, combined with recent evidence that inflammation is a significant risk factor for progressive scarring [1], support the hypothesis that inflammatory cells are required to drive pathological responses in the epithelium. This hypothesis perhaps also explains the lack of miR response in our infected epithelial cell model and suggests that

inflammatory cell stimuli are required for a miR response in the epithelium in *vivo*, as might be the case for miR-184.

We found that miR-184 and miR-4728-3p were down-regulated in follicular trachoma irrespective of Ct infection. MiR-184 was the only miR differentially expressed in uninfected cases of follicular trachoma versus uninfected healthy controls and was highly associated with papillary hypertrophy score after adjustment for Ct load. MiR-184 is known to be enriched in the corneal epithelium [63] and it is the fourth most abundant miR in control individuals (F0P0C0). We previously found that miR-184 was highly abundant (5/502) in a pool of normal healthy adults and adults with scarring trachoma [15], suggesting tissue specific expression does not vary with age. A single base substitution in the seed region of miR-184 is associated with severe keratoconus (thinning of the cornea) [64–66]. In the cornea miR-184 is expressed in basal and supra-basal epithelial cells [63], under which the stromal thinning occurs. MiR-184 is strongly down-regulated during acute corneal injury and expression is restored in the re-epithelialized cornea upon healing [63]. MiR-184 also targets the Wnt receptor frizzled-7 and negatively regulates the Wnt pathway; down-regulation of miR-184 is associated with aberrant activation of the Wnt pathway in ischemia-induced neovascularization of the murine retina [67]. Delivery of miR-184 was able to inhibit induction of the Wnt pathway, conferring miR-184 with significant therapeutic potential. Activation of the canonical Wnt pathway has previously been demonstrated in Ct infected epithelial cells in *ex-vivo* fallopian tube tissue [68], with a paracrine effect that resulted in a loss of epithelial homeostasis. Altogether, these data suggest that a down-regulation of miR-184 in follicular trachoma once Ct has been cleared reflects a prolonged wound healing process and activation of the Wnt pathway, possibly contributing to pathology. Prolonged down-regulation of miR-184 may also contribute to epithelial thinning, which is observed in trachoma, potentially predisposing individuals more to subsequent bacterial infections. Future work should focus on the expression of miR-184 and activity of the Wnt pathway in a longitudinal set of clinical samples to determine the contribution of this pathway to the development of trachomatous pathology.

There was considerable variation in load between the Ct infected follicular trachoma cases in this study. Conjunctival cells obtained by a swab are expected to be heterogeneous in the number of infected and uninfected epithelial cells and the number of immune cells. The majority of epithelial cells are likely to be uninfected; reducing our power to detect miR expression differences in infected epithelial cells and perhaps

explaining why the majority of differentially regulated miR detected *in vivo* were hematopoietic cell-associated. This heterogeneity is a caveat of using clinical samples. In order to investigate the host miR response of Ct infected epithelial cells *in vivo* infected cells could be isolated and subjected to single cell miRNA expression analysis [69].

Conclusions

We identified 7 miR that were up-regulated by current chlamydial infection during follicular trachoma. MiR-184 and miR-4728 were down-regulated during follicular trachoma in the absence of Ct. MiR-155 and miR-184 were inversely correlated with pathological inflammation, which is known to be a major risk factor for scarring trachoma. Future studies using more sophisticated *in vitro* models (such as co-culture) involving miR silencing or overexpression coupled with longitudinal studies *in vivo* will help develop our understanding of the functions of these miR, their use as predictive biomarkers of scarring trachoma and their potential as novel treatment targets.

List of Abbreviations

Ct: *Chlamydia trachomatis*; miR: microRNA; TF: trachomatous inflammation – follicular; TI: trachomatous inflammation – Intense; N: normal healthy control; ΔCT: Delta cycle threshold value; OR: odds ratio; CI: Confidence interval; qPCR: quantitative polymerase chain reaction; hpi: hours post-infection; MOI: multiplicity of infection; TLR: Toll-like receptor; RIN: RNA integrity number; P score: Papillary inflammation score; F score: follicle score.

Competing Interests Statement

The authors declare that they have no competing interests.

Author's Contributions

Conceived and designed the project: MH, DM, RB, MB, AL, TD. Collected and graded clinical samples: AL, MN, EC, TD, SB. Performed laboratory work: TD. Analyzed results: TD, AL, CR, MH. Wrote the manuscript: TD, MH. All authors read, edited and approved the final manuscript.

Acknowledgements

References

1. Burton MJ, Rajak SN, Hu VH, Ramadhani A, Habtamu E, Massae P, Tadesse Z, Callahan K, Emerson PM, Khaw PT, Jeffries D, Mabey DCW, Bailey RL, Weiss HA, Holland MJ: **Pathogenesis of progressive scarring trachoma in Ethiopia and Tanzania and its implications for disease control: two cohort studies.** *PLoS Negl Trop Dis* 2015, **9**:e0003763.

2. Alliance WHO, Elimination G, Trachoma B, Oms A: **Weekly epidemiological record Relevé épidémiologique hebdomadaire**. 2014, **96**:421–428.

3. **Future approaches to Trachoma Control: Report of a Global Scientific Meeting, Geneva, 17-20 June 1996**. *World Heal Organ* 1997.

4. Jimenez V, Gelderblom HC, Mann Flueckiger R, Emerson PM, Haddad D: **Mass Drug Administration for Trachoma: How Long Is Not Long Enough?** *PLoS Negl Trop Dis* 2015, **9**:e0003610.

5. Hu VH, Harding-Esch EM, Burton MJ, Bailey RL, Kadimpeul J, Mabey DCW: **Epidemiology and control of trachoma: systematic review.** *Trop Med Int Health* 2010, **15**:673–91.

6. Burton MJ, Hu VH, Massae P, Burr SE, Chevallier C, Afwamba IA, Courtright P, Weiss HA, Mabey DCW, Bailey RL: **What is causing active trachoma? The role of nonchlamydial bacterial pathogens in a low prevalence setting.** *Invest Ophthalmol Vis Sci* 2011, **52**:6012–7.

7. Jones BR, Collier LH: **Inoculation of man with inclusion Blennorrhea virus**. *Ann N Y Acad Sci* 1962, **98**:212–228.

8. Dawson C, Jawetz E, Hanna L, Rose L, Wood TR, Thygeson P: **Experimental inclusion conjunctivitis in man. II. Partial resistance to reinfection.** *Am J Epidemiol* 1966, **84**:411–25.

9. Grassly NC, Ward ME, Ferris S, Mabey DC, Bailey RL: **The natural history of trachoma infection and disease in a Gambian cohort with frequent follow-up.** *PLoS Negl Trop Dis* 2008, **2**:e341.

10. BAILEY R, DUONG T, Carpenter R, WHITTLE H, Mabey D: **The duration of human ocular Chlamydia trachomatis infection is age dependent**. *Epidemiol Infect* 1999, **123**:479–86.

11. Gambhir M, Blake IM, Basáñez M: **Modelling trachoma : infection , transmission and control A report prepared for the International Trachoma Initiative**. .

12. Solomon AW, Harding-Esch E, Alexander NDE, Aguirre A, Holland MJ, Bailey RL, Foster A, Mabey DCW, Massae PA, Courtright P, Shao JF: **Two doses of azithromycin to eliminate trachoma in a Tanzanian community.** *N Engl J Med*

2008, **358**:1870–1.

13. Haramati S, Chapnik E, Sztainberg Y, Eilam R, Zwang R, Gershoni N, McGlinn E, Heiser PW, Wills A-M, Wirguin I, Rubin LL, Misawa H, Tabin CJ, Brown R, Chen A, Hornstein E: **miRNA malfunction causes spinal motor neuron disease.** *Proc Natl Acad Sci U S A* 2010, **107**:13111–13116.

14. Gregory, P. A., Bert, A. G., Paterson, E. L., Barry, S. C., Tsykin, A., Farshid, G., Vadas, M. A., et al. (2008). The miR-200 family and miR-205 regulate epithelial to mesenchymal transition by targeting ZEB1 and SIP1. Nature cell biology, 10(5) 593-60: **The miR-200 family and miR-205 regulate epithelial to mesenchymal transition by targeting ZEB1 and SIP1.** *Nat Cell Biol* 2008, **10**:593–601.

15. Derrick T, Roberts C h., Rajasekhar M, Burr SE, Joof H, Makalo P, Bailey RL, Mabey DCW, Burton MJ, Holland MJ: **Conjunctival MicroRNA Expression in Inflammatory Trachomatous Scarring**. *PLoS Negl Trop Dis* 2013, **7**:e2117.

16. Yeruva L, Myers GSA, Spencer N, Creasy HH, Adams NE, Maurelli AT, McChesney GR, Cleves MA, Ravel J, Bowlin A, Rank RG: **Early microRNA expression profile as a prognostic biomarker for the development of pelvic inflammatory disease in a mouse model of chlamydial genital infection.** *MBio* 2014, **5**:e01241–14.

17. Gupta R, Arkatkar T, Yu J-J, Wali S, Haskins WE, Chambers JP, Murthy AK, Bakar SA, Guentzel MN, Arulanandam BP: **Chlamydia muridarum Infection Associated Host MicroRNAs in the Murine Genital Tract and Contribution to Generation of Host Immune Response**. *Am J Reprod Immunol* 2015, **73**:126–140.

18. Igietseme JU, Omosun Y, Partin J, Goldstein J, He Q, Joseph K, Ellerson D, Ansari U, Eko FO, Bandea C, Zhong G, Black CM: **Prevention of chlamydia-induced infertility by inhibition of local caspase activity**. *J Infect Dis* 2013, **207**:1095–1104.

19. Dawson CR, Jones BR TM, Dawson CR, Jones BR, Tarizzo ML, World Health Organization: *Guide to Trachoma Control in Programmes for the Prevention of Blindness*. 1981.

20. **WHO simplified trachoma grading system.** *Community Eye Health* 2004, **17**:68.

21. Keenan JD, Lakew T, Alemayehu W, Melese M, Porco TC, Yi E, House JI, Zhou Z, Ray KJ, Acharya NR, Whitcher JP, Gaynor BD, Lietman TM: **Clinical activity and polymerase chain reaction evidence of chlamydial infection after repeated mass antibiotic treatments for trachoma.** *Am J Trop Med Hyg* 2010, **82**:482–7.

22. Last AR, Burr SE, Weiss HA, Harding-Esch EM, Cassama E, Nabicassa M,

Mabey DC, Holland MJ, Bailey RL: **Risk Factors for Active Trachoma and Ocular Chlamydia trachomatis Infection in Treatment-Naïve Trachoma-Hyperendemic Communities of the Bijagós Archipelago, Guinea Bissau**. *PLoS Negl Trop Dis* 2014, **8**:e2900.

23. Kari L, Whitmire WM, Carlson JH, Crane DD, Reveneau N, Nelson DE, Mabey DCW, Bailey RL, Holland MJ, McClarty G, Caldwell HD: **Pathogenic diversity among Chlamydia trachomatis ocular strains in nonhuman primates is affected by subtle genomic variations.** *J Infect Dis* 2008, **197**:449–56.

24. Kari L, Whitmire WM, Olivares-Zavaleta N, Goheen MM, Taylor LD, Carlson JH, Sturdevant GL, Lu C, Bakios LE, Randall LB, Parnell MJ, Zhong G, Caldwell HD: **A live-attenuated chlamydial vaccine protects against trachoma in nonhuman primates.** *J Exp Med* 2011, **208**:2217–23.

25. Roberts CH, Last A, Molina-Gonzalez S, Cassama E, Butcher R, Nabicassa M, McCarthy E, Burr SE, Mabey DC, Bailey RL, Holland MJ: **Development and evaluation of a next-generation digital PCR diagnostic assay for ocular Chlamydia trachomatis infections.** *J Clin Microbiol* 2013, **51**:2195–203.

26. Last AR, Roberts C h, Cassama E, Nabicassa M, Molina-Gonzalez S, Burr SE, Mabey DCW, Bailey RL, Holland MJ: **Plasmid copy number and disease severity in naturally occurring ocular Chlamydia trachomatis infection.** *J Clin Microbiol* 2014, **52**:324–7.

27. Ying S-Y, Walker JM: **MicroRNA Protocols**. *Life Sci* 2013, **531**:375.

28. Robinson MD, McCarthy DJ, Smyth GK: **edgeR: a Bioconductor package for differential expression analysis of digital gene expression data.** *Bioinformatics* 2010, **26**:139–40.

29. Anders S, Huber W: **Differential expression analysis for sequence count data.** *Genome Biol* 2010, **11**:R106.

30. Robles JA, Qureshi SE, Stephen SJ, Wilson SR, Burden CJ, Taylor JM: **Efficient experimental design and analysis strategies for the detection of differential expression using RNA-Sequencing.** *BMC Genomics* 2012, **13**:484.

31. Benjamini Y, Hochberg Y: **Controlling the False Discovery Rate: A Practical and Powerful Approach to Multiple Testing**. *Journal of the Royal Statistical Society. Series B (Methodological)* 1995:289 – 300.

32. Venables, W. N. & Ripley BD: *Modern Applied Statistics with S*. Fourth Edi. Springer, New York; 2002.

33. Package T, Pohlert AT, Kruskal DT: **Package ' PMCMR '**. 2015.

34. Livak KJ, Schmittgen TD: **Analysis of relative gene expression data using real-time quantitative PCR and the 2(-Delta Delta C(T)) Method.** *Methods* 2001,

25:402–8.

35. Carlson JH, Whitmire WM, Crane DD, Wicke L, Virtaneva K, Sturdevant DE, Kupko JJ, Porcella SF, Martinez-Orengo N, Heinzen R a, Kari L, Caldwell HD: **The Chlamydia trachomatis plasmid is a transcriptional regulator of chromosomal genes and a virulence factor.** *Infect Immun* 2008, **76**:2273–83.

36. O'Connell CM, Ingalls RR, Andrews CW, Scurlock AM, Darville T: **Plasmid-deficient Chlamydia muridarum fail to induce immune pathology and protect against oviduct disease.** *J Immunol* 2007, **179**:4027–34.

37. Olivares-Zavaleta N, Whitmire WM, Kari L, Sturdevant GL, Caldwell HD: **CD8+ T cells define an unexpected role in live-attenuated vaccine protective immunity against Chlamydia trachomatis infection in macaques.** *J Immunol* 2014, **192**:4648–54.

38. Yang C, Starr T, Song L, Carlson JH, Sturdevant GL, Beare PA, Whitmire WM, Caldwell HD: **Chlamydial Lytic Exit from Host Cells Is Plasmid Regulated.** *MBio* 2015, **6**.

39. Porcella SF, Carlson JH, Sturdevant DE, Sturdevant GL, Kanakabandi K, Virtaneva K, Wilder H, Whitmire WM, Song L, Caldwell HD: **Transcriptional Profiling of Human Epithelial Cells Infected with Plasmid-Bearing and Plasmid-Deficient Chlamydia trachomatis.** *Infect Immun* 2015, **83**:534–43.

40. Buckner LR, Lewis ME, Greene SJ, Foster TP, Quayle AJ: **Chlamydia trachomatis infection results in a modest pro-inflammatory cytokine response and a decrease in T cell chemokine secretion in human polarized endocervical epithelial cells.** *Cytokine* 2013, **63**:151–65.

41. Schulte LN, Eulalio A, Mollenkopf H-J, Reinhardt R, Vogel J: **Analysis of the host microRNA response to Salmonella uncovers the control of major cytokines by the let-7 family.** *EMBO J* 2011, **30**:1977–89.

42. Jones HW, McKusick VA, Harper PS, Wuu KD: **George Otto Gey. (1899-1970). The HeLa cell and a reappraisal of its origin.** *Obstet Gynecol* 1971, **38**:945–9.

43. Gipson IK: **Mucin Gene Expression in Immortalized Human Corneal-Limbal and Conjunctival Epithelial Cell Lines**. *Invest Ophthalmol Vis Sci* 2003, **44**:2496–2506.

44. Miyairi I, Mahdi OS, Ouellette SP, Belland RJ, Byrne GI: **Different growth rates of Chlamydia trachomatis biovars reflect pathotype.** *J Infect Dis* 2006, **194**:350–7.

45. Sambuy Y, De Angelis I, Ranaldi G, Scarino ML, Stammati A, Zucco F: **The Caco-2 cell line as a model of the intestinal barrier: influence of cell and culture-related factors on Caco-2 cell functional characteristics.** *Cell Biol Toxicol*

2005, **21**:1–26.

46. Yu H, Cook TJ, Sinko PJ: **Evidence for diminished functional expression of intestinal transporters in Caco-2 cell monolayers at high passages.** *Pharm Res* 1997, **14**:757–62.

47. Briske-Anderson MJ, Finley JW, Newman SM: **The influence of culture time and passage number on the morphological and physiological development of Caco-2 cells.** *Proc Soc Exp Biol Med* 1997, **214**:248–57.

48. Wenger SL, Senft JR, Sargent LM, Bamezai R, Bairwa N, Grant SG: **Comparison of established cell lines at different passages by karyotype and comparative genomic hybridization.** *Biosci Rep* 2004, **24**:631–9.

49. Miyairi I, Laxton JD, Wang X, Obert CA, Arva Tatireddigari VRR, van Rooijen N, Hatch TP, Byrne GI: **Chlamydia psittaci Genetic Variants Differ in Virulence by Modulation of Host Immunity.** *J Infect Dis* 2011, **204**:654–63.

50. Buckner LR, Schust DJ, Ding J, Nagamatsu T, Beatty W, Chang TL, Greene SJ, Lewis ME, Ruiz B, Holman SL, Spagnuolo RA, Pyles RB, Quayle AJ: **Innate immune mediator profiles and their regulation in a novel polarized immortalized epithelial cell model derived from human endocervix.** *J Reprod Immunol* 2011, **92**:8–20.

51. Park S-M, Gaur AB, Lengyel E, Peter ME: **The miR-200 family determines the epithelial phenotype of cancer cells by targeting the E-cadherin repressors ZEB1 and ZEB2.** *Genes Dev* 2008, **22**:894–907.

52. Shin VY, Jin H, Ng EKO, Cheng ASL, Chong WWS, Wong CYP, Leung WK, Sung JJY, Chu K-M: **NF-κB targets miR-16 and miR-21 in gastric cancer: involvement of prostaglandin E receptors.** *Carcinogenesis* 2011, **32**:240–5.

53. Iliopoulos D, Jaeger S a., Hirsch H a., Bulyk ML, Struhl K: **STAT3 Activation of miR-21 and miR-181b-1 via PTEN and CYLD Are Part of the Epigenetic Switch Linking Inflammation to Cancer**. *Mol Cell* 2010, **39**:493–506.

54. Zhou Y, Holland MJ, Makalo P, Joof H, Roberts C h, Mabey DC, Bailey RL, Burton MJ, Weinstock GM, Burr SE: **The conjunctival microbiome in health and trachomatous disease: a case control study**. *Genome Med* 2014, **6**:99.

55. Landgraf P, Rusu M, Sheridan R, Sewer A, Iovino N, Aravin A, Pfeffer S, Rice A, Kamphorst AO, Landthaler M, Lin C, Socci ND, Hermida L, Fulci V, Chiaretti S, Foà R, Schliwka J, Fuchs U, Novosel A, Müller R-U, Schermer B, Bissels U, Inman J, Phan Q, Chien M, Weir DB, Choksi R, De Vita G, Frezzetti D, Trompeter H-I, et al.: **A mammalian microRNA expression atlas based on small RNA library sequencing.** *Cell* 2007, **129**:1401–14.

56. Izar B, Mannala GK, Mraheil MA, Chakraborty T, Hain T: **microRNA response

to Listeria monocytogenes infection in epithelial cells. *Int J Mol Sci* 2012, **13**:1173–85.

57. Xiao B, Liu Z, Li B, Tang B, Li W, Guo G, Shi Y, Wang F, Wu Y, Tong W, Guo H, Mao X, Zou Q: **Induction of microRNA‑155 during Helicobacter pylori Infection and Its Negative Regulatory Role in the Inflammatory Response**. *J Infect Dis* 2009, **200**:916–925.

58. Vasilatou D, Papageorgiou S, Pappa V, Papageorgiou E, Dervenoulas J: **The role of microRNAs in normal and malignant hematopoiesis.** *Eur J Haematol* 2010, **84**:1–16.

59. Seddiki N, Brezar V, Ruffin N, Lévy Y, Swaminathan S: **Role of miR-155 in the regulation of lymphocyte immune function and disease.** *Immunology* 2014, **142**:32–8.

60. Godard P, van Eyll J: **Pathway analysis from lists of microRNAs: common pitfalls and alternative strategy.** *Nucleic Acids Res* 2015:gkv249–.

61. Liu G, Friggeri A, Yang Y, Park Y-J, Tsuruta Y, Abraham E: **miR-147, a microRNA that is induced upon Toll-like receptor stimulation, regulates murine macrophage inflammatory responses.** *Proc Natl Acad Sci U S A* 2009, **106**:15819–24.

62. Bertero T, Grosso S, Robbe-Sermesant K, Lebrigand K, Hénaoui I-S, Puisségur M-P, Fourre S, Zaragosi L-E, Mazure NM, Ponzio G, Cardinaud B, Barbry P, Rezzonico R, Mari B: **'Seed-Milarity' Confers to hsa-miR-210 and hsa-miR-147b Similar Functional Activity.** *PLoS One* 2012, **7**:e44919.

63. Ryan DG, Oliveira-Fernandes M, Lavker RM: **MicroRNAs of the mammalian eye display distinct and overlapping tissue specificity.** *Mol Vis* 2006, **12**:1175–84.

64. Bykhovskaya Y, Caiado Canedo AL, Wright KW, Rabinowitz YS: **C.57 C > T Mutation in MIR 184 is Responsible for Congenital Cataracts and Corneal Abnormalities in a Five-generation Family from Galicia, Spain.** *Ophthalmic Genet* 2013.

65. Iliff BW, Riazuddin SA, Gottsch JD: **A single-base substitution in the seed region of miR-184 causes EDICT syndrome.** *Invest Ophthalmol Vis Sci* 2012, **53**:348–53.

66. Hughes AE, Bradley DT, Campbell M, Lechner J, Dash DP, Simpson DA, Willoughby CE: **Mutation altering the miR-184 seed region causes familial keratoconus with cataract.** *Am J Hum Genet* 2011, **89**:628–33.

67. Takahashi Y, Chen Q, Rajala RVS, Ma J-X: **MicroRNA-184 modulates**

canonical Wnt signaling through the regulation of frizzled-7 expression in the retina with ischemia-induced neovascularization. *FEBS Lett* 2015, **589**:1143–9.

68. Kessler M, Zielecki J, Thieck O, Mollenkopf H-J, Fotopoulou C, Meyer TF: **Chlamydia Trachomatis Disturbs Epithelial Tissue Homeostasis in Fallopian Tubes via Paracrine Wnt Signaling.** *Am J Pathol* 2011, **180**:198–186.

69. Wu M, Piccini M, Koh C-Y, Lam KS, Singh AK: **Single cell microRNA analysis using microfluidic flow cytometry.** *PLoS One* 2013, **8**:e55044.

Additional files:

File name: *Additional file 6.1 (see figures 4.2 and 4.4)*
File title*: Chlamydial infection of HEp-2 and HCjE cell lines with three ocular Ct strains.*
File description*: HEp-2 cell monolayers infected with Ct strains A2497 (A), A2497P- (B) and A/HAR-13 (C), and HCjE cell monolayers infected with Ct strains A2497 (D), A2497P- (E) and A/HAR-13 (F) at 48 hpi. Cell nuclei are stained with DAPI (blue) and Ct inclusions are stained with anti-C. trachomatis MOMP antibody (FITC (green)). Cells were infected with an MOI of 1 and viewed at 40X magnification. Representative photographs were taken from one of three replicates for each condition.*

File name: *Additional file 6.2*
File format*: XLS*
File title*: Differential expression analysis of miR from A2497 and A2497P- infected HEp-2 cells.*
File description*: Results of DESeq differential expression analysis of sequencing read count data for uninfected HEp-2 cells versus HEp-2 cells infected with A2497 and A2497P- strains of* Chlamydia trachomatis *at 48hpi. MiR with an average read count <5 were excluded. Three biological replicates of each condition were sequenced and analyzed. MRC = Mean read count, -VE= mock-infected cells.*

File name*: Additional file 6.3*
File format*: XLS*
File title: *Differential expression analysis of miR from A2497 and A2497P- infected HCjE cells.*
File description*: Results of DESeq differential expression analysis of sequencing read count data for uninfected HCjE cells versus HCjE cells infected with A2497 and A2497P- strains of* Chlamydia trachomatis *at 48hpi. MiR with an average read count <5 were excluded. Three biological replicates of each condition were sequenced and analyzed. MRC = Mean read count, -VE= mock-infected cells.*

File name*: Additional file 6.4*
File format*: XLS*
File title*: Differential expression analysis of miR from uninfected HCjE versus HEp-2 cells.*
File description*: Results of DESeq differential expression analysis of sequencing read count data for uninfected HEp-2 cells versus uninfected HCjE cells at 48hpi. MiR with*

an average read count <5 were excluded. Three biological replicates of each condition were sequenced and analyzed. MRC = Mean read count, -VE= mock-infected cells.

N

Other miR
n=204

miR-21-5p

miR-141-3p

miR-26a-5p

miR-184

miR-22-3p

miR-27b-3p

miR-191-5p

Let-7f-5p

TF

Other miR
n=218

miR-21-5p

miR-181a-5p

miR-191-5p

miR-141-3p

miR-22-3p

miR-92a-3p

miR-26a-5p

Let-7f-5p
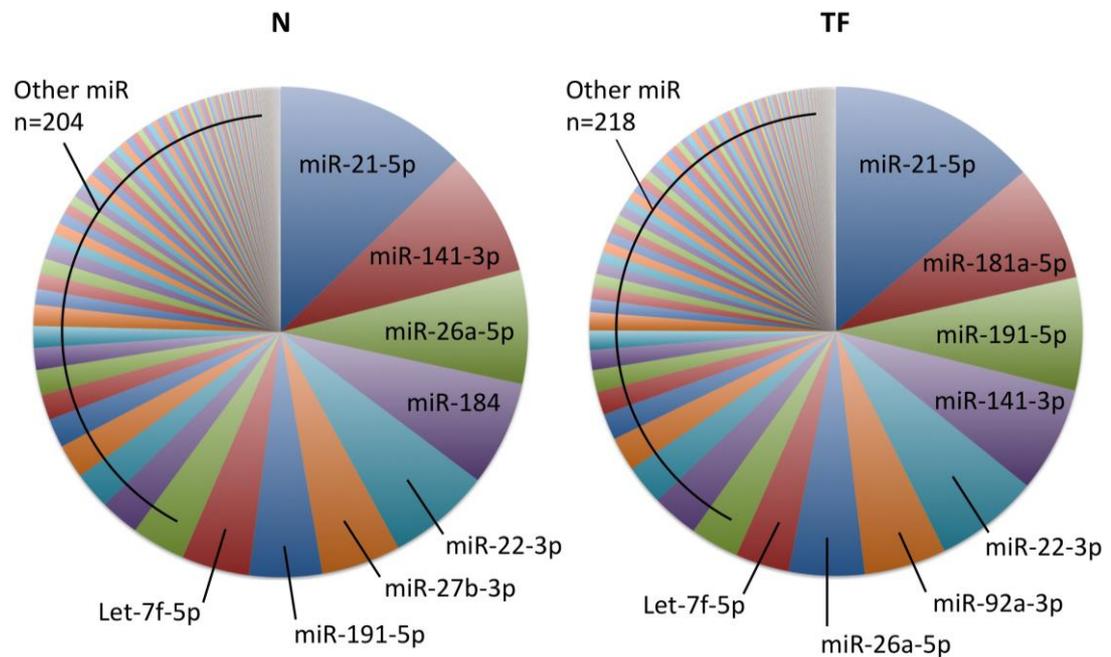
 File name*: Additional file 6.5*

File title*: Relative abundance of miR in the conjunctiva of cases of follicular trachoma (TF) and controls (N).*

File description*: Relative abundance of miR detected in 5 TF cases and 5 controls by small RNA sequencing. MiR with a mean read count in TF cases or controls < 5 were excluded. MiR were ranked by mean read count across all five samples of each phenotype group.*

File name*: Additional file 6.6*

File format*: XLS*

File title*: Differential expression analysis of miR from individuals with follicular trachoma versus healthy controls.*

File description*: Results of DESeq differential expression analysis of sequencing read count data for normal healthy controls (N) versus cases of follicular trachoma (TF) with current* Chlamydia trachomatis *(Ct) infection (five samples of each). MiR with an average read count <5 were excluded. MRC = Mean read count.*

Additional file 6.7. Multivariable regression model of the contribution of miR expression to clinical papillary hypertrophy score.

Independent variable	Adjusted OR[a]	95% CI[b]	P value
Age (years)	1.247	1.034 – 1.503	**0.0210**
Gender (Male)	1.145	0.536 – 2.446	0.7266
Ct load[c]	1.256	1.053 – 1.498	**0.0113**
miR-155	2.533	1.291 – 4.971	**0.0069**
miR-184	0.416	0.300 – 0.578	**$1.61*10^{-7}$**
miR-150	0.654	0.349 – 1.227	0.1861
miR-181a	1.195	0.600 – 2.382	0.6118
miR-181b	1.623	0.779 – 3.381	0.1962
miR-142	1.369	0.794 – 2.357	0.2582
miR-4728	0.718	0.479 – 1.076	0.1084

Collapsed papillary hypertrophy score (P0, P1 or P2/3, as defined by the WHO 1981 FPC scoring system) was used as an ordinal outcome variable to define trachomatous inflammation in 163 clinical samples. Age, gender, Ct load and inverted ΔCT values (40-ΔCT) of miR are included as independent variables. Model AIC (Akaike information criterion) is 227.3725. Significant P values are highlighted in bold font.
[a]OR= Odds ratio, [b]CI= confidence intervals, [c]Ct load is defined as log-(e) omcB copies/swab.

Additional file 6.8. Focused list of published roles for miR that are differentially expressed in TF that relate to inflammation or fibrosis.

miR	Expression in TF	Functions
		Hematopoiesis (1), regulation of T and B cell differentiation (2)
		Essential for the development of Th1 and Th17 pathogen-specific immune responses (3)
		Mainly pro-inflammatory, though some anti-inflammatory roles described
		Induced upon exposure to TLR ligands or TNFα, dependent on transcription factors AP-1 and NFκB (4, 5)
miR-155-5p	Up-regulated	Suppresses negative regulators of inflammation [56,57]
		Hematopoiesis - regulates T and B cell development (8)
miR-150-5p	Up-regulated	Suppresses negative regulators of inflammation (SOCS1), promotes renal fibrosis (9, 10)
miR-142-5p	Up-regulated	Trans-activates miR-150, activates canonical Wnt pathway (11)
		Endotoxin responsive, negatively regulates NFκB signaling (12)
miR-181b-5p	Up-regulated	Upregulated by TGFB1 in deep dermal fibroblasts → myofibroblast differentiation and hypertrophic scar formation [47]
		Regulates lymphoid cell development, critical for T cell receptor selection in the thymus and follicular T helper cell differentiation [44,45]
miR-181a-5p	Up-regulated	Mediates TGFβ-induced epithelial-mesenchymal transition via repression of Smad7 in ovarian cancer [46]
miR-342-3p	Up-regulated	Overexpression inhibits cell proliferation, migration and invasion in cervical cancer (13)
miR-184	Down-regulated	Negatively regulates Wnt pathway (14), inhibits cell migration and proliferation (15)

miR-4728-3p	Down-regulated	Encoded in HER2 locus, targets estrogen receptor 1 alpha through a non-canonical target site (16)
miR-132-3p	Up-regulated	Endotoxin responsive, negatively regulates TLR-induced pro-inflammatory cytokine signaling (5, 17)
miR-375	Down-regulated	Supports differentiation of goblet cells (18)
miR-10a-5p	Up-regulated	Inhibits NFkB pro-inflammatory signaling pathway (19)
miR-146b-3p	Up-regulated	Endotoxin responsive, negatively regulates TLR-induced pro-inflammatory cytokine signaling (5)

References:

1. **Georgantas RW et al.** 2007. Proc Natl Acad Sci U S A **104**:2750–5.

2. **Turner M, Vigorito E.** 2008. Biochem Soc Trans **36**:531–3.

3. **Oertli M et al.** 2011. J Immunol **187**:3578–86.

4. **O'Connell RM et al.** 2007. Proc Natl Acad Sci U S A **104**:1604–9.

5. **Taganov KD, Boldin MP, Chang K-J, Baltimore D.** 2006. Proc Natl Acad Sci U S A **103**:12481–6.

6. **Pathak S et al.** Exp Mol Med **47**:e164.

7. **Wang P et al.** 2010. J Immunol **185**:6226–33.

8. **Zhou B et al.** 2007. Proc Natl Acad Sci U S A **104**:7080–5.

9. **Chen R-F et al.** 2014. J Infect **69**:366–74.

10.   Zhou H et al. 2013. J Am Soc Nephrol **24**:1073–87.

11.   Isobe T et al. 2014. Elife **3**:e01977.

12.   Sun X et al. 2012. J Clin Invest **122**:1973–90.

13.   Li X-R et al. 2014. FEBS Lett **588**:3298–307.

14.   Takahashi Y, Chen Q, Rajala RVS, Ma J-X. 2015. FEBS Lett **589**:1143–9.

15.   Su Z et al. 2015. Exp Ther Med **9**:961–966.

16.   Newie I et al. 2014. PLoS One **9**:e97200.

17.   Shaked I et al. 2009. Immunity **31**:965–73.

18.   Biton M et al. 2011. Nat Immunol **12**:239–46.

19.   Fang Y et al. 2010. Proc Natl Acad Sci U S A **107**:13450–5.

Chapter 7: Investigating the use of miRNA expression as classifiers of trachomatous disease

7.1 The use of miRNA as classifiers

miR are post-transcriptional regulators of gene expression. Individual miR can regulate hundreds of genes [1] and single or small numbers of miR can have profound roles in the regulation of biological processes in health and disease (examples include cancer [2,3], organ aging [4], fibrosis [5] and inflammation [6–8]). In addition to aiding our understanding of the complex transcriptional patterns associated with disease mechanisms, miRNA can be used as predictors or biomarkers of disease. miR are of particular use when measured in longitudinal samples to predict disease progression [9]. The use of miR as prognostic biomarkers of infertility has previously been investigated in chlamydial disease in the murine genital tract [10]. Mice were infected with two strains of *C. muridarum* (Cm) that differ in virulence, however miRNA expression was only assessed at 24 hours post infection [10].

It is thought that all (or the vast majority) of individuals living in trachoma-endemic communities are exposed to Ct throughout childhood and that repeated episodes of Ct infection and associated inflammatory episodes (TI) lead to scarring progression and eventually blindness. It is not understood why only some exposed individuals progress to scarring disease where others do not. A miR transcriptional signature that could classify those at risk of scarring progression before the onset of clinical signs could help target treatment options to prevent or halt progressive scarring. miR could also be used as biomarkers of protective or adverse effects in response to a Ct vaccine if one was made available for testing in human populations.

An association between a biomarker and disease can be tested using regression (Chapter 6). When predicting a binary outcome (disease or no disease), a basic approach to evaluate the performance of the biomarker as a diagnostic test is to use Receiver-Operator Characteristic (ROC) analysis. A ROC curve is a plot of the true positive rate (sensitivity) against the false positive rate (1-specificity), which illustrates the ability of the predictor to diagnose disease as the discrimination threshold varies. The area under the curve (AUC) or 'C statistic' defines the performance of the predictor, with a large AUC (maximum 1) indicative of a perfect test and an AUC 0.5 meaning that the predictor is no better than chance.

Once a predictor or set of predictors is identified, their performance should be evaluated. Essentially a model is fitted to a 'training' data set to detect associations between the predictor and the disease outcome, then the model is tested in a different

dataset and the fit of the model to the new dataset is measured. A perfect predictor would be able to classify cases and controls in the new dataset with complete accuracy. These 'training' and 'testing' steps can be performed within the same dataset by splitting it half, however the fit of the model might depend on how the dataset is split. An alternative approach is to split and test the dataset many times, such as with 'leave one out cross validation' (LOOCV). The model is trained on all samples but one and then tested on that one sample. This is done for every sample in turn therefore the number of dataset splits is as large as the number of samples in the dataset. The optimum method of validating a predictor however, if possible, is to use an external dataset, ideally from a different population.

7.2 miR associated with scarring and inflammatory trachoma as classifiers

The goal of using classifiers in trachoma would be to find one or a few miR that could predict scarring progression. Scarring progression is strongly associated with TI, so miR that associated with TSI (Chapter 3) and TI (Chapter 6) were tested for their ability to classify disease in the same datasets. ROC curves were generated using expression data (delta cycle threshold values) for one or more miR (the classifier). Data were analysed using the Deducer package in R [11].

7.2.1. miR associated with TSI

miR-147b was upregulated in TSI relative to healthy controls (FC = 2.3, P = 0.03) and miR-1285 was upregulated in TSI relative to TS alone (FC = 4.6, P = 0.005) in a cohort of 194 adults (Chapter 3 [12]). Controls were defined as N (F0, P0, C0, n=93) and cases were defined as individuals with TS in the absence of inflammation (C1/2/3, P0/1, n=74). Both miR performed very poorly at diagnosing TS (miR-147b AUC = 0.5; miR-1285 AUC = 0.56) and were no better in combination (AUC = 0.53 (Figure 7.1)). Performance was no better when classifying cases as individuals with TS and TSI (C1/2/3, P1/2/3, n=96) (miR-147b AUC = 0.54; miR-1285 AUC = 0.49; miR-147b and miR-1285 AUC = 0.51 (data not shown)).
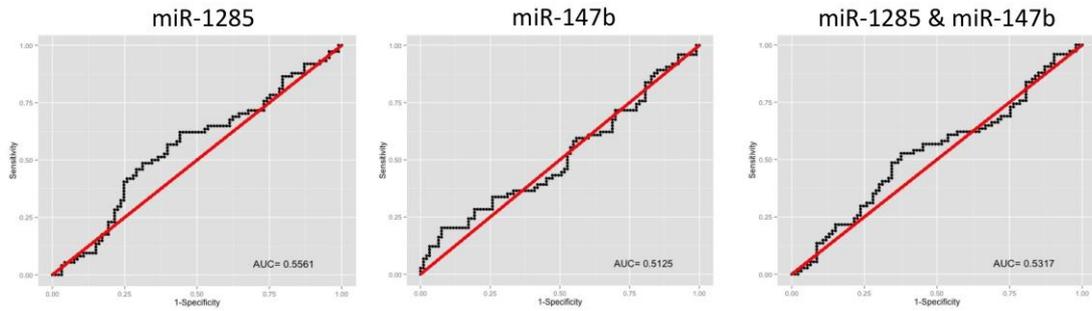
Figure 7.1. ROC curves showing the ability of miR-1285 and miR-147b to diagnose TS. The red line shows an AUC of 0.5. The black line tracks the performance of the predictor as the discrimination threshold varies. Sensitivity is plotted on the Y-axis and 1-Specificity is plotted on the X-axis.

7.2.2. miR associated with TI

miR-184 (P = $1.61*10^{-7}$, OR = 0.4) and miR-155 (P = 0.007, OR = 2.53) were strongly associated with TI in a cohort of 163 children aged between 1-9 years old (Chapter 6 [13]). Individuals were classified as controls (P0 or P1 using the 1981 WHO FPC trachoma grading system [14], n=135) or TI cases (P2 or P3, n=28). miR-155 (AUC = 0.78) and miR-184 (AUC = 0.74) were both good classifiers of TI independently, however the combined expression of miR-184 and miR-155 had an approximate classification accuracy of 91.3% to predict or diagnose TI (AUC = 0.913, Figure 7.2).
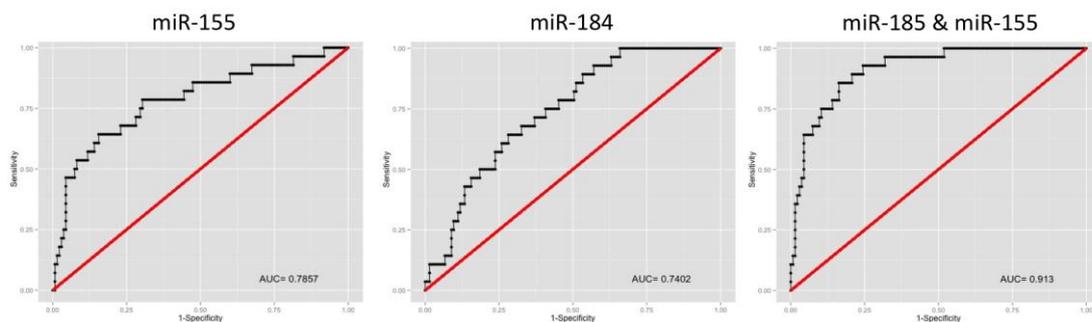
Figure 7.2. ROC curves showing the ability of miR-155 and miR-184 to diagnose TI. The red line shows an AUC of 0.5. The black line tracks the performance of the predictor as the discrimination threshold varies. Sensitivity is plotted on the Y-axis and 1-Specificity is plotted on the X-axis.

7.3 Summary

miR-147b and miR-1285 were upregulated in individuals with TSI and not in TS alone [12], which perhaps explains why they were poor classifiers of TS. This remains true even when cases were defined as individuals with TS and TSI, as the TSI group was much smaller than the TS group. These individuals already had established scarring however. Given that inflammation is a major risk factor for scarring progression [15], miR-147b and miR-1285 may be better able to classify individuals at risk of progressive scarring at an earlier stage of disease. miR-184 and miR-155 in combination were good classifiers of TI, however the number of individuals with TI in this 'training' cohort was small (n=28). The expression of miR-155, miR-184, miR-147b and miR-1285 will be quantified in a longitudinal cohort of 506 Tanzanian individuals with progressive scarring trachoma. Individuals were aged between 6 and 10 at the time of enrollment and were assessed quarterly over the course of four years. The ability of miR-155, miR-184, miR-147b and miR-1285 to classify individuals with progressive scarring relative to non-progressors will be investigated in this cohort, which is also large enough to split into training and testing datasets for appropriate validation. In addition to qualifying the use of these miR as biomarkers of progressive scarring, the results will further our understanding of the role of these miR in chlamydial disease.

7**.4 References**

1.   Ambros V (2004) The functions of animal microRNAs. Nature 431: 350–355. doi:10.1038/nature02871.

2.   Park S-M, Gaur AB, Lengyel E, Peter ME (2008) The miR-200 family determines the epithelial phenotype of cancer cells by targeting the E-cadherin repressors ZEB1 and ZEB2. Genes Dev 22: 894–907. doi:10.1101/gad.1640608.

3.   Korpal M, Lee ES, Hu G, Kang Y (2008) The miR-200 family inhibits epithelial-mesenchymal transition and cancer cell migration by direct targeting of E-cadherin transcriptional repressors ZEB1 and ZEB2. J Biol Chem 283: 14910–14914. doi:10.1074/jbc.C800074200.

4.   Boon RA, Iekushi K, Lechner S, Seeger T, Fischer A, et al. (2013) MicroRNA-34a regulates cardiac ageing and function. Nature 495: 107–110. doi:10.1038/nature11919.

5.   Cushing L, Kuang PP, Qian J, Shao F, Wu J, et al. (2011) miR-29 is a major regulator of genes associated with pulmonary fibrosis. Am J Respir Cell Mol Biol 45: 287–294. doi:10.1165/rcmb.2010-0323OC.

6.   Yao R, Ma Y-L, Liang W, Li H-H, Ma Z-J, et al. (2012) MicroRNA-155 modulates Treg and Th17 cells differentiation and Th17 cell function by targeting SOCS1. PLoS One 7: e46082. doi:10.1371/journal.pone.0046082.

7.   Xiang M, Birkbak NJ, Vafaizadeh V, Walker SR, Yeh JE, et al. (2014) STAT3 induction of miR-146b forms a feedback loop to inhibit the NF-κB to IL-6 signaling axis and STAT3-driven cancer phenotypes. Sci Signal 7: ra11. doi:10.1126/scisignal.2004497.

8.   Rodriguez A, Vigorito E, Clare S, Warren M V, Couttet P, et al. (2007) Requirement of bic/microRNA-155 for normal immune function. Science 316: 608–611. doi:10.1126/science.1139253.

9.   Boeri M, Verri C, Conte D, Roz L, Modena P, et al. (2011) MicroRNA signatures in tissues and plasma predict development and prognosis of computed tomography detected lung cancer. Proc Natl Acad Sci U S A 108: 3713–3718. doi:10.1073/pnas.1100048108.

10.   Yeruva L, Myers GSA, Spencer N, Creasy HH, Adams NE, et al. (2014) Early microRNA expression profile as a prognostic biomarker for the development of pelvic inflammatory disease in a mouse model of chlamydial genital infection. MBio 5: e01241–14. doi:10.1128/mBio.01241-14.

11.   Fellows I (2012) Deducer : A Data Analysis GUI for R. J Stat Softw 49: 1–15.

12.   Derrick T, Roberts C h., Rajasekhar M, Burr SE, Joof H, et al. (2013)

Conjunctival MicroRNA Expression in Inflammatory Trachomatous Scarring. PLoS Negl Trop Dis 7: e2117. doi:10.1371/journal.pntd.0002117.

13. Derrick T, Last AR, Burr SE, Roberts CH, Nabicassa M, et al. (2016) Inverse relationship between microRNA-155 and -184 expression with increasing conjunctival inflammation during ocular Chlamydia trachomatis infection. BMC Infect Dis 16: 60. doi:10.1186/s12879-016-1367-8.

14. Dawson CR, Jones BR TM, Dawson CR, Jones BR, Tarizzo ML, World Health Organization (1981) Guide to trachoma control in programmes for the prevention of blindness. 56 p.

15. Burton MJ, Rajak SN, Hu VH, Ramadhani A, Habtamu E, et al. (2015) Pathogenesis of progressive scarring trachoma in Ethiopia and Tanzania and its implications for disease control: two cohort studies. PLoS Negl Trop Dis 9: e0003763. doi:10.1371/journal.pntd.0003763.

Chapter 8: Induction of inflammation and EMT in *Chlamydia trachomatis* infected HEp-2 epithelial cells

8.1 Introduction

Epithelial cells are thought to play a large role in the immunopathology of chlamydial pathogenesis [1]. Epithelial cells infected with Ct *in vitro* produce a number of pro-inflammatory cytokines (IL-6, IL-8, IL-11, IL-18, IL-1α and granulocyte-macrophage colony-stimulating factor (GM-CSF)), chemokines (CXCL1, CXCL2, CXCL3) and growth factors such as fibroblast growth factor (FGF) [2–5]. Genes involved in cell growth, differentiation, immune suppression and apoptosis have also been shown to be expressed [3]. Pro-inflammatory factors were expressed throughout the developmental cycle of Ct (2-4 days) and required bacterial protein synthesis [2]. More recent evidence in a polarized endocervix-derived epithelial cell model showed that IL-1α, which is thought to amplify the pro-inflammatory response [2], was not expressed until 72 hours post infection (hpi) with Ct [5]. Interestingly, IL-1ra (IL-1 receptor antagonist) was constitutively expressed from the apical membrane in both Ct infected and mock-infected cells, whereas Ct-induced IL-11 expression was localized to the basolateral membrane. In contrast to earlier reports, protein levels of IL-8 and IL-6 were not different between infected and mock-infected cells at any timepoint throughout the developmental cycle, up to 120 hours [5]. What is more, Ct infection suppressed the constitutive expression of T-cell chemokines [5]. This immune evasion strategy presumably protects Ct and promotes growth, possibly increasing pathology long term by preventing prompt clearance of infection and promoting low levels of chronic inflammation. This study ([5]) also highlights the differences in host response to Ct infection between different cell lines and culture conditions. The role of epithelial cells in the immunopathology of chlamydial disease is further supported by studies carried out in individuals with TF, TS and TT. Expression of a number of pro-inflammatory mediators (*IL17A*, *IL1B*, *CXCL5*, *S100A7* (psoriasin), growth factors (*CTGF* (connective tissue growth factor)) and matrix metalloproteinases (*MMP7, MMP9*) were upregulated in TF/TI, TS and TT [6–10]. In TS and TT this occurred even in the absence of detectable Ct infection [6,7,9,8]. Immunohistochemistry (IHC) studies using tissue from a small number of individuals with TF/TI previously found that CTGF, IL-1α and IL-1β were increased in the conjunctival epithelium [11,12].

EMT-2 (EMT) is the process by which an epithelial cell differentiates into a mesenchymal cell upon chronic inflammatory stimulation. Cells undergoing EMT lose their apical-basal polarity, degrade the basement membrane and migrate into the subepithelial layer where they can contribute to fibrosis [13]. Pro-inflammatory

cytokines, growth factors and MMPs have been shown to stimulate EMT *in vivo* and *in vitro* [14–16]. Phenotypic changes related to EMT have previously been observed in response to Ct infection. In Ct infected epithelial cells the N-cadherin/β-catenin complex (a key structural component of adherens junctions) was broken down and β-catenin was recruited to the chlamydial inclusion, associated with a loss of cell-cell adhesion and cell polarity [17,18]. β-catenin is also a Wnt signaling transducer and the paracrine Wnt pathway was activated in Ct infected *ex vivo* fallopian tube tissue [18]. The Wnt pathway has also been shown to stimulate EMT [19], including in response to viral and intracellular bacterial infections [20,21]. A role for the Wnt pathway in trachomatous pathogenesis has also been hinted at in several clinical studies through pathway analysis of transcriptional data [22–24]. It is therefore plausible that Ct-induced epithelial inflammation stimulates EMT, which subsequently contributes to the fibrotic pathology associated with chlamydial disease.

Ct has a 7.5Kb plasmid which was found to be maintained in clinical ocular strains at a median copy number of 5.34 (range 1-18) [25]. Variation in plasmid copy number has been observed and genital strains are thought to have a slightly lower plasmid:genome ratio with a mean around 4 [26]. The chlamydial plasmid has been shown in ocular non-human primate (NHP) and murine genital model systems to be a virulence factor [27–29]. A plasmid-free Ct serovar F strain in a urogenital murine model had reduced infectivity and virulence relative to a plasmid-competent isogenic strain [27]. Plasmid-free Ct serotype A and L strains had identical growth kinetics to their plasmid-competent counterparts *in vitro*, however, virulence *in vivo* was reduced [28,29]. The impact of the Ct plasmid on virulence appears to be binary, as plasmid copy number did not associate with Ct load, papillary hypertrophy or lar score [25]. Plasmid-free Ct did not induce inflammatory pathology in an ocular NHP model [29] and plasmid-free *C. muridarum* (Cm) failed to induce inflammatory pathology in a murine genital tract model and did not stimulate TLR2-dependent cytokine production [30]. In contrast to plasmid-competent Cm, plasmid-free Cm did not induce IL-8 expression in two epithelial cell lines and this was associated with a reduction in neutrophil infiltration into the murine genital tract [30]. IL-8 is chemotactic for neutrophils, the presence of which has been directly correlated with the degree of oviduct pathology in Cm infected mice [31]. This implies a model whereby IL-8 expression is increased following TLR2-mediated recognition of the chlamydial plasmid, leading to neutrophil infiltration and pathology. The plasmid is not a virulence factor however in a murine *C. psittaci* intraperitoneal infection model and in a *C. caviae* urogenital infection model in guinea pigs [32,33]. A recent study examined the impact of the Ct plasmid in a NHP urogenital

model for the first time and found that, in contrast to the ocular Ct NHP model and murine Ct and Cm urogenital models, Ct serovar D plasmid-free and plasmid-competent strains had equal infectivity and induced equal pathology [34]. This might suggest that the impact of the Ct/Cm plasmid varies depending on the chlamydial strains, animal model and anatomical sites under investigation.

Recently a gene expression microarray analysis was performed in an epithelial cell line (HeLa) infected with a serovar A strain of Ct (A2497) and the plasmid-cured isogenic counterpart (A2497P-) [3]. These strains differed in virulence in the ocular NHP model [29]. Gene expression was assessed at 30 minutes, 2, 4, 24, 48 and 72 hours post infection (hpi). Relative to uninfected cells, differences in gene expression were not detected until 24 hpi, where more genes were differentially expressed (DE) in A2497 infected cells relative to A2497P-. The total number of DE genes was highest at 72 hpi and was comparable between A2497 and A2497P-. Differences in DE genes between A2497 and A2497P- were greatest at 48 hpi, with higher expression in A2497 infected cells of *CSF2* (GM-CSF), *CXCL1/2/3*, *IL1A*, *IL6* and *IL8* [3]. Overall fold changes and differences between A2497 and A2497P- were modest.

Infected epithelial cells clearly play an important role in orchestrating the immune response to Ct. The Ct plasmid appears to affect the magnitude of this response, resulting in increased pathology at the infection site with potential implications for later scarring sequelae. The aim of the work presented in this chapter was to investigate the induction of inflammation in Ct infected epithelial cells and to ascertain whether this stimulated EMT. The production of pro-inflammatory mediators, growth factors and EMT biomarkers was assessed by gene expression analysis in epithelial cells infected with plasmid-competent and plasmid-free strains of Ct, in order to understand the contribution of the plasmid to EMT induction. Motility of infected cells was measured using a scratch wound assay. If induction of EMT was detected, the aim was then to test for epigenetic changes and differences in specific protein expression. Due to the failure to achieve productive growth of Ct in a conjunctival epithelial cell line, experiments were performed in HEp-2 (HeLa) cells.

8.2 Methods

In vitro culture and Ct infection of human epithelial cell lines

Human epithelial type 2 (HEp-2) cells were cultured in Minimum Essential Medium (MEM) (Gibco, Life Technologies) supplemented with 1% gentamicin (Gibco), 10% fetal bovine serum (FBS) (Gibco), and 1% L-glutamine (Gibco). For *in vitro* experiments, cells were seeded in 12 well plates at $3x10^5$ cells per well in MEM.

HEp-2 were infected with 3 different ocular-derived serovar A Ct strains: A2497 (described in [35]), the plasmid cured counterpart (A2497P-) [29] and A/HAR-13 [35]. Cells were infected 24 hours after seeding at a multiplicity of infection (MOI) of 1 and without the addition of cycloheximide. EMT positive control cells were treated with 10 mg/ml TGFβ2 and 10 mg/ml EGF (Peprotech) 24 hours after seeding. Ct infected cells, TGFβ2 & EGF treated cells and mock-infected cells were centrifuged at 1800 r.p.m. (750g) for 1 hr to facilitate infection and were incubated at 37°C in 5% CO_2. Six replicates were carried out for each biological condition. At 48 hours post-infection (hpi), media was removed and cells were washed in 1X phosphate-buffered saline (PBS) (Sigma). Three hundred microliters of lysis buffer (Norgen Biotek, Thorold, ON, Canada) was added to each well and cells were harvested by scraping. Total RNA and DNA were extracted using the Norgen RNA and DNA purification kit according to the manufacturers instructions. Total RNA was quantified using Qubit® fluorometric quantitation (Life Technologies).

Confocal microscopy and ddPCR were performed as described previously (Chapter 4).

Scratch wound assay

HEp-2 cells were seeded in 12 well plates at $1x10^5$ cells per well in MEM [with supplements]. Cells were infected 24 hours after seeding with A2497 and A2497P- (as described above) at an MOI of 0.5. Positive control wells were treated with 10 mg/ml TGFβ2 and 10 mg/ml EGF and negative control wells received fresh media alone. Triplicate wells were performed for each condition. Twenty-four hours after infection or addition of TGFβ2 & EGF cells were scratched down the center of the well using a 20µl pipette tip. Media was not changed and cells were not washed. Three marks were made on the underside of each well along the length of the scratch using permanent marker. A photograph was taken of the scratch on the microscope in exactly the same

position at 0, 24 and 48 hours post scratch. Photographs were taken using an OptixCam Summit OCS-10.0X 10MP camera on a Nikon inverted microscope under 4/0.10 objective. Photographs were viewed in OCView software (v1.1). The area of the scratch wound on each image was measured in ImageJ (http://rsb.info.nih.gov/ij/index.html) using the polygon selection tool to outline the leading edge of the monolayer and obtain the area of the scratch. The rate of wound closure was calculated using the equation $[(Tn/T0)*100]$ to express wound area at each timepoint (Tn) as a percentage of the area at timepoint zero (T0).

Quantitative polymerase chain reaction (qPCR)

Total RNA was reverse transcribed using MiScript RTII kits with the HiFlex buffer (Qiagen) to make a cDNA library. qPCR was performed on total RNA extracted from infected, TGFβ2 & EGF treated and mock-infected HEp-2 cells. Primers were designed using NCBI gene data (http://www.ncbi.nlm.nih.gov/gene/), Primer3 (http://primer3.wi.mit.edu) and SIM4 (http://pbil.univ-lyon1.fr/members/duret/cours/inserm210604/exercise4/sim4.html) software. All primers were designed in a standard way for this study and sequences are shown in Table 8.1. Primers were mRNA specific such that the primer sequences either crossed an intron-intron boundary or if that was not possible the DNA amplicon size was deemed too large for amplification using Power SYBR master mix. Ten µl cDNA was diluted in 100µl dH_2O for use in qPCR. Primer efficacy was tested and qPCR was optimized using HEp-2 cell cDNA on an HT7900 thermal cycler (Thermo Fisher Scientific) with Power SYBR Green PCR master mix (Thermo Fisher Scientific). Cycling conditions were 10 minutes at 95°C followed by 40 cycles of 15 seconds at 95°C and 1 minute at 60°C. An initial dissociation curve was included to evaluate primer performance and ensure specificity.

Statistical analysis

Data were analysed in R (www.R-project.org). Fold difference in cycle threshold values were calculated using the 2(-Delta Delta CT) method [36], normalizing to the reference ribosomal gene *RPLP0*. If data were normally distributed, assessed by using a Shapiro Wilk test for normality, differential expression between infections and mock-infected cells were tested using a students t -test. Wilcoxon signed ranks test was used where data were not normally distributed. P values were adjusted for false discovery rate according to Benjamini-Hochberg [37].

Table 8.1. Primers sequences used for qPCR

Target name (Gene symbol)	Forward primer	Reverse primer	Product size
Endogenous control:			
RPLP0	ATCTGCTTGGAGCCCACAT	GCGACCTGGAAGTCCAACTA	101
EMT biomarkers:			
E-cadherin (CDH1)	TATTCCTCCCATCAGCTGCC	AGCGTGAGAGAAGAGAGTGT	232
αSMA (ACTA2)	CGGGACTAAGACGGGAATCC	TCACCCACGTAGCTGTCTTT	211
SNAIL (SNAI1)	GTGGTTCTTCTGCGCTACTG	TGCTGGAAGGTAAACTCTGGA	153
Fibronectin (FN1)	TGGGTGACACTTATGAGCGT	TCAAAACACTTCTCAGCTATGGG	241
SLUG (SNAI2)	CGAACTGGACACACATACAGT	GAGGTGTCAGATGGAGGAGG	225
N-cadherin (CDH2)	TGTTTGACTATGAAGGCAGTGG	TCAGTCATCACCTCCACCAT	152
TWIST (TWIST1)	AGGGCCGGAGACCTAGATG	CACGCCCTGTTTCTTTGAAT	152
FSP-1 (S100A4)	CGTGTTGATCCTGACTGCTG	GCTGTCCAAGTTGCTCATCA	214
Vimentin (VIM)	GATGCCCTTAAAGGAACCAA	AGGCGGCCAATAGTGTCTT	104
ZO-1 (TJP1)	AAGAGAAAGGTGAAACACTGCTGA	GGAAGACACTTGTTTTGCCAGGT	127
Inflammatory genes:			
IL-1β (IL1B)	CCTGAAGCCCTTGCTGTAGT	AGCTGATGGCCCTAAACAGA	112
S100A7 (S100A7)	TCTTGTCATCACGTCTGGTGT	CTACTCGTGACGCTTCCCA	121
IL-1α (IL1A)	CTTAGTGCCGTGAGTTTCCC	TGTGACTGCCCAAGATGAAG	118
CXCL1 (CXCL1)	CTTCCTCCTCCCTTCTGGTC	CCAAACCGAAGTCATAGCCA	133
GM-CSF (CSF2)	GTCTCACTCCTGGACTGGCT	ACTACAAGCAGCACTGCCCT	140
CTGF (CTGF)	TGGAGATTTTGGGAGTACGG	TACCAATGACAACGCCTCCT	128
IL-6 (IL6)	CTGCAGCCACTGGTTCTGT	CCAGAGCTGTGCAGATGAGT	143
IL-8 (IL8)	AGCACTCCTTGGCAAAACTG	CAAGAGCCAGGAAGAAACCA	137

8.3 Results

8.3.1 Ct growth in HEp-2 cells

HEp-2c cells infected with A2497 and A2497P- achieved comparable yields at 48 hours post infection (hpi), measured by *omcB* load and by observation of chlamydial inclusions (Figures 4.1 and 4.2 (Chapter 4)). Plasmid DNA was not detected in DNA extracted from plasmid-free cultures by ddPCR (data not shown). A/HAR-13 did not achieve a comparable yield and was excluded from further qPCR analysis.

8.3.2 Inflammatory gene expression in Ct infected HEp-2 cells

The expression of a number of pro-inflammatory cytokines (IL-1α, IL-1β, IL-6, GM-CSF), chemokines (CXCL1, IL-8), the anti-microbial peptide S100A7 and CTGF was quantified in HEp-2 cells infected with A2497 and A2497P- at 48 hpi. These targets were chosen based on their roles from the literature on Ct infection models and in various stages of trachoma.

CTGF, *CXCL1*, *IL1A*, *IL6* and *IL8* were upregulated in A2497 and A2497P- infected HEp-2 cells relative to mock-infected cells (Figure 8.1, Table 8.2). *CTGF*, *CXCL1* and *IL6* expression were greater in A2497 infected cells compared to A2497P- infected cells. The results of differential gene expression analysis are shown in Table 8.2. *S100A7* expression in infected cells was comparable to mock-infected cells and *CSF2* was slightly downregulated relative to mock-infected cells. *IL1B* had a mean cycle threshold value >35 for each of the conditions tested therefore it was excluded from the analysis.

Table 8.2. Differential expression of inflammatory genes in A2497P- and A2497 infected HEp-2 cells relative to uninfected cells, ordered by Padj.

Target	A2497P-		A2497	
	Padj	FC	Padj	FC
CTGF	0.096	1.76	0.015	1.91
IL6	0.059	2.19	0.015	3.12
CXCL1	0.143	2.20	0.024	2.73
IL8	0.085	2.17	0.146	2.07
IL1A	0.189	3.70	0.126	4.05
S100A7	0.881	1.29	1.000	1.34
CSF2	0.654	0.65	0.758	0.90

FC: Fold change
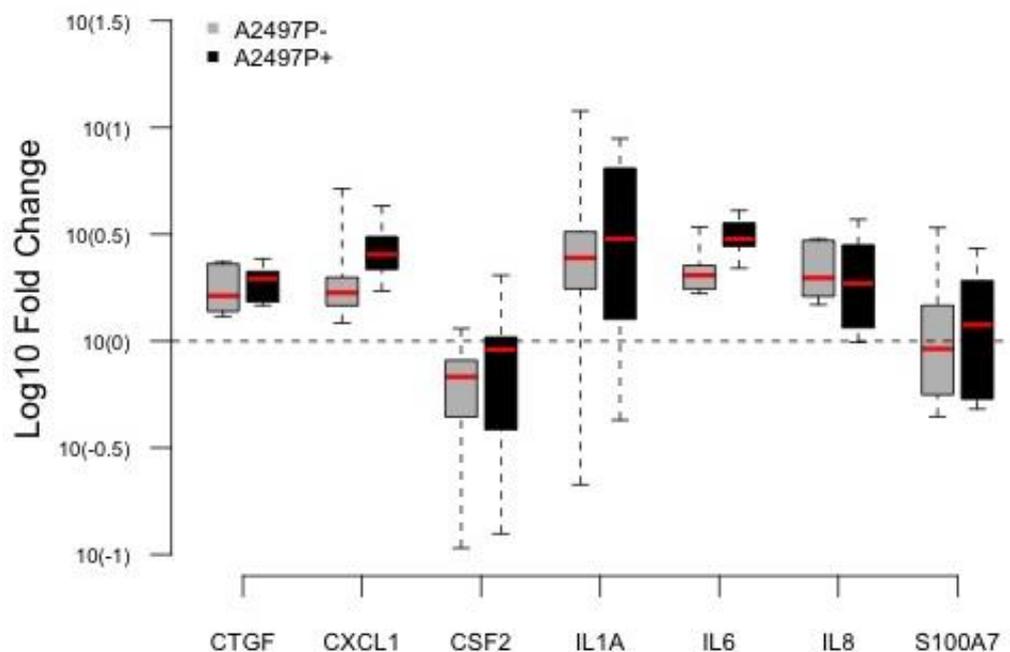
Figure 8.1. Gene expression of pro-inflammatory mediators and growth factors in HEp-2 cells infected with A2497 and A2497P- at 48 hpi. The log(10) fold change is shown relative to target expression in mock-infected cells. The dotted line represents a fold change of one, equivalent to no change in expression. Boxplots show the median (thick red horizontal line), the interquartile range (solid black or grey box) and the minimum and maximum values (dotted lines) of the six replicates for each target and infection. Grey: A2497P-, Black: A2497.

8.3.3 EMT biomarker expression in Ct infected HEp-2 cells

HEp-2 cells were treated with TGFβ2 and EGF in order to stimulate the induction of EMT [38]. Mesenchymal cell markers Fibronectin (FN1), N-cadherin (CDH2), Vimentin (VIM), αSMA (ACTA2), FSP-1 (S100A4), epithelial cell marker ZO-1 (TJP1) and EMT transcription factors TWIST (TWIST1), SLUG (SNAI2) and SNAIL (SNAI1) were tested in HEp-2 cells by qPCR every 24 hours for 5 days to detect those which were characteristic of EMT in this *in vitro* model. CDH2, VIM and FN1 were upregulated in the *in vitro* model with expression peaking at 48 hours post stimulation (data not shown). Cells appeared more fibroblastic and motile compared to untreated epithelial cells, which had a pavement-like morphology (Figure 8.2A and B). These changes were evident as early as 17 hours post stimulation (data not shown). *SNAI1* was slightly upregulated and *S100A4*, *ACTA2*, *TJP1*, *TWIST1* and *SNAI2* were not differentially expressed in this positive control model.
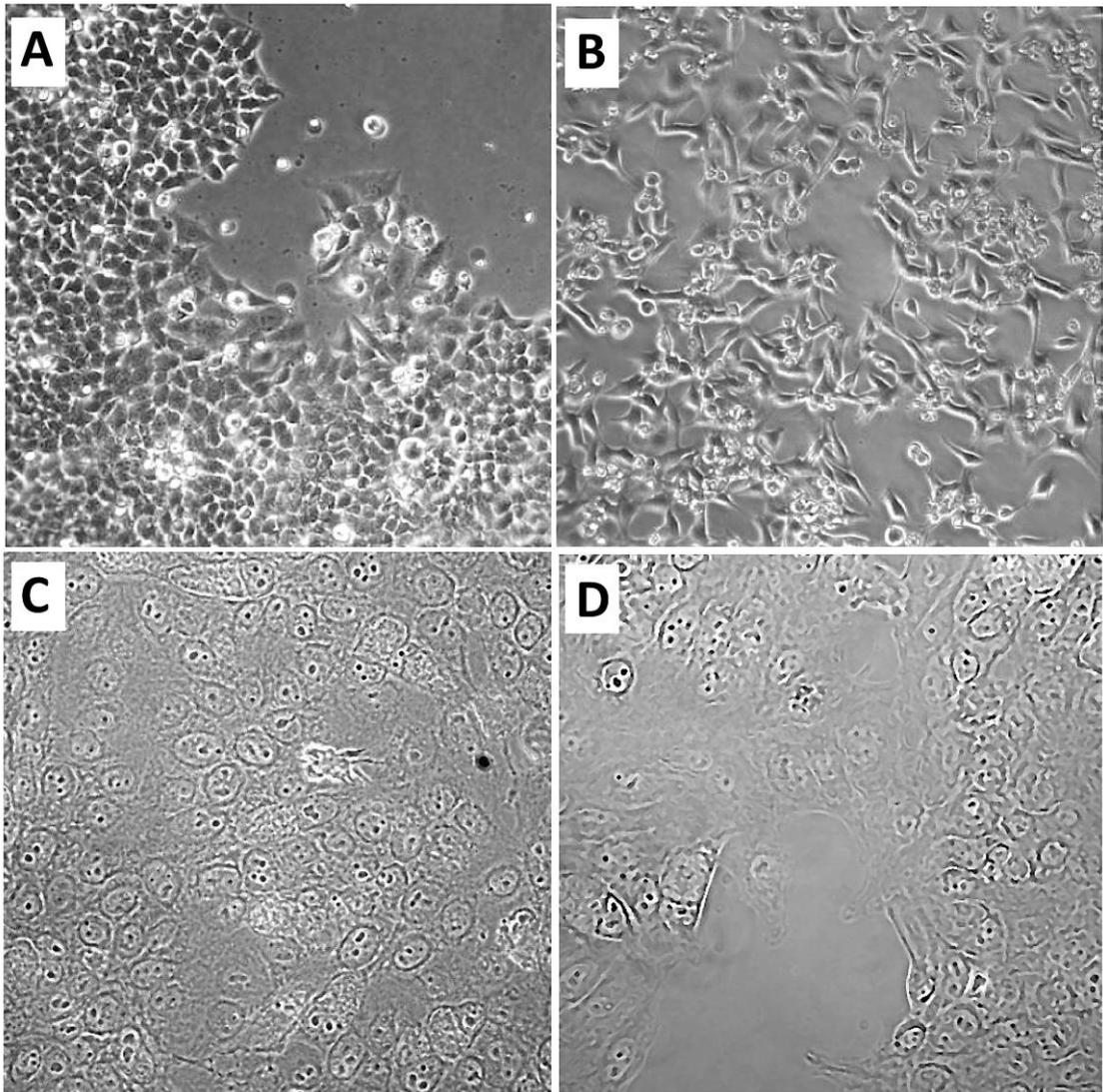
Figure 8.2. Morphology of cells undergoing EMT and Ct infected HEp-2 cells. At 120 hours post stimulation, untreated cells (A) have epithelial pavement-like morphology whereas TGFβ2 and EGF treated cells (B) have acquired and maintained a fibroblastic phenotype. At 48 hours post infection, A2497P- (C) and A2497 infected cells (D) appear to maintain epithelial morphology. Images (A) and (B) were taken of live cells in areas of sub-confluence to show cell morphology more clearly. Images (C) and (D) are phase images derived from confocal microscopy of infected cells. Cells were near confluent therefore it was more difficult to observe cell morphology, however, A2497 infected cells (D) did not appear to be migrating into the space. Images (C) and (D) were taken at 40X magnification.

Expression of *VIM*, *CDH2* and *FN1* was quantified in A2497 and A2497P- infected, TGFβ2 and EGF treated and mock-infected HEp-2 cells at 48 hours post infection or stimulation (Figure 8.3). In TGFβ2 and EGF treated cells *FN1* (P_{adj} = 0.00045, FC =

16.64), *CDH2* (P_{adj} = 0.016, FC = 3.9) and *VIM* (P_{adj} = 0.034, FC = 8.8) were significantly upregulated relative to untreated cells. A2497 and A2497P- infected cells did not differentially express EMT biomarkers in this *in vitro* model at 48 hpi. *FN1* was slightly upregulated in A2497P- infected cells but the difference was not significant (P_{adj} = 0.283, FC = 2.02). Infected cells at 48 hpi appeared to have epithelial pavement type morphology, however, this was difficult to assess as cells were near confluent and images were taken at an earlier timepoint than positive control images (Figure 8.2).
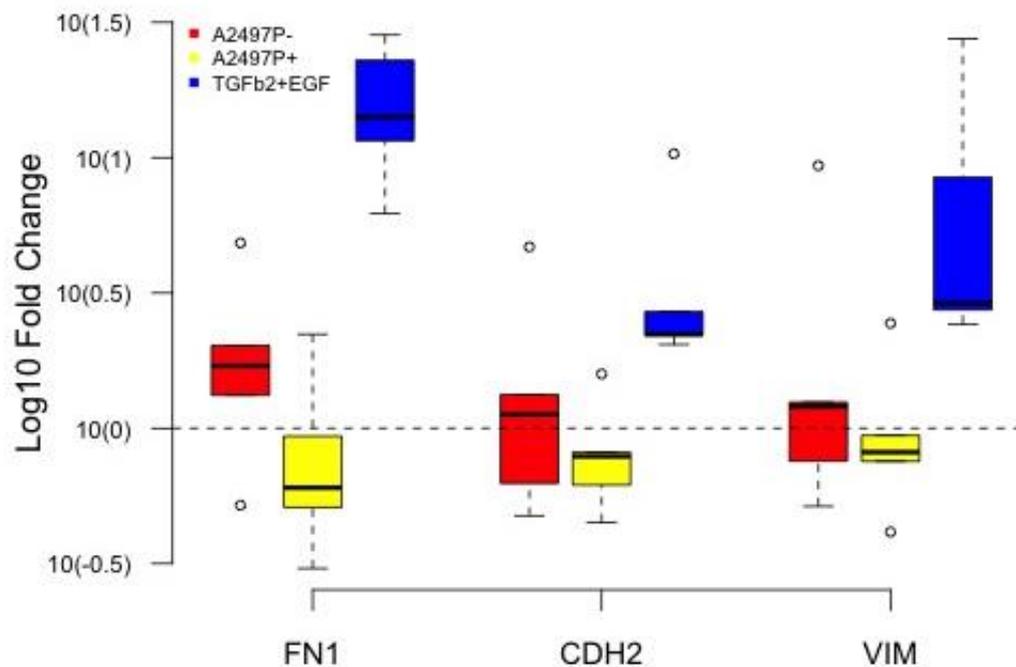
Figure 8.3. Expression of EMT biomarkers in Ct infected and TGFβ2 & EGF treated HEp-2 cells at 48 hpi. The log(10) fold change is shown relative to target expression in mock-infected cells. The dotted line represents a fold change of one, equivalent to no change in expression. Boxplots show the median (thick black horizontal line), the interquartile range (solid coloured box) and the minimum and maximum values (dotted line or circles) of the six replicates for each target and condition. Red: A2497P-, Yellow: A2497, Blue: TGFβ2 & EGF.

8.3.4 Cell motility in Ct infected HEp-2 cells

Increased motility and migration is a hallmark of cells undergoing EMT and these can be measured a using scratch wound assay [39]. The motility of HEp-2 cells infected with A2497 and A2497P- was measured by scratching the monolayer of infected cells at 24 hpi and recording the rate of wound closure. TGFβ2 and EGF treated cells closed

the wound significantly faster than untreated cells at 24 (P_{adj} = 1.32*10^{-15}) and 48 (P_{adj} = 2.26*10^{-12}) hours post scratch (Figure 8.4). Cells infected with A2497 and A2497P- had equal rates of wound closure to untreated cells at 24 (A2497P- P_{adj} = 0.35; A2497 P_{adj} = 0.086) and 48 (A2497P- P_{adj} = 0.61; A2497 P_{adj} = 0.35) hours post scratch (72 hours post infection).
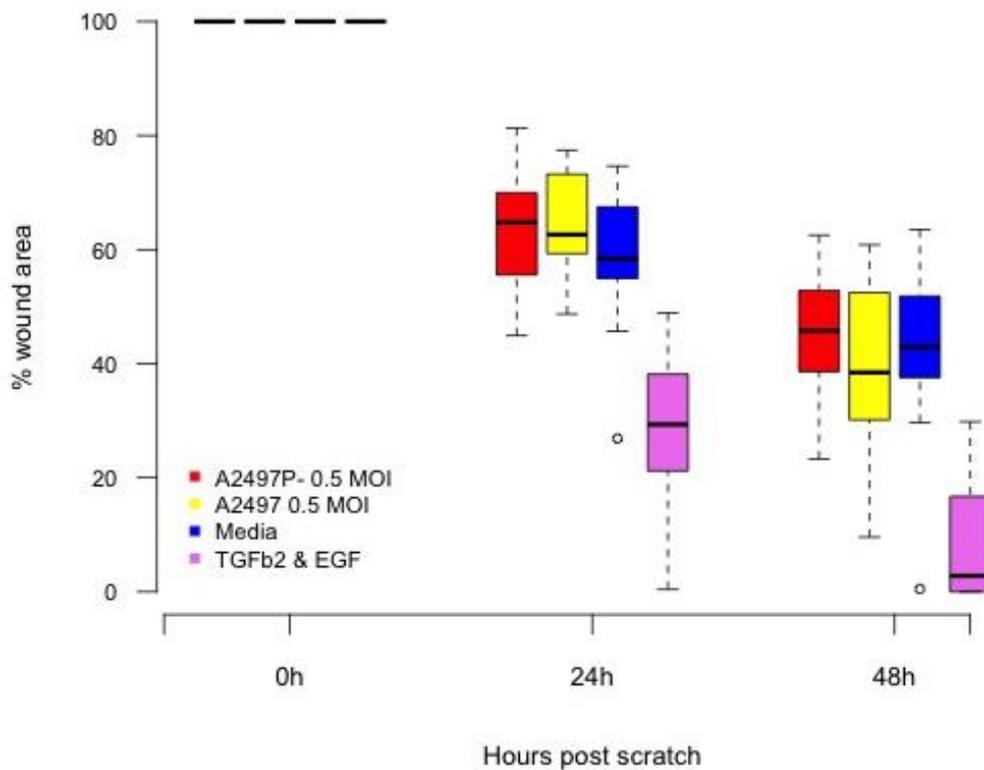
Figure 8.4. Speed of wound closure in A2497 and A2497P- infected, TGFβ2 & EGF treated and uninfected/untreated HEp-2 cells. Cells were scratched 24 hours post infection/treatment and the area of the wound was measured in ImageJ at 0, 24 and 48 hours post scratch. The remaining area at each time point is expressed as a percentage of the wound area at 0 hours. Three measurements were made per well of three replicate wells per experiment. The results of three experiments are shown. Boxplots show the median (thick black horizontal line), the interquartile range (solid coloured box) and the minimum and maximum values (dotted line or circles). Red: A2497P-, Yellow: A2497, Blue: Media (untreated), Pink: TGFβ2 & EGF.

8.4 Discussion

A modest induction of inflammatory cytokines was observed upon infection of HEp-2 cells with A2497 and A2497P-. Infected cells upregulated expression of *IL1A*, *IL6*, *IL8*, *CXCL1* and *CTGF*. *CTGF*, *CXCL1* and *IL6* were significantly upregulated in response to A2497 and expression levels were greater in response to A2497 relative to A2497P-. *S100A7* and *CSF2* were not differentially expressed in response to infection and *IL1B* was expressed at very low levels overall. Optimization of an *in vitro* model of EMT in HEp-2 cells revealed that *FN1*, *VIM* and *CDH2* were upregulated, with expression peaking at 48 hours post stimulation. Despite the induction of inflammatory stimuli and *CTGF* in A2497 and A2497P- infected HEp-2 cells, EMT was not detected by qPCR at 48 hpi and cell motility was equal to uninfected cells at 72 hpi.

The significant upregulation of *IL6* and *CXCL1* and the (non-significant) upregulation of *IL8* and *IL1A* in Ct infected epithelial cells was concordant with the results of other studies [2–5]. IL-8 and CXCL1 are chemoattractant to neutrophils, which kill infected cells and bacteria at the infection site but can also cause collateral tissue damage [31]. IL-6 and IL-1α initiate fever, amplify pro-inflammatory responses and stimulate production of acute phase proteins and neutrophils in the bone marrow. *IL6*, *CXCL1* and *CTGF* expression was highest in response to A2497, despite comparable Ct genome copy numbers in both infections. Porcella *et al.,* reported increased expression of *IL6*, *CXCL1* and *IL8* in response to A2497 relative to A2497P- infected cells [3], however in contrast to this and other reports [30] no difference was observed in *IL8* expression between A2497 and A2497P- infected cells in this study. Surprisingly, *CSF2* was not upregulated in HEp-2 cells in response to A2497 or A2497P-. Porcella *et al.,* reported that *CSF2* was upregulated in HeLa cells infected with A2497 and A2497P- at 72 hpi but there was minimal difference in gene expression relative to mock-infected cells at 48 hpi [3], supporting this result. *IL1B* was expressed at very low levels. IL-1β is translated into an inactive protein and is cleaved into the active form by activated caspase 1; therefore transcription levels may not accurately represent levels of active protein. This could be assessed using ELISA, immunocytochemistry or immunohistochemistry (performed on TT biopsy tissue in Chapter 11 (not in response to Ct)). S100A7 is an antimicrobial peptide that is upregulated in the conjunctiva of individuals with TF/TI, TS and TT [6,8–10]. *S100A7* expression was induced in progesterone-primed endometrial cells in response to Ct [40], however no difference in expression was identified in this study, or by Porcella *et al.,* [3]. These differences could be due to the cell lines and stimuli used. CTGF has not previously been reported

to be upregulated in response to Ct infection of epithelial cells, however it was upregulated in TF/TI, TS and TT [8,32,34, chapter 10]. CTGF can directly induce fibrosis and EMT [15,41,42] and its upregulation has been reported in epithelial cells in response to other bacteria [43]. The finding that *CTGF* expression is upregulated in response to A2497 and A2497P- could provide a possible direct mechanism for Ct induced fibrosis and could contribute to early stage scarring in individuals with TF/TI.

EMT can be induced directly in response to pathogen virulence factors (within 24 hours) [21,44], or as a result of pathogen-induced inflammation [14,45]. The 48 hpi timepoint was used to assess EMT biomarker expression in this study as it was the point at which up-regulation of EMT biomarkers in the *in vitro* positive control model and reported transcriptional differences between A2497 and A2497P- were greatest [3]. This therefore offered the best chance to detect differences in response to the two strains. It is possible that this timepoint was too early for EMT to develop *in vitro* in response to Ct, although there were no differences in cell motility relative to uninfected cells at 72 hpi. *CDH2*, *VIM* and *FN1* were not differentially expressed in A2497 or A2497P- infected HeLa cells at any of the timepoints studied by Porcella *et al.,* up to 72 hpi [3]. There was also no consistent decrease in *CDH1* (E-cadherin) expression [3], which is considered to be an early sign of EMT induction [46]. Transepithelial electrical resistance (TEER) can be used to measure epithelial tight junction integrity and a reduction in TEER occurs during EMT [47]. A slight decrease in TEER was detected between 0 and 4 days post infection of a polarized endocervical epithelial cell model with Ct serovar D, however the decrease was not significant and the TEER measurement remained above the threshold for a polarized epithelium [5,48]. In contrast to this result, CDH1 and occludin localization were disrupted in *ex vivo* fallopian tube tissue 48 hours post infection with Ct serovar D, reflecting a loss of cell-cell adhesion and polarity [18]. These differences could relate to the cellular milieu of the infected cells; it is possible that factors and signals from other cell types may be required to stimulate EMT in response to Ct infection. In an analysis of miRNA expression in the conjunctiva of individuals with TF and current Ct infection versus healthy controls (Chapter 5, supplementary information (DEseq analysis)), miR-204-5p (P_{adj} = 0.018, FC = 0.13), miR-200b-3p (P_{adj} = 0.078, FC = 0.39) and miR-429 (P_{adj} = 0.04, FC = 0.36) were among the top 26 most significantly differentially regulated miRNA out of the 860 miRNA detected. Down-regulation of these miRNA stimulates EMT induction [49,50]. The data also hinted at activation of the Wnt pathway through downregulation of miR-184 [51] (Chapter 5). The expression of EMT biomarkers and members of the Wnt pathway could be investigated further using RNA from individuals

with TF/TI and current Ct infection in order to determine whether a combination of cell types and inflammatory signals, combined with prolonged Ct infections *in vivo,* are required to stimulate EMT.

Despite the induction of inflammation in Ct infected HEp-2 cells, EMT was not detected by expression of EMT biomarkers or changes in cell motility. This data and that of others [3,5] suggest that EMT is not directly stimulated by Ct or Ct-induced inflammation at early timepoints post-infection of epithelial cells *in vitro.* It does not rule out however that EMT might occur in response to Ct *in vivo.* Future *in vitro* work should assess the induction of EMT in polarized ocular epithelial/fibroblast co-culture systems or in an engineered conjunctiva (epithelial cells-collagen basement membrane-stromal cells [52]) that includes inflammatory cell stimuli or in *ex vivo* tissue [53] and at later timepoints post infection, to better mimic the *in vivo* inflammatory environment during active trachoma.

8.5 References

1.   Stephens RS (2003) The cellular paradigm of chlamydial pathogenesis. Trends Microbiol 11: 44–51.

2.   Rasmussen SJ, Eckmann L, Quayle AJ, Shen L, Zhang YX, et al. (1997) Secretion of proinflammatory cytokines by epithelial cells in response to Chlamydia infection suggests a central role for epithelial cells in chlamydial pathogenesis. J Clin Invest 99: 77–87. doi:10.1172/JCI119136.

3.   Porcella SF, Carlson JH, Sturdevant DE, Sturdevant GL, Kanakabandi K, et al. (2015) Transcriptional Profiling of Human Epithelial Cells Infected with Plasmid-Bearing and Plasmid-Deficient Chlamydia trachomatis. Infect Immun 83: 534–543. doi:10.1128/IAI.02764-14.

4.   Kim JH, Jiang S, Elwell CA, Engel JN (2011) Chlamydia trachomatis Co-opts the FGF2 Signaling Pathway to Enhance Infection. PLoS Pathog 7: e1002285. doi:10.1371/journal.ppat.1002285.

5.   Buckner LR, Lewis ME, Greene SJ, Foster TP, Quayle AJ (2013) Chlamydia trachomatis infection results in a modest pro-inflammatory cytokine response and a decrease in T cell chemokine secretion in human polarized endocervical epithelial cells. Cytokine 63: 151–165. doi:10.1016/j.cyto.2013.04.022.

6.   Burton MJ, Rajak SN, Bauer J, Weiss H a, Tolbert SB, et al. (2011) Conjunctival transcriptome in scarring trachoma. Infect Immun 79: 499–511. doi:10.1128/IAI.00888-10.

7.   Hu VH, Weiss HA, Ramadhani AM, Tolbert SB, Massae P, et al. (2012) Innate immune responses and modified extracellular matrix regulation characterize bacterial infection and cellular/connective tissue changes in scarring trachoma. Infect Immun 80: 121–130. doi:10.1128/IAI.05965-11.

8.   Burton MJ, Rajak SN, Hu VH, Ramadhani A, Habtamu E, et al. (2015) Pathogenesis of progressive scarring trachoma in Ethiopia and Tanzania and its implications for disease control: two cohort studies. PLoS Negl Trop Dis 9: e0003763. doi:10.1371/journal.pntd.0003763.

9.   Burton MJ, Rajak SN, Ramadhani A, Weiss HA, Habtamu E, et al. (2012) Post-operative recurrent trachomatous trichiasis is associated with increased conjunctival expression of S100A7 (psoriasin). PLoS Negl Trop Dis 6: e1985. doi:10.1371/journal.pntd.0001985.

10.   Burton MJ, Ramadhani A, Weiss HA, Hu V, Massae P, et al. (2011) Active trachoma is associated with increased conjunctival expression of IL17A and profibrotic cytokines. Infect Immun 79: 4977–4983. doi:10.1128/IAI.05718-11.

11.   Abu el-Asrar a M, Geboes K, Tabbara KF, al-Kharashi S a, Missotten L, et al.

(1998) Immunopathogenesis of conjunctival scarring in trachoma. Eye (Lond) 12 (Pt 3a: 453–460. doi:10.1038/eye.1998.104.

12. Abu El-Asrar a M, Al-Kharashi S a, Missotten L, Geboes K (2006) Expression of growth factors in the conjunctiva from patients with active trachoma. Eye (Lond) 20: 362–369. doi:10.1038/sj.eye.6701884.

13. Kalluri R, Weinberg RA (2009) Review series The basics of epithelial-mesenchymal transition. 119. doi:10.1172/JCI39104.1420.

14. Liu X (2008) Inflammatory cytokines augments TGF-β1-induced epithelial-mesenchymal transition in A549 cells by up-regulating TβR-I. Cell Motil Cytoskeleton 65: 935–944. doi:10.1002/cm.20315.

15. Sonnylal S, Xu S, Jones H, Tam A, Sreeram VR, et al. (2013) Connective tissue growth factor causes EMT-like cell fate changes in vivo and in vitro. J Cell Sci 126: 2164–2175. doi:10.1242/jcs.111302.

16. Radisky ES, Radisky DC (2010) Matrix metalloproteinase-induced epithelial-mesenchymal transition in breast cancer. J Mammary Gland Biol Neoplasia 15: 201–212. doi:10.1007/s10911-010-9177-x.

17. Prozialeck WC, Fay MJ, Lamar PC, Pearson CA, Sigar I, et al. (2002) Chlamydia trachomatis disrupts N-cadherin-dependent cell-cell junctions and sequesters beta-catenin in human cervical epithelial cells. Infect Immun 70: 2605–2613.

18. Kessler M, Zielecki J, Thieck O, Mollenkopf H-J, Fotopoulou C, et al. (2011) Chlamydia Trachomatis Disturbs Epithelial Tissue Homeostasis in Fallopian Tubes via Paracrine Wnt Signaling. Am J Pathol 180: 198–186. doi:10.1016/j.ajpath.2011.09.015.

19. Chen H-C, Zhu Y-T, Chen S-Y, Tseng SCG (2012) Wnt signaling induces epithelial-mesenchymal transition with proliferation in ARPE-19 cells upon loss of contact inhibition. Lab Invest 92: 676–687. doi:10.1038/labinvest.2011.201.

20. Malizia AP, Lacey N, Walls D, Egan JJ, Doran PP (2009) CUX1/Wnt signaling regulates epithelial mesenchymal transition in EBV infected epithelial cells. Exp Cell Res 315: 1819–1831. doi:10.1016/j.yexcr.2009.04.001.

21. Tahoun A, Mahajan S, Paxton E, Malterer G, Donaldson DS, et al. (2012) Salmonella transforms follicle-associated epithelial cells into M cells to promote intestinal invasion. Cell Host Microbe 12: 645–656. doi:10.1016/j.chom.2012.10.009.

22. Holland MJ, Jeffries D, Pattison M, Korr G, Gall A, et al. (2010) Pathway-focused arrays reveal increased matrix metalloproteinase-7 (matrilysin) transcription in trachomatous trichiasis. Invest Ophthalmol Vis Sci 51: 3893–3902.

doi:10.1167/iovs.09-5054.

23. Derrick T, Roberts C h., Rajasekhar M, Burr SE, Joof H, et al. (2013) Conjunctival MicroRNA Expression in Inflammatory Trachomatous Scarring. PLoS Negl Trop Dis 7: e2117. doi:10.1371/journal.pntd.0002117.

24. Natividad A, Freeman TC, Jeffries D, Burton MJ, Mabey DCW, et al. (2010) Human conjunctival transcriptome analysis reveals the prominence of innate defense in Chlamydia trachomatis infection. Infect Immun 78: 4895–4911. doi:10.1128/IAI.00844-10.

25. Last AR, Roberts C h, Cassama E, Nabicassa M, Molina-Gonzalez S, et al. (2014) Plasmid copy number and disease severity in naturally occurring ocular Chlamydia trachomatis infection. J Clin Microbiol 52: 324–327. doi:10.1128/JCM.02618-13.

26. Seth-Smith HMB, Harris SR, Persson K, Marsh P, Barron A, et al. (2009) Co-evolution of genomes and plasmids within Chlamydia trachomatis and the emergence in Sweden of a new variant strain. BMC Genomics 10: 239. doi:10.1186/1471-2164-10-239.

27. Sigar IM, Schripsema JH, Wang Y, Clarke IN, Cutcliffe LT, et al. (2013) Plasmid deficiency in urogenital isolates of Chlamydia trachomatis reduces infectivity and virulence in a mouse model. Pathog Dis: 1–9. doi:10.1111/2049-632X.12086.

28. Carlson JH, Whitmire WM, Crane DD, Wicke L, Virtaneva K, et al. (2008) The Chlamydia trachomatis plasmid is a transcriptional regulator of chromosomal genes and a virulence factor. Infect Immun 76: 2273–2283. doi:10.1128/IAI.00102-08.

29. Kari L, Whitmire WM, Olivares-Zavaleta N, Goheen MM, Taylor LD, et al. (2011) A live-attenuated chlamydial vaccine protects against trachoma in nonhuman primates. J Exp Med 208: 2217–2223. doi:10.1084/jem.20111266.

30. O'Connell CM, Ingalls RR, Andrews CW, Scurlock AM, Darville T (2007) Plasmid-deficient Chlamydia muridarum fail to induce immune pathology and protect against oviduct disease. J Immunol 179: 4027–4034.

31. Frazer LC, O'Connell CM, Andrews CW, Zurenski M a, Darville T (2011) Enhanced neutrophil longevity and recruitment contribute to the severity of oviduct pathology during Chlamydia muridarum infection. Infect Immun 79: 4029–4041. doi:10.1128/IAI.05535-11.

32. Miyairi I, Laxton JD, Wang X, Obert CA, Arva Tatireddigari VRR, et al. (2011) Chlamydia psittaci Genetic Variants Differ in Virulence by Modulation of Host Immunity. J Infect Dis 204: 654–663. doi:10.1093/infdis/jir333.

33. Frazer LC, Darville T, Chandra-Kuntal K, Andrews CW, Zurenski M, et al. (2012)

Plasmid-cured Chlamydia caviae activates TLR2-dependent signaling and retains virulence in the guinea pig model of genital tract infection. PLoS One 7: e30747. doi:10.1371/journal.pone.0030747.

34. Qu Y, Frazer LC, O'Connell CM, Tarantal AF, Andrews CW, et al. (2015) Comparable Genital Tract Infection, Pathology, and Immunity in Rhesus Macaques Inoculated with Wild-Type or Plasmid-Deficient Chlamydia trachomatis Serovar D. Infect Immun 83: 4056–4067. doi:10.1128/IAI.00841-15.

35. Kari L, Whitmire WM, Carlson JH, Crane DD, Reveneau N, et al. (2008) Pathogenic diversity among Chlamydia trachomatis ocular strains in nonhuman primates is affected by subtle genomic variations. J Infect Dis 197: 449–456. doi:10.1086/525285.

36. Livak KJ, Schmittgen TD (2001) Analysis of relative gene expression data using real-time quantitative PCR and the 2(-Delta Delta C(T)) Method. Methods 25: 402–408. doi:10.1006/meth.2001.1262.

37. Benjamini Y, Hochberg Y (1995) Controlling the False Discovery Rate: A Practical and Powerful Approach to Multiple Testing. J R Stat Soc Ser B 57: 289–300. doi:10.2307/2346101.

38. Grände M, Franzen A, Karlsson J-O, Ericson LE, Heldin N-E, et al. (2002) Transforming growth factor-beta and epidermal growth factor synergistically stimulate epithelial to mesenchymal transition (EMT) through a MEK-dependent mechanism in primary cultured pig thyrocytes. J Cell Sci 115: 4227–4236.

39. Meng X, Kong D-H, Li N, Zong Z-H, Liu B-Q, et al. (2014) Knockdown of BAG3 induces epithelial-mesenchymal transition in thyroid cancer cells through ZEB1 activation. Cell Death Dis 5: e1092. doi:10.1038/cddis.2014.32.

40. Wan C, Latter JL, Amirshahi A, Symonds I, Finnie J, et al. (2014) Progesterone activates multiple innate immune pathways in Chlamydia trachomatis-infected endocervical cells. Am J Reprod Immunol 71: 165–177. doi:10.1111/aji.12168.

41. Lipson KE, Wong C, Teng Y, Spong S (2012) CTGF is a central mediator of tissue remodeling and fibrosis and its inhibition can reverse the process of fibrosis. Fibrogenesis Tissue Repair 5: S24. doi:10.1186/1755-1536-5-S1-S24.

42. Burns WC, Twigg SM, Forbes JM, Pete J, Tikellis C, et al. (2006) Connective tissue growth factor plays an important role in advanced glycation end product-induced tubular epithelial-to-mesenchymal transition: implications for diabetic renal disease. J Am Soc Nephrol 17: 2484–2494. doi:10.1681/ASN.2006050525.

43. Wiedmaier N, Müller S, Köberle M, Manncke B, Krejci J, et al. (2008) Bacteria induce CTGF and CYR61 expression in epithelial cells in a lysophosphatidic

acid receptor-dependent manner. Int J Med Microbiol 298: 231–243. doi:10.1016/j.ijmm.2007.06.001.

44.   Baud J, Varon C, Chabas S, Chambonnier L, Darfeuille F, et al. (2013) Helicobacter pylori initiates a mesenchymal transition through ZEB1 in gastric epithelial cells. PLoS One 8: e60315. doi:10.1371/journal.pone.0060315.

45.   Cane G, Ginouvès A, Marchetti S, Buscà R, Pouysségur J, et al. (2010) HIF-1alpha mediates the induction of IL-8 and VEGF expression on infection with Afa/Dr diffusely adhering E. coli and promotes EMT-like behaviour. Cell Microbiol 12: 640–653. doi:10.1111/j.1462-5822.2009.01422.x.

46.   Bolós V, Peinado H, Pérez-Moreno MA, Fraga MF, Esteller M, et al. (2003) The transcription factor Slug represses E-cadherin expression and induces epithelial to mesenchymal transitions: a comparison with Snail and E47 repressors. J Cell Sci 116: 499–511.

47.   Sume SS, Kantarci A, Lee A, Hasturk H, Trackman PC (2010) Epithelial to mesenchymal transition in gingival overgrowth. Am J Pathol 177: 208–218. doi:10.2353/ajpath.2010.090952.

48.   Buckner LR, Schust DJ, Ding J, Nagamatsu T, Beatty W, et al. (2011) Innate immune mediator profiles and their regulation in a novel polarized immortalized epithelial cell model derived from human endocervix. J Reprod Immunol 92: 8–20. doi:10.1016/j.jri.2011.08.002.

49.   Gregory, P. A., Bert, A. G., Paterson, E. L., Barry, S. C., Tsykin, A., Farshid, G., Vadas, M. A., et al. (2008). The miR-200 family and miR-205 regulate epithelial to mesenchymal transition by targeting ZEB1 and SIP1. Nature cell biology, 10(5) 593-60 (2008) The miR-200 family and miR-205 regulate epithelial to mesenchymal transition by targeting ZEB1 and SIP1. Nat Cell Biol 10: 593–601. doi:10.1038/ncb1722.

50.   Zhang L, Wang X, Chen P (2013) MiR-204 down regulates SIRT1 and reverts SIRT1-induced epithelial-mesenchymal transition, anoikis resistance and invasion in gastric cancer cells. BMC Cancer 13: 290. doi:10.1186/1471-2407-13-290.

51.   Takahashi Y, Chen Q, Rajala RVS, Ma J-X (2015) MicroRNA-184 modulates canonical Wnt signaling through the regulation of frizzled-7 expression in the retina with ischemia-induced neovascularization. FEBS Lett 589: 1143–1149. doi:10.1016/j.febslet.2015.03.010.

52.   Auxenfans C, Builles N, Andre V, Lequeux C, Fievet A, et al. (2009) [Porous matrix and primary-cell culture: a shared concept for skin and cornea tissue engineering]. Pathol Biol (Paris) 57: 290–298. doi:10.1016/j.patbio.2008.04.014.

53.   Tovell VE, Dahlmann-Noor AH, Khaw PT, Bailly M (2011) Advancing the treatment of conjunctival scarring: a novel ex vivo model. Arch Ophthalmol (Chicago, Ill 1960) 129: 619–627. doi:10.1001/archophthalmol.2011.91.

Chapter 9: The use of Immunohistochemistry to characterize the expression and localization of inflammatory proteins, growth factors and markers of EMT in the conjunctiva.

9.1 Introduction

Gene expression studies performed using conjunctival swab samples from many different clinical stages of trachoma have revealed a number of genes that are consistently differentially expressed. These include pro-inflammatory cytokines and chemokines (*IL17A*, *IL1B*, *CXCL5*), antimicrobial peptides (*S100A7*), growth factors (*CTGF*), matrix metalloproteinases (*MMP7*, *MMP9*), which were upregulated in TF/TI, TS and TT [1–5]. Expression changes were generally higher when TI was also present [2–5]. In individuals with TS or TT, Ct infection was very rarely detected [3–6].

Many of the cytokines differentially expressed in trachoma are indicative of an active pro-inflammatory epithelium, supporting the cellular model of chlamydial pathogenesis [7]. However, this is also likely to reflect the large number of epithelial cells collected by a swab sample. Two studies that performed flow cytometry on cells collected from the tarsal conjunctiva of healthy donors by brush cytology showed that 67.9% and >95% cells were of epithelial origin [8,9]. In both studies ~4% intra-epithelial lymphocytes were detected. Expression patterns of epithelial-derived cytokines and factors are crucial for determining the role of the epithelium in the pathogenesis of chlamydial disease, as a pro-inflammatory epithelium is likely to drive fibrotic changes in the underlying stroma [7], where scarring occurs. However, by collecting swab samples from the tarsal conjunctiva, the behavior and expression patterns of the cells in the underlying stroma remain relatively hidden.

There have been a number of IHC studies performed using tissue from individuals with TF/TI [10–14], TS and TT [15–17]. In tissue from normal conjunctiva, collagen types I and III were limited to the substantia propria and collagen type V was absent, whereas in TF/TI and TS increased collagen type IV was detected in the thickened basement membrane and new collagen type V was deposited in the upper substantia propria [13,15]. Collagen types I and III were increased amongst epithelial cells in TF/TI and were reduced in TS [15]. Increased overall numbers of inflammatory cells were detected in TF/TI and TS [11,14,16,17]. In TF/TI, CTGF, basic fibroblast growth factor (bFGF), platelet derived growth factor (PDGF), MMP9, IL-1α, IL-1β and TNFα were upregulated in monocytes/macrophages infiltrating the substantia propria [10–12]. Vascular epithelial growth factor (VEGF) was upregulated in vascular and epithelial cells, increased tenascin (extracellular matrix glycoprotein) was noted in the upper substantia propria and angiogenesis was more apparent [12]. MMP9 was upregulated in intravascular polymorphonuclear cells and increased IL-1α and IL-1β were present in

the conjunctival epithelium [10,11]. The expression of cytokines and growth factors was only assessed in individuals with TF/TI and the number of cases and controls used in these studies was small (<10 of each group) [10–12]. More recent work using in vivo confocal microscopy (IVCM) and IHC in TS has revealed enhanced inflammatory cell infiltrates in the upper substantia propria, the presence of 'dendritiform' cells (which fail to stain with the CD83 dendritic cell marker) and connective tissue arranged into discrete bands or sheets [18–20]. The cellular localization of inflammatory cytokines and growth factors in TS has not yet been addressed.

9.2 Biopsy sample processing, IHC staining optimization and grading

The aim of the study described in Chapter 10 was to characterize the expression of EMT biomarkers and targets that were consistently upregulated in trachoma gene expression studies at the protein level, and to identify their cellular localization in TS and TT. Biopsy samples were collected from Tanzanian individuals with TT whilst undergoing tarsal rotation surgery and from controls undergoing ocular surgery for alternative reasons such as cataract or retinal detachment (and who otherwise had healthy conjunctivae). Biopsy samples were formalin fixed and paraffin embedded (FFPE) in Tanzania and brought to London for processing. FFPE samples can be stored indefinitely at room temperature, however formalin fixation can denature proteins through the cross-linking process. Antigen retrieval via heating or enzymatic digestion of the sample is often required to re-expose the antigen for the antibody to bind. For each antibody used in this study, a range of dilutions and retrieval methods were first tested on positive control tissue (any available human tissue that expressed the antigen) in order to find the most specific staining pattern. Example images of positive staining in TT or control conjunctival tissue, for each antibody, after optimization of individual dilution and retrieval protocols (listed in Chapter 10), are shown in Figure 9.1. MMP7 was not detected in any of the 36 conjunctival samples.

Despite reasonable numbers of TT cases (n=20) and controls (n=16) in the study, a limitation was that the biopsy tissue samples were extremely small and did not all contain the same tissue components. For example, some sections did not contain epithelium and others had very little stroma. Only 1/36 samples had enough tissue present to see the "T-sign" of collagen deposition described in sections of conjunctival tissue [18]. Another limitation of the small tissue size was that as few as 20-25 4µm sections could be cut from some samples. For the MMP7 antibody the staining pattern in the positive control tissue was limited to secretions in the lumen of kidney tubules;

no positive staining was detected in any of the other tissues tested (tonsil, appendix, liver, colon, kidney, pancreas and prostate cancer). A broader staining pattern might have been expected however and this could reflect poor antibody sensitivity or inaccessibility of the epitope due to protein folding or denaturation. The lack of any MMP7 staining in TT cases and controls (Chapter 10) might therefore be misleading and requires confirmation with a different antibody. Very few clinical samples stained positive for IL-6 (2/36) and IL-17A (5/36) and those that were positive had a diffuse blush in the epithelium (Figure 9.1). IL-17A is produced by activated T cells (amongst other innate immune cells; neutrophils, macrophages, NK cells and γδ T cells) and in the positive control (colon tissue) staining was limited to individual immune cells that had infiltrated the epithelium (Figure 9.2). Although epithelial cells secrete IL-6, the staining pattern in the positive control was also more specific (Figure 9.3). The staining pattern of IL-17A and IL-6 in clinical samples therefore appears to be non-specific and is perhaps an artifact.
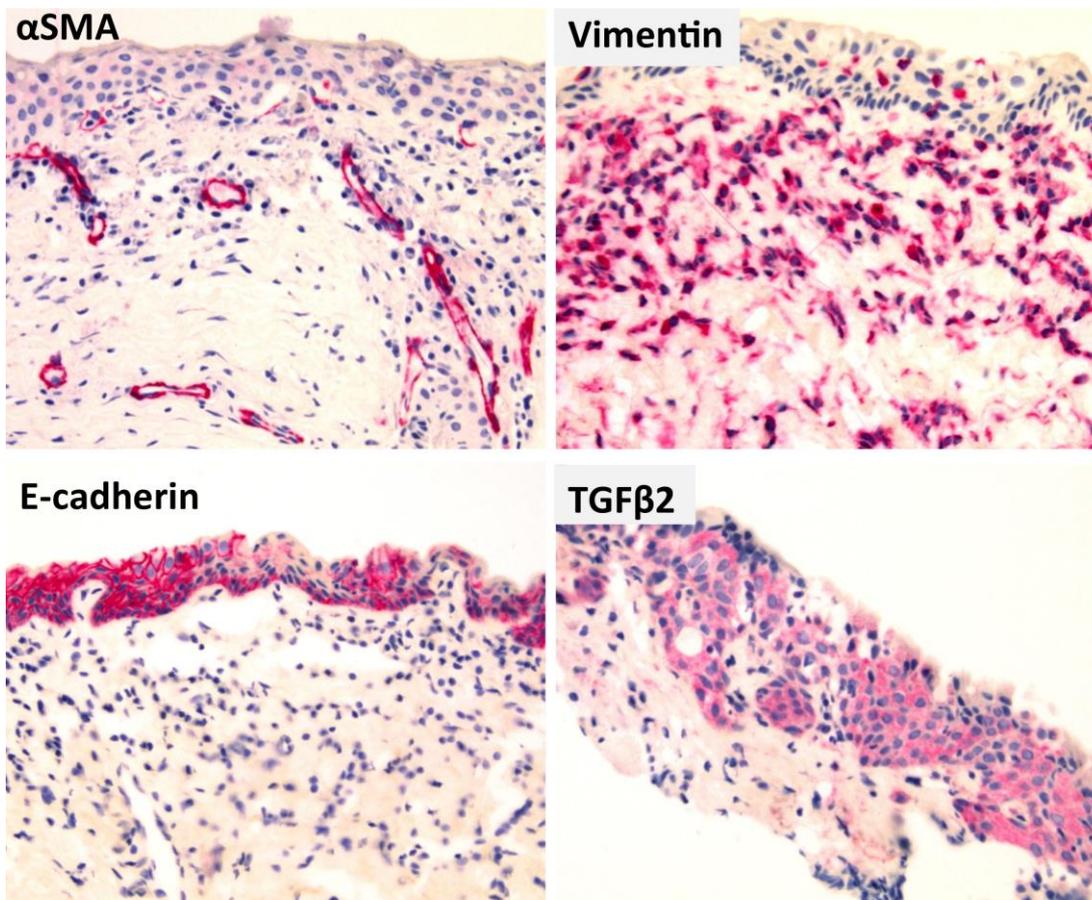
CTGF

PDGF

MMP7

MMP9

IL-1β
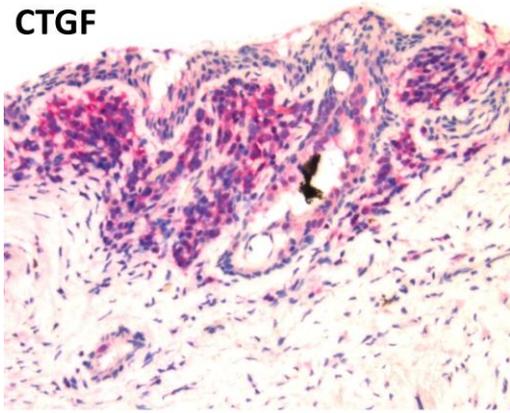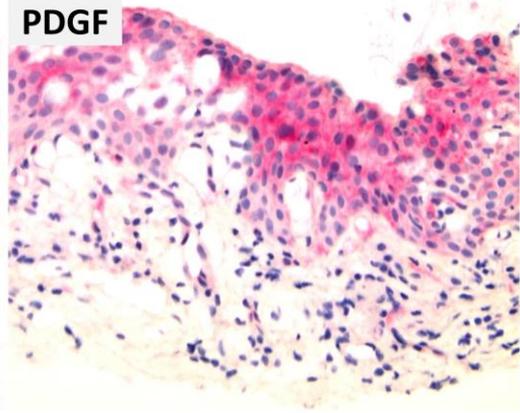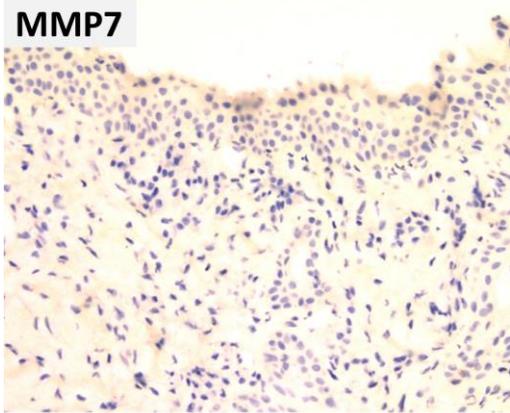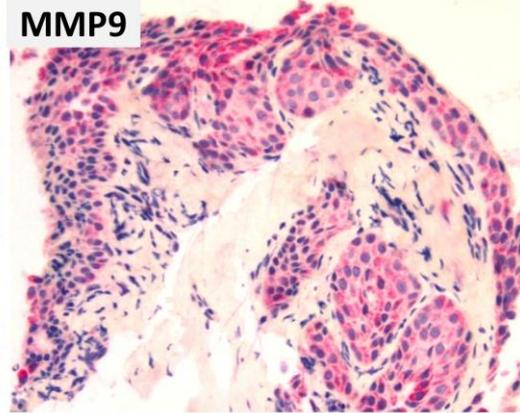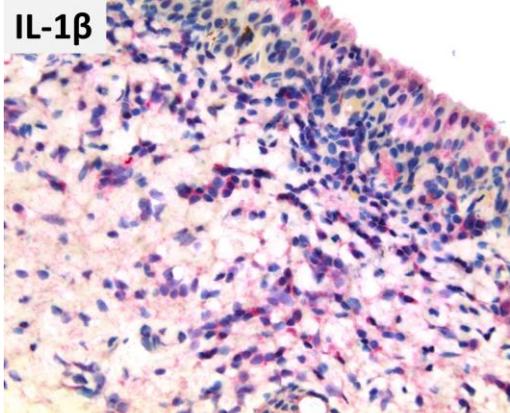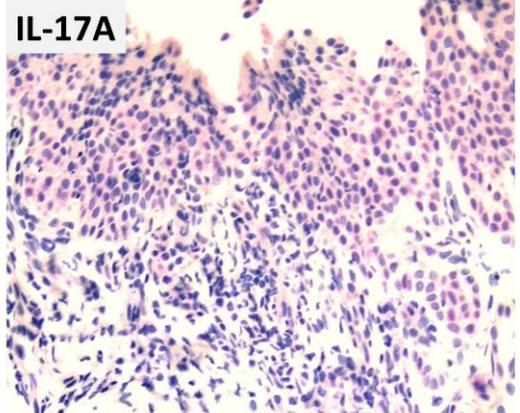
IL-17A

IL-22
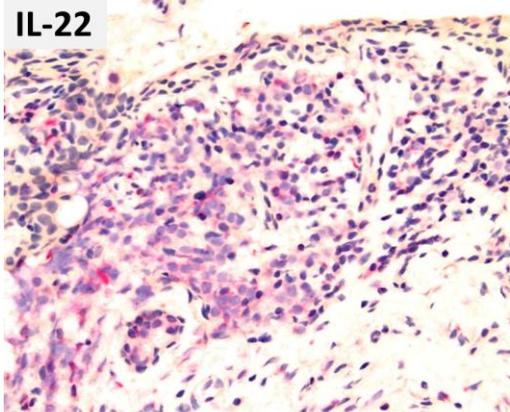
IL-6
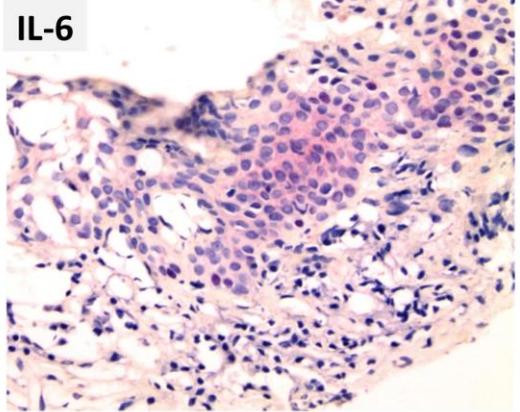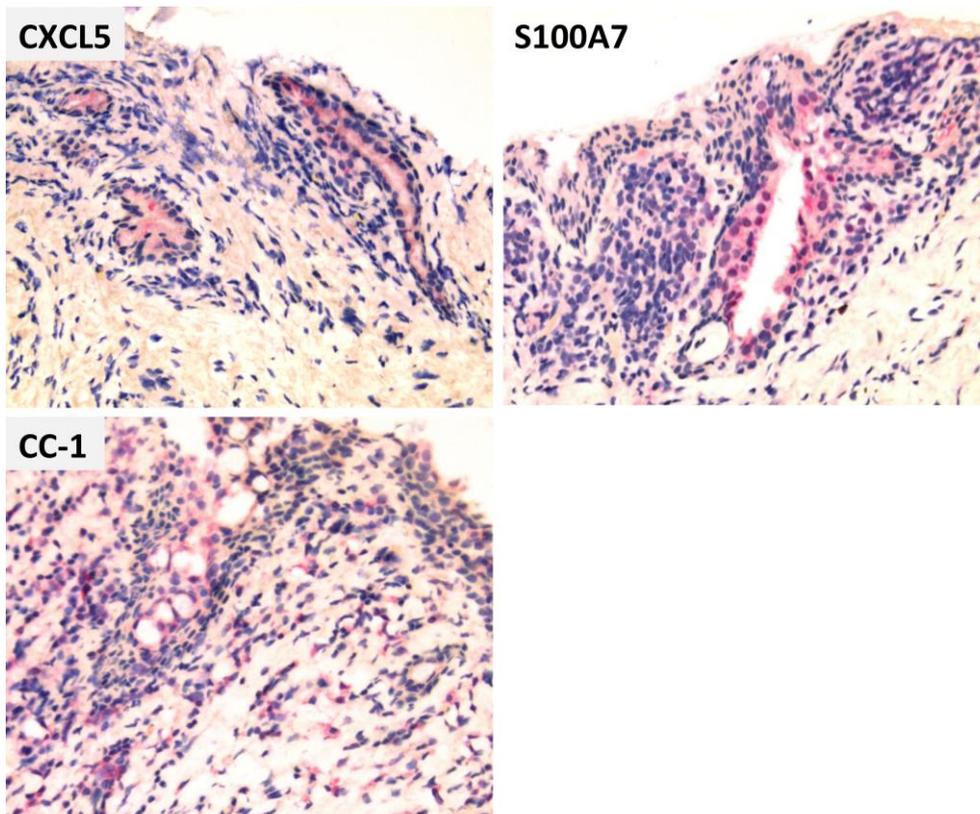
Figure 9.1. Examples of positive staining (pink) in TT case or control conjunctival tissue for each antibody. Images were taken at 200X original magnification.
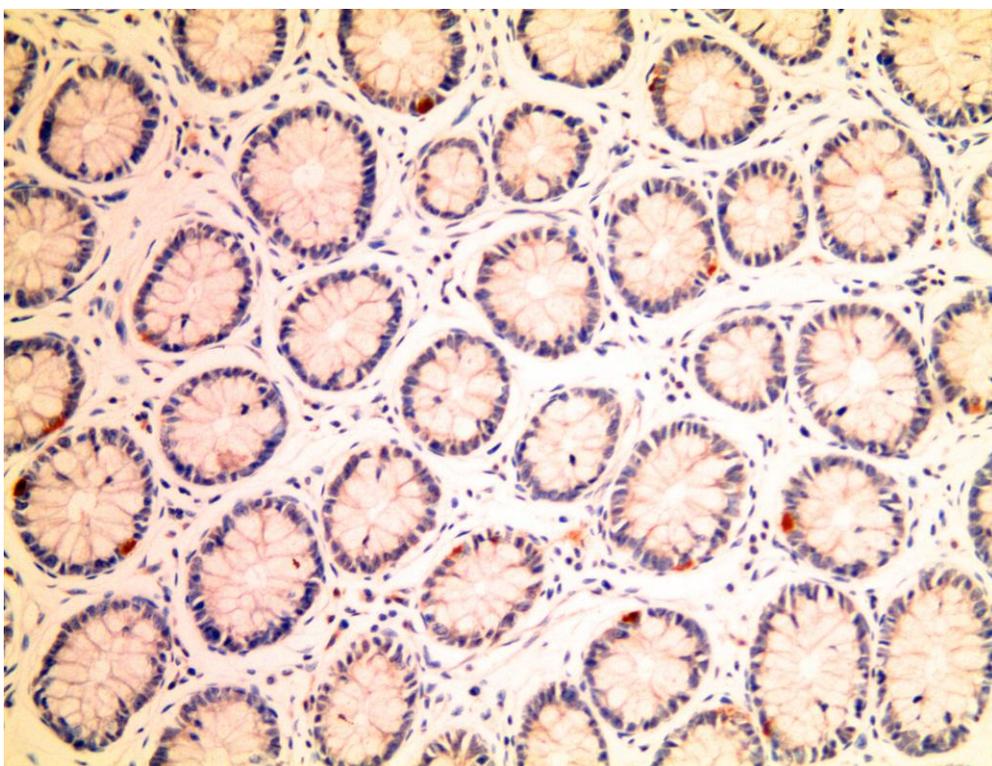
Figure 9.2. IL-17A staining (brown) in a section of human colon. Image was taken at 200X original magnification.
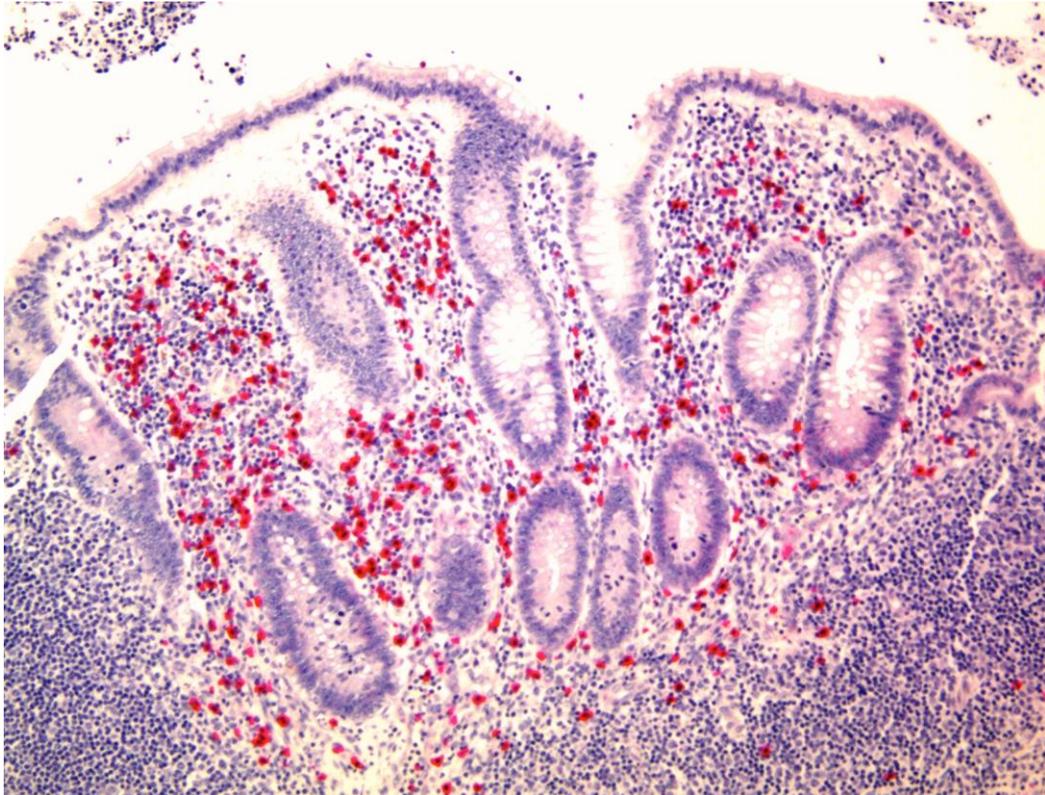
Figure 9.3. IL-6 staining (pink) in a section of human appendix. Image was taken at 200X original magnification.

De-waxing, antigen retrieval and IHC staining were automated on a Leica BOND instrument. This was done to improve staining accuracy and efficiency; a total of 36 samples were stained with 15 antibodies, plus optimization and control slides (around 700 slides in total). Positive and negative control sections were performed for each antibody on each run. Despite the automated process there was occasionally some variation in staining intensity, due to errors in the machines protocol (due to performing up to 30 separate protocols simultaneously) or to fresh antibody dilutions. These staining variations were likely reduced by automation however, relative to processing this number of samples by hand. Positive control slides and sections were stored in runs, such that when masked grading was performed the grader could 'normalize' grading of staining intensity to that of the positive control section for each batch. Due to the size of the sections some lifted off the slide or folded slightly and stained more intensely or non-specifically as a result. There was not sufficient biopsy material to repeat all sections that had lifted slightly or where there was some background, therefore the experience and discretion of the grader was crucial. Due to these limitations and those described above relating to the size and composition of each specimen, it was not practical to grade these samples using an automated grading system [21]. Samples were graded by a single masked grader using the systems

described below (Table 9.1). Antibody staining in each section was graded separately for the epithelial and subepithelial compartments. EMT biomarkers (Vimentin, E-cadherin and αSMA) were scored in the epithelial compartment only in order to detect epithelial cells acquiring a mesenchymal phenotype.

A limitation of IHC is the inability to perform multiplex staining. Double staining is possible by using red and brown dyes, however it is often technically difficult; the staining procedure is performed for each dye sequentially on a single slide, so the two antibodies should require the same antigen retrieval methods for optimal staining. Due to this complexity double staining was not performed in the current study. This was a disadvantage; the ability to identify cells undergoing EMT would be greatly enhanced by double staining for E-cadherin and Vimentin for example, enabling the grader to identify transitioning cells. It was therefore not possible to phenotype the cells producing the cytokines and growth factors of interest. This could be performed using flow cytometry, however it would then not be possible to identify tissue localization of expression. Another study was conducted in parallel with this one, which investigated the phenotypes of immune cells infiltrating the conjunctiva during trichiasis (staining for CD3 (T cells), CD4 (helper T cells), CD8 (cytotoxic T cells and NK cells), NCR1 (NK cells), CD20 (B cells), CD45 (nucleated hematopoietic cells), CD56 (T and NK cells), CD68 (macrophages/monocytes) and CD83 (mature dendritic cells)). The biopsy samples used in both studies were collected as part of an ongoing study at Kilimanjaro Christian Medical Centre, Tanzania. The results of both studies in combination, although limited by the lack of multiplex staining, will increase our understanding of the phenotypes of immune cells infiltrating the conjunctiva and the distribution of cytokines, chemokines and growth factors in trichiasis tissue.

Table 9.1. Systems for grading Hematoxylin & eosin and IHC staining patterns in conjunctival biopsy tissue.

	Grade			
	0	1	2	3
Hematoxylin & eosin				
Epithelial atrophy	No atrophy	Minor atrophy	Moderate atrophy	Severe atrophy
Inflammatory cells, Myofibroblasts	No visible staining	Few cells	Moderate number of cells	Abundant cells
Fibrosis pattern (polarised light): Block, Wavy, Fine	None	Focal patches	Abundant areas	Extensive
Immunohistochemistry				
Subepithelial compartment				
IL-6, IL-1β, IL-17A, IL-22, CXCL5, S100A7, CC1, PDGF, CTGF, TGFβ2, MMP7, MMP9	No visible staining	Few cells	Moderate number of cells	Abundant cells
Epithelial compartment				
IL-6, IL-1β, IL-17A, IL-22, CXCL5, S100A7, CC1, PDGF, CTGF, TGFβ2, MMP7, MMP9, Vimentin, αSMA	No visible staining	Few cells	Moderate number of cells	Abundant cells
E-cadherin*	0-25%	26-50%	51-75%	76-100%

* The percentage of the epithelium that stained positive for E-cadherin was graded quarterly on a scale of 1-4 (rather than 0-3).

9.3 References

1. Burton MJ, Bailey RL, Jeffries D, Mabey DCW, Holland MJ (2004) Cytokine and Fibrogenic Gene Expression in the Conjunctivas of Subjects from a Gambian Community Where Trachoma Is Endemic. Infect Immun 72: 7352–7356. doi:10.1128/IAI.72.12.7352-7356.2004.

2. Burton MJ, Ramadhani A, Weiss HA, Hu V, Massae P, et al. (2011) Active trachoma is associated with increased conjunctival expression of IL17A and profibrotic cytokines. Infect Immun 79: 4977–4983. doi:10.1128/IAI.05718-11.

3. Burton MJ, Rajak SN, Bauer J, Weiss H a, Tolbert SB, et al. (2011) Conjunctival transcriptome in scarring trachoma. Infect Immun 79: 499–511. doi:10.1128/IAI.00888-10.

4. Hu VH, Weiss HA, Ramadhani AM, Tolbert SB, Massae P, et al. (2012) Innate immune responses and modified extracellular matrix regulation characterize bacterial infection and cellular/connective tissue changes in scarring trachoma. Infect Immun 80: 121–130. doi:10.1128/IAI.05965-11.

5. Burton MJ, Rajak SN, Ramadhani A, Weiss HA, Habtamu E, et al. (2012) Post-operative recurrent trachomatous trichiasis is associated with increased conjunctival expression of S100A7 (psoriasin). PLoS Negl Trop Dis 6: e1985. doi:10.1371/journal.pntd.0001985.

6. Burton MJ, Rajak SN, Hu VH, Ramadhani A, Habtamu E, et al. (2015) Pathogenesis of progressive scarring trachoma in Ethiopia and Tanzania and its implications for disease control: two cohort studies. PLoS Negl Trop Dis 9: e0003763. doi:10.1371/journal.pntd.0003763.

7. Stephens RS (2003) The cellular paradigm of chlamydial pathogenesis. Trends Microbiol 11: 44–51.

8. Martínez-Osorio H, Calonge M, Corell A, Reinoso R, López A, et al. (2009) Characterization and short-term culture of cells recovered from human conjunctival epithelium by minimally invasive means. Mol Vis 15: 2185–2195.

9. Reinoso R, Martín-Sanz R, Martino M, Mateo ME, Blanco-Salado R, et al. (2012) Topographical distribution and characterization of epithelial cells and intraepithelial lymphocytes in the human ocular mucosa. Mucosal Immunol 5: 455–467. doi:10.1038/mi.2012.27.

10. El-Asrar a M, Geboes K, Al-Kharashi S a, Al-Mosallam a a, Missotten L, et al. (2000) Expression of gelatinase B in trachomatous conjunctivitis. Br J Ophthalmol 84: 85–91. doi:10.1136/bjo.84.1.85.

11. Abu el-Asrar a M, Geboes K, Tabbara KF, al-Kharashi S a, Missotten L, et al. (1998) Immunopathogenesis of conjunctival scarring in trachoma. Eye (Lond) 12 (Pt 3a: 453–460. doi:10.1038/eye.1998.104.

12. Abu El-Asrar a M, Al-Kharashi S a, Missotten L, Geboes K (2006) Expression of growth factors in the conjunctiva from patients with active trachoma. Eye (Lond) 20: 362–369. doi:10.1038/sj.eye.6701884.

13. Abu el-Asrar a M, Geboes K, al-Kharashi S a, Tabbara KF, Missotten L (1998) Collagen content and types in trachomatous conjunctivitis. Eye (Lond) 12 (Pt 4): 735–739. doi:10.1038/eye.1998.179.

14. el-Asrar a M, Van den Oord JJ, Geboes K, Missotten L, Emarah MH, et al. (1989) Immunopathology of trachomatous conjunctivitis. Br J Ophthalmol 73: 276–282. doi:10.1136/bjo.73.4.276.

15. Abu el-Asrar a M, Geboes K, al-Kharashi S a, al-Mosallam a a, Tabbara KF, et al. (1998) An immunohistochemical study of collagens in trachoma and vernal keratoconjunctivitis. Eye (Lond) 12 (Pt 6): 1001–1006. doi:10.1038/eye.1998.257.

16. Burd EM, Tabbara KF, Nasr AM, Taylor PB (1988) Conjunctival lymphocyte subsets in trachoma. Int Ophthalmol 12: 53–57.

17. Reacher MH, Pe'er J, Rapoza PA, Whittum-Hudson JA, Taylor HR (1991) T cells and trachoma. Their role in cicatricial disease. Ophthalmology 98: 334–341.

18. Hu VH, Holland MJ, Cree I a, Pullin J, Weiss H a, et al. (2013) In vivo confocal microscopy and histopathology of the conjunctiva in trachomatous scarring and normal tissue: a systematic comparison. Br J Ophthalmol 97: 1333–1337. doi:10.1136/bjophthalmol-2013-303126.

19. Hu VH, Massae P, Weiss HA, Cree IA, Courtright P, et al. (2011) In vivo confocal microscopy of trachoma in relation to normal tarsal conjunctiva. Ophthalmology 118: 747–754. doi:10.1016/j.ophtha.2010.08.029.

20. Hu VH, Weiss HA, Massae P, Courtright P, Makupa W, et al. (2011) In vivo confocal microscopy in scarring trachoma. Ophthalmology 118: 2138–2146. doi:10.1016/j.ophtha.2011.04.014.

21. Varghese F, Bukhari AB, Malhotra R, De A (2014) IHC Profiler: an open source plugin for the quantitative evaluation and automated scoring of immunohistochemistry images of human tissue samples. PLoS One 9: e96801. doi:10.1371/journal.pone.0096801.

Chapter 10: Research article: Increased epithelial expression of CTGF and S100A7 with elevated subepithelial expression of IL-1β in trachomatous trichiasis

RESEARCH PAPER COVER SHEET

PLEASE NOTE THAT A COVER SHEET MUST BE COMPLETED FOR EACH RESEARCH PAPER INCLUDED IN A THESIS.

SECTION A – Student Details

Student	Tamsyn Derrick
Principle Supervisor	Martin Holland
Thesis Title	The Role of Epigenetics and Type 2 Epithelial-Mesenchymal Transitions in Trachoma

If the Research Paper has previously been published please complete Section B, if not please move to Section C

SECTION B – Paper already published

Where was the work published?			
When was the work published?			
If the work was published prior to registration for your research degree, give a brief rationale for its inclusion			
Have you retained the copyright for the work?*		Was the work subject to academic peer review?	

*If yes, please attach evidence of retention. If no, or if the work is being included in its published format, please attach evidence of permission from the copyright holder (publisher or other author) to include this work.

SECTION C – Prepared for publication, but not yet published

Where is the work intended to be published?	PLoS Neglected Tropical Diseases
Please list the paper's authors in the intended authorship order:	Tamsyn Derrick, Hodan Jama, Victor H. Hu, Patrick Massae, David Essex, Martin J. Holland, Phil Luthert, Matthew J. Burton
Stage of publication	Under review

SECTION D – Multi-authored work

For multi-authored work, give full details of your role in the research included in the paper and in the preparation of the paper. (Attach a further sheet if necessary)	I performed the laboratory work, analysed the data, interpreted the findings and wrote the manuscript.

Student signature: *Tamsyn Derrick*　　　**Date:** 26.9.15

Supervisor signature: *Martin Holland*　　　**Date:** 28.9.15

Increased epithelial expression of CTGF and S100A7 with elevated subepithelial expression of IL-1β in trachomatous trichiasis

Tamsyn Derrick[1], Philip J. Luthert[2], Hodan Jama[2], Victor H. Hu[3,4], Patrick Massae[4], David Essex[2], Martin J. Holland[1], Matthew J. Burton[3,4]

[1] Department of Clinical Research, Faculty of Infectious and Tropical Diseases, London School of Hygiene and Tropical Medicine, London, UK

[2] UCL Institute of Ophthalmology, London, UK

[3] International Centre for Eye Health, Department of Clinical Research, Faculty of Infectious and Tropical Diseases, London School of Hygiene and Tropical Medicine, London, UK

[4] Kilimanjaro Christian Medical Centre, Moshi, Tanzania.

Corresponding author: Tamsyn Derrick, tamsyn.derrick@lshtm.ac.uk

Conflict of interest: The authors declare that they have no conflicts of interest.

Running head: Cytokine and growth factor expression in trachomatous trichiasis tissue

Key words: Trachoma; trichiasis; scarring; inflammation; immunohistochemistry; conjunctiva; cytokines.

Abstract

Purpose: To characterize the histological appearance and expression of pro-inflammatory mediators, growth factors, matrix metalloproteinases and biomarkers of epithelial-mesenchymal transition (EMT) in healthy control and trachomatous trichiasis (TT) conjunctival tissue.

Methods: Conjunctival biopsies were taken from 20 individuals with TT and from 16 individuals with healthy conjunctiva, which served as controls. Study participants were of varying ethnicity and were living in a trachoma-endemic region of northern Tanzania. Formalin-fixed paraffin-embedded tissue sections were stained using hematoxylin and eosin or by immunohistochemistry using antibodies against: IL-1β, IL-6, IL-17A, IL-22, CXCL5, S100A7, cleaved caspase 1 (CC1), PDGF, CTGF, TGFβ2, MMP7, MMP9, E-cadherin, vimentin, and αSMA.

Results: Tissue from TT cases had a greater inflammatory cell infiltrate relative to controls and greater disruption of collagen structure. CTGF and S100A7 were more highly expressed in the epithelium and IL-1β was more highly expressed in the substantia propria of TT cases relative to controls. Latent TGFβ2 was slightly more abundant in the substantia propria of control tissue. No differences were detected between TT cases and controls in the degree of epithelial atrophy, the number of myofibroblasts or expression of EMT biomarkers.

Conclusions: These data indicate that the innate immune system is active in the immunopathology of trachoma, even in the absence of clinical inflammation. CTGF might provide a direct link between inflammation and fibrosis and could be a suitable target for therapeutic treatment to halt the progression of trachomatous scarring.

Author summary

Progressive scarring of the conjunctiva in individuals with trachoma causes the eyelids to contract, drawing the eyelashes inwards (trichiasis) so that they scratch the cornea, causing pain and eventually blindness. Disease is initiated in childhood by repeated conjunctival infection with *Chlamydia trachomatis* (Ct), however, infection is not commonly found in adults, yet chronic inflammation and fibrosis progress throughout the lives of many individuals. A better understanding of the mechanisms driving inflammation and fibrosis are required in order to develop treatments to halt disease progression. The tissue expression and localization of a number of pro-inflammatory cytokines, growth and matrix factors were investigated in eyelid tissue from 20 individuals with trichiasis and from 16 control individuals. By staining tissue sections with dyes and specific antibodies, pro-inflammatory signaling molecules IL-1β and S100A7 and pro-fibrotic growth factor CTGF were found to be more highly expressed in individuals with trichiasis. CTGF and S100A7 were highly expressed in the epithelium; the outermost layer of the conjunctiva, whereas IL-1β was more highly expressed deeper in the tissue, where scarring occurs. Numerous inflammatory cells were found in the tissue of trichiasis patients even in the absence of clinically apparent inflammation. Future research should seek to describe a causative mechanism linking these factors.

Introduction

Trachoma is a blinding disease initiated by infection of the conjunctival epithelium with the intracellular bacterium *Chlamydia trachomatis* (Ct). Individuals living in trachoma-endemic communities are repeatedly infected with Ct, which causes a follicular conjunctivitis. Chronic, recurrent inflammation, even in the absence of detectable Ct infection, is associated with progressive scarring [1]. The fibrotic response results in the inward turning of the lid margin (entropion) and abrasion of the cornea by the eyelashes (trichiasis). Mechanical damage to the cornea and subsequent opportunistic infections eventually lead to corneal opacity and blindness.

Trachoma is endemic in 51 countries and impairs the eyesight of 2.2 million people worldwide, 1.2 million of whom are irreversibly blind [2]. Although trachoma control programs have made good progress in reducing active disease, there is now some evidence that established scarring disease continues to progress even when chlamydial infection appears well controlled [1]. Therefore, a large number of people remain at risk of developing incident trichiasis, especially in areas where mass drug administration has had a partial effect [3,4]. In order to develop a vaccine or therapeutic treatments to prevent the progression to trichiasis, a better understanding of the immunopathology of scarring trachoma is required.

A number of clinical studies have shown that transcriptional signatures in trachomatous scarring (TS) and trichiasis (TT) are consistent with a pro-inflammatory epithelial response and tissue remodeling, supporting the cellular paradigm of chlamydial disease pathogenesis [5]. The gene expression of a number of pro-inflammatory mediators (*IL17A*, *IL1B*, *CXCL5*, *S100A7* (psoriasin), growth factors (*CTGF* (connective tissue growth factor)) and matrix metalloproteinases (*MMP7, MMP9*) were up-regulated in TS and TT [1,6–9]. Expression was increased further when clinical inflammation was present [1,6,7]. Immunohistochemistry (IHC) studies using tissue from a small number of individuals with active trachoma have shown that MMP9, CTGF, platelet derived growth factor (PDGF) and IL-1β were up-regulated in infiltrating monocytes/macrophages and that IL-1β was increased in the conjunctival epithelium [10–12].

Inflammatory mediators, growth factors and MMPs can stimulate epithelial cells to differentiate into pro-fibrotic mesenchymal cells, a process known as epithelial-mesenchymal transition (EMT) [13–15]. Epithelial cells undergoing EMT lose

expression of E-cadherin and gain mesenchymal 'expression' markers vimentin and α-smooth muscle actin (αSMA) as they migrate through the basement membrane into the stroma, where they contribute to fibrosis [16]. Inflammation-induced EMT normally ceases when inflammation resolves; therefore EMT only becomes pathological in an environment of chronic inflammation. The evidence of chronic pro-inflammatory cytokine and growth factor expression in various stages of trachoma combined with a fibrotic tissue response suggests that EMT may contribute to the pathology of trachoma.

The aim of this IHC study of trachomatous conjunctival tissue was to investigate the relative protein level and tissue localization of pro-inflammatory mediators, growth factors, EMT biomarkers and MMPs and to characterize the changes in tissue architecture that occur in TT. Molecular markers studied include factors that were previously shown to be up-regulated in TS/TT (S100A7, IL-1β, IL-17A, CXCL5, CTGF, MMP7/9), EMT biomarkers (αSMA, vimentin, E-cadherin) and other factors that may play a role in immunopathology (IL-6 (pleiotropic pro-inflammatory cytokine), IL-22 (mucosal defense and epithelial integrity), PDGF, transforming growth factor beta 2 (TGFβ2) (both growth factors associated with fibrosis), and cleaved Caspase 1 (CC1), a marker of inflammasome activation).

Methods

Ethical permission

This study adhered to the tenets of the Declaration of Helsinki and was approved by the London School of Hygiene and Tropical Medicine Ethics Committee, the Tanzanian National Institute of Medical Research Ethics Committee and the Kilimanjaro Christian Medical Centre Ethics Committee. Written, informed consent was obtained from individuals before enrollment in the study.

Clinical assessment and biopsy sampling

Study participants were examined using a bright torch and x2.5 loupes. The clinical phenotype of individuals for follicles, papillary inflammation and trichiasis was graded using the World Health Organization 1981 FPC trachoma grading system [17]. Conjunctival scarring was graded in finer detail using the system described by Hu *et al* [18]. Biopsy samples were collected from individuals undergoing bilamellar tarsal rotation surgery for TT (cases) and from individuals without clinical evidence of trachoma undergoing cataract surgery (controls), matched by age and sex where possible. The eyelid was anaesthetized with an injection of 2% lignocaine (Vital Healthcare, Mumbai, India) and the eye was cleaned with 5% povidone iodine. Biopsy samples were taken from the upper tarsal conjunctiva using a 3mm trephine: 2mm from the lid margin at the junction of the medial ⅔ and lateral ⅓ of the everted lid. Samples were fixed in 10% neutral buffered formalin and subsequently embedded in paraffin wax.

Staining

Formalin-fixed paraffin-embedded (FFPE) samples were cut perpendicular to the conjunctival surface in 4µm thick sections. Sections were stained with hematoxylin and eosin (H&E) for examination of tissue health and composition. Sections for IHC staining were dewaxed and stained with antibodies for pro-inflammatory cytokines and chemokines (IL-6, IL-1β, IL-17A, IL-22, CXCL5), antimicrobial peptide psoriasin (S100A7), cleaved caspase 1 (CC1), growth factors (PDGF, CTGF, TGFβ2), matrix metalloproteinases (MMP7, MMP9) and biomarkers of EMT (E-cadherin, vimentin, αSMA). Antibodies and retrieval methods used are listed in Table S10.1. IHC staining was automated and performed using Novocastra Bond Polymer Refine Red Detection

reagents on a Leica BOND instrument (Leica Biosystems, Milton Keynes, UK). Sections were covered with a cover-slip for microscopic examination.

H&E grading protocol

Tissue sections were graded by an ophthalmic pathologist masked to the clinical status of the samples. Where more than one H&E section was available for a sample the slide with the most tissue was analyzed. H&E slides were graded on a scale of 0 to 3 for the degree of epithelial atrophy (where 0 is none and 3 is severe atrophy), the number of inflammatory cells present and the number of myofibroblasts present (0= no visible staining, 1= few cells, 2= moderate number of cells and 3= abundant cells). H&E sections were viewed under cross-polarized light in order to view collagen fiber deposition and grade fibrosis. Fibrotic scarring was graded for 3 patterns, 'block', 'wavy' and 'fine', each on a scale of 0 to 3: 0=none seen, 1=focal patches, 2=abundant areas and 3=extensive.

IHC grading protocol

Antibodies were graded according to strength and location of staining. For each antibody the section was graded separately for the epithelial and the subepithelial compartments. The subepithelial compartment (substantia propria) contained the stroma and inflammatory cell infiltrate if present. Antibody staining was recorded on a scale of: 0=no visible staining, 1= few cells, 2= moderate number of cells and 3= abundant cells. For the antibodies targeting E-Cadherin, vimentin and αSMA staining was recorded in the epithelial compartment only. For E-cadherin, the total area of the epithelium that stained positive was recorded in quartiles: 0-25% = 1, 26-50% = 2, 51-75% = 3 and 76-100% = 4.

Data analysis

Data were analysed in R (https://www.r-project.org). Fishers Exact Tests were used to test for differences between case-control status and: age (categorized by decade), sex, ethnic group, H&E and IHC scores. IHC targets were excluded from the analysis where ≤2/36 sections had a grade >0. Radial plots were generated by calculating the average score per person for TT cases and controls for each antibody or H&E feature.

Results

Sample phenotypes

Thirty-six conjunctival biopsy specimens were collected from 20 individuals with TT (cases) and 16 individuals with no clinical signs of trachoma (controls). The demographic and clinical phenotypes of individuals whose samples were used in this study are described in Table 10.1. There was no significant difference in sex (P=0.31) or age (P=0.074) between cases and controls. There was a significant difference in ethnic groups between cases and controls (p<0.0001); 18/20 cases were of the Massai ethnic group whereas only one control subject was Massai. No follicles were detected in cases or controls. One TT case had a papillary inflammation grade of 3, equivalent to *trachomatous inflammation – intense* using the simplified grading system [19]. All cases had varied degrees of conjunctival scarring. None of the controls had papillary inflammation, scarring or trichiasis (Table 10.1).

Table 10.1. Demographic and clinical characteristics of samples

Variable	Cases N = 20	Controls N = 16
Gender, male (%)	7 (35%)	9 (56%)
Age, mean in years (range)	74.6 (41-91)	70.3 (50-83)
Ethnic group		
Massai	18	1
Chagga	2	7
Other	0	8
Scarring grade		
0	0	16
S1b	4	0
S1c	8	0
S2	3	0
3	5	0
Papillary Inflammation grade		
0	9	16
1	8	0
2	2	0
3	1	0
Trichiasis Grade		
0	2	16
1	1	0
2	9	0
3	8	0

Footnote: 2 TT cases that scored 0 for trichiasis grade had marked entropion and had epilated lashes.

Tissue morphology

H & E staining was used to visualize tissue structure and prevalence of inflammatory cells in sections. There was no difference in the degree of epithelial atrophy or in the number of myofibroblasts between cases and controls (Table 10.2). There were significantly more inflammatory cells evident in cases (P=0.001). Three patterns of subepithelial tissue deposition became apparent when sections were viewed under cross-polarized light: "block", "wavy" and "fine". Representative photographs of these phenotypes are shown in Figure S10.1. Tissue from cases had significantly more wavy (P=0.0075) and fine patterns (P=0.0005) of subepithelial tissue deposition, whereas individuals with healthy conjunctiva had more block type patterns (P = 0.0005), Table 10.2 and Figure 10.1.

Table 10.2. Sample characteristics by Hematoxylin and Eosin staining

	Cases	Controls	P value[*]
Epithelial Atrophy			0.65
0	6	7	
1	7	3	
2	5	4	
3	1	0	
NA[†]	1	2	
Inflammatory cell infiltrate			0.0025
0	0	1	
1	7	13	
2	12	1	
3	1	1	
Myofibroblasts			1
0	2	2	
1	8	7	
2	8	6	
NA[†]	2	1	
Fibrosis: Block pattern			0.0005

0	5	0
1	11	1
2	3	4
3	1	11
Fibrosis: Wavy pattern			0.0075
0	6	13
1	10	3
2	4	0
Fibrosis: Fine pattern			0.0005
0	0	9
1	15	6
2	5	1

[*] Fishers exact test was used to test for differences between groups.

[†] Sections received "NA" when there was not enough tissue present to grade a parameter and were not included in the significance calculation.
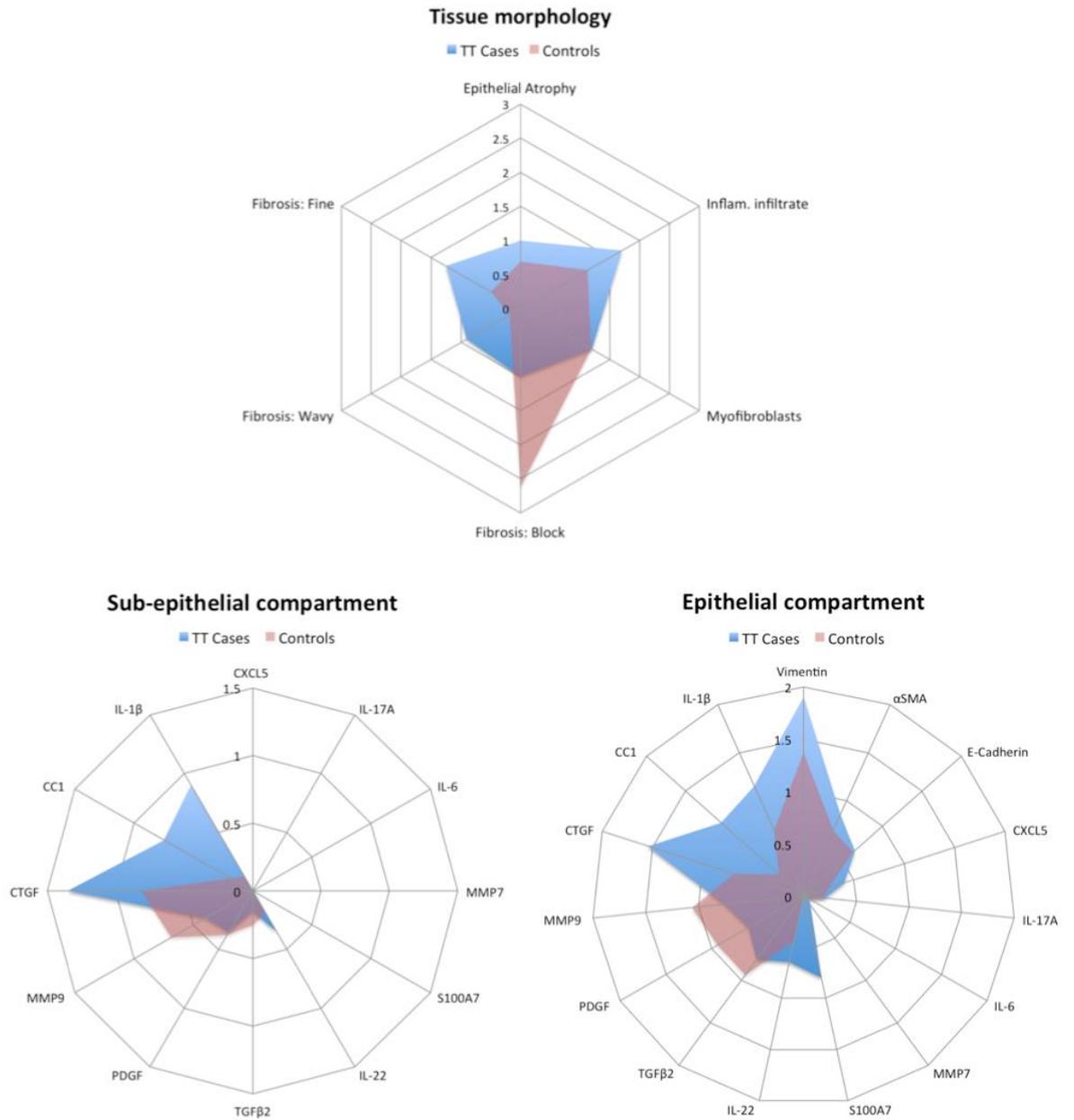
Figure 10.1. Radial plots summarizing overall changes in tissue morphology and expression of molecular markers. Molecular marker expression was quantified by IHC in the epithelial and subepithelial compartments. The average score per person for TT cases (blue) and controls (red) was plotted for each target or H&E feature.

The relative expression of the different molecular markers detected by IHC in the epithelial and subepithelial compartments were analysed by case-control status and the results are shown in Table 10.3. The average IHC score per person for TT cases and controls for each molecular marker is also represented in Figure 10.1. Staining was generally highest in the epithelium of TT cases. CTGF, IL-1β and CC1 had greater average expression in TT cases in both epithelial and subepithelial compartments.

Table 10.3. Expression of specific molecular markers in the epithelial and subepithelial compartments by IHC.

Category	Target	Epithelial Compartment			Subepithelial Compartment		
		Cases (N=20)	Controls (N=16)	*P**	Cases (N=20)	Controls (N=16)	*P**
Pro-inflammatory mediators	IL-1β			0.312			0.012
	0	9	9		11	14	
	1	1	3		1	2	
	2	8	4		7	0	
	3	2	0		1	0	
	IL-17A			1			NA
	0	17	14		20	16	
	1	2	1		0	0	
	2	1	1		0	0	
	3	0	0		0	0	
	CXCL5			0.241			NA
	0	14	14		20	16	
	1	4	0		0	0	
	2	2	2		0	0	
	3	0	0		0	0	
	S100A7			0.009			NA
	0	11	16		20	16	
	1	5	0		0	0	
	2	1	0		0	0	
	3	3	0		0	0	
	IL-22			0.280			0.806
	0	9	11		16	14	
	1	9	3		1	1	
	2	2	2		3	1	
	3	0	0		0	0	
	IL-6			NA			NA

		0	19	15		20	16	
		1	1	1		0	0	
		2	0	0		0	0	
		3	0	0		0	0	
Inflammasome	**CC1**			0.213			0.197
	0	9	12		11	14	
	1	4	3		5	1	
	2	4	1		2	1	
	3	3	0		2	0	
Growth Factors	**PDGF**			0.689			0.541
	0	12	7		15	12	
	1	4	4		3	3	
	2	4	4		2	0	
	3	0	1		0	1	
	TGFβ2			0.359			0.037
	0	13	7		19	12	
	1	1	4		0	4	
	2	4	4		0	0	
	3	2	1		1	0	
	CTGF			0.008			0.099
	0	2	10		5	7	
	1	6	2		8	5	
	2	11	3		2	4	
	3	1	1		5	0	
Matrix	**MMP9**			0.263			0.556
	0	11	8		15	10	
	1	3	0		2	1	
	2	6	7		3	5	
	3	0	1		0	0	
	MMP7			NA			NA
	0	18	16		20	14	
	1	2	0		0	2	
	2	0	0		0	0	
	3	0	0		0	0	
EMT	**E-Cadherin**			0.314			
	0	1	0				
	1	0	3				
	2	2	2				
	3	3	1				
	4	14	10				
	Vimentin			0.180			
	0	0	3				

	1	7	5
	2	8	7
	3	5	1
αSMA			1
	0	12	11
	1	1	0
	2	5	4
	3	2	1

* Fishers exact test was used to test for differences between groups. To account for the burden of repeated statistical tests applied, critical p-value thresholds of (0.05/13) <0.004 for the epithelial compartment and (0.05/7) <0.007 in the subepithelial compartment would be required.

CTGF expression was greater in the epithelium of TT cases relative to controls (P = 0.0085). Of the samples that scored >0 for CTGF, 10/23 had a clinical papillary inflammation grade >0. Epithelial expression of CTGF was localized in 14/24 of the samples that stained positive. In 4/24 CTGF positive samples (two cases, two controls) expression was more concentrated in the deep epithelium (Figure 10.2A). CTGF expression was slightly greater in the subepithelial tissue of cases but the difference was not significant.
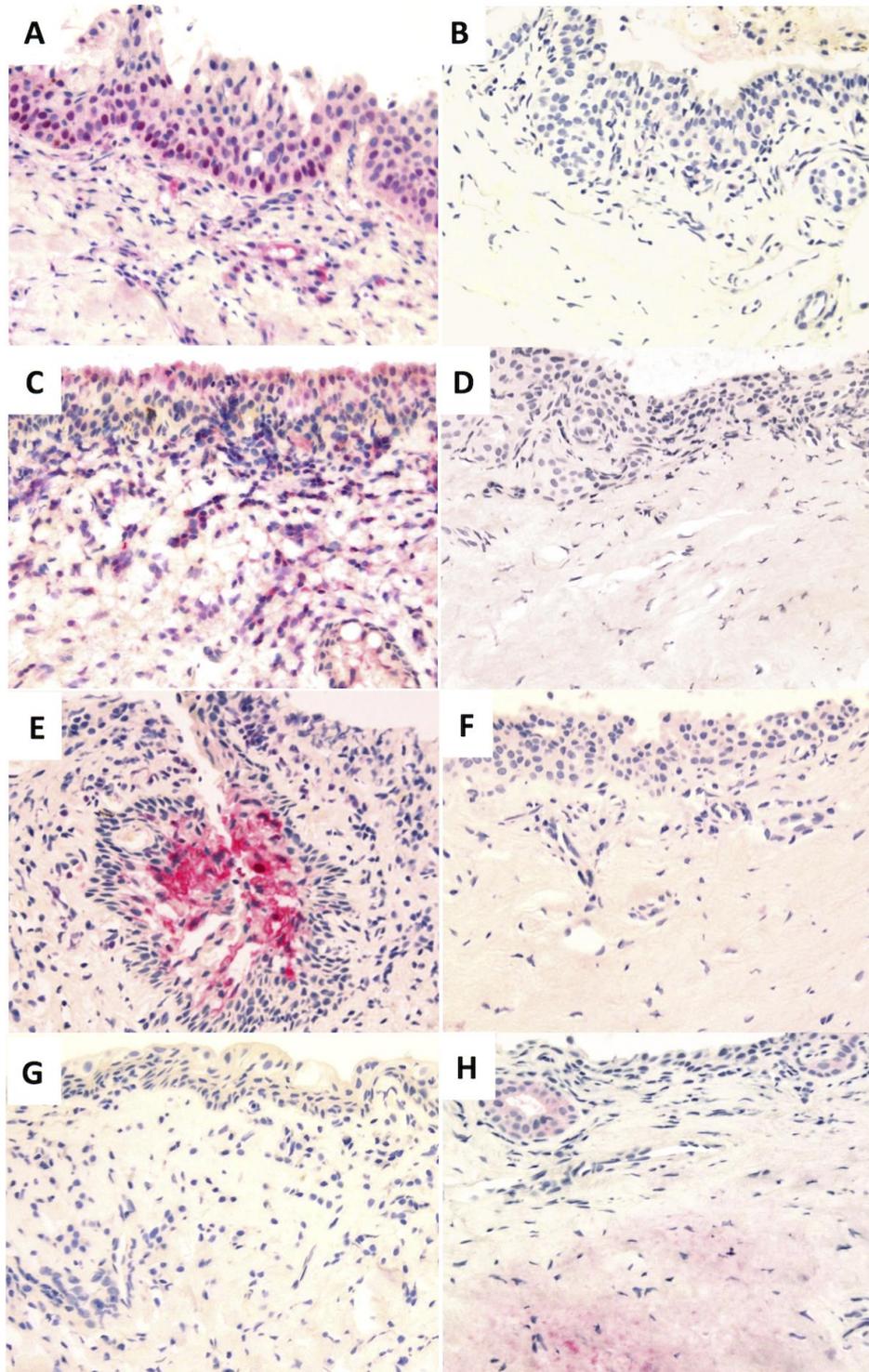
Figure 10.2. Example images of IHC staining. CTGF in the deep epithelium of TT cases (A) and controls (B), IL-1β in TT cases (C) and controls (D), S100A7 in a pseudogland of Henle of a TT case (E) and S100A7 staining in controls (F) and TGFβ2 staining in TT cases (G) and in controls (H). Images were taken at 200x original magnification.

Significantly more expression of IL-1β was detected in the subepithelial tissue of TT cases relative to controls (P = 0.012). IL-1β expression was localized around the inflammatory cell infiltrate (Figure 10.2C), however, only 5/11 of samples that stained >0 for IL-1β had a clinical papillary grade >0. Expression of IL-1β tended to be higher in the epithelium of TT cases but the difference was not statistically significant.

S100A7 expression was significantly higher in the epithelium of TT cases (P = 0.0095). Expression of S100A7 within the epithelium was patchy and in 2 samples expression was localized to pseudoglands of Henle (Figure 10.2E). All controls stained negative for S100A7. Six of the nine samples that scored >0 for S100A7 had a clinical papillary grade >0. S100A7 was not detected in the subepithelial tissue in any sample.

TGFβ2 expression was slightly greater in the subepithelial tissue of controls (P = 0.037). Four controls were weakly positive (Figure 10.2H) and one case (papillary grade 3) had stronger expression of TGFβ2 in the subepithelial tissue. For the remaining 31 samples TGFβ2 was not detected in the subepithelial tissue. Epithelial expression of TGFβ2 was not different between cases and controls.

There were no statistical differences in the expression of EMT biomarkers E-cadherin, vimentin and αSMA in the epithelium between cases and controls. There were also no statistical differences between cases and controls in epithelial or subepithelial tissue expression of CC1, MMP9, PDGF, IL-17A, IL-22 and CXCL5 (Table 10.3). IL-17A and CXCL5 were not detected in the subepithelial tissue in any samples. IL-6 and MMP7 were detected in ≤2 of the 36 samples tested.

Discussion

In this study we found that conjunctival tissue of TT cases had significantly greater S100A7 and CTGF expression in the epithelium and significantly greater IL-1β expression in the subepithelial tissue. The average expression of CTGF, IL-1β and CC1 was greater in TT cases in both epithelial and subepithelial compartments. Controls tended to have more expression of TGFβ2 in the subepithelial tissue. We did not detect an increase in the expression of EMT biomarkers in the epithelium of samples from individuals with TT. We found that individuals with TT had different patterns of collagen deposition and an increased inflammatory cell infiltrate in the subepithelial compartment relative to individuals without clinical evidence of trachoma.

In this study the age distribution of cases and controls was comparable. There were more females among the TT cases, however, this was not a statistically significant. There were substantially more Maasai people among the cases. This probably reflects greater environmental and behavioral risk factors [20,21]. Maasai people live in close contact with their livestock (flies are often abundant) and in areas with fairly limited access to water. Furthermore the uptake of antibiotics for trachoma control may be lower in these communities [22]. Although genetic risk factors in Maasai people cannot be excluded, the behavioral and environmental risk factors leading to increased exposure to *C. trachomatis* infection probably account for the higher proportion of Maasai among TT cases.

Changes in tissue morphology were clearly evident with a transition from a "block" type pattern of collagen deposition in controls to "wavy" and "fine" type patterns in cases. This probably reflects the progressive disruption of normal connective tissue. Degradation of organized bundles of collagen fibers running parallel with the epithelium ("block" type) by MMPs or oedema could create the fragmented "wavy" and "fine" patterns observed. A similar observation has previously been shown in the subepithelial tissue of individuals with scarring trachoma and was found to correlate with tissue scarring determined by *in vivo* confocal microscopy (IVCM) [23]. There is an apparent mismatch in the features of TS when tissue is observed by the 2 different methods; using IVCM, defined bands of scarring were observed, whereas by histology collagen bundles appear fragmented and amorphous. It is possible that the bands of scarring (observed by IVCM in 3 dimensions) disrupt the parallel collagen bundles (seen on a section in 2 dimensions) to produce wavy and fine patterns of collagen in cases. It was not possible to grade fibrosis in subepithelial tissue with the same

grading system described in Hu *et al* [23] as tissue sections were not sufficient in size. The baseline "T" collagen structure indicative of healthy tissue in controls was visible only in one control section.

More inflammatory cells were identified in tissue from TT cases. This result is in keeping with the range of clinical inflammatory grades observed in cases, whereas all controls had a clinical inflammation grade of 0. It is perhaps surprising that epithelial atrophy, thought to be a common feature of scarring trachoma, and the number of myofibroblasts were not different between cases and controls. Epithelial atrophy has been reported in two studies that used samples from 11 and 29 individuals with TT and entropion, however neither study included controls [24,25]. The same two studies also reported epithelial hyperplasia and psuedogland formation [24,25]. Persistent and recurrent conjunctival inflammation and associated hyperplasia are thought to promote the formation of pseudoglands of Henle, which are crypts formed by invagination of the epithelium [26]. Bacteria and debris can become trapped by mucus within these crypts and entrapped secretions within pseudoglands were observed in individuals with TT [24,26]. Myofibroblasts have contractile properties therefore one might speculate that they have an increased role during TS and TT. In line with our observations we did not detect any significant differences in the epithelial expression of the EMT biomarkers vimentin, αSMA or E-cadherin between cases and controls, although vimentin expression was slightly increased in TT cases. The number of samples in this study was relatively small and there was only one sample from an individual with *trachomatous inflammation – intense*, therefore it is possible we did not have sufficient power within the study to detect subtle, transient or rare events. We only graded loss of E-cadherin and gain of vimentin and αSMA expression in the epithelium, as it would not be possible to distinguish cells expressing vimentin and αSMA in the subepithelial tissue from normal fibroblasts/myofibroblasts. Future work such as multiplex staining or application of new techniques such as laser ablation mass cytometry are required to distinguish complex cell phenotypes and rare events such as cells undergoing EMT [27].

IHC staining was generally greater in the epithelial compartment relative to the subepithelial compartment. CC1, CTGF and IL-1β were increased in both epithelial and subepithelial compartments in TT cases (Figure 1) and S100A7 was increased in the epithelium. CC1 cleaves IL-1β into its active form and the concomitant upregulation of CC1 and IL-1β reflects activation of the inflammasome [28]. In the subepithelial tissue of TT cases IL-1β was localized around the inflammatory cell infiltrate. Just over half of

the samples that stained positive for IL-1β in the subepithelial tissue had no evidence of clinical inflammation; therefore considerable levels of IL-1β were expressed in the absence of clinical signs. Recent evidence showed that IL-1β expression was weakly associated with progressive scarring trachoma and strongly associated with inflammatory episodes [1]. It is possible that IL-1β remains up-regulated in the subepithelial tissue in individuals without evidence of clinical inflammation, as this study might suggest, but that cytokines expressed in the subepithelial tissue are less readily detected when samples are collected using a superficial conjunctival swab. Chronic IL-1 induced inflammation is known to result in tissue remodeling [29,30].

CTGF modulates the interaction of cells with the extracellular matrix; promoting collagen deposition, mesenchymal cell activation and differentiation (including EMT) and tissue remodeling [14,31]. CTGF was previously shown by IHC to be upregulated in infiltrating monocytes/macrophages of children with active trachoma [12], however we demonstrate an upregulation of CTGF in both the subepithelium and epithelium of TT cases. This difference could reflect the different clinical stages of trachoma in the samples studied. TGFβ induces CTGF expression in fibroblasts and epithelial cells therefore it is surprising that we did not see a concomitant up-regulation of TGFβ in TT cases alongside CTGF [32–34]. A number of bacteria have been shown to stimulate CTGF expression in epithelial cells via the lysophosphatidic acid receptor [35], therefore it is possible that CTGF is directly induced in the epithelium by the altered ocular microbiota observed in individuals with trachoma [18,36]. Over-expression of CTGF drives fibrosis in a number of diseases [32,37,38] and it has become apparent that epithelial-derived CTGF can drive fibrosis in the underlying subepithelial tissue [34,39]. CTGF was detected in the basal epithelium in four samples (Figure 2A). CTGF staining in the basal epithelium has previously been reported in the context of gingival fibrosis, where it was thought to have a role in cell proliferation and epithelial hyperplasia [40]. This could drive the formation of pseudoglands in addition to driving fibrosis in the underlying tissue. CTGF was strongly associated with clinical inflammation in adults with progressive scarring trachoma [1], however in the present study CTGF did not appear to be preferentially detected in adults with evidence of clinical inflammation.

S100A7 is a pro-inflammatory antimicrobial peptide secreted by epithelial cells. S100A7 was only detected in the epithelium of TT cases in this study and expression was generally patchy, possibly suggesting a localized antimicrobial response. In addition to direct antibacterial action, S100A7 recruits CD4+ T cells and neutrophils

and amplifies pro-inflammatory cytokine responses [41–43]. In two samples staining was detected around pseudoglands of Henle, possibly reflecting a local inflammatory response to bacteria that had accumulated within the pseudogland. Positive staining of the epithelium around these pseudoglands was also noted for IL-1β in 4 TT cases. No positive staining was detected around pseudoglands in control tissue for any of the antibodies tested. Due to the small size of the tissue sections it was not possible to compare the number of pseudoglands between cases and controls. Further study is required to identify whether trachomatous inflammation promotes pseudogland formation and whether bacteria trapped within pseudoglands have a role in exacerbating inflammation.

Latent TGFβ2, PDGF and MMP9 expression tended to be slightly higher in controls. TGFβ2 expression in controls was relatively weak and non-specific therefore could be attributed to a high background. The antibody used detected the latent form of TGFβ2, therefore it is possible that more latent TGFβ2 was present in controls whereas cases had activated and released TGFβ2. Despite having a well-defined role in tissue fibrosis, no previous associations have been found between TGFβ2 and trachoma at both expression and protein levels (Holland, Mabey and Bailey; personal communication) [44]. Full characterization of the role of TGFβ2 in trachoma has been limited due to its complex post-translational modifications.

IL-17A, CXCL5, PDGF, MMP7 and MMP9 have previously been associated with various stages of trachoma (*trachomatous inflammation – follicular* [10,11,44,45], TS [1,6,7] and TT [8,9]) at mRNA and protein expression levels, however they were not demonstrably up-regulated in TT cases in the present study. MMP7, CXCL5 and IL-17A were strongly associated with inflammatory episodes but not with progressive scarring in two large cohorts of individuals with trachoma [1]. The failure to detect differences in staining in this study could be due to the lack of clinical inflammation in the individuals from whom samples were obtained, or due to a lack of study power to detect more subtle differences. It could also be biological and might suggest that differences at the expression level are not maintained at the protein level. The failure to detect MMP7 and IL-6 could likewise be due to a lack of clinical inflammation, a lack of expression or due to the sensitivity of the antibodies used. IL-22 is released alongside IL-17 by Th17 cells and contributes to mucosal defense and maintenance of epithelial integrity but also to the pathogenesis of psoriasis [46,47]. Although IL-22 has not previously been associated with trachoma we hypothesized it might have a role in

conjunctival epithelial inflammation or health [48], however no differences in expression were detected.

We did not to collect swabs for *C. trachomatis* PCR because the swabbing process would have probably altered the surface tissue appearance. However, from contemporary studies it is known that the prevalence of *C. trachomatis* infection in this region among individuals with trachomatous scarring is very low, and therefore it is likely that few if any of these case would have been infected [1]. Similarly, it was not possible to collect conjunctival swab samples for mRNA gene expression analysis from these individuals as this would have affected the histological analysis. Our previous gene expression work used mRNA collected from surface swabs. Therefore, we would not necessarily expect these to exactly correspond to this immunohistochemistry study, which is assessing protein mostly in deeper levels.

We have demonstrated that individuals with TT had significantly increased levels of CTGF and S100A7 in the epithelium and IL-1β in the subepithelial tissue, even in the absence of marked clinical inflammation. CTGF, IL-1β and CC1 were increased in TT cases in both epithelial and subepithelial compartments. We suggest that microbial stimulation of the epithelium, ongoing sub-clinical inflammation and inflammasome activation in the connective tissue and CTGF-driven fibrosis contribute to the pathology of trachoma. We also described a potential role for pseudoglands of Henle in trachoma that warrants further investigation. CTGF could be responsible for driving inflammation-induced fibrosis in trachoma, making it a potential therapeutic target [49]. Future research should focus on the stimuli that lead to up-regulation of CTGF, S100A7 and IL-1β and potential inhibitors that could halt the progression of scarring.

Acknowledgements

The authors would like to express great thanks to the study participants and to the theatre staff of the Eye Department at Kilimanjaro Christian Medical Centre.

Protein accession numbers

Target	Swiss-Prot ID
IL-1β	P01584
IL-6	P05231
IL-17A	Q16552
CXCL5	P42830
S100A7	P31151
IL-22	Q9GZX6
PDGF	P04085
TGFβ2	P61812
CTGF	P29279
E-cadherin	P12830
Vimentin	P08670
αSMA	P62736
MMP7	P09237
MMP9	P14780
CC1	P29466

1. Burton MJ, Rajak SN, Hu VH, Ramadhani A, Habtamu E, et al. (2015) Pathogenesis of progressive scarring trachoma in Ethiopia and Tanzania and its implications for disease control: two cohort studies. PLoS Negl Trop Dis 9: e0003763. doi:10.1371/journal.pntd.0003763.

2. Alliance WHO, Elimination G, Trachoma B, Oms A (2014) Weekly epidemiological record Relevé épidémiologique hebdomadaire. 96: 421–428.

3. Hu VH, Harding-Esch EM, Burton MJ, Bailey RL, Kadimpeul J, et al. (2010) Epidemiology and control of trachoma: systematic review. Trop Med Int Health 15: 673–691. doi:10.1111/j.1365-3156.2010.02521.x.

4. Jimenez V, Gelderblom HC, Mann Flueckiger R, Emerson PM, Haddad D (2015) Mass Drug Administration for Trachoma: How Long Is Not Long Enough? PLoS Negl Trop Dis 9: e0003610. doi:10.1371/journal.pntd.0003610.

5. Stephens RS (2003) The cellular paradigm of chlamydial pathogenesis. Trends Microbiol 11: 44–51.

6. Burton MJ, Rajak SN, Bauer J, Weiss H a, Tolbert SB, et al. (2011) Conjunctival transcriptome in scarring trachoma. Infect Immun 79: 499–511. doi:10.1128/IAI.00888-10.

7. Hu VH, Weiss HA, Ramadhani AM, Tolbert SB, Massae P, et al. (2012) Innate immune responses and modified extracellular matrix regulation characterize bacterial infection and cellular/connective tissue changes in scarring trachoma. Infect Immun 80: 121–130. doi:10.1128/IAI.05965-11.

8. Burton MJ, Rajak SN, Ramadhani A, Weiss HA, Habtamu E, et al. (2012) Post-operative recurrent trachomatous trichiasis is associated with increased conjunctival expression of S100A7 (psoriasin). PLoS Negl Trop Dis 6: e1985. doi:10.1371/journal.pntd.0001985.

9. Holland MJ, Jeffries D, Pattison M, Korr G, Gall A, et al. (2010) Pathway-focused arrays reveal increased matrix metalloproteinase-7 (matrilysin) transcription in trachomatous trichiasis. Invest Ophthalmol Vis Sci 51: 3893–3902. doi:10.1167/iovs.09-5054.

10. El-Asrar a M, Geboes K, Al-Kharashi S a, Al-Mosallam a a, Missotten L, et al. (2000) Expression of gelatinase B in trachomatous conjunctivitis. Br J Ophthalmol 84: 85–91. doi:10.1136/bjo.84.1.85.

11. Abu el-Asrar a M, Geboes K, Tabbara KF, al-Kharashi S a, Missotten L, et al. (1998) Immunopathogenesis of conjunctival scarring in trachoma. Eye (Lond) 12 (Pt 3a: 453–460. doi:10.1038/eye.1998.104.

12. Abu El-Asrar a M, Al-Kharashi S a, Missotten L, Geboes K (2006) Expression of growth factors in the conjunctiva from patients with active trachoma. Eye (Lond)

20: 362–369. doi:10.1038/sj.eye.6701884.

13. Liu X (2008) Inflammatory cytokines augments TGF-β1-induced epithelial-mesenchymal transition in A549 cells by up-regulating TβR-I. Cell Motil Cytoskeleton 65: 935–944. doi:10.1002/cm.20315.

14. Sonnylal S, Xu S, Jones H, Tam A, Sreeram VR, et al. (2013) Connective tissue growth factor causes EMT-like cell fate changes in vivo and in vitro. J Cell Sci 126: 2164–2175. doi:10.1242/jcs.111302.

15. Radisky ES, Radisky DC (2010) Matrix metalloproteinase-induced epithelial-mesenchymal transition in breast cancer. J Mammary Gland Biol Neoplasia 15: 201–212. doi:10.1007/s10911-010-9177-x.

16. Kalluri R, Weinberg RA (2009) Review series The basics of epithelial-mesenchymal transition. 119. doi:10.1172/JCI39104.1420.

17. Dawson CR, Jones BR TM, Dawson CR, Jones BR, Tarizzo ML, World Health Organization (1981) Guide to trachoma control in programmes for the prevention of blindness. 56 p.

18. Hu VH, Massae P, Weiss HA, Chevallier C, Onyango JJ, et al. (2010) Bacterial Infection in Scarring Trachoma. Invest Ophthalmol Vis Sci 52: 2181–2186. doi:10.1167/iovs.10-5829.

19. WHO simplified trachoma grading system. (2004). Community Eye Health 17: 68.

20. Lawson DW, Borgerhoff Mulder M, Ghiselli ME, Ngadaya E, Ngowi B, et al. (2014) Ethnicity and child health in northern Tanzania: Maasai pastoralists are disadvantaged compared to neighbouring ethnic groups. PLoS One 9: e110447. doi:10.1371/journal.pone.0110447.

21. Mahande MJ, Mazigo HD, Kweka EJ (2012) Association between water related factors and active trachoma in Hai district, Northern Tanzania. Infect Dis poverty 1: 10. doi:10.1186/2049-9957-1-10.

22. Kiringe JW (2005) Ecological and Anthropological Threats to Ethno-Medicinal Plant Resources and their Utilization in Maasai Communal Ranches in the Amboseli Region of Kenya. Ethnobot Res Appl 3: 231–241.

23. Hu VH, Holland MJ, Cree I a, Pullin J, Weiss H a, et al. (2013) In vivo confocal microscopy and histopathology of the conjunctiva in trachomatous scarring and normal tissue: a systematic comparison. Br J Ophthalmol 97: 1333–1337. doi:10.1136/bjophthalmol-2013-303126.

24. al-Rajhi AA, Hidayat A, Nasr A, al-Faran M (1993) The histopathology and the mechanism of entropion in patients with trachoma. Ophthalmology 100: 1293–1296.

25. Guzey M, Ozardali I, Basar E, Aslan G, Satici A, et al. (2000) A survey of trachoma: the histopathology and the mechanism of progressive cicatrization of eyelid tissues. Ophthalmologica 214: 277–284. doi:27504.

26. William T, Edward J, editors (n.d.) Duane's Ophthalmology Lippincott Williams & Wilkins.

27. Giesen C, Wang HAO, Schapiro D, Zivanovic N, Jacobs A, et al. (2014) Highly multiplexed imaging of tumor tissues with subcellular resolution by mass cytometry. Nat Methods 11: 417–422. doi:10.1038/nmeth.2869.

28. Martinon F, Burns K, Tschopp J (2002) The Inflammasome. Mol Cell 10: 417–426. doi:10.1016/S1097-2765(02)00599-3.

29. Dinarello C a (2009) Immunological and inflammatory functions of the interleukin-1 family. Annu Rev Immunol 27: 519–550. doi:10.1146/annurev.immunol.021908.132612.

30. Kolb M, Margetts PJ, Anthony DC, Pitossi F, Gauldie J (2001) Transient expression of IL-1beta induces acute lung injury and chronic repair leading to pulmonary fibrosis. J Clin Invest 107: 1529–1536. doi:10.1172/JCI12568.

31. Shi-Wen X, Leask A, Abraham D (2008) Regulation and function of connective tissue growth factor/CCN2 in tissue repair, scarring and fibrosis. Cytokine Growth Factor Rev 19: 133–144. doi:10.1016/j.cytogfr.2008.01.002.

32. Chen MM, Lam A, Abraham JA, Schreiner GF, Joly AH (2000) CTGF expression is induced by TGF- beta in cardiac fibroblasts and cardiac myocytes: a potential role in heart fibrosis. J Mol Cell Cardiol 32: 1805–1819. doi:10.1006/jmcc.2000.1215.

33. Igarashi A, Okochi H, Bradham DM, Grotendorst GR (1993) Regulation of connective tissue growth factor gene expression in human skin fibroblasts and during wound repair. Mol Biol Cell 4: 637–645. doi:10.1091/mbc.4.6.637.

34. Yang J, Velikoff M, Canalis E, Horowitz JC, Kim KK (2014) Activated alveolar epithelial cells initiate fibrosis through autocrine and paracrine secretion of connective tissue growth factor. Am J Physiol Lung Cell Mol Physiol 306: L786–L796. doi:10.1152/ajplung.00243.2013.

35. Wiedmaier N, Müller S, Köberle M, Manncke B, Krejci J, et al. (2008) Bacteria induce CTGF and CYR61 expression in epithelial cells in a lysophosphatidic acid receptor-dependent manner. Int J Med Microbiol 298: 231–243. doi:10.1016/j.ijmm.2007.06.001.

36. Zhou Y, Holland MJ, Makalo P, Joof H, Roberts C h, et al. (2014) The conjunctival microbiome in health and trachomatous disease: a case control study. Genome Med 6: 99. doi:10.1186/s13073-014-0099-x.

37. Ito Y, Aten J, Bende RJ, Oemar BS, Rabelink TJ, et al. (1998) Expression of connective tissue growth factor in human renal fibrosis. Kidney Int 53: 853–861. doi:10.1111/j.1523-1755.1998.00820.x.

38. Ponticos M, Holmes AM, Shi-wen X, Leoni P, Khan K, et al. (2009) Pivotal role of connective tissue growth factor in lung fibrosis: MAPK-dependent transcriptional activation of type I collagen. Arthritis Rheum 60: 2142–2155. doi:10.1002/art.24620.

39. Yang J, Wheeler SE, Velikoff M, Kleaveland KR, LaFemina MJ, et al. (2013) Activated alveolar epithelial cells initiate fibrosis through secretion of mesenchymal proteins. Am J Pathol 183: 1559–1570. doi:10.1016/j.ajpath.2013.07.016.

40. Kantarci A, Black SA, Xydas CE, Murawel P, Uchida Y, et al. (2006) Epithelial and connective tissue cell CTGF/CCN2 expression in gingival fibrosis. J Pathol 210: 59–66. doi:10.1002/path.2000.

41. Lee KC, Eckert RL (2007) S100A7 (Psoriasin)--mechanism of antibacterial action in wounds. J Invest Dermatol 127: 945–957. doi:10.1038/sj.jid.5700663.

42. Zheng Y, Niyonsaba F, Ushio H, Ikeda S, Nagaoka I, et al. (2008) Microbicidal protein psoriasin is a multifunctional modulator of neutrophil activation. Immunology 124: 357–367. doi:10.1111/j.1365-2567.2007.02782.x.

43. Jinquan T, Vorum H, Larsen CG, Madsen P, Rasmussen HH, et al. (1996) Psoriasin: a novel chemotactic protein. J Invest Dermatol 107: 5–10.

44. Burton MJ, Bailey RL, Jeffries D, Mabey DCW, Holland MJ (2004) Cytokine and Fibrogenic Gene Expression in the Conjunctivas of Subjects from a Gambian Community Where Trachoma Is Endemic. Infect Immun 72: 7352–7356. doi:10.1128/IAI.72.12.7352-7356.2004.

45. Burton MJ, Ramadhani A, Weiss HA, Hu V, Massae P, et al. (2011) Active trachoma is associated with increased conjunctival expression of IL17A and profibrotic cytokines. Infect Immun 79: 4977–4983. doi:10.1128/IAI.05718-11.

46. Rutz S, Eidenschenk C, Ouyang W (2013) IL-22, not simply a Th17 cytokine. Immunol Rev 252: 116–132. doi:10.1111/imr.12027.

47. Zheng Y, Danilenko DM, Valdez P, Kasman I, Eastham-Anderson J, et al. (2007) Interleukin-22, a T(H)17 cytokine, mediates IL-23-induced dermal inflammation and acanthosis. Nature 445: 648–651. doi:10.1038/nature05505.

48. Sonnenberg GF, Fouser LA, Artis D (2011) Border patrol: regulation of immunity, inflammation and tissue homeostasis at barrier surfaces by IL-22. Nat Immunol 12: 383–390. doi:10.1038/ni.2025.

49. Lipson KE, Wong C, Teng Y, Spong S (2012) CTGF is a central mediator of

tissue remodeling and fibrosis and its inhibition can reverse the process of fibrosis. Fibrogenesis Tissue Repair 5: S24. doi:10.1186/1755-1536-5-S1-S24.

Supporting information

Table S10.1. Antibodies and retrieval methods used in this study

Category	Target	Dilution	Retrieval	Supplier	Antibody
Pro-inflammatory mediators	IL-1β	1:75	H2*(20)[‡]	ABCAM	AB2105
	IL-6	1:400	NR[§]	LEICA	NCL-L-IL6
	IL-17A	1:350	H1[†](30)	ABCAM	AB136668
	CXCL5	1:200	H2(20)	ABCAM	AB9802
	S100A7	1:400	H1(10)	ABCAM	AB13680
	IL-22	1:100	H2(20)	ABCAM	AB18499
Growth Factors	PDGF	1:200	H2(20)	ABCAM	AB178409
	TGFβ2	1:100	H1(20)	ABCAM	AB36495
	CTGF	1:300	H1(10)	ABCAM	AB6992
EMT	E-cadherin	1:200	H2(20)	DAKO	NCH-38
	Vimentin	1:3000	H2(20)	DAKO	M0725
	αSMA	1:500	NR	DAKO	M0851
Matrix	MMP7	1:50	H2(20)	ABCAM	AB4044
	MMP9	1:200	H2(20)	LEICA	NCL-MMP9-439
Inflammasome	CC1	1:50	H2(20)	ABCAM	AB1872

*H2 = Bond (Leica) epitope retrieval solution 2; pH9 EDTA based buffer and surfactant at 25°C.

[‡](10) = 10 minutes; (20) = 20 minutes; (30) = 30 minutes.

[§]NR = no retrieval.

[†]H1 = Bond (Leica) epitope retrieval solution 1; pH6 citrate based buffer and surfactant at 25°C.
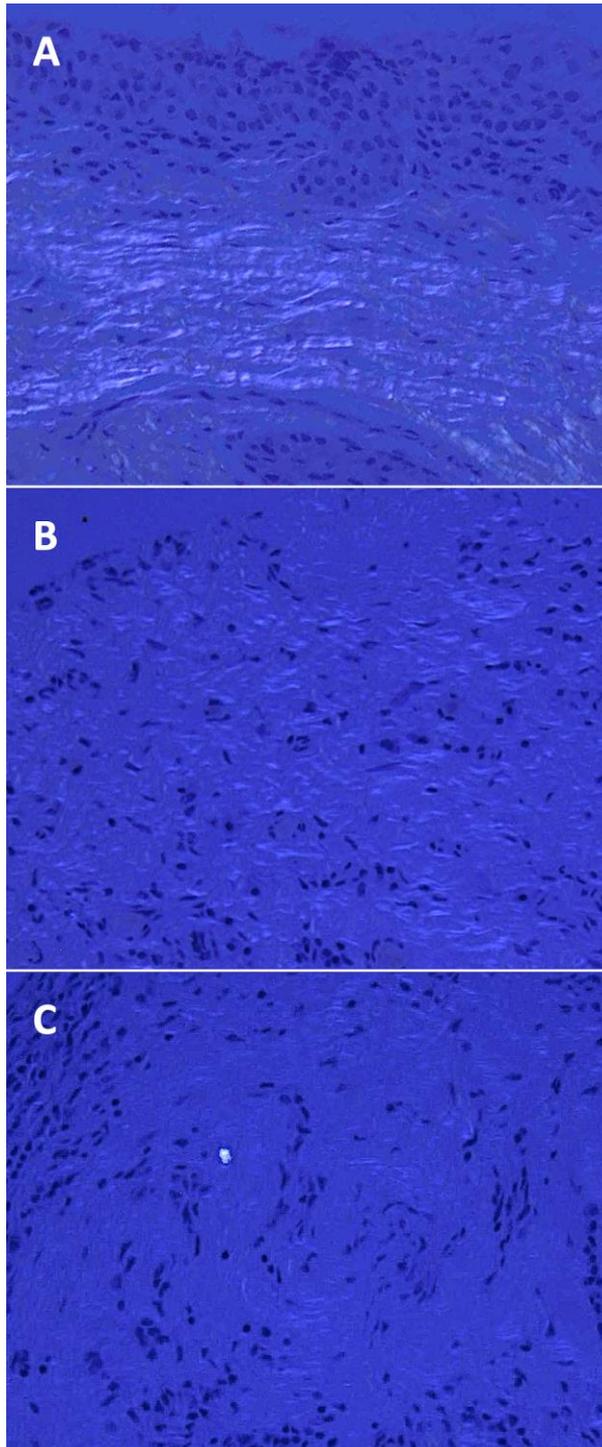
Figure S10.1. Cross-polarized light images of haemotoxylin and eosin stained tissue sections. Example images representative of "block" (A), "wavy" (B) and "fine" (C) patterns of fibrosis are shown. Images were taken at 200X original magnification.

Chapter 11: Conclusions

11.1 Overall conclusions

Data from transcriptomic studies in active and scarring trachoma have shown that many thousands of genes were differentially regulated [1,2]. In order to reduce some of this complexity and to find key pathways that were dysregulated in different stages of trachomatous disease, miR expression was investigated (chapter 3; chaper 6 [3,4]). miR were not differentially regulated in response to Ct infection in epithelial cells *in vitro. In vivo*, miR-155 and miR-184 were dysregulated in TF and were strongly associated with TI. Dysregulation of miR-155 and miR-184 in TF and TI likely reflects the activation and increased presence of immune cells in the epithelium, regulation of inflammation and epithelial wound healing, possibly including prolonged activation of cell proliferation and pro-fibrotic pathways [5–8]. miR-1285 and miR-147b were upregulated in individuals with TSI but not in individuals with TS alone. Upregulation of miR-147b and miR-1285 in TSI alludes to the regulation of cell proliferation pathways and inflammation [9–11]. Regulation of the immune cell inflammatory response appears to be a key process in both stages of disease, which perhaps explains why no differences were seen in miR expression in Ct infected epithelial cells *in vitro*. These data suggest that miR expression in TF, TI and TSI is indicative of the host's attempts to control clinical inflammation, which is a major risk factor for scarring progression [12].

Ct infected epithelial cells *in vitro* upregulated expression a number of pro-inflammatory cytokines and the growth factor CTGF and expression was slightly greater in response to plasmid-competent Ct (Chapter 8). This supports the data of others [13] and could explain why pathology is more severe in some animal models in response to plasmid-competent Ct [14–16]. Ct infection is rarely found in adults with established scarring disease however, yet inflammation and fibrosis continues [12]. The factors driving this pathological inflammation in the absence of Ct infection remain unclear. Non-chlamydial bacteria are thought to have a role in driving inflammation and disease in the absence of Ct (reviewed in [17]) however mechanistic links have not yet been identified and it is unclear whether the differential species diversity detected in trachoma is causal or an effect of the altered physiological environment. It seems reasonable to speculate that repeated bouts of Ct-induced inflammation and the associated wound healing response throughout childhood alters or damages the architecture of the conjunctiva, such that it is more susceptible to inflammation throughout adulthood in response to stimuli (e.g. dust, commensal bacteria) that might be innocuous in an individual with an uncompromised conjunctiva. It is also possible

that individuals who resolve inflammation quickly are at lower risk of these changes and later scarring complications. Squamous metaplasia, loss of goblet cells and epithelial atrophy have previously been observed in histology samples from individuals with TS and TT, supporting this hypothesis [18,19]. No differences in epithelial atrophy were detected however between TT cases and controls in more recent studies with larger sample sizes (Chapter 10; Victor Hu, manuscript in preparation), perhaps indicating that this dogma should be readdressed.

Conjunctival tissue from individuals with TT had increased expression of CTGF, IL-1β and S100A7 and expression of IL-1β and S100A7 was often located around Pseudoglands of Henle (Chapter 10). Epithelial hyperplasia has been observed in individuals with TF/TI [20], which could be driven by upregulation of the Wnt pathway, mediated by downregulation of miR-184 (chapter 6), and by the upregulation of CTGF (Chapters 8 and 10). In some TT cases CTGF expression was highest in the basal epithelium, which has previously been reported in the context of gingival fibrosis (associated with epithelial hyperplasia) and in corneal scarring following injury [21,22]. This could lead to epithelial invagination and the development of pseudoglands that become blocked with debris, bacteria and mucus. An increased presence of psuedoglands containing entrapped secretions, as has been previously noted in individuals with TT [19,18], might promote localized inflammatory responses that further drive fibrosis and hyperplasia. This could also be supported by the upregulation of miR-1285 in TSI (related to cell proliferation). These results and hypotheses are outlined in a graphical summary (Figure 11.1). In vivo confocal microscopy (IVCM) could be investigated as a non-invasive method to detect conjunctival psuedoglands in trachoma in order to investigate this hypothesis further. EMT was not detected in response to Ct infection of epithelial cells *in vitro* (Chapter 8) or in trichiasis tissue (Chapter 10). EMT might be a rare and transient event therefore it is possible that the experiments performed were not optimally designed or well powered enough to detect the transition. Further experiments to address this are described in section 11.3 below.
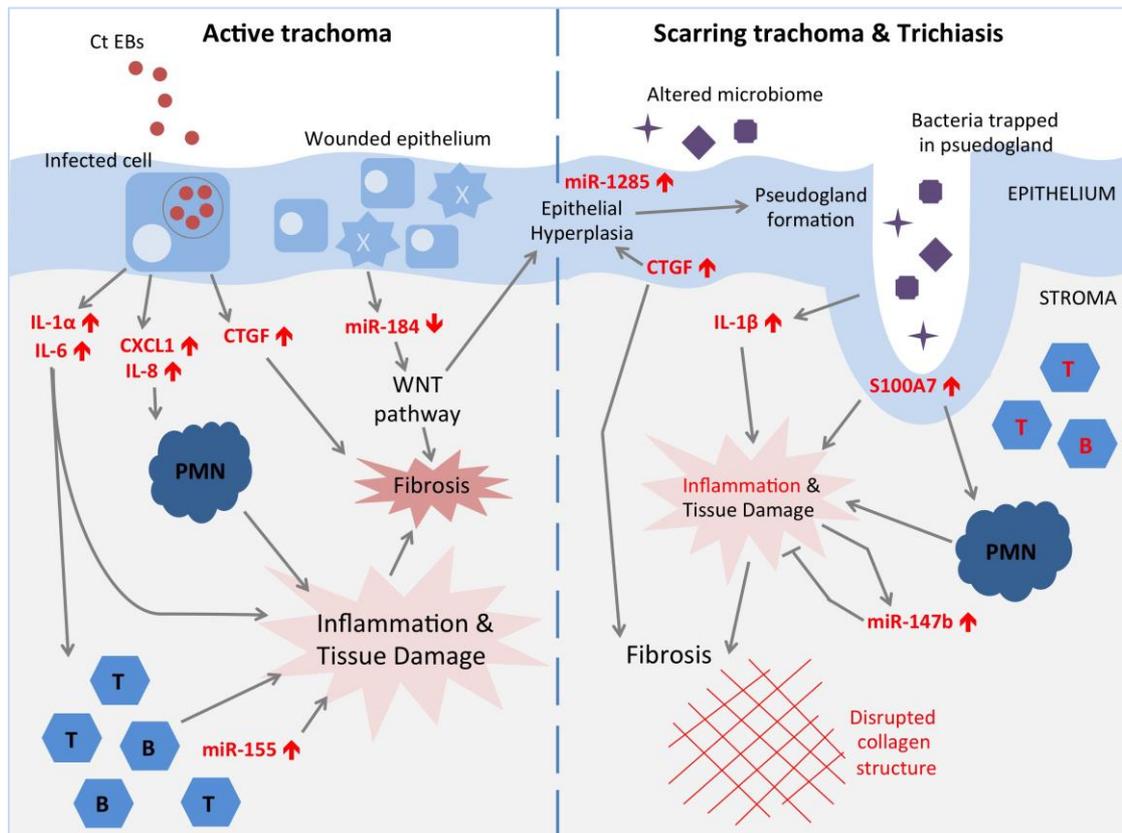
Figure 11.1. Graphical summary of the results of this thesis, in the form of a cross-sectional diagram of the conjunctival epithelium in TF/TI (left) and in TS and TT (right). "T" and "B" are infiltrating T and B lymphocytes and "PMN" are neutrophils. Factors highlighted in red font are direct findings of this thesis. Processes in black font are hypothesized contributors to, or results of, the factors in red.

11.2 Wider relevance

It is not clear whether the immunology and pathology of ocular and urogenital chlamydial disease share exactly the same mechanisms. There is a paucity of studies of human urogenital chlamydial histopathology, largely due to the inherent difficulties of obtaining biopsy samples from this anatomical site and of knowing a persons chlamydial exposure. For ocular disease one can estimate chlamydial exposure using the population prevalence of clinical signs, disease progression can be simply assessed by observation of the up-turned conjunctiva, and biopsy material can be collected during tarsal rotation surgery for trichiasis. Early urogenital histology studies in Ct culture-positive individuals found intense neutrophil infiltration in the epithelium and stroma and stromal infiltration of lymphocytes [23,24]. There was focal loss of surface columnar epithelial cells however stromal architecture remained intact. Neutrophils were not distinguished in the IHC study described in Chapter 10, however

the results are in agreement regarding the stromal lymphocyte infiltration, although it should be noted that these studies are not directly comparable due to the different stages of disease investigated (active infection versus long-term sequelae). Epithelial hyperplasia was not reported, however the focal degradation of the epithelium supports the damaged or altered ocular epithelium hypothesis. Faults in the integrity of the epithelium can also lead to chronic pathological inflammation in other diseases. A breakdown of epithelial barrier function during Inflammatory Bowel Disease perpetuates the cycle of chronic inflammation as the stroma is exposed to foreign antigens (reviewed in [25]), and it thus becomes increasingly difficult to repair the epithelial barrier and restore tissue homeostasis.

IL-1β, CTGF and S100A7 expression have repeatedly been shown to be associated with active trachoma and scarring trachoma at the expression level [1,12,26–30]. IL-1β and S100A7 were in fact the only transcripts associated with scarring progression in a longitudinal trachoma cohort [12]. The results described in Chapter 10 corroborate these data at the protein level and suggest that these factors may be key components in the mechanism of scarring progression. Cervical epithelial cells from women with fertility disorders secreted higher levels of IL-1β in response to Chlamydial antigens relative to women thought to have had equal exposure (deduced through anti-Ct antibody levels) but without fertility problems [31]. Associations between S100A7 and CTGF and human urogenital sequelae of chlamydial infection have not been reported, however as described above there are a limited number of studies and they are often targeted to investigate more classical immune response factors [31–34]. S100A7 was upregulated in progesterone-primed endometrial cells in response to Ct *in vitro* [35]. CTGF has been reported to be associated with C. pneumoniae (Cp) infection; at 1 day post infection in a HeLa cell *in vitro* persistence model [36] and in atheromatous plaques from Cp HSP60 antibody positive individuals with coronary artery disease relative to Cp HSP60 antibody negative individuals [37]. It is unclear if and how S100A7, IL-1β and CTGF may interact to induce fibrosis. Research on transgenic animals has shown that CTGF is not necessarily pro-fibrotic in isolation and might require co-stimulation from factors induced by development or injury and wound healing [38,39]. Following corneal injury of mice and rabbits CTGF was expressed immediately prior to scarring and staining was strongest in the basal epithelium [22]. These data support the hypothesis that CTGF, driven by inflammatory signals such as IL-1β and S100A7, is upregulated in the basal epithelium and directly or indirectly stimulates the activation of myofibroblasts in the stroma, leading to fibrosis. Knock-out of CTGF in the corneal injury model led to a 40% reduction in wound re-

epithelialization [22]. Whilst inhibition of CTGF would be detrimental in the context of an open and healing wound, it may have therapeutic value during trichiasis. CTGF might be a key factor driving inflammation-induced fibrosis in scarring trachoma and as such warrants further research.

Despite many similarities between ocular and urogenital chlamydial infections, it is possible that some aspects of the immunology and pathology are distinct to each anatomical site. miR-184 is highly enriched in ocular tissues [8] and was downregulated in children with TF (Chapter 6). Its downregulation is associated with activation of the WNT pathway and cell proliferation and a genetic deletion in the coding sequence of miR-184 can lead to keratoconus [7,40]. miR-184 is not reported to be highly abundant in the urogenital epithelium, therefore it is unclear whether miR-184 could have a parallel role in urogenital pathology. Human miR expression during urogenital Ct infection has not yet been reported and it would be of interest to compare miR expression profiles during urogenital infection with those described in Chapter 6. miRNA expression has been investigated upon urogenital chlamydia infection of mice however (discussed in Chapter 1) and some miR exhibit similar expression profiles. miR-155 was upregulated upon infection with avirulent but not virulent Cm [41], and miR-146 was upregulated 6 days post Cm infection [42]. miR-146b was upregulated during active trachoma and Ct infection in the sequencing results, however this was not significant upon qPCR validation. These results show that regulation of inflammation is an important component of the host miR response to chlamydial infection.

A few studies have investigated miRNA expression in other ocular infectious and scarring diseases. Downregulation of miR-215 in Pterygium (an ocular surface disorder of excessive fibroblast proliferation and matrix deposition) is associated with fibroblast proliferation and addition of exogenous miR-215 decreased this proliferation [43]. miR-215 was expressed at an average of 2 reads per sample in the small RNA sequencing analysis described in Chapter 6 therefore the read depth was too low to ascertain whether miR-215 was differentially expressed, however there was no difference in expression in scarring trachoma. Small RNA sequencing was recently used to investigate the miR expression profile of the cornea during fungal keratitis caused by *Aspergillus flavus* [44]. Many of the differentially expressed miR were also differentially expressed in active trachoma with Ct infection: miR-142-5p, miR-155-5p and miR-146b were upregulated and miR-184 was downregulated in the sequencing results of both studies. This suggests that common inflammatory pathways occur in the cornea and the conjunctiva in response to bacterial and fungal infection, as miR-155, -142 and -

146b regulate immune response pathways. These data also substantiate the downregulation of miR-184 upon epithelial damage and its possible role in the wound healing response. Resolution of microbial keratitis often results in corneal scarring and poor visual acuity [45]. In both microbial keratitis and active trachoma an appropriate inflammatory response is required to fight infection; too much inflammation can cause pathology however too little inflammation can lead to chronic infection. Broad-spectrum anti-inflammatory drugs such as steroids are therefore not used. A specific miR-184 targeted therapy could have the potential to inhibit excessive cell proliferation and fibrosis whilst allowing the host's immune response to appropriately fight infection. miR therapy has been successfully used in human clinical trials to prevent Hepatitis C virus infection [46]. An antisense oligonucleotide was injected subcutaneously to bind to and sequester mature miR-122, which the virus requires for survival. Exogenous miR-184, given as an eye drop for example, could have therapeutic value in trachoma and microbial keratitis and potentially other ocular fibrotic diseases, and research on its function should be pursued.

11.3 Limitations and future studies

The failure to establish productive chlamydial growth in HCjE cells was a major limitation for the *in vitro* section of this thesis work. Despite the possession of appropriate pathogen recognition receptors (Chapter 4), HEp-2 cells are likely to have an aberrant genetic background [47] (derived through their isolation from a carcinoma) and are not a relevant cell line from which to extrapolate *in vitro* results to a clinical situation. The differences between results derived in commonly used cell lines and more clinically relevant cell models have been highlighted several times and relate to many aspects of chlamydial biology, not just the inflammatory responses induced [48–51]. The up-regulation of growth factors and inflammatory cytokines upon Ct infection should therefore be validated in a more appropriate *in vitro* model. The lack of differential miRNA expression in infected epithelial cells could also be reassessed, as HEp-2 cells had a very different background miRNA expression profile to HCjE cells (Chapter 6) and the HCjE cells examined were not productively infected with Ct. It is therefore possible that significant changes in miRNA expression might be observed upon productive infection of conjunctival epithelial cells with Ct. The differential regulation of epithelial-derived miR such as miR-184 in TF also suggests that external stimuli from other cell types may be required to generate epithelial miR responses *in vivo*. In order to examine the functions of miR that were differentially regulated in trachoma (miR-155, miR-184, miR-147b, miR-1285), co-culture systems could be

developed with epithelial, fibroblast and immune cells. A synthetic conjunctiva could be engineered *in vitro* by culturing fibroblasts in a collagen gel scaffold and seeding epithelial cells on the surface. Following infection of the epithelial layer by Ct or exposure to inflammatory cell factors, cell behavior could be assessed by gene/protein expression, immunocytochemistry or by measuring the tensile properties of the fibroblast layer using a previously established contraction model [52]. This could potentially reveal the relative contribution of each cell type to the response in question. Different methods of infection could be investigated in HCjE cells, such as the rocking method that was previously used successfully [53], or, an alternative source of conjunctival epithelial cells could be used such as the IOBA-NHC cell line or primary conjunctival epithelial cells.

The clinical studies in this project had relatively limited sample sizes. Although larger sample sizes would have had more power to detect differences, there existed a trade off between how many samples it was feasible to collect and the costs associated with processing them. Small RNA sequencing was only performed on 10 samples (5 TF cases with current Ct infection, 5 controls). The top differentially regulated miR mainly reflected the increased activity and presence of adaptive immune cells in TF, therefore subtler changes associated with disease pathogenesis may have been obscured. For example several miR associated with EMT were differentially regulated (discussed in Chapter 8), however the adjusted P values were below the cut-off chosen for validation. Increased depth of sequencing and higher total RNA input concentrations might have increased the statistical power to detect differences, which could have been confirmed by validation of a wider range of miR in all 163 samples. Future experiments, beyond the scope of this PhD project, could include fluorescence-activated cell sorting directly from clinical conjunctival swab samples. This could allow identification of the expression levels of miR at the single cell level using fluorescent intracellular probes. This, in combination with extracellular dyes for cell phenotyping would enable us to identify the cellular sources of miRNA of interest. Additionally, cells could be sorted based on epithelial or lymphocytic cell markers (such as E-cadherin (epithelial cells), CD3 (T cells), CD19 (B cells), CD16 and CD56 (NK cells) for example) and then subjected to small RNA sequencing to ascertain the full miR expression profiles of distinct cell lineages in the conjunctival epithelium.

The evidence suggests that EMT is not induced by Ct infection of epithelial cells *in vitro* (Chapter 8), however it is possible that EMT occurs *in vivo* in response to inflammation and stimuli from a variety of cell types. A role for EMT was not detected in tissue from

TT cases by IHC, although Vimentin was slightly increased in the epithelium of TT cases (Chapter 10). It was difficult to differentiate cells expressing Vimentin from lymphocytes infiltrating the epithelium however, particularly as lymphocytes infiltrating the epithelium can change their morphology. Double staining could be used to address this and to detect rare or subtle changes associated with EMT. Alternatively more complex multiplex staining could be used, such as mass cytometry coupled to laser ablation of tissue sections [54]. This technique radiolabels up to 35 targets of interest using heavy metal isotopes, uses the laser to ablate the tissue and then performs mass spectrometry. The heavy-metal tagged targets can then be mapped to the previously intact tissue section. This technique is still in development, however the ability to stain for 35 targets in one tissue section would offer considerable advantages for investigating marker expression in conjunctival biopsies. Currently however, the data suggest that EMT does not have a major role in the fibrotic pathology associated with trachoma.

miR-147b and miR-1285 were upregulated in TSI however they had a poor ability to classify TS. miR-155 and miR-184 were strong biomarkers for TI, however the real value of a miR classifier would be one that could predict scarring progression. In order to determine the ability of miR-155, miR-184, miR-147b and miR-1285 to predict scarring progression, their expression will be quantified by qPCR in a longitudinal cohort of 506 Tanzanians. These individuals were aged between 6-10 at enrollment and will be followed for four years, with sub-clinical progressive scarring measured using IVCM. This cohort will provide a unique opportunity to investigate whether these miR are associated with or predictive of progressive scarring in trachoma and these data will further our knowledge of miR biology in trachoma.

11.3 Summary

These data suggest that EMT is not a prominent mechanism in the scarring process, however, it may have a more transient or subtle role that the studies performed in this PhD project were not able to detect. Epithelial cells did not differentially express miR *in vitro* in response to chlamydial infection and there was no effect of the chlamydial plasmid on miR expression. However, the establishment of productive Ct infection in a conjunctival epithelial cell line is required to confirm these results. This thesis has described human miR expression in various stages of ocular chlamydial disease and has revealed key factors involved in the scarring process. Future research on these targets will further our knowledge of the mechanisms leading to scarring trachoma,

reveal opportunities for therapeutic intervention and might aid vaccine design and assessment of efficacy.

11.4 References

1. Burton MJ, Rajak SN, Bauer J, Weiss H a, Tolbert SB, et al. (2011) Conjunctival transcriptome in scarring trachoma. Infect Immun 79: 499–511. doi:10.1128/IAI.00888-10.

2. Natividad A, Freeman TC, Jeffries D, Burton MJ, Mabey DCW, et al. (2010) Human conjunctival transcriptome analysis reveals the prominence of innate defense in Chlamydia trachomatis infection. Infect Immun 78: 4895–4911. doi:10.1128/IAI.00844-10.

3. Derrick T, Roberts C h., Rajasekhar M, Burr SE, Joof H, et al. (2013) Conjunctival MicroRNA Expression in Inflammatory Trachomatous Scarring. PLoS Negl Trop Dis 7: e2117. doi:10.1371/journal.pntd.0002117.

4. Derrick T, Last AR, Burr SE, Roberts CH, Nabicassa M, et al. (2016) Inverse relationship between microRNA-155 and -184 expression with increasing conjunctival inflammation during ocular Chlamydia trachomatis infection. BMC Infect Dis 16: 60. doi:10.1186/s12879-016-1367-8.

5. Yao R, Ma Y-L, Liang W, Li H-H, Ma Z-J, et al. (2012) MicroRNA-155 modulates Treg and Th17 cells differentiation and Th17 cell function by targeting SOCS1. PLoS One 7: e46082. doi:10.1371/journal.pone.0046082.

6. Thai T-H, Calado DP, Casola S, Ansel KM, Xiao C, et al. (2007) Regulation of the germinal center response by microRNA-155. Science 316: 604–608. doi:10.1126/science.1141229.

7. Takahashi Y, Chen Q, Rajala RVS, Ma J-X (2015) MicroRNA-184 modulates canonical Wnt signaling through the regulation of frizzled-7 expression in the retina with ischemia-induced neovascularization. FEBS Lett 589: 1143–1149. doi:10.1016/j.febslet.2015.03.010.

8. Ryan DG, Oliveira-Fernandes M, Lavker RM (2006) MicroRNAs of the mammalian eye display distinct and overlapping tissue specificity. Mol Vis 12: 1175–1184.

9. Tian S, Huang S, Wu S, Guo W, Li J, et al. (2010) MicroRNA-1285 inhibits the expression of p53 by directly targeting its 3' untranslated region. Biochem Biophys Res Commun 396: 435–439. doi:10.1016/j.bbrc.2010.04.112.

10. Hidaka H, Seki N, Yoshino H, Yamasaki T, Yamada Y, et al. (2012) Tumor suppressive microRNA-1285 regulates novel molecular targets: aberrant expression and functional significance in renal cell carcinoma. Oncotarget 3: 44–57.

11. Liu G, Friggeri A, Yang Y, Park Y-J, Tsuruta Y, et al. (2009) miR-147, a

microRNA that is induced upon Toll-like receptor stimulation, regulates murine macrophage inflammatory responses. Proc Natl Acad Sci U S A 106: 15819–15824. doi:10.1073/pnas.0901216106.

12. Burton MJ, Rajak SN, Hu VH, Ramadhani A, Habtamu E, et al. (2015) Pathogenesis of progressive scarring trachoma in Ethiopia and Tanzania and its implications for disease control: two cohort studies. PLoS Negl Trop Dis 9: e0003763. doi:10.1371/journal.pntd.0003763.

13. Porcella SF, Carlson JH, Sturdevant DE, Sturdevant GL, Kanakabandi K, et al. (2015) Transcriptional Profiling of Human Epithelial Cells Infected with Plasmid-Bearing and Plasmid-Deficient Chlamydia trachomatis. Infect Immun 83: 534–543. doi:10.1128/IAI.02764-14.

14. Kari L, Whitmire WM, Olivares-Zavaleta N, Goheen MM, Taylor LD, et al. (2011) A live-attenuated chlamydial vaccine protects against trachoma in nonhuman primates. J Exp Med 208: 2217–2223. doi:10.1084/jem.20111266.

15. Sigar IM, Schripsema JH, Wang Y, Clarke IN, Cutcliffe LT, et al. (2013) Plasmid deficiency in urogenital isolates of Chlamydia trachomatis reduces infectivity and virulence in a mouse model. Pathog Dis: 1–9. doi:10.1111/2049-632X.12086.

16. O'Connell CM, Ingalls RR, Andrews CW, Scurlock AM, Darville T (2007) Plasmid-deficient Chlamydia muridarum fail to induce immune pathology and protect against oviduct disease. J Immunol 179: 4027–4034.

17. Derrick T, Roberts C, Last AR, Burr SE, Holland MJ (2015) Trachoma and Ocular Chlamydial Infection in the Era of Genomics. Mediators Inflamm.

18. Guzey M, Ozardali I, Basar E, Aslan G, Satici A, et al. (2000) A survey of trachoma: the histopathology and the mechanism of progressive cicatrization of eyelid tissues. Ophthalmologica 214: 277–284. doi:27504.

19. al-Rajhi AA, Hidayat A, Nasr A, al-Faran M (1993) The histopathology and the mechanism of entropion in patients with trachoma. Ophthalmology 100: 1293–1296.

20. el-Asrar a M, Van den Oord JJ, Geboes K, Missotten L, Emarah MH, et al. (1989) Immunopathology of trachomatous conjunctivitis. Br J Ophthalmol 73: 276–282. doi:10.1136/bjo.73.4.276.

21. Kantarci A, Black SA, Xydas CE, Murawel P, Uchida Y, et al. (2006) Epithelial and connective tissue cell CTGF/CCN2 expression in gingival fibrosis. J Pathol 210: 59–66. doi:10.1002/path.2000.

22. Gibson DJ, Pi L, Sriram S, Mao C, Petersen BE, et al. (2014) Conditional knockout of CTGF affects corneal wound healing. Invest Ophthalmol Vis Sci 55: 2062–2070. doi:10.1167/iovs.13-12735.

23. Kiviat NB, Wølner-Hanssen P, Eschenbach DA, Wasserheit JN, Paavonen JA, et al. (1990) Endometrial histopathology in patients with culture-proved upper genital tract infection and laparoscopically diagnosed acute salpingitis. Am J Surg Pathol 14: 167–175.

24. Kiviat NB, Paavonen JA, Wølner-Hanssen P, Critchlow CW, Stamm WE, et al. (1990) Histopathology of endocervical infection caused by Chlamydia trachomatis, herpes simplex virus, Trichomonas vaginalis, and Neisseria gonorrhoeae. Hum Pathol 21: 831–837.

25. Pastorelli L, De Salvo C, Mercado JR, Vecchi M, Pizarro TT (2013) Central role of the gut epithelial barrier in the pathogenesis of chronic intestinal inflammation: lessons learned from animal models and human genetics. Front Immunol 4: 280. doi:10.3389/fimmu.2013.00280.

26. Burton MJ, Bailey RL, Jeffries D, Mabey DCW, Holland MJ (2004) Cytokine and Fibrogenic Gene Expression in the Conjunctivas of Subjects from a Gambian Community Where Trachoma Is Endemic. Infect Immun 72: 7352–7356. doi:10.1128/IAI.72.12.7352-7356.2004.

27. Burton MJ, Ramadhani A, Weiss HA, Hu V, Massae P, et al. (2011) Active trachoma is associated with increased conjunctival expression of IL17A and profibrotic cytokines. Infect Immun 79: 4977–4983. doi:10.1128/IAI.05718-11.

28. Faal N, Bailey RL, Sarr I, Joof H, Mabey DCW, et al. (2005) Temporal cytokine gene expression patterns in subjects with trachoma identify distinct conjunctival responses associated with infection. Clin Exp Immunol 142: 347–353. doi:10.1111/j.1365-2249.2005.02917.x.

29. Hu VH, Weiss HA, Ramadhani AM, Tolbert SB, Massae P, et al. (2012) Innate immune responses and modified extracellular matrix regulation characterize bacterial infection and cellular/connective tissue changes in scarring trachoma. Infect Immun 80: 121–130. doi:10.1128/IAI.05965-11.

30. Burton MJ, Rajak SN, Ramadhani A, Weiss HA, Habtamu E, et al. (2012) Post-operative recurrent trachomatous trichiasis is associated with increased conjunctival expression of S100A7 (psoriasin). PLoS Negl Trop Dis 6: e1985. doi:10.1371/journal.pntd.0001985.

31. Agrawal T, Gupta R, Dutta R, Srivastava P, Bhengraj AR, et al. (2009) Protective or pathogenic immune response to genital chlamydial infection in women--a possible role of cytokine secretion profile of cervical mucosal cells. Clin Immunol 130: 347–354. doi:10.1016/j.clim.2008.10.004.

32. Cohen CR, Koochesfahani KM, Meier AS, Shen C, Karunakaran K, et al. (2005) Immunoepidemiologic profile of Chlamydia trachomatis infection: importance of

heat-shock protein 60 and interferon- gamma. J Infect Dis 192: 591–599. doi:10.1086/432070.

33. Wiesenfeld HC, Heine RP, Krohn MA, Hillier SL, Amortegui AA, et al. (2002) Association between elevated neutrophil defensin levels and endometritis. J Infect Dis 186: 792–797. doi:10.1086/342417.

34. Debattista J, Timms P, Allan J (2002) Reduced levels of gamma-interferon secretion in response to chlamydial 60 kDa heat shock protein amongst women with pelvic inflammatory disease and a history of repeated Chlamydia trachomatis infections. Immunol Lett 81: 205–210.

35. Wan C, Latter JL, Amirshahi A, Symonds I, Finnie J, et al. (2014) Progesterone activates multiple innate immune pathways in Chlamydia trachomatis-infected endocervical cells. Am J Reprod Immunol 71: 165–177. doi:10.1111/aji.12168.

36. Peters J, Hess S, Endlich K, Thalmann J, Holzberg D, et al. (2005) Silencing or permanent activation: host-cell responses in models of persistent Chlamydia pneumoniae infection. Cell Microbiol 7: 1099–1108. doi:10.1111/j.1462-5822.2005.00534.x.

37. Jha HC, Srivastava P, Vardhan H, Singh LC, Bhengraj AR, et al. (2011) Chlamydia pneumoniae heat shock protein 60 is associated with apoptotic signaling pathway in human atheromatous plaques of coronary artery disease patients. J Cardiol 58: 216–225. doi:10.1016/j.jjcc.2011.07.010.

38. Brigstock DR (2010) Connective tissue growth factor (CCN2, CTGF) and organ fibrosis: lessons from transgenic animals. J Cell Commun Signal 4: 1–4. doi:10.1007/s12079-009-0071-5.

39. Tong Z, Chen R, Alt DS, Kemper S, Perbal B, et al. (2009) Susceptibility to liver fibrosis in mice expressing a connective tissue growth factor transgene in hepatocytes. Hepatology 50: 939–947. doi:10.1002/hep.23102.

40. Hughes AE, Bradley DT, Campbell M, Lechner J, Dash DP, et al. (2011) Mutation altering the miR-184 seed region causes familial keratoconus with cataract. Am J Hum Genet 89: 628–633. doi:10.1016/j.ajhg.2011.09.014.

41. Yeruva L, Myers GSA, Spencer N, Creasy HH, Adams NE, et al. (2014) Early microRNA expression profile as a prognostic biomarker for the development of pelvic inflammatory disease in a mouse model of chlamydial genital infection. MBio 5: e01241–14. doi:10.1128/mBio.01241-14.

42. Gupta R, Arkatkar T, Yu J-J, Wali S, Haskins WE, et al. (2015) Chlamydia muridarum Infection Associated Host MicroRNAs in the Murine Genital Tract and Contribution to Generation of Host Immune Response. Am J Reprod Immunol 73: 126–140. doi:10.1111/aji.12281.

43. Lan W, Chen S, Tong L (2015) MicroRNA-215 Regulates Fibroblast Function: Insights from a Human Fibrotic Disease. Cell Cycle 14: 1973–1984. doi:10.1080/15384101.2014.998077.

44. Boomiraj H, Mohankumar V, Lalitha P, Devarajan B (2015) Human Corneal MicroRNA Expression Profile in Fungal Keratitis. Investig Opthalmology Vis Sci 56: 7939. doi:10.1167/iovs.15-17619.

45. Gopinathan U, Sharma S, Garg P, Rao GN Review of epidemiological features, microbiological diagnosis and treatment outcome of microbial keratitis: experience of over a decade. Indian J Ophthalmol 57: 273–279. doi:10.4103/0301-4738.53051.

46. Janssen HL, Reesink HW, Lawitz EJ, Zeuzem S, Rodriguez-Torres M, et al. (2013) Treatment of HCV infection by targeting microRNA. N Engl J Med 368: 1685–1694. doi:10.1056/NEJMoa1209026.

47. Landry JJM, Pyl PT, Rausch T, Zichner T, Tekkedil MM, et al. (2013) The Genomic and Transcriptomic Landscape of a HeLa Cell Line. G3 (Bethesda). doi:10.1534/g3.113.005777.

48. Wyrick PB, Choong J, Davis CH, Knight ST, Royal MO, et al. (1989) Entry of genital Chlamydia trachomatis into polarized human epithelial cells. Infect Immun 57: 2378–2389.

49. Guseva N V, Dessus-Babus S, Moore CG, Whittimore JD, Wyrick PB (2007) Differences in Chlamydia trachomatis serovar E growth rate in polarized endometrial and endocervical epithelial cells grown in three-dimensional culture. Infect Immun 75: 553–564. doi:10.1128/IAI.01517-06.

50. Buckner LR, Lewis ME, Greene SJ, Foster TP, Quayle AJ (2013) Chlamydia trachomatis infection results in a modest pro-inflammatory cytokine response and a decrease in T cell chemokine secretion in human polarized endocervical epithelial cells. Cytokine 63: 151–165. doi:10.1016/j.cyto.2013.04.022.

51. Wyrick PB, Davis CH, Knight ST, Choong J (1993) In-vitro activity of azithromycin on Chlamydia trachomatis infected, polarized human endometrial epithelial cells. J Antimicrob Chemother 31: 139–150.

52. Li H, Ezra DG, Burton MJ, Bailly M (2013) Doxycycline prevents matrix remodeling and contraction by trichiasis-derived conjunctival fibroblasts. Invest Ophthalmol Vis Sci 54: 4675–4682. doi:10.1167/iovs.13-11787.

53. Miyairi I, Mahdi OS, Ouellette SP, Belland RJ, Byrne GI (2006) Different growth rates of Chlamydia trachomatis biovars reflect pathotype. J Infect Dis 194: 350–357. doi:10.1086/505432.

54. Giesen C, Wang HAO, Schapiro D, Zivanovic N, Jacobs A, et al. (2014) Highly

multiplexed imaging of tumor tissues with subcellular resolution by mass cytometry. Nat Methods 11: 417–422. doi:10.1038/nmeth.2869.

Appendix

Review Article

Trachoma and Ocular Chlamydial Infection in the Era of Genomics

Tamsyn Derrick, Chrissy h. Roberts, Anna R. Last, Sarah E. Burr, and Martin J. Holland

Department of Clinical Research, Faculty of Infectious Tropical Diseases, London School of Hygiene and Tropical Medicine, London WC1E 7HT, UK

Correspondence should be addressed to Tamsyn Derrick; tamsyn.derrick@lshtm.ac.uk

Trachoma is a blinding disease usually caused by infection with *Chlamydia trachomatis (Ct)* serovars A, B, and C in the upper tarsal conjunctiva. Individuals in endemic regions are repeatedly infected with *Ct* throughout childhood. A proportion of individuals experience prolonged or severe inflammatory episodes that are known to be significant risk factors for ocular scarring in later life. Continued scarring often leads to trichiasis and in-turning of the eyelashes, which causes pain and can eventually cause blindness. The mechanisms driving the chronic immunopathology in the conjunctiva, which largely progresses in the absence of detectable *Ct* infection in adults, are likely to be multifactorial. Socioeconomic status, education, and behavior have been identified as contributing to the risk of scarring and inflammation. We focus on the contribution of host and pathogen genetic variation, bacterial ecology of the conjunctiva, and host epigenetic imprinting including small RNA regulation by both host and pathogen in the development of ocular pathology. Each of these factors or processes contributes to pathogenic outcomes in other inflammatory diseases and we outline their potential role in trachoma.

1. Introduction

Sightsavers International estimates that every 15 minutes a person loses sight as a result of trachoma [1]. As such, trachoma remains the world's leading infectious cause of blindness despite significant efforts to control and eliminate the disease [2]. Trachoma is currently considered endemic in 51 countries worldwide and only seven formerly endemic countries have reached target elimination thresholds [2]. The Alliance for the Global Elimination of Blinding Trachoma has set the goal of 2020 for the elimination of trachoma. The aim is to control trachoma through the implementation of surgery for trichiasis, antibiotics to treat infection, facial cleanliness, and environmental improvements to reduce transmission (SAFE). Currently 31 trachoma endemic countries implement SAFE, which is effective in controlling trachoma if well conducted. Azithromycin is the antibiotic of choice used in mass drug administration (MDA) programmes for trachoma control. There are additional beneficial effects of azithromycin MDA, including reduced all-cause mortality [3] and potential to reduce clinical disease through its anti-inflammatory

properties [4]. There remains a need to pursue vaccine development as there are circumstances when SAFE is poorly effective and there is uncertainty about its universal application. The lack of randomized controlled trials examining the effectiveness of the F and E components for the interruption of transmission, alongside the historical lack of molecular laboratory tools able to identify transmission events, raises questions on the basic understanding of their effectiveness. Additional concerns with the A component include the long-term use of antibiotics in populations where MDA has failed to control disease [5], introduction of resistance in other bacterial species [6], and the continued progression of scarring and trichiasis in populations where MDA has been implemented [7]. It is also not currently understood whether effective mass treatment leads to arrested immunity and it is unclear what impact the elimination of ocular chlamydial exposure in childhood might exert later in adolescent and adult urogenital disease. Chlamydiae can reside in the gastrointestinal tract in the absence of clinical disease and this has led to the suggestion that azithromycin treatment failures (at least in urogenital disease) may be because gastrointestinal

Chlamydiae are refractory to azithromycin treatment and can act as a source for autoinoculation [8, 9]. A vaccine offering effective long-term protection against disease in both ocular and urogenital chlamydial disease therefore remains desirable.

Trachoma is initiated by infection of the tarsal conjunctiva with the intracellular bacteria *Chlamydia trachomatis* (*Ct*). There are a number of classification systems for the clinical signs of trachoma. Under the WHO simplified grading system, the presence of five or more follicles on the conjunctival surface is classified as trachomatous inflammation follicular (TF). *Ct* infection is independently associated with TF (OR = 11.2 (95% CI 6.9–18.1) [10]), although this value varies between populations depending on disease sign prevalence and becomes disassociated from TF once prevalence is low. Repeated *Ct* infection in endemic communities can trigger chronic conjunctival inflammation (trachomatous inflammation intense, TI) in some individuals, causing conjunctival fibrosis (trachomatous scarring, TS). Progressive fibrosis may lead to entropion, inward turning, or misdirected lashes (trachomatous trichiasis, TT), all of which abrade the corneal surface. This abrasive damage may lead to corneal opacity (CO) and blindness. Figure 1 shows reflective *in vivo* confocal microscopy scans, histology sections, and photographs of the tarsal conjunctiva that illustrate the changes in tissue architecture that occur in the different stages of trachomatous disease.

The human trachoma vaccine trials that took place in the 1960s concluded that some short-term strain-specific protection from infection was induced, amidst concerns that pathology was exacerbated in some cases, supported by data from monkey models [13]. The data from these large placebo-controlled trials has been recently reinterpreted in the context of current grading systems and our current knowledge of disease pathogenesis. Only trial III in The Gambia recorded evidence of conjunctival scarring. Two doses of prophylactic vaccination made from two live strains in mineral oil were given three weeks apart to children aged 0–4 years. There was no protection from active trachoma; however the vaccinated group had a reduced prevalence of scarring disease two years later [14]. When all three Gambian trials are reviewed in the context of what is now known about disease pathogenesis, vaccine-induced exacerbation of disease may not be a significant concern, raising hopes that current vaccine formulations may be successful [15, 16].

2. Immunopathology of Trachoma

Despite extensive research, the mechanistic link between chronic inflammation and progressive scarring remains elusive [7]. The scarring observed in both trachoma and urogenital disease is thought to be a result of the host response to infection rather than a direct effect of the bacteria. Defining the features of protective versus pathogenic immunological responses in chlamydial disease (reviewed in [17]) is crucial to the understanding of disease and for efficacious vaccine design.

Currently, two models have been put forward to explain the immunopathogenesis of chlamydial disease: the immunological and cellular paradigms. The traditional immunological paradigm implicates the adaptive immune system.

Initial studies on chlamydial infection found that repeated infection exacerbated inflammation and that inflammatory pathology continued in the absence of *Ct*. At first, a delayed type hypersensitivity (DTH) reaction triggered by a chlamydial antigen was hypothesized. The chlamydial heat shock protein 60 (HSP60) was considered a candidate antigen to trigger DTH but was not found to exacerbate pathology when tested in a guinea-pig model [18]. Antibodies to HSP60 predicted a 2-3-fold higher risk of *Ct* pelvic inflammatory disease (PID) in humans and higher levels of antibodies specific to HSP60 were found in women with the most severe forms of urogenital disease [19]. Likewise antibodies to HSP60 were associated with tubal factor infertility (TFI) and inflammatory trachoma [20, 21]; however it remains unclear whether these antibodies cause pathology or are a result of a greater number or more severe episodes of infection. More recent screening of sera from trichiasis patients and controls detected differential patterns of antibody recognition for a number of *Ct* antigens; however HSP60 responses were not significantly different [22].

Previous research demonstrated that individuals with scarring trachoma had Th2 patterns of cytokine expression [23], whereas those with strong Th1 responses efficiently cleared infection [24]. This opposed the DTH theory and suggested that a Th2 response either was ineffectual at clearing infection or led to enhanced pathology and that CD4+ Th1 IFNγ responses were a key element of protective immunity in trachoma. Both CD8+ and CD4+ T cell infiltrates are associated with the conjunctival follicles that are characteristic of TF; however CD4+ T cells are thought to outnumber CD8+ [25]. NK cells have more recently been identified as a major early source of IFNγ in response to *Ct* [26]. Despite the primary function of CD8+ T cells in defense against intracellular pathogens, data from murine models previously found a limited role for CD8+ T cells in anti-*Ct* immunity [27]. Recent evidence in the macaque model of trachoma challenges this theory and suggests that depletion of CD8+ T cells can abrogate protective immunity [28]. Characterization of the roles of each of these cell types in chronic scarring trachoma has proved difficult to address, however, largely due to the natural history of scarring disease.

Stephens suggested an alternative model of disease [29] in which epithelial cells at the infection site play a central role as mediators of the innate immune response. Epithelial cells infected with *Ct* secrete a number of proinflammatory cytokines and growth factors, such as IL-8, GROα, IL-1α, IL-6, and granulocyte-macrophage colony-stimulating factor (GM-CSF). The secretion of these cytokines is delayed compared to the kinetics of secretion upon infection with other invasive bacteria and persists throughout the 2–4-day developmental cycle of *Ct*. The secretion of IL-1α by infected cells was shown to upregulate proinflammatory cytokine production by neighboring uninfected cells, promoting a strong inflammatory response [30]. Lymphocytes of the adaptive immune system are attracted to the infection site by the chemotactic gradient and subsequent infections include memory populations that amplify the response. *Ct* infected cells also secreted the profibrotic cytokine IL-11, a member of the IL-6 family [31, 32]. Recent evidence from a primary-like
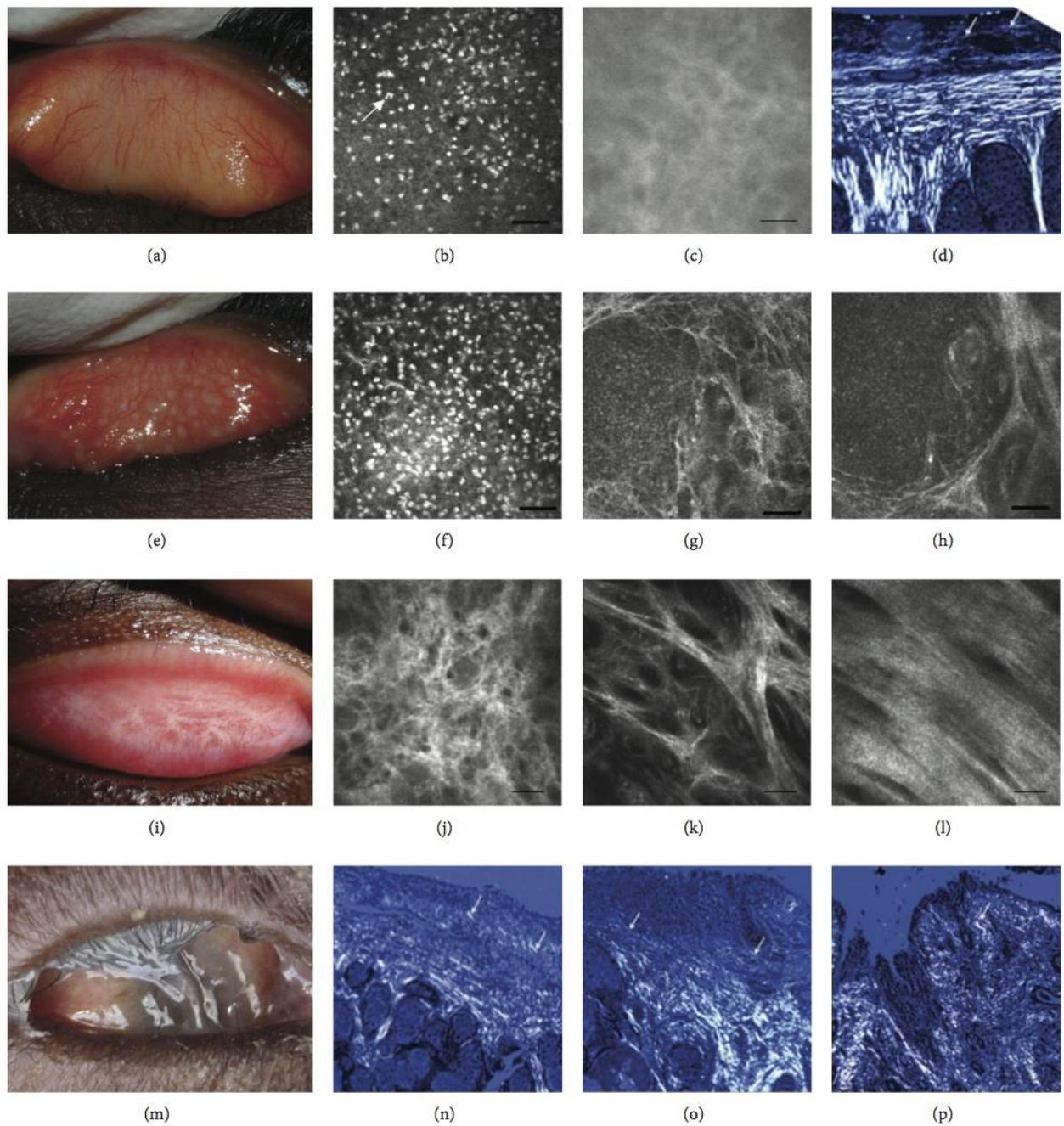
FIGURE 1: Images from a normal healthy eye (a–d) and from individuals with follicular trachoma (e–h), trachomatous scarring (i–l), and trichiasis and progressive scarring (m–p). (a), (e), (i), and (m) are photographs of the tarsal conjunctiva showing normal appearance (a), papillary inflammation and follicles (e), bands of trachomatous scarring (i), and extreme trichiasis and corneal opacity (m). (b), (c), (f), (g), (h), (j), (k), and (l) are *in vivo* confocal microscopy images of the tarsal conjunctiva at various depths (the bar represents 50 μm). A moderate number of inflammatory nuclei are present in the subepithelium of a healthy eye (b), whereas a higher number are present in trachomatous inflammation (f). Follicles can be seen in (g) and (h). The connective tissue of the healthy conjunctiva is amorphous (c), whereas successive grades of trachomatous scarring are seen as a heterogeneous clumpy appearance (j), defined tissue bands that make up <50% of the scan area (k), and defined bands that make up >50% of the scan area (l). (d) and (n–p) are histological images of tissue scarring using polarized light (original magnification ×100). In the healthy conjunctiva, collagen fibers are parallel (arrows) with the surface epithelium (d), whereas progressive disorganization of this appearance is observed in scarring (n–p). Images are kindly provided with permission from Matthew Burton and Victor Hu and are adapted from Hu et al. 2011 [11] and Hu et al. 2013 [12].

polarized epithelial cell model showed that IL-11 was secreted preferentially from the basolateral membrane and IL1ra from the apical membrane in *Ct* infected cells [33]. The T cell chemokines RANTES and IP10 were also downregulated in productively *Ct* infected cells, suggesting that *Ct* attempts to avoid stimulation of the immune response in order to maintain its intracellular niche, potentially leading to longer infections and chronic pathology [33]. Recent genome-wide scale array studies from clinical samples support Stephens's hypothesis. Expression profiling of children in The Gambia with active trachoma versus healthy controls revealed a strong upregulation of the innate immune response [34]. Along with the expected infiltration of neutrophils, lymphocytes, and the inflammatory cytokine pathways consistent with histopathology [35], the natural killer (NK) cell response was also enhanced. A transcriptome study conducted in Ethiopian adults with either trachomatous trichiasis (TT) or TT with inflammation (TTI) versus healthy controls found that despite less than 1% *Ct* infection prevalence, markers of ongoing subclinical inflammation and tissue remodeling were evident in the TT group and were more pronounced in the TTI group [36]. These markers were consistent with an activated and proinflammatory epithelium. There was a lack of evidence for a profibrotic Th2 response and a very limited Th1 response. Subsequent targeted quantitative-PCR studies have reemphasized the role of the innate immune response in trachoma in both children and adults [37, 38]. These studies found antimicrobial peptides psoriasin (*S100A7*), *DEFb4A*, and *SAA1*, inflammatory cytokines *IL17*, *IL1β*, and *TNF*, inflammatory chemokines (*CCL18* and *CXCL5*), *MMPs*, and *CTGF* were upregulated in trachomatous disease. Increased *IL17* expression was highlighted as characteristic of active trachoma and is thought to coordinate the proinflammatory response [37].

Overall these studies suggest that clearance of *Ct* infection requires an appropriate acute Th1 response with IFNγ and CD8+ T cells. They also support the case for the central role of epithelial cells in ongoing trachomatous inflammation and pathogenesis that leads to TT. This would imply that neither the cellular nor the immunological paradigm can fully explain disease but that active cross talk between cellular (innate epithelial cell responses) and immunological (adaptive immunity) systems is required.

3. Host Genetic Association Studies and Trachoma

The assumed link between immune driven inflammation and conjunctival scarring and its blinding sequelae led to the first genetic association studies which focused on immune response genes. Immune response genes located within the Major Histocompatibility Complex (MHC) drive the adaptive cellular response and initial studies focused on the association of trachomatous scarring disease with alleles in HLA class I and class II loci. The intracellular nature of chlamydial infection suggested that class I restricted CD8+ T cell responses would be important in controlling infection and that these might be related to later scarring disease. MHC class II loci would be expected to contribute by defining the profile of anti-*Ct* antibody responses and cytokines via CD4+ class II restricted T cells.

The first reported genetic association study in trachoma in Gambians [39] found evidence that a specific HLA class I serological determinant of the HLA-A2 supertype (HLA-A28) was associated with scarring trachoma (OR = 1.88, *P* = 0.046) and observed that approximately 26% of scarring cases had HLA-A28, compared to 16% of controls. HLA-A28 is made up of at least 3 molecular subtypes (HLA-A*68:01, HLA-A*68:02, and HLA-A*69:01), of which HLA-A*68:02 was thought to be the most frequent allele in Gambians. In a subset analysis of a limited number of samples from the same study, molecular typing showed that the HLA-A*68:02 allele was strongly associated with scarring trachoma (OR = 3.14, CI 1.32–7.44, and *P* = 0.009). No alleles of either of the MHC class II genes, HLA-DRB1 or HLA-DQB1, were found to be associated with scarring. Antibody responses to chlamydial HSP60 were positively correlated with the allele HLA-DRB1*07:01 (OR = 2.6, *P* = 0.02) and negatively correlated with both HLA-DQB1*03:01 (OR = 0.42, *P* < 0.001) and HLA-DQB1*05:01 (OR = 0.55, *P* = 0.046) [40]. Later studies also linked HLA class II alleles to anti-*Ct* antibody prevalence and quantity in the clinical context of sexually transmitted *Ct* infections [41, 42].

It had previously been shown that synthetic peptides based on chlamydial sequences (MOMP and HSP60) could elicit *HLA-B8* and *HLA-B35* restricted CD8+ CTL responses in peripheral blood of individuals from trachoma endemic regions [43]. In an attempt to link the observed *HLA-A*68:02 association to an effector mechanism, a follow-up study [44] investigated whether *HLA-A*68:02 restricted CD8+ CTLs or IFNγ producing cells were associated with *Ct* specific immune responses in a small number of scarring cases and disease-free controls. Peptides from 3 chlamydial antigens that were predicted to bind HLA-A*68:02 were used to stimulate cells but no chlamydia-peptide specific responses were detected. This led the authors to suggest either that the peptides that were chosen did not represent natural epitopes or that *HLA-A*68:02 restricted CD8+ T cells were not important mediators in ocular disease. An alternative experimental approach and one that did not require *in vitro* restimulation used *HLA-A2*-MOMP tetramers and found that increased frequencies of CD8+ tetramer positive cells were coincident with current ocular *Ct* infection and longer durations of infection [45]. Effector functions of these cells were not investigated but it was noted that the tetramers used to identify cells also bound to the TCR of HLA-A28 restricted T cells. This supported a model under which the HLA-A*68:02 allele might contribute to scarring disease via prolonged or chronic ocular infections.

Outside of trachoma, antichlamydial CD8+ MHC class I restricted cells have been clearly demonstrated in murine models [46] and in humans exposed to urogenital infections [47]. Recently there has been a resurgence of interest in the importance of CD8+ MHC class I restricted T cells, following work in a murine model of urogenital disease [48] and in vaccinated monkeys [49]. Following vaccination with the plasmid-free attenuated strain of *Ct*, monkeys with a common MHC class II haplotype (M1) were protected from virulent ocular challenge. Subsequent work found that protection was mediated through CD8+ T cell recognition of soluble

chlamydial antigens [28] and not through class II restricted CD4+ T cells. Most recently, an immune-proteomic screening approach in mice showed that only a small percentage (~3%) of the *Ct* proteome is processed for presentation by MHC class II molecules. *Ct* proteins that were processed were the expected immunodominant proteins such as MOMP, PmpE, PmpF, and PmpG and were presented on a wide range of I-A and I-E MHC haplotypes [50]. The immunogenicity of these proteins was also subject to both MHC class II selection and chlamydial peptide sequence diversity. Overall, this suggests that studies of sufficient size and power to account for the high degree of polymorphism and small effect size are required to further investigate HLA class II disease susceptibility. Overall, reports of associations between human MHC polymorphisms and chlamydial infection and disease have been inconsistent and have not identified a specific causal pathway. Collectively these studies do suggest an important but complex role for the MHC in chlamydial host resistance and disease.

Following the early MHC class I and class II genetic association studies in Gambians, a trachoma-HLA association study was conducted in Omanis using a serologically based typing system. This found some evidence of association between TT and the HLA class II DR16 and DR53 antigens [51]. Further studies in Tanzanians [52] found that trichiasis was less common in women carrying *HLA-DRB1**11 alleles (OR = 0.48, CI 0.26–0.90, and P = 0.02) and more common in those carrying *HLA-B**07 (OR = 3.26, CI 1.42–7.49, and P = 0.004) or *HLA-B**08 (OR = 5.12, CI 1.74–15.05, and P = 0.001). More recently, a much larger study in Gambian families also highlighted the association between *HLA-B**08:01 alleles and scarring [53], but analysis based on current knowledge of the HLA system would suggest that HLA-B*08:01 could be a proxy marker for the HLA-C epitope of the Killer Cell Immunoglobulin-like Receptors (KIRs). This epitope is defined by a dichotomous amino acid polymorphism at position 80 of the HLA-C heavy chain [54]. HLA-C alleles carry Asn^{80} and are designated C1 whilst those with Lys^{80} are C2. The HLA-C KIR epitope determines which KIR can bind the ligand, with KIR2DL1 binding to HLA-C2 and both KIR2DL2 and KIR2DL3 binding to HLA-C1 [55–57]. KIR are a polymorphic family of membrane-bound immune-receptors found on natural killer (NK) cells [58–60], where they are usually considered to control the licensing [61] and responsiveness [62, 63] of the NK cytotoxic immune response. KIRs are also present on NK-T cells and T cells [64, 65], though the functional contribution of KIRs to T cell reactivity is relatively less well studied [66, 67]. The finding that HLA-C2 was a significant predictor [53] of increased risk of scarring in Gambian families (OR$_{C1/C2}$ = 2.29, $P_{C1/C2}$ = 0.0061 | OR$_{C2/C2}$ = 3.97, $P_{C2/C2}$ = 0.0004) further suggested a role for NK cells in trachomatous scarring. Epistatic effects were observed since KIR (Chromosome 19) genotype modified the risk of scarring depending on HLA-C (Chromosome 6) genotype; HLA-C2 showed additive gene dosage effects and individuals carrying both *KIR2DL2* and *KIR2DL3* had the highest relative risk (OR$_{C1/C2}$ = 2.33, $P_{C1/C2}$ = 0.1 | OR$_{C2/C2}$ = 5.95, $P_{C2/C2}$ = 0.0025). NK cells are likely to be important in the initial host response to ocular challenge,

since it has been shown that they are the main cellular source of IFNγ in response to *in vitro* elementary body stimulation [26]. There was no evidence in the study of scarring trachoma in Gambian families that the previously identified *HLA-A**68:02 allele was associated with early scarring (P = 0.27).

MHC class I and class II association studies were also extended into class III loci. A polymorphism in the tumour necrosis factor (*TNF*) promoter region was found to associate with scarring under an additive model (OR$_{A/G}$ = 1.59, OR$_{A/A}$ = 3.4, and P = 0.03) [68]. Whilst scarring disease was also associated with increased detection of TNF protein in tear fluid (OR$_{add}$ = 2.5, P = 0.013), TNF levels in the tear fluid did not associate with the genotypes of the TNF-308 polymorphism. A later study of trichiasis patients and controls found an association between TNF-308A and disease, which was significant under a dominant, rather than additive, genetic model (OR$_{dom}$ = 1.52, P = 0.016) [69]. These later data also suggested evidence for heterozygote advantage (OR$_{A/G}$ = 1.48, P = 0.048 | OR$_{A/A}$ = 1.11, P = 0.12) in the context of a simple genotype model; however adjustments for multiple testing were not included. Lymphocytes from TNF-308A individuals had increased TNF secretion *in vitro* in response to challenge with *Ct* elementary bodies. Curiously, the TNF-308A polymorphism has also been identified [70] as a protective factor in trichiasis (OR$_{A/G}$ = 0.45 [0.25–0.81], P = 0.008 | OR$_{A/A}$ = 0.19 [0.04–1.08], P = 0.062) in a study that also identified homozygosity at a lymphotoxin alpha (LTA) polymorphism (LTA252 OR$_{A/A}$ = 0.25 [0.09–0.63], P = 0.004), heterozygosity at an Interleukin 9 polymorphism (IL9-T113M OR$_{C/T}$ = 0.25 [0.1–0.64], P = 0.004), and heterozygosity at the vascular cell adhesion molecule 1 (VCAM1, OR = 0.47 [0.25–0.86], P = 0.015) as protective factors for trichiasis [70]. The same authors suggested that epistasis between the polymorphisms was potentially key to unraveling the host genetic background of trachoma. TT risk increased substantially (OR = 13.5, P = 0.001) when the TNFA (-308G), VDR (intron G), IL4R (50 V), and ICAM1 (56 M) polymorphisms were considered as genetic constellations under a "logic regression" model [70], but the number of samples contributing to this analysis was small (controls n = 232 and TT n = 135).

A series of studies used SNP genotypes and linkage disequilibrium data to predict haplotypes and then carried out haplotype based association tests in genes including *IFNγ* [71], *IL8* [72], *IL10* [71, 73], haptoglobin (*HP*), *GM-CSF2* [72], and matrix metalloproteinase 9 (*MMP9*) [74]. The *MMP9* gene is consistently differentially expressed between cases and controls of several stages of trachomatous disease [34, 36]. A study of the *IL8/CSF2* loci [72] also noted some evidence for epistatic interactions between polymorphisms in *MMP9* and each of the *IL8* and *CSF2* genes. Other epistatic interactions were also found in the same dataset, in particular, an *MMP9-IL10* interaction (Figure 2). In the analysis of a cohort of 651 scarring case-control pairs, main effects for the *IL10-1082* allele were null; however interaction between *IL10*-1082 and *MMP9* Q279R contributed to risk. The protective effects of the *MMP9* Q279R G allele were transformed to risk in the copresence of a SNP (*IL10*-1082) tagging the trachoma risk haplotype (*IL10*-3575A~*IL10*-1082C~*IL10*-592G~*IL10*+5009G).
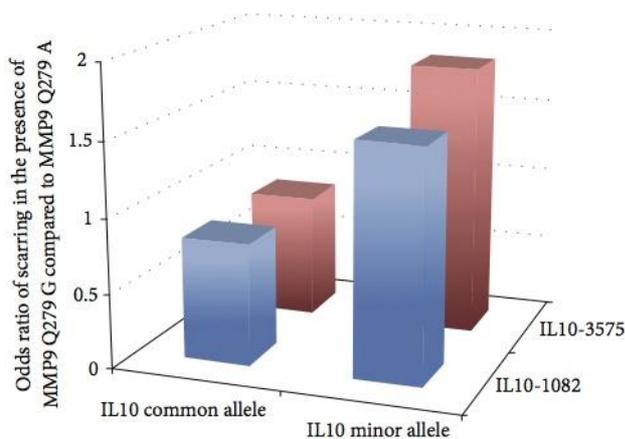
FIGURE 2: Evidence for MMP9-IL10 epistasis in Gambians with trachomatous scarring. The protective effect of *MMP9* allele (Q279R) is modulated by host genetic background at the *IL10* locus such that protective effects of the G allele are lost in the presence of either of 2 minor frequency risk alleles (*IL10*-1082C or *IL10*-3575A). The interaction between these nonallelic genes (or risk genotypes) has a dominant effect over other combinations. The interaction between risk genotypes was examined by conditional likelihood ratio tests (LRT) (main effects) log p/1 − p = a + b (SNP1) + c (SNP2). Interaction terms were defined as Log p/1 − p = a + b(SNP1) + c(SNP2) + d(SNP1∗SNP2) and when significant identified statistical epistasis. This approach was applied to 651 Gambian case-control pairs of TS. The *MMP9* Q279R and *IL10*-3575 loci showed strong evidence for statistical interaction affecting risk of TS (LRT χ^2 = 7.23, P = 0.007). Carriers of the (protective) *MMP9* Q279R G allele who also had the *IL10*-3575A minor allele were at significantly increased risk of TS (OR = 1.83 (1.06–3.19)) when compared to subjects with the *IL10*-3575 T allele (common allele) (OR = 0.84 (0.69–1.02)). The *IL10*-1082 C minor allele in combination with the *MMP9* Q279R G allele had an increased risk of TS (OR = 1.51 (1.02–2.24)) relative to IL10-1082 C in the presence of the *MMP9* Q279R A allele (OR = 0.82 (0.67–1.01)) (LRT χ^2 = 7.53, P = 0.006 for the interaction between the *IL10*-1082 and *MMP9* risk alleles). Interaction between *IL10*-1082 and *MMP9* Q279R affects risk despite the null single SNP main effect for *IL10*-1082 [71]. The individually protective *MMP9* Q279R G allele was therefore associated with an increased risk of scarring in the presence of *IL10* risk alleles (*IL10*-1082C or *IL10*-3575A minor alleles) and a decreased risk in the presence of common *IL10* (protective) alleles. Similar modelling at other loci previously investigated in this cohort (IFNγ-1616, +3234; LTA -252, +77; IkBL -63; IL-8 -251; GM-CSF2 27348, 27438) showed significant or marginally significant evidence for two-way interactions, at the genotype or allelic level, with the MMP9 Q279R SNP. Some of these SNPs are in high LD and therefore not all the hypotheses tested are independent. The existence both of LD between loci and of potential biological interdependence between loci raises methodological difficulties in correction for multiple testing. We did not attempt any correction for multiple testing: and therefore a contribution of chance to these results is difficult to exclude as we point out in the main text. Comparing main and additional two-way epistatic effects in the final model suggested that the inclusion of interaction terms improved the fit of the model to the data, so that the final best model included both main and epistatic effects. For TS this model suggested that two-way interactions of *MMP9*-Q279R with *IFNγ*-1616, *IFNγ*+3234, *IL10*-1082, *IL8*-251, *LTA*+77, *LTA*-252, and *IkBL*-63 improved the fit of the model (data courtesy of Natividad, Mabey, Holland, and Bailey).

This allele or haplotype is associated with higher levels of *IL10* transcription [73]. This may suggest that premature or excessive downregulation of MMP9 activity by IL-10 ultimately increases risk. Each of these studies suffers from limited sample size and large numbers of parallel statistical tests under several different genetic models, whilst sometimes also considering multiple phenotypes (i.e., scarring and trichiasis). Consequently the results should be interpreted in the context of potential type I and type II errors.

The candidate gene approach has helped reinforce current lines of investigation but has yet to resolve the paradigm of the cellular versus immunological hypotheses or generate new avenues of investigation into the basic biology of chlamydial ocular disease. A genome-wide association scan (GWAS) is an alternative to the candidate gene method and provides an opportunity to generate new hypotheses in an unbiased manner. GWAS requires much larger sample sizes than have been previously described in trachoma and chlamydial urogenital disease and has its own limitations, particularly when applied to samples from African populations [75]. There are also relatively few GWAS in infectious disease [76]. The West African malaria GWAS is perhaps a cautionary example [77]. The study showed that SNP markers in very close proximity to the well-characterized causal SNP (rs334) of the "sickle-cell trait" protective effect failed to reach genome-wide significance, even though the study was well powered. This was largely due to the low degree of linkage disequilibrium (LD) between SNPs in African populations. The rs334 SNP, when directly genotyped, was highly significant ($P = 1.3 \times 10^{-28}$), whilst the best marker in the GWAS SNPs ($P = 3.9 \times 10^{-7}$) did not reach genome-wide significance. The use of more densely populated GWAS SNP arrays and imputation methods can increase the likelihood of finding significant SNPs [78], but imputation is essentially dependent on LD structures and the imputation of rs334 in the malaria GWAS was far less effective ($P = 4.5 \times 10^{-14}$) than direct genotyping of the locus [77]. GWAS in African populations are less likely to directly identify SNPs or alleles in association with disease than equivalently sized studies in other populations. Therefore the utility of a trachoma GWAS will most likely be in prioritizing the best candidates and biologically plausible pathways. The small effects of numerous polymorphisms in functionally linked networks potentially have much greater contribution to disease when tested *en masse*. Several groups are currently pursuing genome-wide approaches to the understanding of the host genetics of chlamydial diseases, either in human clinical populations of pelvic inflammatory disease [79], trachoma [80], and advanced recombinant inbred mouse models [81] or in "cellular GWAS," which uses *in vitro* infection of extensively genotyped host cell lines [82, 83]. The potential power of a pathway-focus in genome-wide studies is evident from the preliminary reports in trachoma [80] and a mouse model system [81], both of which emphasize the importance of G-protein coupled receptor signaling pathways in disease processes relating to chlamydial infections.

4. Chlamydial Genomics and Pathogenesis

Initial single gene, multilocus sequence typing, and subsequent whole genome sequencing (WGS) of chlamydial species have provided insight into the processes involved in

chlamydial pathogenesis. The first fully sequenced *Chlamydia trachomatis* genome was a laboratory reference strain (D/UW-3/Cx) passaged in the laboratory for more than 30 years after its initial isolation from a cervical swab in 1965. The genome was completed by shotgun sequencing using highly purified *Ct* genomic DNA obtained by bulk culture to produce sufficient genomic DNA to generate the M13 linker-adaptor library. More than 28,000 sequencing reactions using dye-labeled primers and almost 4,700 dye-terminator reactions were required to complete the genome [84]. Ten to twelve years later, the first ocular chlamydial genomes were fully sequenced prior to the wide scale introduction of next generation sequencing (NGS) [85, 86]. Comparative genomic analysis of these and subsequent chlamydial isolates demonstrated overall similarity in gene content and order across biovars and between chlamydial species [87–90]. This high level synteny is correlated with the extent of evolutionary divergence [90]. Application of NGS technologies has rapidly advanced and expanded our understanding of chlamydial comparative and evolutionary dynamics. Recent WGS analysis demonstrated that there is extensive recombination within and between biovars [91] (also noted in other studies [92, 93]) and that there is evidence for genetic exchange and recombination within the cryptic plasmid [91]. This has challenged our knowledge of chlamydial diversity and highlighted the implications of recombination in pathogenesis. Other significant advances including genetic manipulation of Chlamydiae [94, 95], mutagenesis studies [95–98], and axenic culture [99] facilitate the study of chlamydial metabolism and physiology in the context of genetic studies. Novel presequencing enrichment techniques such as immunomagnetic separation and DNA-baiting techniques (SureSelect) have removed technical barriers to obtaining WGS data directly from clinical specimens [100, 101]. Moreover, the ability to obtain WGS data directly from clinical samples without the need for culture obviates the problem of *in vitro* propagation and subsequent loss of genomic diversity reflecting differences between *in vitro* and *in vivo* evolutionary environments, as has been demonstrated in *Ct* [102–104] and herpesvirus species (Varicella Zoster Virus and *Cytomegalovirus*) [105, 106]. This allows the study of genetic variants associated with disease, including those under positive selective pressure through interaction with the host. Direct and targeted deep resequencing has also enabled discovery of mixed infections within seed stocks of cultures and from clinical isolates [104, 107]. Putative virulence factors identified through WGS analysis and *in vitro* and animal studies include the polymorphic outer membrane protein family (Pmps) [84, 108–110], type three secretion system (T3SS) and effectors [111–113], genes involved in tryptophan [114–116] and glycogen [94, 117] biosynthesis, members of the *incA* [118, 119] and phospholipase-D [120, 121] families, genes from the heat shock protein family [122, 123], the chlamydial cytotoxin [124], and plasmid-encoded genes implicated in the regulation of chromosomal virulence factors [97, 125, 126].

Pmps appear to fulfill several biological functions, but the full extent of their role is not entirely clear. These exported bacterial proteins have been shown to function as autotransporters within the chlamydial outer membrane [127–129]. Several chlamydial Pmps have been detected on the chlamydial elementary body surface [127]. Some are strongly immunogenic and elicit a proinflammatory response [127]. They may play a role in virulence regarding modulation of inflammation and adherence to and invasion of host cells [129].

The chlamydial plasticity zone (PZ) is the site of extensive genomic variation between the chlamydial serovars [88, 90]. The PZ contains a toxin whose function is thought to involve GTPase inactivation and guanylate binding protein neutralization resulting in interferon gamma (IFNγ) resistance [124, 130, 131]. IFNγ stimulation of cells *in vitro* and *in vivo* induces transcription of genes that cooperate to eliminate intracellular bacteria, suggesting that inhibition of this mechanism may contribute to the pathogenesis of chlamydial disease [131]. The genomic organisation of the cytotoxin varies such that oculogenital strains have a single gene with a large deletion and lymphogranuloma venereum (LGV) strains lack the gene entirely, whilst the closely related *C. muridarum* (*Cm*) has three intact copies [132, 133]. This most likely reflects the IFNγ evasion mechanism employed by *Cm* in the mouse compared with that employed by urogenital strains in humans [133]. Since ocular strains lack a functional *trp* operon and only have a partial toxin, how they evade IFNγ is not fully understood. The membrane attack complex/perforin protein (CT153) and members of the phospholipase-D (PLD) family are also encoded within the PZ [90]. The PZ PLDs are present in *Ct* [120] and other Chlamydiaceae [87, 134, 135]. These proteins are known to modify lipids and membranes and may be secreted and localize to the inclusion membrane [121]. Reactivation of *Ct* from an IFNγ-induced persistent state is blocked by primary alcohols (potent PLD inhibitors), implying a role for PZ PLDs in this process [136].

Genomic analysis has shown that many Inc proteins are produced by each chlamydial species and several are produced early in development. Inc proteins, which are T3SS effector proteins, may be important antigens in cell-mediated immune responses following infection. IncA has been defined as an effector protein proposed to mediate inclusion fusion in *Ct* [118, 119]. IncA proteins exhibit an innate ability to form vesicles and enter the membrane of intracellular compartments [137]. A recent study of the Inc-human "interactome" using affinity-purification mass spectrometry identified that 38/58 Incs interacted with human proteins [138]. Many of the host targets were also targeted by viral proteins implying conserved mechanisms of intracellular pathogenesis. IncE bound to components of the retromer, which restricted chlamydial growth [138].

Work on the chlamydial T3SS [112] in combination with the advent of WGS demonstrated that a family of chlamydial proteins that localize to the inclusion membrane during intracellular growth were a candidate T3SS [111]. This system is important in bacterial pathogenesis and is essential for virulence of a number of bacterial species [139]. In most of these pathogens, the structural and effector genes are located on distinct pathogenicity islands [140]. In Chlamydiae, these genes are scattered across a number of operons and use a sigma factor for constitutive gene expression, suggesting that additional activators or repressors are required if components

of the T3SS are developmentally regulated [113]. Given the intracellular existence of Chlamydiae, these T3 secreted products are likely to be important in pathogenesis.

The chlamydial plasmid has been shown to function as a virulence factor in animal models [49, 141]. Phenotypic differences vary between plasmid-cured and wild-type strains with respect to infectivity, glycogen accumulation, induction of inflammation, and activation of toll-like receptor pathways [117, 142]. Plasmid deletion mutagenesis studies showed that deletion of the plasmid-encoded *pgp4* gene results in an *in vitro* phenotype identical to that of a plasmid-free strain [97]. Bacterial transcriptome analysis found a decrease in transcript levels of a subset of chromosomal genes in a naturally occurring plasmid-free strain of *Ct*, demonstrating that the plasmid is a transcriptional regulator of virulence-associated genes [125]. Maintenance of the plasmid at the relatively low copy number of 5-6 plasmids per genome [143] carries inherent risk of plasmid-loss during cell partition [144], but naturally occurring plasmid-free strains are rare [145–147]. This suggests that 5-6 plasmid copies may maximize infectivity or intracellular survival whilst provoking minimal host immune response. Recent host transcriptome studies suggest that the plasmid may stimulate host cell expression of PD-L1, which induces programmed cell death in immune effector cells [48, 148]. The plasmid is clearly strongly selected for during successful infection or transmission [142] and recent studies have shown that a plasmid-cured *Ct* strain is less virulent in ocular infection of macaques and can function as a live attenuated vaccine [49].

The ability to obtain WGS data directly from clinical samples enables a genome-wide approach to investigate associations with disease phenotype and chlamydial load in naturally occurring *Ct* infections. Pathogen GWAS studies are a powerful tool to assess the association between a SNP or locus and defined phenotypes. It has also been shown to be a robust approach for discovering novel loci of interest in other bacterial pathogens [149, 150]. A small number of bacterial GWAS have revealed pathogen genetic associations with host adaptation in *Campylobacter jejuni* and *Escherichia coli* [151], drug resistance in *Mycobacterium tuberculosis* [152], methicillin-resistant *Staphylococcus aureus* (MRSA) [153], and *Streptococcus pneumoniae* [154] and resulted in the identification of virulence loci in methicillin-resistant *Staphylococcus aureus* [149]. Rapid advances in WGS techniques will enhance our understanding of chlamydial biology and diseases pathogenesis.

5. Bacterial Ecology of the Conjunctiva and Trachoma

Persistent, severe inflammation is associated with conjunctival scarring yet *C. trachomatis* is rarely detected in the eyes of adults with disease signs [7]. This has led to the suggestion that the inflammation seen in trachomatous disease is driven, at least in part, by nonchlamydial pathogens and there is now a growing evidence to support this hypothesis [155].

Studies carried out in The Gambia in the early 2000s found that whilst viable bacteria, including *Staphylococcus aureus* and *Streptococcus* species, could be cultured from the eyes of healthy controls, bacterial infection was more frequently identified in the eyes of cases with trachomatous trichiasis [156]; *Streptococcus pneumonia* was the dominant pathogen isolated. In trachoma endemic communities in Tanzania, individuals with TS have been shown to be more frequently infected with *Streptococcus pneumoniae*, *Haemophilus influenzae*, coagulase-negative *Staphylococcus*, and *Corynebacterium* species than individuals with normal conjunctivae [155]. Similar findings have been reported in Ethiopians where comparison of the bacterial flora of conjunctivae with trachomatous trichiasis versus trachomatous scarring revealed increased frequency of isolation of *Streptococcus pneumoniae*, *Haemophilus influenzae*, coagulase-negative *Staphylococcus*, *Corynebacterium*, and viridans streptococci species [157].

More recent studies have examined the presence of viable bacteria in the eyes of children in regions of Tanzania and The Gambia where there is a low prevalence of clinical signs of active trachoma with correspondingly low levels of ocular *C. trachomatis* infection. In both studies, children with TF were more likely to have nonchlamydial bacteria in their eyes, namely, *Streptococcus pneumoniae* or *Haemophilus influenzae*, than children who had no clinical signs of disease [158, 159]. In the Tanzanian studies, culture of these nonchlamydial bacterial infections was associated with increased host conjunctival expression of *IL17A*, *CXCL5*, *CCL18*, and *KLRD1* [37]. Of these, *IL17A*, *CXCL5*, and *CCL18* were also associated with follicular and papillary inflammation.

The suggestion that nonchlamydial bacterial infection of the eye contributes to the maintenance of an inflammatory state that drives the scarring process is further supported by immunological studies. In Tanzania, a study of individuals with TS in the absence of TT found that nonchlamydial bacterial infection was associated with increased expression of *INDO*, *S100A7*, *DEFB4A*, and *MMP12* and decreased expression of *MMP10*, *SPARCL1*, and *CFH* [38]. Clinical inflammation, which is consistently identified as a major risk factor for progressive scarring, was associated with increased *INDO*, *IL1B*, *DEFB4A*, *CXCL5*, *MMP7*, *MMP9*, *MMP12*, and *CD83* and decreased *MMP10*, *SPARCL1*, and *CFH*. Data from longitudinal studies on recurrent trichiasis in The Gambia have indicated that bacterial infection, particularly with *Streptococcus pneumonia*, and clinical inflammation are associated with recurrence following surgery [160]. Clinical inflammation and nonchlamydial bacteria were also associated with increased expression of *IL1B* and *MMP9* in this cohort [161].

The isolation, often at high loads, of bacteria such as *Streptococcus pneumoniae* from the eyes of individuals with trachoma may suggest that colonization exacerbates clinical signs of the disease or, alternatively, that those with conjunctival inflammation are more susceptible to colonization and conjunctival scarring. Findings indicating increased numbers of what are largely regarded as commensal bacteria (such as coagulase-negative staphylococci and *Corynebacterium* species) in trachomatous eyes are also of particular interest, as alterations or dysbiosis of the microbiota could be a contributing factor to disease.

The study of the "normal" or indigenous microbiota that colonizes the human body has seen huge advances in

the past decade with the application of NGS techniques that enable the identification of viral, fungal, and bacterial species. These methods have been particularly useful in the identification of noncultivable bacteria directly from clinical samples. These techniques have been perhaps best utilized to describe the microbiota of the human gastrointestinal tract and, in particular, changes in the microbiota associated with inflammatory disease including inflammatory bowel syndrome and Crohn's disease. Biopsied intestinal tissue that is inflamed tends to have reduced bacterial species diversity and altered species composition as compared to tissue taken from healthy controls [162–164]. The species composition of the microbiota has also been found to play an important role in the health of the epithelial barrier via induction and maintenance of IL-17, IL-22, and regulatory T cells [165–167].

In the female genital tract, dysbiosis of the microbiota (characterized by decreased numbers of lactobacilli and polymicrobial overgrowth of anaerobic bacteria) is associated with bacterial vaginosis. This and other alterations in the vaginal microbiota are thought to be risk factors for reduced fertility [168]. While the mechanism behind this is not yet clear, bacterial vaginosis has been associated with elevated cervical levels of IL-1β and IL-8, leading to the suggestion that the induction of proinflammatory cytokines by the altered vaginal microbiota is an unrecognized cause of infertility [169].

At present, the metagenome of the ocular surface has not been characterized and, to date, only a handful of studies have applied NGS techniques, namely, deep-sequencing of the 16S rRNA gene, to the characterization of the conjunctival microbiota. A study of four healthy American volunteers described a "core" conjunctival microbiota consisting of *Pseudomonas, Propionibacterium, Bradyrhizobium, Coryne-bacterium, Acinetobacter, Brevundimonas, Staphylococcus, Aquabacterium, Sphingomonas,* and *Streptococcus* species [170]. In contrast, the core members of the conjunctival microbiota of a West African population were identified as *Corynebacterium, Streptococcus, Propionibacterium, Bacillus,* and *Staphylococcus* species [171, 172]. Amongst ophthalmologists and microbiologists, these results have been questioned since the traditional view regards the ocular surface as a sterile site of low biomass. This view is not confined to those studying the ocular surface; there are many parallels with those investigating the lung microbiome where there was initial resistance to the concept that the lung was not a "sterile" environment but in fact that healthy lung harbors a complex community of bacteria [173].

Later studies on the conjunctival microbiota in Gambians with trachoma used a case-control study design with and without trachomatous disease (TF, TS, and TT) [172]. In common with other pathologies of the mucosal epithelia, this study found a disequilibrium of the normal flora, as defined by the decreased richness (number of genera) and diversity (number of genera and their abundance within the community) associated with clinical signs of TS and TT when compared with those with healthy eyes [172]. The decrease in bacterial diversity seen in individuals with TS was largely driven by an increase in *Corynebacterium* species in those with trachomatous disease, which is consistent with earlier

studies characterizing the bacterial profile of the eye using culture techniques. The ocular microbiota of children was found to have greater richness and diversity in comparison to that of adults. While few significant differences were found in the microbiota of children with follicles versus normal controls, the microbiota of one child with clinical inflammation was dominated by *Haemophilus* species again pointing to the potential role of nonchlamydial bacteria in driving inflammation.

One drawback of the 16S rRNA gene sequencing approach, particularly in low biomass samples such as conjunctival swabs, is the potential for contamination from environmental sources and the inability to distinguish between viable and nonviable bacteria. Low biomass samples also currently preclude WGS approaches that would facilitate more a complete characterisation of the bacterial species and the full metagenome (archaea, fungi, and viruses). Using 16S-amplicon sequencing, it is difficult to distinguish those bacteria that actively colonize the conjunctival surface from those that are transiently introduced into this niche [172]. Primer-bias, which can lead to misrepresentation in the population [174], and bias introduced by sequencing depth, which limits the ability to characterise those bacteria that comprise the minority of the population [175], are also limitations of the 16S sequencing approach. As a result, there have been attempts to develop methods that might distinguish viable from nonviable bacteria before entry into the sequencing pipeline, such as the introduction of a DNase I predigestion [176], or the use of community transcriptomics to identify expressed bacterial components.

Culturomics is a relatively new field that couples high-throughput culture with matrix-assisted laser desorption ionization time-of-flight mass spectrometry (MALDI-TOF MS) identification and is a technique that may provide further means of addressing some of these issues. Studies of the gut microbiota have developed culturomics to identify bacterial species never before associated with the human gastrointestinal tract as well as novel species not previously described [177, 178]. As this technique targets viable cells, it is less prone to artefacts resulting from bacterial DNA contamination. The technique has also been used to establish cell-free *Chlamydia trachomatis* culture, using radiolabelled amino acids to demonstrate metabolic activity [99]. Culturomics therefore offers the potential to close the gap between 16S-amplicon sequencing and traditional microbiological culture [177, 179].

New applications of NGS continue to evolve in infectious disease immunology and the study of the role of the microbiota and specific microorganisms. One such technique is IgA-SEQ, a method that utilizes flow cytometry based sorting to separate bacteria coated with IgA from noncoated bacteria in a complex sample. The sorted fractions are then analysed by 16S-amplicon sequencing to identify the bacteria. In two recent studies, IgA-coated intestinal bacteria identified from human volunteers suffering inflammatory bowel disease and impaired gut-barrier function were cultured. These cultures were then able to induce intestinal inflammation in germ-free mice [180, 181]. These findings suggested that those bacteria that are able to penetrate the mucin barrier are more likely

to stimulate an immune inflammatory response. The IgA-SEQ method thereby provides an elegant means of identifying and isolating those bacteria within the microbiota that drive disease.

The application of sophisticated techniques to the study of the conjunctival microbiota may offer better opportunities to distinguish bacterial colonizers from bystanders as well as identifying those bacteria that stimulate the immune responses that drive inflammation and the scarring process. The analysis of metagenomic data alongside host transcriptome arrays may also aid in this search; unraveling the interactions between the conjunctival microbiota and the gene expression networks and pathways of inflammation that lead to fibrosis is key to further understanding of microbiota-host interactions in scarring disease.

6. Epigenetics and Chlamydial Infection

One possible explanation for the chronic inflammation and continued presence of active disease signs in populations once ocular *Ct* infection has been controlled is epigenetic change of the host cell state. "Epigenetics" describes changes in gene expression that are heritable through cell division, without alteration to the DNA sequence itself. These changes can be applied directly to DNA (CpG methylation), to the proteins DNA is packaged around (chromatin modifications such as histone methylation or acetylation), and to the transcribed message (microRNA mediated silencing).

Bacteria and infection-induced inflammation are both known to induce epigenetic changes in host cells, particularly to genes in the MAPK, NFkB, and IFNγ signaling pathways, all of which are integral to the immune response (reviewed in [182]). *Helicobacter pylori* induces genome-wide aberrant hypermethylation of DNA in the gastric mucosa of pediatric and adult samples [183]. In particular, methylation of E-cadherin (and its downregulation, which is a characteristic of epithelial-mesenchymal transition (EMT), discussed further below) is induced by *H. pylori* infection via IL-1β stimulation of NFkB, resulting in nitric oxide production and activation of DNA methyltransferases [184]. In a similar manner, the Bacille Calmette-Guerin (BCG) vaccine induces long-lasting and nonspecific increases in cytokine expression in human monocytes via NOD2-dependent histone methylation of H2K4me3 [185]. *Chlamydia* encode SET (suppressor of variegation-enhancer of zeste-trithorax) domain proteins, which function as methyltransferases [186]. *Ct* encodes nuclear effector (NUE), a SET domain histone methyltransferase which is secreted through the T3SS and shows activity toward histones H2B, H3, and H4 in the host cell nucleus [187]. As of yet, the targets and function of NUE in the host remain to be identified. Humphrys and colleagues found that a number of host genes encoding histones were differentially expressed at 1 hour after infection, perhaps reflecting an early modulatory effect of *Ct* infection on the host epigenetic profile [188]. It is tempting to speculate that *Ct* stimulation of pathogen recognition receptors may induce CpG or histone methylation changes, or in fact that *Ct* may directly induce host histone changes via NUE, causing an abnormal state of chronic inflammation in the conjunctival epithelium.

7. The Role of Small RNAs in Chlamydial Disease

Only 20% of transcription across the human genome is associated with protein-coding genes [189] and it has become clear that many of the non-protein-coding RNA species that are transcribed have important regulatory roles. These noncoding RNA species include microRNA (miRNA), short interfering RNA (siRNA), piwi-interacting RNA (piRNA), small nucleolar RNAs (snoRNA), other small RNAs, and long noncoding RNA (lncRNA (>200 nucleotides)).

miRNA encoding sequences make up only around 2% of the human genome but are estimated to regulate >60% of protein-coding genes [190]. miRNA (miR) are short (18–22 nucleotides) single stranded sequences of RNA. miR regulate gene expression through binding to complementary messenger RNA (mRNA) sequences in the cytosol in association with Argonaute proteins, forming a RNA-induced silencing complex (RISC), leading to inhibition or degradation of the target mRNA [191]. The "seed sequence" of the miR, nucleotides 2–7 from the five prime ends, guides target selection [192]. Half of known miR are found in polycistronic units and are expressed in parallel, often sharing structure and function [193, 194]. Due to flexibility in binding complementarity, an individual miR can target hundreds of different genes and a gene might be targeted by many different miR [194], forming a complex network of regulation. Abnormal expression of miR may occur by the same factors regulating expression of any gene, including epigenetic control of pre-miR transcription or SNPs in the miR coding sequence. miR expression can also be regulated at the posttranscriptional level (as pre-miR or mature miR), by RNA-binding proteins or by circular RNAs that can act as "sponges" [195–198]. Due to the far-reaching and complex roles of miR, a small change in expression can have a profound effect on tissue homeostasis.

miR are an important part of the host response to bacteria, both pathogenic and commensal. Inflammation must be tightly regulated; excess can lead to organ damage whereas insufficient inflammation may facilitate the dissemination of infection. Several miR are well characterized as having important roles in the immune response against bacteria (reviewed in [199–201]). miR-146 and miR-155 are upregulated in immune cells following infection with a range of bacteria, including *Helicobacter pylori*, *Salmonella enterica*, *Listeria monocytogenes*, *Francisella tularensis*, and *Mycobacterium* species. Both miR-155 and miR-146 function in negative feedback loops to prevent excessive inflammation by silencing targets in the TLR4 signalling pathway. miR-155 also maintains TNF expression and is essential for an appropriate adaptive immune response. Distinct patterns of miR expression are elicited by two strains of *Cm* that vary in virulence in the murine genital tract [202]. miR-223-3p and miR-18a-5p were induced in mice by both strains at 24 hours after infection. Interestingly, miR-155 expression was increased in response to avirulent *Cm* but not in response to the virulent strain of *Cm*. The failure to upregulate miR-155 in the virulent infection could indicate an absence of the negative feedback loop that is required to prevent excessive

inflammation, leading to the increased pathology that was observed. Gupta and colleagues investigated miR expression following *Cm* infection in the murine genital model at a later time point. At 6 days after bacterial challenge, miR-125b-5p, miR-135a, miR-16, miR-214, miR-30c, miR-30e, miR-182, miR-183, and miR-23b were downregulated in the lower genital tract and miR-146 and miR-451 were upregulated [203]. These changes were not maintained at 12 days after infection. Knockdown of miR-125b-5p, miR-30c, and miR-182 led to a failure to control *Cm* infection and, in $CD4^{-/-}$ mice, levels of miR-125b-5p, miR-182, miR-183, and miR-135 were upregulated relative to wild-type infected mice. miR-125b maintains the naivety of T cells and is downregulated upon their differentiation and maturation [204]. miR-125b also targets TNF and is thought to maintain the inactivity of macrophages in the absence of bacterial TLR stimulation [199]. miR-125b downregulation may therefore be required for an appropriate immune response. Igietseme and colleagues have shown that, upon urogenital infection of mice with a virulent LGV *Ct* strain (L2), murine miR-21, miR-103, miR-107, let-7i, and miR-92b were downregulated in the oviducts, though the time point at which these changes in expression are observed is unclear [205].

Overexpression of miR-146a in psoriatic skin lesions has been linked to a SNP in the miR-146 gene in a large cohort of Chinese patients [206]. Wang and colleagues looked at the association of polymorphisms in miR-146a and the NRLP3 inflammasome in association with susceptibility and severity of urogenital *Ct* infection in two cohorts of Dutch and Finnish women [207]. A SNP in NLRP3 was found to associate with lower abdominal pain in *Ct* positive women; however, no link with miR-146a was found. Our previous work has identified that miR-147b is upregulated in scarring and inflammatory trachoma and miR-1285 is upregulated in scarring and inflammation when compared to scarring alone [208]. miR-147b acts in a similar manner to miR-146a; it is induced by TLR signaling and prevents excessive inflammation in murine macrophages [209] and is thought to have a homologous role in humans [210]. The upregulation of miR-147b in diseased individuals could represent repeated TLR stimulation, perhaps by an abnormal microbiome. miR-1285 has conflicting roles in regulation of the cell cycle [211, 212]. Abnormal regulation of inflammation and cell cycle could drive the chronic inflammation and fibrotic proliferation associated with trachomatous pathology.

Transcriptome arrays comparing gene expression at various stages of trachomatous disease have found that many thousands of genes are differentially regulated [34, 36]. In an attempt to reduce this complexity, we used a data mining approach (MSigDB) and found miR that were enriched for targets within lists of differentially regulated genes of four trachoma transcriptomes (Table 1). Of interest are the miR with known roles in the regulation of EMT, which we discuss further below. A number of miR that have been identified as differentially expressed in *Ct* and *Cm* infection are enriched for targets in these datasets, particularly in the comparison of active disease with *Ct* infection against controls, which is closest biologically to these murine models. Many of the miR were predicted to have roles regulating cell proliferation

and apoptosis. This could be reflective of *Ct* preventing host cell apoptosis to maintain the intracellular niche or T cell and fibroblast proliferation contributing to inflammation and fibrosis; however, a drawback of using data mining techniques is the relative abundance of cancer-related miR associations and pathways that dominate the literature. Pathogens and commensals express their own regulatory RNAs and it is emerging that these can be translocated into host cells to subvert or manipulate the response. Several DNA viruses express miR that target viral and host mRNAs to enhance their own success and some express virulence factors that manipulate host miR levels (reviewed in [213, 214]). *Mycobacterium tuberculosis* secreted effector ESAT-6 downregulates let-7f in macrophages, releasing expression of A20, which is a negative feedback regulator of the NFkB pathway [215]. This results in a reduction of inflammatory cytokine production and increased *M. tuberculosis* survival. miR from the parasitic nematodes *Heligmosomoides polygyrus* and *Litomosoides sigmodontis* have recently been found in the serum of mice and in discrete parasite-secreted exosomes, resulting in systemic immune regulation and suppression following uptake by host cells [216]. Little is known about bacterial miR and their ability to modulate host responses. *Mycobacterium marinum* expresses a candidate miR (23 nt long) that can be bound by host RISC and silence an mRNA target, though a functional role has not yet been identified [217]. *Ct* does not appear to express any authentic miR species in human cells, as defined by association with RISC proteins and a length of 22 ± 2 nt [217]. *Ct* does, however, encode a number of noncoding RNAs with distinct expression patterns throughout the developmental cycle, one of which regulates the transcription of a *Ct* gene [218, 219]. Some lncRNA encoding sequences are located on the *Ct* plasmid, a known virulence factor [220]. No effect on chlamydial gene transcription was identified by "knockout" of one of these plasmid-encoded miR, but an effect on host transcription was not examined [97].

8. Epithelial-Mesenchymal Transition and Chlamydial Disease

EMT is a reversible process by which epithelial cells differentiate into mesenchymal cells. Currently 3 types of EMT are recognised. In type-I EMT, epithelial cells differentiate into mesenchymal cells to migrate around the growing embryo during fetal development. These mesenchymal cells can then transform back into epithelia through the reverse process of mesenchymal-epithelial transition (MET) to establish new distant sites of epithelial tissue. Type-II EMT is associated with inflammation-induced tissue fibrosis and type-III EMT occurs in cancer when epithelial tumors metastasize. It is thought that the 3 types of EMT have similar stimuli, signaling cascades, and regulation [221, 222]. Endothelial cells also differentiate into mesenchymal cells when subjected to the same stimuli (EndMT) and can contribute to cardiac fibrosis [223].

Type-II EMT (EMT-2) occurs in response to inflammation and can lead to loss of organ function through pathological fibrosis. Inflammatory cytokines, growth factors, and MMPs activate a chain of transcription factors that

TABLE 1: miR predicted to regulate differentially expressed transcripts from four array datasets.

miR functional categories	MsigDb predicted miR based on differentially regulated mRNA transcripts (FC > 1.5 Adj. P < 0.01) from 4 trachoma transcriptomes			
	Active disease with *Ct* infection (GSE20436)	Active disease (GSE20430)	Trachomatous scarring disease with inflammation (GSE24383)	Trachomatous trichiasis with inflammation (GSE23705)
Inflammation/infection	**let-7 family** [205] **miR-125a/b** [203] miR-19a/b		miR-511	**let-7 family** [205] miR-19a/b miR-224 miR-29a/b/c
EMT/fibrosis	miR-200b/c, miR-429 miR-506			miR-200b/c, miR-429 miR-29a/b/c miR-506 miR-520d
Cell cycle/cancer	**let-7 family** [205] miR-124a **miR-125a/b** [203] miR-15 family miR-17-5p, miR-20a/b, miR-106a/b, and miR-519d miR-19a/b miR-218 **miR-23a/b** [203] **miR-30a/b/c/d/e-5p** [203] miR-519a/b/c miR-524 miR-9	miR-518a-2 miR-186 miR-130a/b, miR-301	miR-128a/b **miR-21** [202, 205] miR-26a/b miR-519a/b/c	**let-7 family** [205] miR-19a/b miR-22 miR-224 miR-25, miR-32, **miR-92**, miR-363, and miR-367 [205] miR-516-3p miR-519a/b/c miR-520d
Other	miR-130a/b, miR-301		miR-153	miR-27a/b miR-516-5p

Phenotype comparisons are as follows: normal healthy (N) children aged 1–9 versus those with active trachoma (TF) and *Ct* infection (GSE20436); children aged 1–9 with TF (with or without *Ct* infection) versus N (GSE20430); N adults versus adults with trachomatous scarring and clinical inflammation (TSI) (GSE24383); and N adults versus adults with trichiasis and clinical inflammation (TTI) (GSE23705). Enriched miR are grouped into functional categories based on well-characterized roles in the literature. References show published studies that identify miR in bold as differentially expressed in chlamydial infection.

cause downregulation of epithelial characteristics in cells and gain of mesenchymal properties. The basement membrane is degraded by MMPs, allowing differentiating cells to migrate into the interstitial tissue [224]. New mesenchymal cells can then acquire a myofibroblast phenotype [225], secreting collagen 1 and expressing α-smooth muscle actin and therefore contributing to extracellular matrix deposition and "wound" contraction. EMT-2 is known to contribute to the pathology of many fibrotic diseases, including kidney fibrosis [225], idiopathic pulmonary fibrosis [226], and cardiac and liver fibrosis [223, 227]. In a murine model of liver fibrosis, up to 45% of fibroblasts were found to have originated from hepatocytes [227]. Evidence of EMT has been shown both in acute wound healing and in chronic fibrotic (hypertrophic) scars where there is also evidence of unresolved inflammation [228]. EMT-2 ceases when inflammatory stimuli stop; therefore it appears that EMT-2 only become pathological in an environment of chronic inflammation. Having said that, EMT cells can be resistant to apoptosis (reviewed in [229]), possibly arising from the need for resilient cells to seed new sites of epithelial tissue in embryonic development. In addition to resisting apoptosis, EMT cells can acquire stem-cell-like properties allowing self-renewal [230–232], a property which is known to play a role in various cancers and which could contribute to the chronic fibrosis that is observed in trachoma. EMT-activating transcription factor ZEB1 represses expression of the stemness-inhibiting miR-200 family, therefore releasing expression of stem-cell factors and leading to EMT and self-renewal. From the evidence of our *in silico* analysis (Table 1), we suggest that the miR-200 family may be associated with trachoma.

Epigenetic changes can fix the expression of genes that induce EMT, contributing to chronic fibrosis and cancer. TGFβ-induced EMT is associated with global loss of

heterochromatin mark H3K9Me2 and gain of euchromatin marks H3K4Me3 and H3K36Me3 [233]. In cancer-related EMT, hypermethylation of E-cadherin is found [234, 235]. SNAIL, a transcription factor associated with EMT, is thought to contribute to this effect by recruiting DNA methyltransferase-1 to the E-cadherin promoter [236] and has been shown to modify the chromatin structure at the site through recruitment of the Sin3A/histone deacetylase 1 (HDAC1)/HDAC2 complex [237].

Primary hepatocytes infected with hepatitis C virus *in vitro* have been shown to upregulate biomarkers of EMT [238]. LPS-treated intrahepatic biliary epithelial cells upregulate TGFβ1 *in vitro* and stimulate EMT through the TGFβ1/SMAD2/3 pathway [239]. EMT-2 has also been observed during herpes virus infection *in vitro* and *in vivo* and following *E. coli* infection *in vitro* [240, 241]. *Helicobacter pylori* virulence factors VacA and CagA disrupt epithelial cell tight junctions and polarity [242–244] and upregulation of EMT transcription factors and biomarkers in gastric cell lines requires both the *cag* pathogenicity island and NFkB activation [245, 246]. EMT can thus be stimulated indirectly through inflammatory signals or directly by pathogens. *Ct* infected epithelial cells in *ex vivo* fallopian tube tissue show phenotypic changes characteristic of EMT, such as decreased polarity and cell adhesion [247]. The WNT pathway was upregulated and β-catenin was recruited to the chlamydial inclusion. Loss of epithelial cell-cell adhesion, N-cadherin/β-catenin complex formation, and recruitment of β-catenin to the chlamydial inclusion have also been observed *in vitro* [248]. Nectin-1, an integral molecule of epithelial cell tight junctions and adherens junctions, was downregulated at the posttranscriptional level by 85% in *Ct* infected HeLa cells, which was dependent on live infection [249]. Disruptions to key components of the WNT and Notch signaling pathways, intercellular junctions and adhesion, and cytoskeletal remodeling have been identified by RNA-sequencing as early as one hour after infection of HeLa cells with serovar E [188]. Transcriptomic profiling of TT and subsequent gene-set enrichment analysis has also shown significant enrichment in members of the WNT pathway [36, 250]. These data therefore support a role for WNT signaling in both active infection and later stages of chlamydial disease. Given that WNT signaling stimulates EMT *in vitro* [251] and the Akt/β-catenin pathway mediates EMT activation following HCV and *H. pylori* infection [238, 244], it is therefore tempting to speculate that *Ct* induces EMT-2 in the conjunctival epithelium, either directly or via *Ct*-induced inflammation.

9. Conclusions

The development of scarring trachoma represents a complex multigenic system where each host factor contributes a small protective or deleterious risk. Interaction of each of these factors adds a further layer of complexity to understanding of the disease process. Outside of host genetic factors, balance or dysbiosis of the ocular surface microbiome coupled to *Ct* genetic variation and environmental risk factors each contributes to a multilayered disease network that determines protection or pathology. Excessive or uncontrolled prolonged inflammation is the main risk factor for pathology. Genes and pathways that are dysregulated in inflammation, infection, and scarring have been identified, but clear causative links between inflammation and scarring remain elusive. To address this, we need *in vitro* studies and longitudinal clinical studies of infection, inflammation, and progressive scarring in childhood when scarring evolves. Unlike human sexually transmitted chlamydial infections, studies such as these are still possible in trachoma endemic populations. The current trend [252, 253] and emerging toolkit [254–263] for using a systems-wide or systems biology analysis of data promise to look beyond single markers towards entire molecular and cellular pathways across multiple layers of disease. The ultimate goal of the systems approaches should be to define a model that integrates data from these multiple layers including the host genetic background, composition of the microbiome, host response (transcriptome, proteome, and epigenome), and pathogen variation [188, 264] in order to explain the route to scarring or protection.

Conflict of Interests

The authors declare that there is no conflict of interests regarding the publication of this paper.

References

[1] Sightsavers, "Sightsavers Annual Review: 24," MISC12, 2012.

[2] WHO Alliance, "Weekly epidemiologicalrecord," *Relevé épidémiologique Hebdomadaire*, vol. 96, pp. 421–428, 2014.

[3] J. D. Keenan, B. Ayele, T. Gebre et al., "Childhood mortality in a cohort treated with mass azithromycin for trachoma," *Clinical Infectious Diseases*, vol. 52, no. 7, pp. 883–888, 2011.

[4] E. J. Giamarellos-Bourboulis, "Macrolides beyond the conventional antimicrobials: a class of potent immunomodulators," *International Journal of Antimicrobial Agents*, vol. 31, no. 1, pp. 12–20, 2008.

[5] V. Jimenez, H. C. Gelderblom, R. Mann Flueckiger, P. M. Emerson, D. Haddad, and T. M. Lietman, "Mass drug administration for trachoma: how long is not long enough?" *PLoS Neglected Tropical Diseases*, vol. 9, no. 3, Article ID e0003610, 2015.

[6] C. L. Coles, K. Mabula, J. C. Seidman et al., "Mass distribution of azithromycin for trachoma control is associated with increased risk of azithromycin-resistant *Streptococcus pneumoniae* carriage in young children 6 months after treatment," *Clinical Infectious Diseases*, vol. 56, no. 11, pp. 1519–1526, 2013.

[7] M. J. Burton, S. N. Rajak, V. H. Hu et al., "Pathogenesis of progressive scarring trachoma in Ethiopia and Tanzania and its implications for disease control: two cohort studies," *PLoS Neglected Tropical Diseases*, vol. 9, no. 5, Article ID e0003763, 2015.

[8] R. G. Rank and L. Yeruva, "Hidden in plain sight: chlamydial gastrointestinal infection and its relevance to persistence in human genital infection," *Infection and Immunity*, vol. 82, no. 4, pp. 1362–1371, 2014.

[9] A. P. Craig, F. Y. S. Kong, L. Yeruva et al., "Is it time to switch to doxycycline from azithromycin for treating genital chlamydial infections in women? Modelling the impact of autoinoculation from the gastrointestinal tract to the genital tract," *BMC Infectious Diseases*, vol. 15, article 200, 2015.

[10] A. R. Last, S. E. Burr, H. A. Weiss et al., "Risk factors for active trachoma and ocular *Chlamydia trachomatis* infection in treatment-naïve trachoma-hyperendemic communities of the Bijagós Archipelago, Guinea Bissau," *PLoS Neglected Tropical Diseases*, vol. 8, no. 6, Article ID e2900, 2014.

[11] V. H. Hu, P. Massae, H. A. Weiss et al., "In vivo confocal microscopy of trachoma in relation to normal tarsal conjunctiva," *Ophthalmology*, vol. 118, no. 4, pp. 747–754, 2011.

[12] V. H. Hu, M. J. Holland, I. A. Cree et al., "In vivo confocal microscopy and histopathology of the conjunctiva in trachomatous scarring and normal tissue: a systematic comparison," *British Journal of Ophthalmology*, vol. 97, no. 10, pp. 1333–1337, 2013.

[13] D. C. W. Mabey, V. Hu, R. L. Bailey, M. J. Burton, and M. J. Holland, "Towards a safe and effective chlamydial vaccine: lessons from the eye," *Vaccine*, vol. 32, no. 14, pp. 1572–1578, 2014.

[14] S. Sowa, J. Sowa, L. H. Collier, and W. A. Blyth, "Trachoma vaccine field trials in The Gambia," *Journal of Hygiene*, vol. 67, no. 4, pp. 699–717, 1969.

[15] R. L. Bailey, M. J. Burton, and D. C. W. Mabey, "Trachoma vaccine trials in the Gambia," in *Chlamydial Infections. Proceedings of the Thirteenth International Symposium on Human Chlamydial Infections*, J. Schachter, G. Byrne, and M. A. Chernesky, Eds., pp. 485–488, Asilomar Conference Grounds, Pacific Grove, Calif, USA, 2014.

[16] D. C. W. Mabey, V. H. Hu, R. L. Bailey et al., "Towards a safe and effective chlamydial vaccine: lessons from the eye," in *Proceedings of the 13th International Symposium on Human Chlamydial Infections*, J. Schachter, G. Byrne, M. A. Chernesky, and etal, Eds., pp. 489–492, Asilomar Conference Grounds, Pacific Grove, Calif, USA, June 2014.

[17] V. H. Hu, M. J. Holland, and M. J. Burton, "Trachoma: protective and pathogenic ocular immune responses to *Chlamydia trachomatis*," *PLoS Neglected Tropical Diseases*, vol. 7, no. 2, Article ID e2020, 2013.

[18] R. G. Rank, C. Dascher, A. K. Bowlin, and P. M. Bavoil, "Systemic immunization with Hsp60 alters the development of chlamydial ocular disease," *Investigative Ophthalmology and Visual Science*, vol. 36, no. 7, pp. 1344–1351, 1995.

[19] E. A. Wagar, J. Schachter, P. Bavoil, and R. S. Stephens, "Differential human serologic response to two 60,000 molecular weight *Chlamydia trachomatis* antigens," *Journal of Infectious Diseases*, vol. 162, no. 4, pp. 922–927, 1990.

[20] T. Skwor, R. P. Kandel, S. Basravi, A. Khan, B. Sharma, and D. Dean, "Characterization of humoral immune responses to chlamydial HSP60, CPAF, and CT795 in inflammatory and severe trachoma," *Investigative Ophthalmology & Visual Science*, vol. 51, no. 10, pp. 5128–5136, 2010.

[21] N. M. Budrys, S. Gong, A. K. Rodgers et al., "Chlamydia trachomatis antigens recognized in women with tubal factor infertility, normal fertility, and acute infection," *Obstetrics and Gynecology*, vol. 119, no. 5, pp. 1009–1016, 2012.

[22] C. Lu, M. J. Holland, S. Gong et al., "Genome-wide identification of *Chlamydia trachomatis* antigens associated with trachomatous trichiasis," *Investigative Ophthalmology & Visual Science*, vol. 53, no. 6, pp. 2551–2559, 2012.

[23] M. J. Holland, R. L. Bailey, L. J. Hayes, H. C. Whittle, and D. C. W. Mabey, "Conjunctival scarring in trachoma is associated with depressed cell-mediated immune responses to chlamydial antigens," *Journal of Infectious Diseases*, vol. 168, no. 6, pp. 1528–1531, 1993.

[24] M. J. Holland, R. L. Bailey, D. J. Conway et al., "T helper type-1 (Th1)/Th2 profiles of peripheral blood mononuclear cells (PBMC); responses to antigens of *Chlamydia trachomatis* in subjects with severe trachomatous scarring," *Clinical & Experimental Immunology*, vol. 105, pp. 429–435, 1996.

[25] A. M. Abu El-Asrar, K. Geboes, K. F. Tabbara, S. A. Al-Kharashi, L. Missotten, and V. Desmet, "Immunopathogenesis of conjunctival scarring in trachoma," *Eye*, vol. 12, no. 3, pp. 453–460, 1998.

[26] A. Gall, A. Horowitz, H. Joof et al., "Systemic effector and regulatory immune responses to chlamydial antigens in trachomatous trichiasis," *Frontiers in Microbiology*, vol. 2, article 10, 2011.

[27] R. C. Brunham and J. Rey-Ladino, "Immunology of Chlamydia infection: implications for a *Chlamydia trachomatis* vaccine," *Nature Reviews Immunology*, vol. 5, no. 2, pp. 149–161, 2005.

[28] N. Olivares-Zavaleta, W. M. Whitmire, L. Kari, G. L. Sturdevant, and H. D. Caldwell, "CD8+ T cells define an unexpected role in live-attenuated vaccine protective immunity against *Chlamydia trachomatis* infection in macaques," *The Journal of Immunology*, vol. 192, no. 10, pp. 4648–4654, 2014.

[29] R. S. Stephens, "The cellular paradigm of chlamydial pathogenesis," *Trends in Microbiology*, vol. 11, no. 1, pp. 44–51, 2003.

[30] S. J. Rasmussen, L. Eckmann, A. J. Quayle et al., "Secretion of proinflammatory cytokines by epithelial cells in response to Chlamydia infection suggests a central role for epithelial cells in chlamydial pathogenesis," *The Journal of Clinical Investigation*, vol. 99, no. 1, pp. 77–87, 1997.

[31] S. Dessus-Babus, T. L. Darville, F. P. Cuozzo, K. Ferguson, and P. B. Wyrick, "Differences in innate immune responses (in vitro) to HeLa cells infected with nondisseminating serovar E and disseminating serovar L2 of *Chlamydia trachomatis*," *Infection and Immunity*, vol. 70, no. 6, pp. 3234–3248, 2002.

[32] Z. Zhu, C. G. Lee, T. Zheng et al., "Airway inflammation and remodeling in asthma. Lessons from interleukin 11 and interleukin 13 transgenic mice," *American Journal of Respiratory and Critical Care Medicine*, vol. 164, no. 10, pp. S67–S70, 2001.

[33] L. R. Buckner, M. E. Lewis, S. J. Greene, T. P. Foster, and A. J. Quayle, "Chlamydia trachomatis infection results in a modest pro-inflammatory cytokine response and a decrease in T cell chemokine secretion in human polarized endocervical epithelial cells," *Cytokine*, vol. 63, no. 2, pp. 151–165, 2013.

[34] A. Natividad, T. C. Freeman, D. Jeffries et al., "Human conjunctival transcriptome analysis reveals the prominence of innate defense in *Chlamydia trachomatis* infection," *Infection and Immunity*, vol. 78, no. 11, pp. 4895–4911, 2010.

[35] A. L. Barron, *Microbiology of Chlamydia*, edited by: A. L. Barron, CRC Press, 1988.

[36] M. J. Burton, S. N. Rajak, J. Bauer et al., "Conjunctival transcriptome in scarring trachoma," *Infection and Immunity*, vol. 79, no. 1, pp. 499–511, 2011.

[37] M. J. Burton, A. Ramadhani, H. A. Weiss et al., "Active trachoma is associated with increased conjunctival expression of IL17A and profibrotic cytokines," *Infection and Immunity*, vol. 79, no. 12, pp. 4977–4983, 2011.

[38] V. H. Hu, H. A. Weiss, A. M. Ramadhani et al., "Innate immune responses and modified extracellular matrix regulation characterize bacterial infection and cellular/connective tissue changes in scarring trachoma," *Infection and Immunity*, vol. 80, no. 1, pp. 121–130, 2012.

257

[39] D. J. Conway, M. J. Holland, A. E. Campbell et al., "HLA class I and II polymorphisms and trachomatous scarring in a *Chlamydia trachomatis*—endemic population," *The Journal of Infectious Diseases*, vol. 174, no. 3, pp. 643–646, 1996.

[40] R. W. Peeling, R. L. Bailey, D. J. Comvay et al., "Antibody response to the 60-kDa chlamydial heat-shock protein is associated with scarring trachoma," *The Journal of Infectious Diseases*, vol. 177, no. 1, pp. 256–259, 1998.

[41] L. K. Gaur, R. W. Peeling, M. Cheang et al., "Association of *Chlamydia trachomatis* heat-shock protein 60 antibody and HLA class II DQ alleles," *Journal of Infectious Diseases*, vol. 180, no. 1, pp. 234–237, 1999.

[42] C. R. Cohen, S. S. Sinei, E. A. Bukusi, J. J. Bwayo, K. K. Holmes, and R. C. Brunham, "Human leukocyte antigen class II DQ alleles associated with *Chlamydia trachomatis* tubal infertility," *Obstetrics and Gynecology*, vol. 95, no. 1, pp. 72–77, 2000.

[43] M. J. Holland, D. J. Conway, T. J. Blanchard et al., "Synthetic peptides based on *Chlamydia trachomatis* antigens identify cytotoxic T lymphocyte responses in subjects from a trachoma-endemic population," *Clinical & Experimental Immunology*, vol. 107, no. 1, pp. 44–49, 1997.

[44] O. S. M. Mahdi, H. C. Whittle, H. Joof, D. C. W. Mabey, and R. L. Bailey, "Failure to detect HLA-A*6802-restricted CD8$^+$ T cells specific for Chlamydia trachomatis antigens in subjects from trachoma-endemic communities," *Clinical and Experimental Immunology*, vol. 123, no. 1, pp. 68–72, 2001.

[45] M. J. Holland, N. Faal, I. Sarr et al., "The frequency of *Chlamydia trachomatis* major outer membrane protein-specific CD8$^+$ T lymphocytes in active trachoma is associated with current ocular infection," *Infection and Immunity*, vol. 74, no. 3, pp. 1565–1572, 2006.

[46] M. N. Starnbach, M. J. Bevan, and M. F. Lampe, "Protective cytotoxic T lymphocytes are induced during murine infection with *Chlamydia trachomatis*," *The Journal of Immunology*, vol. 153, no. 11, pp. 5183–5189, 1994.

[47] S.-K. Kim, L. Devine, M. Angevine, R. DeMars, and P. B. Kavathas, "Direct detection and magnetic isolation of *Chlamydia trachomatis* major outer membrane protein-specific CD8$^+$ CTLs with HLA class I tetramers," *Journal of Immunology*, vol. 165, no. 12, pp. 7285–7292, 2000.

[48] S. C. Fankhauser and M. N. Starnbach, "PD-L1 limits the mucosal CD8$^+$ T cell response to *Chlamydia trachomatis*," *The Journal of Immunology*, vol. 192, no. 3, pp. 1079–1090, 2014.

[49] L. Kari, W. M. Whitmire, N. Olivares-Zavaleta et al., "A live-attenuated chlamydial vaccine protects against trachoma in nonhuman primates," *The Journal of Experimental Medicine*, vol. 208, no. 11, pp. 2217–2223, 2011.

[50] K. P. Karunakaran, H. Yu, X. Jiang et al., "Outer membrane proteins preferentially load MHC class II peptides: implications for a *Chlamydia trachomatis* T cell vaccine," *Vaccine*, vol. 33, no. 18, pp. 2159–2166, 2015.

[51] A. G. White, J. Bogh, W. Leheny et al., "HLA antigens in Omanis with blinding trachoma: markers for disease susceptibility and resistance," *British Journal of Ophthalmology*, vol. 81, no. 6, pp. 431–434, 1997.

[52] M. Abbas, L. D. Bobo, Y.-H. Hsieh et al., "Human leukocyte antigen (HLA)-B, DRB1, and DQB1 allotypes associated with disease and protection of trachoma endemic villagers," *Investigative Ophthalmology and Visual Science*, vol. 50, no. 4, pp. 1734–1738, 2009.

[53] C. H. Roberts, S. Molina, P. Makalo et al., "Conjunctival scarring in trachoma is associated with the HLA-C Ligand of KIR and is exacerbated by heterozygosity at KIR2DL2/KIR2DL3," *PLoS Neglected Tropical Diseases*, vol. 8, no. 3, Article ID e2744, 2014.

[54] C. C. Winter, J. E. Gumperz, P. Parham, E. O. Long, and N. Wagtmann, "Direct binding and functional transfer of NK cell inhibitory receptors reveal novel patterns of HLA-C allotype recognition," *The Journal of Immunology*, vol. 161, no. 2, pp. 571–577, 1998.

[55] E. Ciccone, D. Pende, M. Vitale et al., "Self class I molecules protect normal cells from lysis mediated by autologous natural killer cells," *European Journal of Immunology*, vol. 24, no. 4, pp. 1003–1006, 1994.

[56] M. Colonna, E. G. Brooks, M. Falco, G. B. Ferrara, and J. L. Strominger, "Generation of allospecffic natural killer cells by stimulation across a polymorphism of HLA-C," *Science*, vol. 260, no. 5111, pp. 1121–1124, 1993.

[57] M. Colonna, G. Borsellino, M. Falco, G. B. Ferrara, and J. L. Strominger, "HLA-C is the inhibitory ligand that determines dominant resistance to lysis by NK1- and NK2-specific natural killer cells," *Proceedings of the National Academy of Sciences of the United States of America*, vol. 90, no. 24, pp. 12000–12004, 1993.

[58] R. Biassoni, C. Cantoni, M. Falco et al., "The human leukocyte antigen (HLA)-C-specific 'activatory' or 'inhibitory' natural killer cell receptors display highly homologous extracellular domains but differ in their transmembrane and intracytoplasmic portions," *The Journal of Experimental Medicine*, vol. 183, no. 2, pp. 645–650, 1996.

[59] E. O. Long, M. Colonna, and L. L. Lanier, "Inhibitory MHC class I receptors on NK and T cells: a standard nomenclature," *Immunology Today*, vol. 17, no. 2, article 100, 1996.

[60] M. Colonna and J. Samaridis, "Cloning of immunoglobulin-superfamily members associated with HLA-C and HLA-B recognition by human natural killer cells," *Science*, vol. 268, no. 5209, pp. 405–408, 1995.

[61] S. Kim, J. Poursine-Laurent, S. M. Truscott et al., "Licensing of natural killer cells by host major histocompatibility complex class I molecules," *Nature*, vol. 436, no. 7051, pp. 709–713, 2005.

[62] A. Moretta, C. Bottino, D. Pende et al., "Identification of four subsets of human CD3–CD16+ natural killer (NK) cells by the expression of clonally distributed functional surface molecules: correlation between subset assignment of NK clones and ability to mediate specific alloantigen recognition," *Journal of Experimental Medicine*, vol. 172, no. 6, pp. 1589–1598, 1990.

[63] A. Moretta, G. Tambussi, C. Bottino et al., "A novel surface antigen expressed by a subset of human CD3$^-$CD16$^+$ natural killer cells. Role in cell activation and regulation of cytolytic function," *The Journal of Experimental Medicine*, vol. 171, no. 3, pp. 695–714, 1990.

[64] B. Huard and L. Karlsson, "A subpopulation of CD8$^+$ T cells specific for melanocyte differentiation antigens expresses killer inhibitory receptors (KIR) in healthy donors: evidence for a role of KIR in the control of peripheral tolerance," *European Journal of Immunology*, vol. 30, no. 6, pp. 1665–1675, 2000.

[65] S. Ferrini, A. Cambiaggi, R. Meazza et al., "T cell clones expressing the natural killer cell-related p58 receptor molecule display heterogeneity in phenotypic properties and p58 function," *European Journal of Immunology*, vol. 24, no. 10, pp. 2294–2298, 1994.

[66] N.-K. S. Al Basatena, A. MacNamara, A. M. Vine et al., "KIR2DL2 enhances protective and detrimental HLA class I-mediated immunity in chronic viral infection," *PLoS Pathogens*, vol. 7, no. 10, Article ID e1002270, 2011.

[67] W. K. Chan, P. Rujkijyanont, G. Neale et al., "Multiplex and genome-wide analyses reveal distinctive properties of KIR+ and CD56+ T cells in human blood," *The Journal of Immunology*, vol. 191, no. 4, pp. 1625–1636, 2013.

[68] D. J. Conway, M. J. Holland, R. L. Bailey et al., "Scarring trachoma is associated with polymorphism in the tumor necrosis factor alpha (TNF-α) gene promoter and with elevated TNF-α levels in tear fluid," *Infection and Immunity*, vol. 65, no. 3, pp. 1003–1006, 1997.

[69] A. Natividad, N. Hanchard, M. J. Holland et al., "Genetic variation at the *TNF* locus and the risk of severe sequelae of ocular *Chlamydia trachomatis* infection in Gambians," *Genes & Immunity*, vol. 8, no. 4, pp. 288–295, 2007.

[70] B. Atik, T. A. Skwor, R. P. Kandel et al., "Identification of novel single nucleotide polymorphisms in inflammatory genes as risk factors associated with trachomatous trichiasis," *PLoS ONE*, vol. 3, no. 10, Article ID e3600, 2008.

[71] A. Natividad, J. Wilson, O. Koch et al., "Risk of trachomatous scarring and trichiasis in Gambians varies with SNP haplotypes at the interferon-gamma and interleukin-10 loci," *Genes and Immunity*, vol. 6, no. 4, pp. 332–340, 2005.

[72] A. Natividad, J. Hull, G. Luoni et al., "Innate immunity in ocular *Chlamydia trachomatis* infection: contribution of IL8 and CSF2 gene variants to risk of trachomatous scarring in Gambians," *BMC Medical Genetics*, vol. 10, article 138, 2009.

[73] A. Natividad, M. J. Holland, K. A. Rockett et al., "Susceptibility to sequelae of human ocular chlamydial infection associated with allelic variation in IL10 cis-regulation," *Human Molecular Genetics*, vol. 17, no. 2, pp. 323–329, 2008.

[74] M. Savy, B. J. Hennig, C. P. Doherty et al., "Haptoglobin and sickle cell polymorphisms and risk of active trachoma in gambian children," *PLoS ONE*, vol. 5, no. 6, Article ID e11075, 2010.

[75] Y.-Y. Teo, K. S. Small, and D. P. Kwiatkowski, "Methodological challenges of genome-wide association analysis in Africa," *Nature Reviews Genetics*, vol. 11, no. 2, pp. 149–160, 2010.

[76] M. J. Newport and C. Finan, "Genome-wide association studies and susceptibility to infectious diseases," *Briefings in Functional Genomics*, vol. 10, no. 2, pp. 98–107, 2011.

[77] M. Jallow, Y. Y. Teo, K. S. Small et al., "Genome-wide and fine-resolution association analysis of malaria in West Africa," *Nature Genetics*, vol. 41, pp. 657–665, 2009.

[78] B. Howie, C. Fuchsberger, M. Stephens, J. Marchini, and G. R. Abecasis, "Fast and accurate genotype imputation in genome-wide association studies through pre-phasing," *Nature Genetics*, vol. 44, no. 8, pp. 955–959, 2012.

[79] SA. Morré, S. Ouburg, V.-D. Margreet, S. Ioana, and F. Fabrizio, "EpiGenChlamydia Consortium," 2015, http://www.epigenchlamydia.eu/cms/.

[80] C. H. Roberts, C. Franklin, S. Molina-Gonzalez et al., "A genome wide association scan reveals pathway—wide genomic differences between cases of scarring trachoma and controls," in *Proceedings of the 13th International Symposium on Human Chlamydial Infections*, J. Schachter, G. Byrne, M. A. Chernesky, and etal, Eds., pp. 501–504, Asilomar Conference Grounds, Pacific Grove, Calif, USA, June 2014.

[81] Y. Su, X. Wang, J. Enitra et al., "Host genetics and upper genital tract disease in *Chlamydia muridarum* infected mice: a forward genetic approach with translational implications," in *Proceedings of the 13th International Symposium on Human Chlamydial Infections*, J. Schachter, G. Byrne, M. A. Chernesky, and etal, Eds., pp. 261–264, Asilomar Conference Grounds, Pacific Grove, Calif, USA, June 2014.

[82] D. C. Ko, K. P. Shukla, C. Fong et al., "A genome-wide in vitro bacterial-infection screen reveals human variation in the host response associated with inflammatory disease," *The American Journal of Human Genetics*, vol. 85, no. 2, pp. 214–227, 2009.

[83] D. C. Ko and T. J. Urban, "Understanding human variation in infectious disease susceptibility through clinical and cellular GWAS," *PLoS Pathogens*, vol. 9, no. 8, Article ID e1003424, 2013.

[84] R. S. Stephens, S. Kalman, C. Lammel et al., "Genome sequence of an obligate intracellular pathogen of humans: *Chlamydia trachomatis*," *Science*, vol. 282, no. 5389, pp. 754–759, 1998.

[85] L. Kari, W. M. Whitmire, J. H. Carlson et al., "Pathogenic diversity among *Chlamydia trachomatis* ocular strains in nonhuman primates is affected by subtle genomic variations," *Journal of Infectious Diseases*, vol. 197, no. 3, pp. 449–456, 2008.

[86] H. M. B. Seth-Smith, S. R. Harris, K. Persson et al., "Co-evolution of genomes and plasmids within *Chlamydia trachomatis* and the emergence in Sweden of a new variant strain," *BMC Genomics*, vol. 10, article 239, 2009.

[87] S. Kalman, W. Mitchell, R. Marathe et al., "Comparative genomes of *Chlamydia pneumoniae* and *C. trachomatis*," *Nature Genetics*, vol. 21, no. 4, pp. 385–389, 1999.

[88] T. D. Read, R. C. Brunham, C. Shen et al., "Genome sequences of *Chlamydia trachomatis* MoPn and *Chlamydia pneumoniae* AR39," *Nucleic Acids Research*, vol. 28, no. 6, pp. 1397–1406, 2000.

[89] M. Shirai, H. Hirakawa, M. Kimoto et al., "Comparison of whole genome sequences of *Chlamydia pneumoniae* J138 from Japan and CWL029 from USA," *Nucleic Acids Research*, vol. 28, no. 12, pp. 2311–2314, 2000.

[90] T. D. Read, G. S. A. Myers, R. C. Brunham et al., "Genome sequence of *Chlamydophila caviae* (*Chlamydia psittaci* GPIC): examining the role of niche-specific genes in the evolution of the Chlamydiaceae," *Nucleic Acids Research*, vol. 31, no. 8, pp. 2134–2147, 2003.

[91] S. R. Harris, I. N. Clarke, H. M. B. Seth-Smith et al., "Whole-genome analysis of diverse *Chlamydia trachomatis* strains identifies phylogenetic relationships masked by current clinical typing," *Nature Genetics*, vol. 44, no. 4, pp. 413–419, 2012.

[92] J. P. Gomes, W. J. Bruno, A. Nunes et al., "Evolution of *Chlamydia trachomatis* diversity occurs by widespread interstrain recombination involving hotspots," *Genome Research*, vol. 17, no. 1, pp. 50–60, 2007.

[93] B. M. Jeffrey, R. J. Suchland, K. L. Quinn, J. R. Davidson, W. E. Stamm, and D. D. Rockey, "Genome sequencing of recent clinical *Chlamydia trachomatis* strains identifies loci associated with tissue tropism and regions of apparent recombination," *Infection and Immunity*, vol. 78, no. 6, pp. 2544–2553, 2010.

[94] Y. Wang, S. Kahane, L. T. Cutcliffe, R. J. Skilton, P. R. Lambden, and I. N. Clarke, "Development of a transformation system for chlamydia trachomatis: restoration of glycogen biosynthesis by acquisition of a plasmid shuttle vector," *PLoS Pathogens*, vol. 7, no. 9, Article ID e1002258, 2011.

[95] Y. Wang, S. Kahane, L. T. Cutcliffe et al., "Genetic transformation of a clinical (genital tract), plasmid-free isolate of *Chlamydia trachomatis*: engineering the plasmid as a cloning vector," *PLoS ONE*, vol. 8, no. 3, Article ID e59195, 2013.

[96] Y. Wang, L. T. Cutcliffe, R. J. Skilton, K. Persson, C. Bjartling, and I. N. Clarke, "Transformation of a plasmid-free, genital tract isolate of *Chlamydia trachomatis* with a plasmid vector carrying a deletion in CDS6 revealed that this gene regulates inclusion phenotype," *Pathogens and Disease*, vol. 67, no. 2, pp. 100–103, 2013.

[97] L. Song, J. H. Carlson, W. M. Whitmire et al., "Chlamydia trachomatis plasmid-encoded pgp4 is a transcriptional regulator of virulence-associated genes," *Infection and Immunity*, vol. 81, no. 3, pp. 636–644, 2013.

[98] L. Kari, M. M. Goheen, L. B. Randall et al., "Generation of targeted *Chlamydia trachomatis* null mutants," *Proceedings of the National Academy of Sciences of the United States of America*, vol. 108, no. 17, pp. 7189–7193, 2011.

[99] A. Omsland, J. Sager, V. Nair, D. E. Sturdevant, and T. Hackstadt, "Developmental stage-specific metabolic and transcriptional activity of *Chlamydia trachomatis* in an axenic medium," *Proceedings of the National Academy of Sciences of the United States of America*, vol. 109, no. 48, pp. 19781–19785, 2012.

[100] H. M. B. Seth-Smith, S. R. Harris, R. J. Skilton et al., "Whole-genome sequences of *Chlamydia trachomatis* directly from clinical samples without culture," *Genome Research*, vol. 23, no. 5, pp. 855–866, 2013.

[101] M. T. Christiansen, A. C. Brown, S. Kundu et al., "Whole-genome enrichment and sequencing of *Chlamydia trachomatis* directly from clinical samples," *BMC Infectious Diseases*, vol. 14, article 591, 2014.

[102] V. Borges, R. Ferreira, A. Nunes et al., "Effect of long-term laboratory propagation on *Chlamydia trachomatis* genome dynamics," *Infection, Genetics and Evolution*, vol. 17, pp. 23–32, 2013.

[103] P. M. Bavoil, G. Myers, B. Ma et al., "Eco-pathogenomics of chlamydial reproductive tract infection (EPCRTI)," in *Proceedings of the 13th International Symposium on Human Chlamydial Infections*, J. Schachter, G. Byrne, M. A. Chernesky et al., Eds., pp. 63–66, Asilomar Conference Grounds, Pacific Grove, Calif, USA, June 2014.

[104] C. Bonner, H. D. Caldwell, J. H. Carlson et al., "*Chlamydia trachomatis* virulence factor CT135 is stable *in vivo* but highly polymorphic *in vitro*," *Pathogens and Disease*, vol. 73, Article ID ftv043, 2015.

[105] S. D. Tyler, G. A. Peters, C. Grose et al., "Genomic cartography of varicella-zoster virus: a complete genome-based analysis of strain variability with implications for attenuation and phenotypic differences," *Virology*, vol. 359, no. 2, pp. 447–458, 2007.

[106] D. J. Dargan, E. Douglas, C. Cunningham et al., "Sequential mutations associated with adaptation of human cytomegalovirus to growth in cell culture," *Journal of General Virology*, vol. 91, pp. 1535–1546, 2010.

[107] N. L. Bachmann, M. J. Sullivan, M. Jelocnik, G. S. A. Myers, P. Timms, and A. Polkinghorne, "Culture-independent genome sequencing of clinical samples reveals an unexpected heterogeneity of infections by *Chlamydia pecorum*," *Journal of Clinical Microbiology*, vol. 53, no. 5, pp. 1573–1581, 2015.

[108] D. Longbottom, M. Russell, S. M. Dunbar, G. E. Jones, and A. J. Herring, "Molecular cloning and characterization of the genes coding for the highly immunogenic cluster of 90-kilodalton envelope proteins from the *Chlamydia psittaci* subtype that causes abortion in sheep," *Infection & Immunity*, vol. 66, no. 4, pp. 1317–1324, 1998.

[109] D. R. Stothard, G. A. Toth, and B. E. Batteiger, "Polymorphic membrane protein H has evolved in parallel with the three disease-causing groups of Chlamydia trachomatis," *Infection and Immunity*, vol. 71, no. 3, pp. 1200–1208, 2003.

[110] J. P. Gomes, A. Nunes, W. J. Bruno, M. J. Borrego, C. Florindo, and D. Dean, "Polymorphisms in the nine polymorphic membrane proteins of *Chlamydia trachomatis* across all serovars: evidence for serovar da recombination and correlation with tissue tropism," *Journal of Bacteriology*, vol. 188, no. 1, pp. 275–286, 2006.

[111] D. D. Rockey, R. A. Heinzen, and T. Hackstadt, "Cloning and characterization of a *Chlamydia psittaci* gene coding for a protein localized in the inclusion membrane of infected cells," *Molecular Microbiology*, vol. 15, no. 4, pp. 617–626, 1995.

[112] R.-C. Hsia, Y. Pannekoek, E. Ingerowski, and P. M. Bavoil, "Type III secretion genes identify a putative virulence locus of *Chlamydia*," *Molecular Microbiology*, vol. 25, no. 2, pp. 351–359, 1997.

[113] P. S. Hefty and R. S. Stephens, "Chlamydial type III secretion system is encoded on ten operons preceded by Sigma 70-like promoter elements," *Journal of Bacteriology*, vol. 189, no. 1, pp. 198–206, 2006.

[114] H. D. Caldwell, H. Wood, D. Crane et al., "Polymorphisms in *Chlamydia trachomatis* tryptophan synthase genes differentiate between genital and ocular isolates," *The Journal of Clinical Investigation*, vol. 111, no. 11, pp. 1757–1769, 2003.

[115] H. Wood, C. Fehlner-Gardner, J. Berry et al., "Regulation of tryptophan synthase gene expression in *Chlamydia trachomatis*," *Molecular Microbiology*, vol. 49, no. 5, pp. 1347–1359, 2003.

[116] J. H. Carlson, H. Wood, C. Roshick, H. D. Caldwell, and G. McClarty, "*In vivo* and *in vitro* studies of *Chlamydia trachomatis* TrpR:DNA interactions," *Molecular Microbiology*, vol. 59, no. 6, pp. 1678–1691, 2006.

[117] C. M. O'Connell, Y. M. AbdelRahman, E. Green et al., "Toll-like receptor 2 activation by *Chlamydia trachomatis* is plasmid dependent, and plasmid-responsive chromosomal loci are coordinately regulated in response to glucose limitation by *C. trachomatis* but not by *C. muridarum*," *Infection and Immunity*, vol. 79, no. 3, pp. 1044–1056, 2011.

[118] T. Hackstadt, M. A. Scidmore-Carlson, E. I. Shaw, and E. R. Fischer, "The *Chlamydia trachomatis* IncA protein is required for homotypic vesicle fusion," *Cellular Microbiology*, vol. 1, no. 2, pp. 119–130, 1999.

[119] R. J. Suchland, D. D. Rockey, J. P. Bannantine, and W. E. Stamm, "Isolates of *Chlamydia trachomatis* that occupy nonfusogenic inclusions lack IncA, a protein localized to the inclusion membrane," *Infection and Immunity*, vol. 68, no. 1, pp. 360–367, 2000.

[120] D. E. Nelson, D. D. Crane, L. D. Taylor, D. W. Dorward, M. M. Goheen, and H. D. Caldwell, "Inhibition of chlamydiae by primary alcohols correlates with the strain-specific complement of plasticity zone phospholipase D genes," *Infection and Immunity*, vol. 74, no. 1, pp. 73–80, 2006.

[121] L. D. Taylor, D. E. Nelson, D. W. Dorward, W. M. Whitmire, and H. D. Caldwell, "Biological characterization of *Chlamydia trachomatis* plasticity zone MACPF domain family protein CT153," *Infection and Immunity*, vol. 78, no. 6, pp. 2691–2699, 2010.

[122] D. LaVerda, L. N. Albanese, P. E. Ruther et al., "Seroreactivity to *Chlamydia trachomatis* Hsp10 correlates with severity of human genital tract disease," *Infection & Immunity*, vol. 68, no. 1, pp. 303–309, 2000.

[123] A. Kol, A. H. Lichtman, R. W. Finberg, P. Libby, and E. A. Kurt-Jones, "Cutting edge: heat shock protein (HSP) 60 activates the innate immune response: CD14 is an essential receptor for HSP60 activation of mononuclear cells," *Journal of Immunology*, vol. 164, no. 1, pp. 13–17, 2000.

[124] J. H. Carlson, S. Hughes, D. Hogan et al., "Polymorphisms in the *Chlamydia trachomatis* cytotoxin locus associated with ocular and genital isolates," *Infection and Immunity*, vol. 72, no. 12, pp. 7063–7072, 2004.

[125] J. H. Carlson, W. M. Whitmire, D. D. Crane et al., "The *Chlamydia trachomatis* plasmid is a transcriptional regulator of chromosomal genes and a virulence factor," *Infection and Immunity*, vol. 76, no. 6, pp. 2273–2283, 2008.

[126] L. C. Frazer, T. Darville, K. Chandra-Kuntal et al., "Plasmid-cured *Chlamydia caviae* activates TLR2-dependent signaling and retains virulence in the guinea pig model of genital tract infection," *PLoS ONE*, vol. 7, no. 1, Article ID e30747, 2012.

[127] C. Tan, J. K. Spitznagel, H.-Z. Shou et al., "The polymorphic membrane protein gene family of the Chlamydiaciae," in *Chlamydia: Genomics and Pathogenesis*, P. M. Bavoil and P. B. Wyrick, Eds., pp. 195–218, Horizon Bioscience, Norfolk, UK, 2006.

[128] K. A. Swanson, L. D. Taylor, S. D. Frank et al., "Chlamydia trachomatis polymorphic membrane protein D is an oligomeric autotransporter with a higher-order structure," *Infection and Immunity*, vol. 77, no. 1, pp. 508–516, 2009.

[129] W. Wehrl, V. Brinkmann, P. R. Jungblut, T. F. Meyer, and A. J. Szczepek, "From the inside out—processing of the Chlamydial autotransporter PmpD and its role in bacterial adhesion and activation of human host cells," *Molecular Microbiology*, vol. 51, no. 2, pp. 319–334, 2004.

[130] R. J. Belland, M. A. Scidmore, D. D. Crane et al., "*Chlamydia trachomatis* cytotoxicity associated with complete and partial cytotoxin genes," *Proceedings of the National Academy of Sciences of the United States of America*, vol. 98, no. 24, pp. 13984–13989, 2001.

[131] I. Tietzel, C. El-Haibi, and R. A. Carabeo, "Human guanylate binding proteins potentiate the anti-chlamydia effects of interferon-gamma," *PLoS ONE*, vol. 4, no. 8, Article ID e6499, 2009.

[132] N. R. Thomson, M. T. G. Holden, C. Carder et al., "*Chlamydia trachomatis*: genome sequence analysis of lymphogranuloma venereum isolates," *Genome Research*, vol. 18, no. 1, pp. 161–171, 2008.

[133] B. Fan, B. van der Pol, and D. Nelson, "Do chlamydial cytotoxins mediate IFN-γ immune evasion," in *Proceedings of the European Society for Chlamydia Research*, vol. 6, pp. 165–171, 2008.

[134] M. Sait, M. Livingstone, E. M. Clark et al., "Genome sequencing and comparative analysis of three *Chlamydia pecorum* strains associated with different pathogenic outcomes," *BMC Genomics*, vol. 15, article 23, 2014.

[135] A. Ciervo, F. Mancini, and A. Cassone, "Transcription, expression, localization and immunoreactivity of *Chlamydophila pneumoniae* Phospholipase D protein," *Microbial Pathogenesis*, vol. 43, no. 2, pp. 96–105, 2007.

[136] D. R. Clifton, K. A. Fields, S. S. Grieshaber et al., "A chlamydial type III translocated protein is tyrosine-phosphorylated at the site of entry and associated with recruitment of actin," *Proceedings of the National Academy of Sciences of the United States of America*, vol. 101, no. 27, pp. 10166–10171, 2004.

[137] W. M. Geisler, R. J. Suchland, D. D. Rockey, and W. E. Stamm, "Epidemiology and clinical manifestations of unique *Chlamydia trachomatis* isolates that occupy nonfusogenic inclusions," *Journal of Infectious Diseases*, vol. 184, no. 7, pp. 879–884, 2001.

[138] K. M. Mirrashidi, C. A. Elwell, E. Verschueren et al., "Global mapping of the inc-human interactome reveals that retromer restricts *Chlamydia* infection," *Cell Host & Microbe*, vol. 18, no. 1, pp. 109–121, 2015.

[139] C. J. Hueck, "Type III protein secretion systems in bacterial pathogens of animals and plants," *Microbiology and Molecular Biology Reviews*, vol. 62, no. 2, pp. 379–433, 1998.

[140] J. J. Mecsas and E. J. Strauss, "Molecular mechanisms of bacterial virulence: type III secretion and pathogenicity islands," *Emerging Infectious Diseases*, vol. 2, no. 4, pp. 270–288, 1996.

[141] I. M. Sigar, J. H. Schripsema, Y. Wang et al., "Plasmid deficiency in urogenital isolates of *Chlamydia trachomatis* reduces infectivity and virulence in a mouse model," *Pathogens and Disease*, vol. 70, no. 1, pp. 61–69, 2014.

[142] M. Russell, T. Darville, K. Chandra-Kuntal, B. Smith, C. W. Andrews Jr., and C. M. O'Connell, "Infectivity acts as in vivo selection for maintenance of the chlamydial cryptic plasmid," *Infection and Immunity*, vol. 79, no. 1, pp. 98–107, 2011.

[143] A. R. Last, C. H. Roberts, E. Cassama et al., "Plasmid copy number and disease severity in naturally occurring ocular *Chlamydia trachomatis* infection," *Journal of Clinical Microbiology*, vol. 52, no. 1, pp. 324–327, 2014.

[144] A. J. Twigg and D. Sherratt, "Trans-complementable copy-number mutants of plasmid ColE1," *Nature*, vol. 283, no. 5743, pp. 216–218, 1980.

[145] N. S. Thomas, M. Lusher, C. C. Storey, and I. N. Clarke, "Plasmid diversity in *Chlamydia*," *Microbiology*, vol. 143, no. 6, pp. 1847–1854, 1997.

[146] Q. An, G. Radcliffe, R. Vassallo et al., "Infection with a plasmid-free variant chlamydia related to *Chlamydia trachomatis* identified by using multiple assays for nucleic acid detection," *Journal of Clinical Microbiology*, vol. 30, no. 11, pp. 2814–2821, 1992.

[147] E. M. Peterson, B. A. Markoff, J. Schachter, and L. M. de la Maza, "The 7.5-kb plasmid present in *Chlamydia trachomatis* is not essential for the growth of this microorganism," *Plasmid*, vol. 23, no. 2, pp. 144–148, 1990.

[148] S. F. Porcella, J. H. Carlson, D. E. Sturdevant et al., "Transcriptional profiling of human epithelial cells infected with plasmid-bearing and plasmid-deficient *Chlamydia trachomatis*," *Infection and Immunity*, vol. 83, no. 2, pp. 534–543, 2015.

[149] M. Laabei, M. Recker, J. K. Rudkin et al., "Predicting the virulence of MRSA from its genome sequence," *Genome Research*, vol. 24, no. 5, pp. 839–849, 2014.

[150] T. D. Read and R. C. Massey, "Characterizing the genetic basis of bacterial phenotypes using genome-wide association studies: a new direction for bacteriology," *Genome Medicine*, vol. 6, no. 11, article 109, 2014.

[151] S. K. Sheppard, X. Didelot, G. Meric et al., "Genome-wide association study identifies vitamin B5 biosynthesis as a host specificity factor in Campylobacter," *Proceedings of the National Academy of Sciences of the United States of America*, vol. 110, no. 29, pp. 11923–11927, 2013.

[152] M. R. Farhat, B. J. Shapiro, K. J. Kieser et al., "Genomic analysis identifies targets of convergent positive selection in drug-resistant *Mycobacterium tuberculosis*," *Nature Genetics*, vol. 45, no. 10, pp. 1183–1189, 2013.

[153] M. T. Alam, R. A. Petit, E. K. Crispell et al., "Dissecting van-comycin-intermediate resistance in *Staphylococcus aureus* using genome-wide association," *Genome Biology and Evolution*, vol. 6, no. 5, pp. 1174–1185, 2014.

[154] C. Chewapreecha, P. Marttinen, N. J. Croucher et al., "Comprehensive identification of single nucleotide polymorphisms associated with beta-lactam resistance within pneumococcal mosaic genes," *PLoS Genetics*, vol. 10, no. 8, Article ID e1004547, 2014.

[155] V. H. Hu, P. Massae, H. A. Weiss et al., "Bacterial infection in scarring trachoma," *Investigative Ophthalmology & Visual Science*, vol. 52, pp. 2181–2186, 2011.

[156] M. J. Burton, R. A. Adegbola, F. Kinteh et al., "Bacterial infection and trachoma in the Gambia: a case-control study," *Investigative Ophthalmology and Visual Science*, vol. 48, no. 10, pp. 4440–4444, 2007.

[157] V. Cevallos, J. P. Whitcher, M. Melese et al., "Association of conjunctival bacterial infection and female sex in cicatricial trachoma," *Investigative Ophthalmology & Visual Science*, vol. 53, no. 9, pp. 5208–5212, 2012.

[158] M. J. Burton, V. H. Hu, P. Massae et al., "What Is causing active trachoma? The role of nonchlamydial bacterial pathogens in a low prevalence setting," *Investigative Ophthalmology and Visual Science*, vol. 52, no. 8, pp. 6012–6017, 2011.

[159] S. E. Burr, J. D. Hart, T. Edwards et al., "Association between ocular bacterial carriage and follicular trachoma following mass azithromycin distribution in The Gambia," *PLoS Neglected Tropical Diseases*, vol. 7, no. 7, Article ID e2347, 2013.

[160] M. J. Burton, R. J. C. Bowman, H. Faal et al., "Long term outcome of trichiasis surgery in the Gambia," *British Journal of Ophthalmology*, vol. 89, no. 5, pp. 575–579, 2005.

[161] M. J. Burton, R. L. Bailey, D. Jeffries et al., "Conjunctival expression of matrix metalloproteinase and proinflammatory cytokine genes after trichiasis surgery," *Investigative Ophthalmology and Visual Science*, vol. 51, no. 7, pp. 3583–3590, 2010.

[162] D. N. Frank, A. L. St Amand, R. A. Feldman, E. C. Boedeker, N. Harpaz, and N. R. Pace, "Molecular-phylogenetic characterization of microbial community imbalances in human inflammatory bowel diseases," *Proceedings of the National Academy of Sciences of the United States of America*, vol. 104, no. 34, pp. 13780–13785, 2007.

[163] B. Willing, J. Halfvarson, J. Dicksved et al., "Twin studies reveal specific imbalances in the mucosa-associated microbiota of patients with ileal Crohn's disease," *Inflammatory Bowel Diseases*, vol. 15, no. 5, pp. 653–660, 2009.

[164] A. W. Walker, J. D. Sanderson, C. Churcher et al., "High-throughput clone library analysis of the mucosa-associated microbiota reveals dysbiosis and differences between inflamed and non-inflamed regions of the intestine in inflammatory bowel disease," *BMC Microbiology*, vol. 11, article 7, 2011.

[165] A. J. McDermott and G. B. Huffnagle, "The microbiome and regulation of mucosal immunity," *Immunology*, vol. 142, no. 1, pp. 24–31, 2014.

[166] M. Valentini, A. Piermattei, G. Di Sante, G. Migliara, G. Delogu, and F. Ria, "Immunomodulation by gut microbiota: role of Toll-like receptor expressed by T cells," *Journal of Immunology Research*, vol. 2014, Article ID 586939, 8 pages, 2014.

[167] M. M. Kosiewicz, A. L. Zirnheld, and P. Alard, "Gut microbiota, immunity, and disease: a complex relationship," *Frontiers in Microbiology*, vol. 2, article 180, 2011.

[168] N. Van Oostrum, P. De Sutter, J. Meys, and H. Verstraelen, "Risks associated with bacterial vaginosis in infertility patients: a systematic review and meta-analysis," *Human Reproduction*, vol. 28, no. 7, pp. 1809–1815, 2013.

[169] S. D. Spandorfer, A. Neuer, P. C. Giraldo, Z. Rosenwaks, and S. S. Witkin, "Relationship of abnormal vaginal flora, proinflammatory cytokines and idiopathic infertility in women undergoing IVF," *Journal of Reproductive Medicine for the Obstetrician and Gynecologist*, vol. 46, no. 9, pp. 806–810, 2001.

[170] Q. Dong, J. M. Brulc, A. Iovieno et al., "Diversity of bacteria at healthy human conjunctiva," *Investigative Ophthalmology and Visual Science*, vol. 52, no. 8, pp. 5408–5413, 2011.

[171] Y. Zhou, H. Gao, K. A. Mihindukulasuriya et al., "Biogeography of the ecosystems of the healthy human body," *Genome Biology*, vol. 14, article R1, 2013.

[172] Y. Zhou, M. J. Holland, P. Makalo et al., "The conjunctival microbiome in health and trachomatous disease: a case control study," *Genome Medicine*, vol. 6, article 99, 2014.

[173] R. P. Dickson, J. R. Erb-Downward, and G. B. Huffnagle, "The role of the bacterial microbiome in lung disease," *Expert Review of Respiratory Medicine*, vol. 7, no. 3, pp. 245–257, 2013.

[174] D.-P. Mao, Q. Zhou, C.-Y. Chen, and Z.-X. Quan, "Coverage evaluation of universal bacterial primers using the metagenomic datasets," *BMC Microbiology*, vol. 12, article 66, 2012.

[175] G. Dubourg, J. C. Lagier, F. Armougom et al., "The gut microbiota of a patient with resistant tuberculosis is more comprehensively studied by culturomics than by metagenomics," *European Journal of Clinical Microbiology and Infectious Diseases*, vol. 32, no. 5, pp. 637–645, 2013.

[176] A. A. Pezzulo, P. H. Kelly, B. S. Nassar et al., "Abundant dnase I-sensitive bacterial DNA in healthy porcine lungs and its implications for the lung microbiome," *Applied and Environmental Microbiology*, vol. 79, no. 19, pp. 5936–5941, 2013.

[177] J.-C. Lagier, F. Armougom, M. Million et al., "Microbial culturomics: paradigm shift in the human gut microbiome study," *Clinical Microbiology and Infection*, vol. 18, no. 12, pp. 1185–1193, 2012.

[178] J.-C. Lagier, M. Million, P. Hugon, F. Armougom, and D. Raoult, "Human gut microbiota: repertoire and variations," *Frontiers in Cellular and Infection Microbiology*, vol. 2, article 136, 2012.

[179] A. Omsland, T. Hackstadt, and R. A. Heinzen, "Bringing culture to the uncultured: *Coxiella burnetii* and lessons for obligate intracellular bacterial pathogens," *PLoS Pathogens*, vol. 9, no. 9, Article ID e1003540, 2013.

[180] N. W. Palm, M. R. de Zoete, T. W. Cullen et al., "Immunoglobulin A coating identifies colitogenic bacteria in inflammatory bowel disease," *Cell*, vol. 158, no. 5, pp. 1000–1010, 2014.

[181] A. L. Kau, J. D. Planer, J. Liu et al., "Functional characterization of IgA-targeted bacterial taxa from undernourished Malawian children that produce diet-dependent enteropathy," *Science Translational Medicine*, vol. 7, no. 276, Article ID 276ra24, 2015.

[182] H. Bierne, M. Hamon, and P. Cossart, "Epigenetics and bacterial infections," *Cold Spring Harbor Perspectives in Medicine*, 2012.

[183] S.-H. Shin, S.-Y. Park, J.-S. Ko, N. Kim, and G. H. Kang, "Aberrant CpG island hypermethylation in pediatric gastric mucosa in association with helicobacter pylori infection," *Archives of Pathology & Laboratory Medicine*, vol. 135, no. 6, pp. 759–765, 2011.

[184] F.-Y. Huang, A. O.-O. Chan, A. Rashid, D. K.-H. Wong, C.-H. Cho, and M.-F. Yuen, "*Helicobacter pylori* induces promoter methylation of E-cadherin via interleukin-1β activation of nitric oxide production in gastric cancer cells," *Cancer*, vol. 118, no. 20, pp. 4969–4980, 2012.

[185] J. Kleinnijenhuis, J. Quintin, F. Preijers et al., "Bacille Calmette-Guérin induces NOD2-dependent nonspecific protection from reinfection via epigenetic reprogramming of monocytes," *Proceedings of the National Academy of Sciences of the United States of America*, vol. 109, no. 43, pp. 17537–17542, 2012.

[186] M. Murata, Y. Azuma, K. Miura et al., "Chlamydial SET domain protein functions as a histone methyltransferase," *Microbiology*, vol. 153, no. 2, pp. 585–592, 2007.

[187] M. E. Pennini, S. Perrinet, A. Dautry-Varsat, and A. Subtil, "Histone methylation by NUE, a novel nuclear effector of the intracellular pathogen *Chlamydia trachomatis*," *PLoS Pathogens*, vol. 6, no. 7, Article ID e1000995, pp. 1–12, 2010.

[188] M. S. Humphrys, T. Creasy, Y. Sun et al., "Simultaneous transcriptional profiling of bacteria and their host cells," *PLoS ONE*, vol. 8, no. 12, Article ID e80597, 2013.

[189] P. Kapranov, J. Cheng, S. Dike et al., "RNA maps reveal new RNA classes and a possible function for pervasive transcription," *Science*, vol. 316, no. 5830, pp. 1484–1488, 2007.

[190] R. C. Friedman, K. K.-H. Farh, C. B. Burge, and D. P. Bartel, "Most mammalian mRNAs are conserved targets of microRNAs," *Genome Research*, vol. 19, no. 1, pp. 92–105, 2009.

[191] J. Martinez, A. Patkaniowska, H. Urlaub, R. Lührmann, and T. Tuschl, "Single-stranded antisense siRNAs guide target RNA cleavage in RNAi," *Cell*, vol. 110, no. 5, pp. 563–574, 2002.

[192] C. E. Vejnar and E. M. Zdobnov, "11673," *Nucleic Acids Research*, vol. 40, no. 22, pp. 11673–11683, 2012.

[193] D. P. Bartel, "MicroRNAs: genomics, biogenesis, mechanism, and function," *Cell*, vol. 116, no. 2, pp. 281–297, 2004.

[194] V. Ambros, "The functions of animal microRNAs," *Nature*, vol. 431, no. 7006, pp. 350–355, 2004.

[195] S. Memczak, M. Jens, A. Elefsinioti et al., "Circular RNAs are a large class of animal RNAs with regulatory potency," *Nature*, vol. 495, no. 7441, pp. 333–338, 2013.

[196] T. B. Hansen, T. I. Jensen, B. H. Clausen et al., "Natural RNA circles function as efficient microRNA sponges," *Nature*, vol. 495, no. 7441, pp. 384–388, 2013.

[197] M. Van Kouwenhove, M. Kedde, and R. Agami, "MicroRNA regulation by RNA-binding proteins and its implications for cancer," *Nature Reviews Cancer*, vol. 11, no. 9, pp. 644–656, 2011.

[198] S. R. Viswanathan, G. Q. Daley, and R. I. Gregory, "Selective blockade of microRNA processing by Lin28," *Science*, vol. 320, no. 5872, pp. 97–100, 2008.

[199] C. Staedel and F. Darfeuille, "MicroRNAs and bacterial infection," *Cellular Microbiology*, vol. 15, no. 9, pp. 1496–1507, 2013.

[200] A. Eulalio, L. N. Schulte, and J. Voge, "The mammalian microRNA response to bacterial infections," *RNA Biology*, vol. 9, no. 6, pp. 742–750, 2012.

[201] C. Maudet, M. Mano, and A. Eulalio, "microRNAs in the interaction between host and bacterial pathogens," *FEBS Letters*, vol. 588, no. 22, pp. 4140–4147, 2014.

[202] L. Yeruva, G. S. Myers, N. Spencer et al., "Early microRNA expression profile as a prognostic biomarker for the development of pelvic inflammatory disease in a mouse model of chlamydial genital infection," *mBio*, vol. 5, no. 3, Article ID e01241-14, 2014.

[203] R. Gupta, T. Arkatkar, J.-J. Yu et al., "Chlamydia muridarum infection associated host MicroRNAs in the murine genital tract and contribution to generation of host immune response," *The American Journal of Reproductive Immunology*, vol. 73, no. 2, pp. 126–140, 2015.

[204] R. L. Rossi, G. Rossetti, L. Wenandy et al., "Distinct microRNA signatures in human lymphocyte subsets and enforcement of the naive state in CD4+ T cells by the microRNA miR-125b," *Nature Immunology*, vol. 12, no. 8, pp. 796–803, 2011.

[205] J. U. Igietseme, Y. Omosun, J. Partin et al., "Prevention of chlamydia-induced infertility by inhibition of local caspase activity," *The Journal of Infectious Diseases*, vol. 207, no. 7, pp. 1095–1104, 2013.

[206] W. Zhang, X. Yi, S. Guo et al., "A single-nucleotide polymorphism of miR-146a and psoriasis: an association and functional study," *Journal of Cellular and Molecular Medicine*, vol. 18, no. 11, pp. 2225–2234, 2014.

[207] W. Wang, F. R. Stassen, H.-M. Surcel et al., "Analyses of polymorphisms in the inflammasome-associated NLRP3 and miRNA-146A genes in the susceptibility to and tubal pathology of *Chlamydia trachomatis* infection," *Drugs of Today*, vol. 45, pp. 95–103, 2009.

[208] T. Derrick, C. h. Roberts, M. Rajasekhar et al., "Conjunctival MicroRNA expression in inflammatory trachomatous scarring," *PLoS Neglected Tropical Diseases*, vol. 7, no. 3, p. e2117, 2013.

[209] G. Liu, A. Friggeri, Y. Yang, Y.-J. Park, Y. Tsuruta, and E. Abraham, "miR-147, a microRNA that is induced upon toll-like receptor stimulation, regulates murine macrophage inflammatory responses," *Proceedings of the National Academy of Sciences of the United States of America*, vol. 106, no. 37, pp. 15819–15824, 2009.

[210] T. Bertero, S. Grosso, K. Robbe-Sermesant et al., "'Seed-milarity' confers to hsa-miR-210 and hsa-miR-147b similar functional activity," *PLoS ONE*, vol. 7, Article ID e44919, 2012.

[211] S. Tian, S. Huang, S. Wu, W. Guo, J. Li, and X. He, "MicroRNA-1285 inhibits the expression of p53 by directly targeting its 3′ untranslated region," *Biochemical and Biophysical Research Communications*, vol. 396, no. 2, pp. 435–439, 2010.

[212] H. Hidaka, N. Seki, H. Yoshino et al., "Tumor suppressive microRNA-1285 regulates novel molecular targets: aberrant expression and functional significance in renal cell carcinoma," *Oncotarget*, vol. 3, no. 1, pp. 44–57, 2012.

[213] B. R. Cullen, "Viruses and microRNAs: RISCy interactions with serious consequences," *Genes & Development*, vol. 25, no. 18, pp. 1881–1894, 2011.

[214] W. de Vries and B. Berkhout, "RNAi suppressors encoded by pathogenic human viruses," *The International Journal of Biochemistry & Cell Biology*, vol. 40, no. 10, pp. 2007–2012, 2008.

[215] M. Kumar, S. K. Sahu, R. Kumar et al., "microRNA let-7 modulates the immune response to *Mycobacterium tuberculosis* infection via control of A20, an inhibitor of the NF-κB pathway," *Cell Host & Microbe*, vol. 17, no. 3, pp. 345–356, 2015.

[216] A. H. Buck, G. Coakley, F. Simbari et al., "Exosomes secreted by nematode parasites transfer small RNAs to mammalian cells and modulate innate immunity," *Nature Communications*, vol. 5, article 5488, 2014.

[217] Y. Furuse, R. Finethy, H. A. Saka et al., "Search for microRNAs expressed by intracellular bacterial pathogens in infected mammalian cells," *PLoS ONE*, vol. 9, no. 9, Article ID e106434, 2014.

[218] Y. M. Abdelrahman, L. A. Rose, and R. J. Belland, "Developmental expression of non-coding RNAs in *Chlamydia trachomatis* during normal and persistent growth," *Nucleic Acids Research*, vol. 39, no. 5, pp. 1843–1854, 2011.

[219] M. Albrecht, C. M. Sharma, R. Reinhardt, J. Vogel, and T. Rudel, "Deep sequencing-based discovery of the *Chlamydia trachomatis* transcriptome," *Nucleic Acids Research*, vol. 38, no. 3, Article ID gkp1032, pp. 868–877, 2009.

[220] S. Ricci, R. Cevenini, E. Cosco, M. Comanducci, G. Ratti, and V. Scarlato, "Transcriptional analysis of the *Chlamydia trachomatis* plasmid pCT identifies temporally regulated transcripts, antisense RNA and σ^{70}-selected promoters," *Molecular & General Genetics*, vol. 237, no. 3, pp. 318–326, 1993.

[221] R. Kalluri and R. A. Weinberg, "The basics of epithelial-mesenchymal transition," *The Journal of Clinical Investigation*, vol. 119, no. 6, pp. 1420–1428, 2009.

[222] M. Zeisberg and E. G. Neilson, "Biomarkers for epithelial-mesenchymal transitions," *Journal of Clinical Investigation*, vol. 119, no. 6, pp. 1429–1437, 2009.

[223] E. M. Zeisberg, O. Tarnavski, M. Zeisberg et al., "Endothelial-to-mesenchymal transition contributes to cardiac fibrosis," *Nature Medicine*, vol. 13, no. 8, pp. 952–961, 2007.

[224] H. Okada, F. Strutz, T. M. Danoff, R. Kalluri, and E. G. Neilson, "Possible mechanisms of renal fibrosis," *Contributions to Nephrology*, vol. 118, pp. 147–154, 1996.

[225] M. Iwano, D. Plieth, T. M. Danoff, C. Xue, H. Okada, and E. G. Neilson, "Evidence that fibroblasts derive from epithelium during tissue fibrosis," *The Journal of Clinical Investigation*, vol. 110, no. 3, pp. 341–350, 2002.

[226] M. Chilosi, V. Poletti, A. Zamò et al., "Aberrant Wnt/beta-catenin pathway activation in idiopathic pulmonary fibrosis," *American Journal of Pathology*, vol. 162, no. 5, pp. 1495–1502, 2003.

[227] M. Zeisberg, C. Yang, M. Martino et al., "Fibroblasts derive from hepatocytes in liver fibrosis via epithelial to mesenchymal transition," *Journal of Biological Chemistry*, vol. 282, no. 32, pp. 23337–23347, 2007.

[228] C. Yan, W. A. Grimm, W. L. Garner et al., "Epithelial to mesenchymal transition in human skin wound healing is induced by tumor necrosis factor-alpha through bone morphogenic protein-2," *American Journal of Pathology*, vol. 176, no. 5, pp. 2247–2258, 2010.

[229] J. P. Thiery, H. Acloque, R. Y. J. Huang, and M. A. Nieto, "Epithelial-mesenchymal transitions in development and disease," *Cell*, vol. 139, no. 5, pp. 871–890, 2009.

[230] A.-P. Morel, M. Lièvre, C. Thomas, G. Hinkal, S. Ansieau, and A. Puisieux, "Generation of breast cancer stem cells through epithelial-mesenchymal transition," *PLoS ONE*, vol. 3, no. 8, Article ID e2888, 2008.

[231] U. Wellner, J. Schubert, U. C. Burk et al., "The EMT-activator ZEB1 promotes tumorigenicity by repressing stemness-inhibiting microRNAs," *Nature Cell Biology*, vol. 11, no. 12, pp. 1487–1495, 2009.

[232] S. A. Mani, W. Guo, M.-J. Liao et al., "The epithelial-mesenchymal transition generates cells with properties of stem cells," *Cell*, vol. 133, no. 4, pp. 704–715, 2008.

[233] O. G. McDonald, H. Wu, W. Timp, A. Doi, and A. P. Feinberg, "Genome-scale epigenetic reprogramming during epithelial-to-mesenchymal transition," *Nature Structural & Molecular Biology*, vol. 18, no. 8, pp. 867–874, 2011.

[234] M. Lombaerts, T. van Wezel, K. Philippo et al., "E-cadherin transcriptional downregulation by promoter methylation but not mutation is related to epithelial-to-mesenchymal transition in breast cancer cell lines," *British Journal of Cancer*, vol. 94, no. 5, pp. 661–671, 2006.

[235] N. Dumont, M. B. Wilson, Y. G. Crawford, P. A. Reynolds, M. Sigaroudinia, and T. D. Tlsty, "Sustained induction of epithelial to mesenchymal transition activates DNA methylation of genes silenced in basal-like breast cancers," *Proceedings of the National Academy of Sciences of the United States of America*, vol. 105, no. 39, pp. 14867–14872, 2008.

[236] S.-O. Lim, J.-M. Gu, M. S. Kim et al., "Epigenetic changes induced by reactive oxygen species in hepatocellular carcinoma: methylation of the E-cadherin promoter," *Gastroenterology*, vol. 135, no. 6, pp. 2128–2140.e8, 2008.

[237] H. Peinado, E. Ballestar, M. Esteller, and A. Cano, "Snail mediates E-cadherin repression by the recruitment of the Sin3A/histone deacetylase 1 (HDAC1)/HDAC2 complex," *Molecular and Cellular Biology*, vol. 24, no. 1, pp. 306–319, 2004.

[238] S. K. Bose, K. Meyer, A. M. Di Bisceglie, R. B. Ray, and R. Ray, "Hepatitis C virus induces epithelial-mesenchymal transition in primary human hepatocytes," *Journal of Virology*, vol. 86, no. 24, pp. 13621–13628, 2012.

[239] L. Zhao, R. Yang, L. Cheng, M. Wang, Y. Jiang, and S. Wang, "LPS-induced epithelial-mesenchymal transition of intrahepatic biliary epithelial cells," *Journal of Surgical Research*, vol. 171, no. 2, pp. 819–825, 2011.

[240] V. Pozharskaya, E. Torres-González, M. Rojas et al., "Twist: a regulator of epithelial-mesenchymal transition in lung fibrosis," *PLoS ONE*, vol. 4, no. 10, Article ID e7559, 2009.

[241] G. Cane, A. Ginouvès, S. Marchetti et al., "HIF-1alpha mediates the induction of IL-8 and VEGF expression on infection with Afa/Dr diffusely adhering *E. coli* and promotes EMT-like behaviour," *Cellular Microbiology*, vol. 12, no. 5, pp. 640–653, 2010.

[242] E. Papini, B. Satin, N. Norais et al., "Selective increase of the permeability of polarized epithelial cell monolayers by *Helicobacter pylori* vacuolating toxin," *The Journal of Clinical Investigation*, vol. 102, no. 4, pp. 813–820, 1998.

[243] M. R. Amieva, R. Vogetmann, A. Covacci, L. S. Tompkins, W. J. Nelson, and S. Falkow, "Disruption of the epithelial apical-junctional complex by *Helicobacter pylori* CagA," *Science*, vol. 300, no. 5624, pp. 1430–1434, 2003.

[244] N. Murata-Kamiya, Y. Kurashima, Y. Teishikata et al., "*Helicobacter pylori* CagA interacts with E-cadherin and deregulates the β-catenin signal that promotes intestinal transdifferentiation in gastric epithelial cells," *Oncogene*, vol. 26, no. 32, pp. 4617–4626, 2007.

[245] F. Yin, A. M. Grabowska, P. A. Clarke et al., "*Helicobacter pylori* potentiates epithelial:mesenchymal transition in gastric cancer: links to soluble HB-EGF, gastrin and matrix metalloproteinase-7," *Gut*, vol. 59, no. 8, pp. 1037–1045, 2010.

[246] J. Baud, C. Varon, S. Chabas, L. Chambonnier, F. Darfeuille, and C. Staedel, "*Helicobacter pylori* initiates a mesenchymal transition through ZEB1 in gastric epithelial cells," *PLoS ONE*, vol. 8, no. 4, Article ID e60315, 2013.

[247] M. Kessler, J. Zielecki, O. Thieck, H.-J. Mollenkopf, C. Fotopoulou, and T. F. Meyer, "*Chlamydia trachomatis* disturbs epithelial tissue homeostasis in fallopian tubes via paracrine Wnt signaling," *American Journal of Pathology*, vol. 180, no. 1, pp. 186–198, 2012.

[248] W. C. Prozialeck, M. J. Fay, P. C. Lamar, C. A. Pearson, I. Sigar, and K. H. Ramsey, "*Chlamydia trachomatis* disrupts N-cadherin-dependent cell-cell junctions and sequesters beta-catenin in human cervical epithelial cells," *Infection and Immunity*, vol. 70, no. 5, pp. 2605–2613, 2002.

[249] J. Sun, J. Kintner, and R. V. Schoborg, "The host adherens junction molecule nectin-1 is downregulated in *Chlamydia trachomatis*-infected genital epithelial cells," *Microbiology*, vol. 154, no. 5, pp. 1290–1299, 2008.

[250] M. J. Holland, D. Jeffries, M. Pattison et al., "Pathway-focused arrays reveal increased matrix metalloproteinase-7 (Matrilysin) transcription in trachomatous trichiasis," *Investigative Ophthalmology and Visual Science*, vol. 51, no. 8, pp. 3893–3902, 2010.

[251] H.-C. Chen, Y.-T. Zhu, S.-Y. Chen, and S. C. G. Tseng, "Wnt signaling induces epithelial-mesenchymal transition with proliferation in ARPE-19 cells upon loss of contact inhibition," *Laboratory Investigation*, vol. 92, no. 5, pp. 676–687, 2012.

[252] D. A. Cusanovich, C. Billstrand, X. Zhou et al., "The combination of a genome-wide association study of lymphocyte count and analysis of gene expression data reveals novel asthma candidate genes," *Human Molecular Genetics*, vol. 21, no. 9, pp. 2111–2123, 2012.

[253] P. Jia and Z. Zhao, "Network-assisted analysis to prioritize GWAS results: principles, methods and perspectives," *Human Genetics*, vol. 133, no. 2, pp. 125–138, 2014.

[254] P. Holmans, E. K. Green, J. S. Pahwa et al., "Gene ontology analysis of GWA study data sets provides insights into the biology of bipolar disorder," *The American Journal of Human Genetics*, vol. 85, no. 1, pp. 13–24, 2009.

[255] R. Braun and K. Buetow, "Pathways of distinction analysis: a new technique for multi-SNP analysis of GWAS data," *PLoS Genetics*, vol. 7, no. 6, Article ID e1002101, 2011.

[256] C. S. Greene, N. M. Penrod, J. Kiralis, and J. H. Moore, "Spatially uniform reliefF (SURF) for computationally-efficient filtering of gene-gene interactions," *BioData Mining*, vol. 2, article 5, 2009.

[257] M. D. Ritchie, L. W. Hahn, N. Roodi et al., "Multifactor-dimensionality reduction reveals high-order interactions among estrogen-metabolism genes in sporadic breast cancer," *The American Journal of Human Genetics*, vol. 69, no. 1, pp. 138–147, 2001.

[258] P. Jia and Z. Zhao, "Searching joint association signals in CATIE schizophrenia genome-wide association studies through a refined integrative network approach," *BMC Genomics*, vol. 13, supplement 6, article S15, 2012.

[259] S. Purcell, B. Neale, K. Todd-Brown et al., "PLINK: a tool set for whole-genome association and population-based linkage analyses," *The American Journal of Human Genetics*, vol. 81, no. 3, pp. 559–575, 2007.

[260] L. S. Chen, C. M. Hutter, J. D. Potter et al., "Insights into colon cancer etiology via a regularized approach to gene set analysis of GWAS data," *The American Journal of Human Genetics*, vol. 86, no. 6, pp. 860–871, 2010.

[261] D. Knights, M. S. Silverberg, R. K. Weersma et al., "Complex host genetics influence the microbiome in inflammatory bowel disease," *Genome Medicine*, vol. 6, article 107, 2014.

[262] B. P. Fairfax, S. Makino, J. Radhakrishnan et al., "Genetics of gene expression in primary immune cells identifies cell type-specific master regulators and roles of HLA alleles," *Nature Genetics*, vol. 44, no. 5, pp. 502–510, 2012.

[263] D. Wong, W. Lee, P. Humburg et al., "Genomic mapping of the MHC transactivator CIITA using an integrated ChIP-seq and genetical genomics approach," *Genome Biology*, vol. 15, no. 10, p. 494, 2014.

[264] D. E. Sturdevant, K. Virtaneva, C. Martens et al., "Host-microbe interaction systems biology: lifecycle transcriptomics and comparative genomics," *Future Microbiology*, vol. 5, no. 2, pp. 205–219, 2010.

PostScript

LETTER

Eyescores: an open platform for secure electronic data and photographic evidence collection in ophthalmological field studies

In ophthalmological studies, the need to take photographs as evidence introduces additional complications to fieldwork. A recent report[1] highlighted the usefulness of smartphones in the collection and grading of photographic evidence of trachoma. We have recently considered the wider potential of portable computerised equipment to integrate the recording and management of trachoma photographs with field data and biological specimens.

While the overall resolution of smartphone cameras increases rapidly, an outstanding issue with smartphone photography is the phenomenon of shutter lag, a significant time interval between actuation and the recording of an image. Shutter lag is associated with image blurring as the subject or camera may have moved out of focus by the time of image recording. Recently released smartphones such as the HTC One X and Samsung Galaxy S3 are robust against shutter lag, but are currently the exceptions in a telephony market that has responded slowly to the problem. Light Field Photography (LFP) technology (http://www.lytro.com) has the potential to eliminate blurring and increase the amount of information available to the researcher. LFP cameras generate images that can be viewed and analysed on multiple focal planes. With portable LFP cameras as yet untested in a medical setting and with shutter lag a continuing problem for smartphone cameras, we continue to view digital single lens reflex (SLR) photography as the gold standard for trachoma studies. Smartphone applications such as Epicollect[2] and OpenDataKit (http://www.opendatakit.org) have made attempts to integrate electronic data capture with photographic evidence, but while smartphones may be convenient for photographic purposes, a previous study found that Netbooks may be superior to smartphones for high-quality electronic data collection[3] and our own experiences support this.

With these issues in mind, we developed 'Eyescores', a flexible, open and modifiable software/hardware platform for the collection and management of data, bio-samples and photographs in trachoma and other ophthalmological field studies. Integral to the system is the use of an Eye-Fi memory card (EYE-FI Inc. Mountain View, California, USA) in a digital SLR camera. This inexpensive (~$50) hardware device is used to create a local wi-fi connection between any camera with a secure digital (SD) memory slot and a netbook computer. Eyescores allows data transfers, watermarking and renaming of photograph image files in real time with almost zero user involvement. Eyescores is customisable, minimises user involvement in data entry and validates data using the powerful language of regular expressions. Data is stored in customisable formats and is automatically backed up to external solid-state USB hard drive. Eyescores performs on-the-fly encryption of subjects' personal data using openSSL (secure sockets layer) protocols (http://www.openssl.org). This makes the transfer of data files by email, cloud server or other similar electronic connections a secure and practical option for data management and sharing between sites. From the point of collection, Eyescores data is fully protected against loss or theft of the computer.

We trialled Eyescores on 93 samples from The Gambia which had been surveyed using paper forms 2 years previously. We found good accordance between the two data sets and being satisfied with the outcome of our trial, we have now fully deployed Eyescores in our ongoing trachoma field studies in Tanzania. Since February 2012 we have collected more than 800 samples without significant incident or error and with zero missing data.

Eyescores is written in the programming language Perl. It runs on very low-specification hardware, is cross platform and is reasonably simple to install. Support is available from the authors if you wish to implement Eyescores. This software is released under the GNU General Public License. To download Eyescores in its current beta version or to view examples of the data output, please visit http://chrissyhroberts.lshtm.ac.uk/eyescores/

Chrissy h Roberts,[1] Tara Mtuy,[1,2] Tamsyn Derrick,[1] Matthew J Burton,[1] Martin J Holland[1]

[1]Clinical Research Department, London School of Hygiene and Tropical Medicine, London, UK
[2]Kilimanjaro Centre for Community Ophthalmology, KCMC Hospital, Moshi, Tanzania

Correspondence to Dr Chrissy h Roberts, Clinical Research Department, London School of Hygiene and Tropical Medicine, London WC1E 7HT, UK; chrissyhroberts@yahoo.co.uk

OPEN ACCESS

REFERENCES

1 Bhosai SJ, Amza A, Beido N, et al. Application of smartphone cameras for detecting clinically active trachoma. Br J Ophthalmol 2012;96:1350–1.
2 Aanensen DM, Huntley DM, Feil EJ, et al. EpiCollect: linking smartphones to web applications for epidemiology, ecology and community data collection. PLoS ONE 2009;4:7.
3 Walther B, Hossin S, Townend J, et al. Comparison of electronic data capture (EDC) with the standard data capture method for clinical trial data. PLoS one 2011;6:e25348.

Comité Nacional de Ética na Saúde

Nº Refª _OI2_/CNES/INASA/2013   Bissau, 22 de março de 2013

À

Dra. Anna Last
London School Of Higiene & Tropical Medicine
Keppel Street, London WCIE 7HT
Tel: +44 020-7927-2419 direct line
Fax: +44 020-7637-4314
E-mail: martin.holland@lshtm.ac.uk
Projeto de Saúdem Bandim
Apartado 861, 1004 Bissau Codex

BISSAU

ASSUNTO: Aprovação de Emendas ao Protocolo de Pesquisa

Com os melhores cumprimentos.

O Comité Nacional de Ética na Saúde reunido na sua segunda sessão extraordinária no dia 20 de março de 2013, ao analisar o Protocolo de Projeto de Pesquisa que lhe foi submetido cujo título: "*Proposta de triagem e identificação dos padrões de expressão de microRNA da conjuntivite associados com tracoma activo no Arquipélago dos Bijagós da Guiné-Bissau*", após compulsar o Protocolo aprovado na sua segunda sessão ordinária no dia 25 de Junho de 2011, intitulado "**Mapeamento do Tracoma no Arquipélago dos Bijagós de GNB usando técnicas especial e moleculares epidemiológicos**" verificou que esta constitui uma das fases de realização dos seus achados pelo que, face aos argumentos que suportam a necessidade de recolha de amostras para a realização deste estudo nos moldes que se apresentam na metodologia, o coletivo deu por aprova-lo por unanimidade.

Com elevada consideração.

O Presidente

Dr. Cunhate Na Bangna

Instituto Nacional de Saúde Pública • Avenida Combatente da Liberdade de Pátria, Hospital "3 de Agosto" •
Apartado: 861 Bissau, 1004 Bissau Cedex • Administração TM: + 245 551 5150 • TM: (+ 245) 693 8511/590 4960.
E-mail: inasagb@gmail.com/nabangna.julho2009@gmail.com & djicoblama@hotmail.com

Observational / Interventions Research Ethics Committee

Tamsyn Derrick
Research Degree Student
CR / ITD
LSHTM

11 July 2013

Dear Ms. Derrick,

Study Title: **miR expression in active trachoma**
LSHTM ethics ref: **6433**

Thank you for your letter of 4 July 2011, responding to the Observational Committee's request for further information on the above research and submitting revised documentation.

The further information has been considered on behalf of the Committee by the Chair.

Confirmation of ethical opinion

On behalf of the Committee, I am pleased to confirm a favourable ethical opinion for the above research on the basis described in the application form, protocol and supporting documentation as revised, subject to the conditions specified below.

Conditions of the favourable opinion

Approval is dependent on local ethical approval having been received, where relevant.

Approved documents

The final list of documents reviewed and approved by the Committee is as follows:

Document	Version	Date
LSHTM ethics application	2	
miRNA Information Sheet & Consent form		
miRNA data collection form		

After ethical review

Any subsequent changes to the application must be submitted to the Committee via an E2 amendment form. All studies are also required to notify the ethics committee of any serious adverse events which occur during the project via form E4. At the end of the study, please notify the committee via form E5.

Yours sincerely,

Professor John DH Porter
Chair
ethics@lshtm.ac.uk
http://intra.lshtm.ac.uk/management/committees/ethics/

Improving health worldwide

Observational / Interventions Research Ethics Committee

Tamsyn Derrick
Research Degree Student
CR / ITD
LSHTM

7 November 2013

Dear Miss Derrick,

Study Title:	**miR expression in active trachoma**
LSHTM ethics ref:	**6433**
LSHTM amend no:	**A460**

Thank you for your application of 4 October 2013 for the amendment above to the existing ethically approved study and submitting revised documentation. The amendment application has been considered by the Observational Committee.

Confirmation of ethical opinion

On behalf of the Committee, I am pleased to confirm a favourable ethical opinion for the above amendment to research on the basis described in the application form, protocol and supporting documentation as revised, subject to the conditions specified below.

Conditions of the favourable opinion

Approval is dependent on local ethical approval for the amendment having been received, where relevant.

Approved documents

The final list of documents reviewed and approved by the Committee is as follows:

Document	Version	Date
LSHTM amendment application	n/a	4/10/2013
miRNA info consent form for GB_amended_4.10.13	2	04.10.2013
miRNA data collection form GB_amended_4.10.13	2	04.10.2013

After ethical review

Any further changes to the application must be submitted to the Committee via an E2 amendment form. The Principal Investigator is reminded that all studies are also required to notify the ethics committee of any serious adverse events which occur during the project via form E4. At the end of the study, please notify the committee via form E5.

Yours sincerely,

Professor John DH Porter
Chair
ethics@lshtm.ac.uk
http://www.lshtm.ac.uk/ethics/

Improving health worldwide

ANEXO 4: Pesquisa de miRNA da conjuntiva no Arquipélago dos Bijagós

Formulário de Registo

Examinador/a _____ Assistente de Laboratório _____ Fotógrafo/a_____

Número UID

__ __ / __ __ __ / __ __ __ __

Formulário de consentimento preenchido?   Sim   Não

A criança tem menos de 10 anos de idade?   Sim   Não

A criança tem tracoma activo?   Sim   Não

Se Não, DESISTA! Preencha o formulário de consentimento.

Nome _____   Apelido____ _____

Exame Clínico e Amostragem

OLHO ESQUERDA   TF   TI   N | AMOSTRA 'AIR' |
                     F [ ]   P [ ]   C [ ]

| Etiqueta Adesiva de AMOSTRA 1 | Números dos fotos | 1 |
                                                          | 2 |
| Etiqueta Adesiva de AMOSTRA 2 | | 3 |

| Etiqueta Adesiva amostra de saliva |

(vii)

ANEXO 2
Informações adicionais e Formulário de Consentimento para Participantes
Triagem e identificação dos padrões de expressão do microRNA da conjuntiva associados com tracoma activo
Estudo: Mapeamento do Tracoma no Arquipélago dos Bijagós na Guiné Bissau
Responsável: Dra Anna Last
Escola de Higiene e Medicina Tropical de Londres no Reino Unido com o Programa Nacional da Saúde da Visão (PNSV) da Guiné Bissau

A respeito do que é este estudo?
Sabemos que o tracoma é um grande problema nas ilhas Bijagós. Nós não sabemos porque o problema é tão grande. A fim de compreender porque é que há um problema tão grande, queremos observar as defezas oculares (imunidade) contra a infecção.

Quem está fazendo este estudo?
Escola de Higiene e Medicina Tropical de Londres no Reino Unido juntamente com o Programa Nacional da Saúde da Visão (PNSV) da Guiné Bissau.

Da ajuda de quem precisamos?
Precisamos da ajuda de cerca de 200 crianças com menos de 10 anos de idade que vivam em comunidades nas ilhas.

O que vamos pedir-lhe para fazer?
Precisamos examinar seus olhos e tomar 2 amostras (com um cotonete) do seu olho esquerdo para fazer testes para investigar as defezas oculares (imunidade) contra a infecção e testes de infecção no laboratório. Vamos tomar uma foto de cada olho que examinarmos. Pedimos-lhe para cuspir em um tubo para que possamos coletar sua saliva. De sua saliva podemos aprender sobre sua genética.

Quais são os benefícios de participar deste estudo?
O tracoma é um grande problema nas ilhas Bijagós. O tracoma pode ser tratado eficazmente com o antibiótico azitromicina, um comprimido. Este tratamento pode curar a infecção e prevenir a cegueira por tracoma. Nós, juntamente com o PNSV, vamos a tratar as comunidades com tracoma (com comprimidos) e fazer a cirurgia de triquíase para prevenir a cegueira. No futuro este trabalho pode ajudar-nos a desenvover colírios ou pomadas para serem usadas como tratamento para inflamação e infecção para prevenir a cegueira e as consequências do tracoma.

Existem riscos causados por participar neste estudo?
O exame e a lavagem são apenas um pouco desconfortáveis mas não vão danificar o olho de maneira nenhuma. Vai demorar apenas poucos minutos. Não há riscos no processo de colheita de amostras. Já foi feita sem problemas em muitos países.

Que testes serão feitos com as amostras?
Vamos testar as amostras no laboratório no Reino Unido para aumentar a nossa compreensão do tracoma.

O que vamos fazer com os registos e as fotos que fizermos dos seus olhos?
Todas as informações que colhermos serão confidenciais. Somente os organizadores do estudo terão acesso a elas.

Sou obrigado a participar deste estudo?
Não, a participação é completamente voluntária. É sua decisão participar deste estudo. Você pode negar-se a participar do estudo quando quiser sem dar explicação. E em caso de nao querer participar, isso não afectará o seu relacionamento com o hospital ou o seu tratamento de tracoma ou outras doenças de maneira nenhuma.

Data _____   Assistente _____   Estudo do Tracoma

Muito obrigada por considerar estar envolvido neste trabalho importante. Se você tiver alguma dúvida, pergunte-nos:

     Dra Anna Last (Médica e Coodenadora do Estudo) 00245 650 6554
     Sra Eunice Cassama (Enfermeira ofthalmológica) 00245 628 8282
     Dr Meno Nabicassa, Programa Nacional da Saúde da Visão, Ministério da Saúde Pública, Bissau
     Dr Jose Nacutum, Hospital Regional da Bubaque 'Marcelino Banca'

Nome Próprio _____   Apelido _____

Número de identificação (UID)   __ __ / __ __ __ / __ __ __ __

Eu li/recebi explicações sobre o estudo. O assistente respondeu todas as minhas perguntas sobre o estudo.

Eu entendo as informações e permito que esta cirança participe   Sim   Não

Confirmação do pai / responsável (porque a criança tiver menos de 10 anos)

Assinatura/Impressão digital   _____

Nome   _____

Data   _____

Confimação do Assistente

Eu expliquei o objetivo do estudo e estou convencido de que ele/ela concorda em participar voluntariamente.

Assinatura   _____

Nome   _____

Data   _____

Declaração de testemunha se o participante não puder ler as informações de consentimento

Eu sou testemunha das explicações fornecidas ao participante e do consentimento dado do participante acima mencionado para o estudo.

Assinatura/Impressão digital   _____

Nome   _____

Data   _____